Holography and Strongly Correlated Systems

by

Nabil Iqbal

Submitted to the Department of Physics
in partial fulfillment of the requirements for the degree of

PhD

at the

MASSACHUSETTS INSTITUTE OF TECHNOLOGY

June 2011

Author .....
Department of Physics
May 20, 2011

Certified by .....
Hong Liu
Professor
Thesis Supervisor

Accepted by .....
Krishna Rajagopal
Associate Department Head for Education

Holography and Strongly Correlated Systems

by

Nabil Iqbal

Submitted to the Department of Physics
on May 20, 2011, in partial fulfillment of the
requirements for the degree of
PhD

Abstract

In this thesis we apply techniques arising from string theory – gauge-gravity/duality, or holography – to problems associated with strongly coupled quantum field theories under extreme conditions such as finite temperature or density.

We first study a strongly coupled field theory at finite temperature. We demonstrate that its low frequency limit is determined by the horizon geometry of its gravity dual, i.e. by the "membrane paradigm" fluid of classical black hole mechanics. Thus generic boundary theory transport coefficients can be expressed in terms of geometric quantities evaluated at the horizon, providing a simple understanding of results such as the universality of the shear viscosity in theories with gravity duals. Away from the low frequency limit we find a nontrivial radial flow from the black hole horizon to the boundary of the spacetime; we derive equations governing this flow and demonstrate their use in the simple examples of charge and momentum diffusion.

Next, we turn to the study of strongly coupled theories with a finite density of a $U(1)$ charge. The near-horizon geometry of the gravity dual of such a state has an AdS_2 factor, indicating the existence of a nontrivial emergent conformal symmetry in the infrared with nontrivial scaling only in the time direction. We review earlier work indicating that fermionic perturbations of such a state reveal *non-Fermi-liquid* behavior, i.e. gapless fermionic excitations that are not those of Fermi liquid theory. We perform a one-loop calculation in the bulk to compute the contribution from these Fermi surfaces to the conductivity of the full system. Interestingly, within this class of non-Fermi liquids we find examples whose single-particle spectral function and transport behavior both resemble those of *strange metals*, i.e. the anomalous metallic state existing in the real-life high T_c cuprates above their superconducting transition temperature. In particular, for these examples the contribution to the conductivity is inversely proportional to temperature. In our treatment these properties can be understood as being controlled by the scaling dimension of the fermion operator in the emergent IR fixed point.

We then turn to models of symmetry breaking in holographic models at finite density. We observe that the presence of the AdS_2 factor can result in the condensation of a neutral scalar operator. This can be used to model an "antiferromagnetic" phase in which a global $SU(2)$ symmetry is broken down to $U(1)$. We study the collective modes of the ordered phase and recover the expected spin waves from a gravitational treatment. We then note that the phase transition can be driven to zero temper-

ature by tuning various bulk couplings, resulting in a quantum phase transition of the Berezinskii-Kosterlitz-Thouless type. We study this transition in detail, revealing novel critical behavior, including locally quantum critical dynamics and the existence of an infinite tower of excited states related by a discrete subgroup of the original emergent conformal symmetry.

Throughout this thesis we focus on how the novel viewpoint provided by holography can help us gain new insights into the physics of strongly correlated systems.

Thesis Supervisor: Hong Liu
Title: Professor

Dedication

To Ammu and Abbu, my first teachers and the ones who taught me the most important lessons.

Acknowledgments

I would first like to thank my advisor Hong Liu for being a source not only of scholarly knowledge and guidance, but also of infectious enthusiasm and excitement, and in general for being a spectacular mentor in every way.

I thank all the people at the Center for Theoretical Physics who made it such a delightful place to work. In particular, thank you to my friends Thomas Faulkner, Vijay Kumar, and David Guarrera for many good times, both inside and outside CTP. Thank you also to my fellow students David Vegh, Mark Mezei, Mindaugas Leckaveckas, Ethan Dyer, and Koushik Balasubramanian. A very special thank you goes to my wonderful friend Christiana Athanasiou, who somehow made the day-to-day grind of theoretical physics into something that was not merely fun, but usually absolutely hilarious.

I thank John McGreevy for many physics discussions that were always as entertaining as they were illuminating, and I thank Sean Hartnoll and Harvey Meyer, for collaboration from which I learned much.

I thank my other friends Danial Lashkari, Shamim Nemati, Hila Hashemi, Evan Graham, Dionysios Anninos, and Parthi Santhanam, who are entirely responsible for making the past five years in Cambridge as much fun as they were. Thank you also to Palak Amin, for her laughter, her smile, and her encouragement while this document was being prepared.

Finally, I would like to thank my family. Thank you to Yeshim Iqbal, for being a sister I am proud to be related to, and thank you to Ammu and Abbu, for more than I can ever say.

Contents

List of Figures

Chapter 1

Introduction

1.1 The problem of interactions

Our current most precise understanding of the universe is in terms of quantum field theory. Traditionally, we organize our understanding of quantum field theory in terms of particle excitations. Let us consider the simplest example, defined by the Lagrangian:

$$\mathcal{L} = \int d^4x \left[\frac{1}{2}(\nabla\phi)^2 + \frac{1}{2}m^2\phi^2\right] \tag{1.1}$$

This system contains free particles of mass m, who stream past each other without interaction. Not much happens in this system, but this is precisely what makes it the traditional starting point for an understanding of quantum field theory.

Nevertheless, this is currently a bad caricature of reality, and so in an attempt to capture more interesting physics we add an interaction term that allows these particles to scatter:

$$\mathcal{L}_I = \int d^4x \frac{\lambda}{4!}\phi^4, \tag{1.2}$$

and now life is made far more interesting by the fact that the theory is no longer soluble. We are forced to resort to approximation, perturbation expansions in λ and the computation of Feynman diagrams. The resulting structure of perturbative quantum field theory is wildly successful, and is indeed the framework on which our current understanding of physical reality is built. Yet even within the simple example of $\lambda\phi^4$ theory one can easily be frustrated by the fact that our starting point – free particles – is necessarily built around the thoroughly unphysical assumption that the constituent particles do not talk to each other. Consider, for example, heating this theory up to a finite temperature. We are now considering a plasma of interacting ϕ particles, and general principles (i.e. essentially common sense) tell us that on long distances the system should be governed by the rules of hydrodynamics: disturbances should dissipate into the plasma, and one should be able to understand the emergence of hydrodynamics and compute the quantities characterizing the dissipation, such as viscosities.

Yet the computation of the viscosity of the $\lambda\phi^4$ plasma from the Lagrangian (1.2) is

rather nontrivial, requiring the summation of an infinite tower of Feynman diagrams that capture the many ways in which thermally excited ϕ particles scatter off of each other (for example, see [1]). This difficulty is perhaps not entirely unexpected; a viscosity is something whose very existence requires interactions and is rather ill-defined in the free-field limit, yet our current formalism for calculation is based around a starting point in which interactions do not even exist.

1.1.1 A foray into real life

This problem is of course not at all academic. There are many systems in real life whose dynamics is governed by strong interactions and in which the questions of interest depend critically on the nature of these interactions, thus resisting a conventional field-theoretical treatment. I mention here only two of the most famous examples.

Consider for example quantum chromodynamics, the theory of quarks and gluons. The microscopic action describing this theory takes a very simple form

$$S = \int d^4x \left(-\frac{1}{4g^2} F^2 + \sum_i \bar{\psi}_i (\not{D} - m) \psi_i \right), \tag{1.3}$$

where F is the field strength for an the $SU(3)$ gauge field that represents the gluons and each ψ_i represents the field for a light quark that is charged in the fundamental under this gauge field. Staring at this Lagrangian it is clear that its fundamental degrees of freedom – massless gluons and almost massless quarks – look nothing like the heavy particles, protons, neutrons, that make up the universe we see. Famously, the gauge coupling of this theory runs with energy [2]; even though at high energies the theory defined by (1.3) is free, at low energies the coupling becomes strong and the quarks and gluons *confine*, resulting in a spectrum of massive particles that are held together by strong interactions.

Textbook theoretical techniques starting about free quarks and gluons – the summation of Feynman diagrams – are clearly not very useful in understanding confinement; nevertheless tremendous progress has been achieved via direct simulation of the path integral on a discrete lattice using a computer. One might even argue that the confined phase represents a gapped state of matter whose low-energy excitations – the hadrons – are understood, at least qualitatively.

However, there are other phases of QCD. Consider heating up the theory – one expects that at temperatures higher than the confinement scale, hadrons will dissociate and quarks and gluons will again be the fundamental degrees of freedom. This is precisely what happens at the Relativistic Heavy Ion Collider, where gold nuclei are smashed together at energies sufficient to rip apart their hadronic pieces into the quarks and gluons from whence they came. Due to the high multiplicities and energies involved, the resulting soup of strongly interacting quarks and gluons may be thought of as QCD at a *finite temperature*. Remarkably, this appears to form a completely new *liquid* phase of matter – the quark-gluon plasma – whose properties are tremendously mysterious from a weakly coupled point of view.

We present here only one piece of experimental evidence illustrating this fact. The

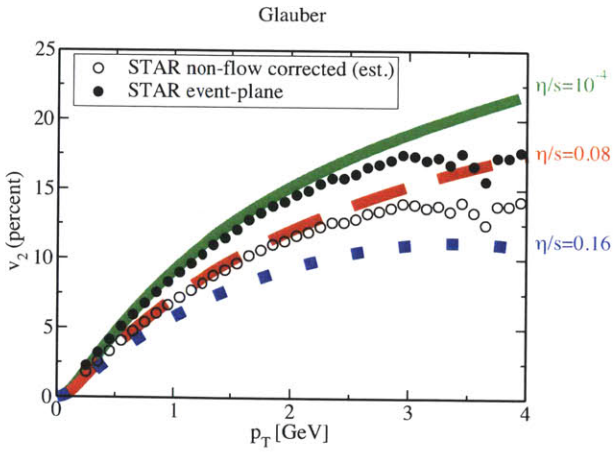

Figure 1-1: Elliptic flow observable v_2 versus transverse momentum p_T observed in heavy ion collisions, together with theoretical predictions from ideal hydrodynamics. Taken from [3].

data shown in Figure 1-1 displays the elliptic flow observable v_2 in heavy ion collisions. We will not develop the concept of the elliptic flow here, as it will play absolutely no role in any of our further discussion: what *is* important, even for us, is that the different dashed lines on the plot display theoretical calculations performed in the context of ideal hydrodynamics. Hydrodynamics is meant to be a valid description on scales much longer than the mean free path of the constituents of the system; the agreement between these theoretical calculations and the experimental result actually indicates that the system must have a small mean free path – and thus be very strongly interacting – indeed.

We can obtain a semi-quantitative measure of precisely how strong these interactions are by examining the value of $\frac{\eta}{s}$, the dimensionless ratio of the shear viscosity to entropy density. Consider this ratio first for a weakly coupled theory such as the $\lambda\phi^4$ theory mentioned above. Elementary arguments (see e.g. [1] or [4]) show that in perturbation theory we have $\frac{\eta}{s} \sim \frac{1}{\lambda^2}$, i.e. it *diverges* as the coupling is taken to 0. For the quark-gluon plasma the precise value obtained depends on details of the hydrodynamic models used; however we do see from Figure 1-1 that the fit to hydrodynamic calculations requires a *very small* $\frac{\eta}{s}$, on the order of 10^{-1}, clearly indicating that a small λ expansion is not a suitable starting point. This miniscule viscosity is thus a testament both to the remarkable properties of the quark-gluon plasma and to our lack of a theoretical framework in which to understand it.

Another famous example arises from condensed matter physics. Before turning to strongly correlated phenomena let us first understand the canonical example of a well-understood metallic state, the *Fermi liquid*. This describes weakly interacting fermions filling up a Fermi surface: excitations about the Fermi surface may be

represented by the momentum-space Lagrangian

$$S_{FL} = \int dt d^{d-2}k dk_\perp \bar{\psi}(k)(i\partial_t - k_\perp v_F)\psi(k), \tag{1.4}$$

where $k_\perp$ is a momentum vector perpendicular to the Fermi surface and k represents the other components of the momentum. The theory defined by (1.4) is quadratic, representing non-interacting fermions with a linear dispersion about the Fermi surface.

Now consider adding interactions; remarkably, the effect of Fermi statistics together with the kinematics of scattering about the Fermi surface greatly constrain the possible effects of any such (sufficiently well-behaved) interaction, essentially making it unimportant at low energies. In the language of the renormalization group, the free fixed point defined by (1.4) has almost *no* relevant perturbations[1] [7, 8]. Thus one expects the free theory to be an excellent model of electronic behavior, and indeed this is true for the vast majority of metals, making Fermi liquid theory one of the foundations on which our understanding of the structure of matter is built. One can compute any desired physical property in this weakly-coupled framework, but we mention only one here: the resistivity is quadratic in temperature, $\rho_{FL} \sim T^2$.

However, since 1986 there has been a great deal of experimental study of metallic states that do *not* fit into the Fermi liquid framework. The most well-known example is the normal phase of the high-T_c superconductors (see e.e. [6]); these are (mostly) copper-based compounds that are superconducting at low temperatures. However, when heated above their superconducting transition temperature T_c they form a novel metallic state, the "strange metal." Essentially every transport property measured of these strange metals is different from that of a Fermi liquid. We cannot resist the temptation to display one such experimental measurement in Figure 1-2; as is obvious, the resistivity of these materials is linear in temperature over a huge range of temperatures, $\rho_{strange} \sim T$, clearly demonstrating incompatibility with the free Fermi liquid picture.

Thus something must replace (1.4) as the effective theory for the *non*-Fermi liquid representing the strange metals. What is it? This is unclear, and and despite considerable progress I believe it is appropriate to say that these systems have so far resisted a unified theoretical treatment. However, even from our qualitative discussion so far, it seems clear that strong interactions are likely to play an important role, again because the free theory (1.4) is not a good starting point.

1.1.2 A new approach

It is thus fortunate, if unexpected, that recent developments in string theory have resulted in the discovery of a completely new approach to strongly correlated physics. As I will attempt to motivate in the remainder of this introduction, it turns out that certain gauge theories are actually *exactly equivalent* to theories of gravity in

[1] This is not strictly true; there are interactions that are marginally relevant connecting points on the Fermi surface and leading to various ordering phenomena, of which BCS superconductivity is one example.

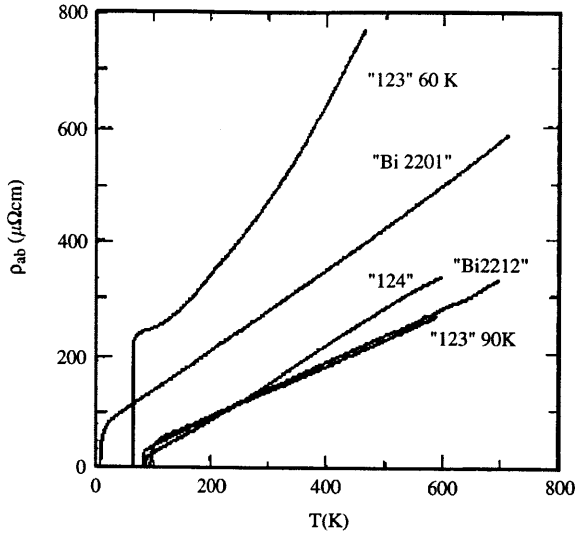

Figure 1-2: Resistivity as a function of temperature for various high-temperature superconductors. Taken from [5].

one higher dimension [9, 10, 11]. Just as a two-dimensional hologram contains the illusion of a three-dimensional image, these three-dimensional quantum field theories can contain the illusion of a four-dimensional theory of quantum gravity. This is both conceptually startling and practically useful: when the field theory is strongly coupled this illusory gravity theory is weakly coupled and classical, and indeed one can now use it to calculate field theory observables that would be otherwise utterly inaccessible. We will see that difficult problems in many-body physics are typically mapped to beautiful geometric structures on the gravity side, often resulting in new field-theoretical insights.

However, I should stress at this point that the holographic approach taken in this thesis simply does *not* apply *directly* to either of the two real life systems mentioned above. There is currently no simple gravity dual to QCD and we are even further from understanding what a true gravity dual to the cuprates would look like. The questions we will ask and answer will be in the context of models that lack many of the complications and interesting physics that the real-life examples provide. However we will argue that many of the features of the gravity models both provide a *caricature* of some of the observed features of the real-life systems. Fascinatingly, we will find both small viscosities and linear resistivities. Perhaps more importantly, we will find that this new approach will often offer a new way of organizing our thinking about strongly correlated systems, something that perturbation theory does not provide. The approach described here is only a starting point, but I will argue that it is a useful starting point, and one from which we can see many attractive pathways winding down.

1.2 Holography in a nutshell

In this section we will take an idiosyncratic route to motivating the holographic correspondence. In particular, it was mentioned above that certain problems in strongly coupled quantum field theories can be mapped to problems in classical gravity. More specifically, holographic duality relates certain *gauge* theories (whose gauge groups we will take to be $SU(N)$) to theories of gravity. When the rank of the gauge group N is taken large, the corresponding gravity theory is classical. This is actually not unexpected, as we now (very briefly) review:

1.2.1 Large N is classical

We will forget completely about gravity for a moment and think only about gauge theory with gauge group $SU(N)$, where we consider N large. Consider gauge-invariant operators made from the gluon fields $\mathcal{O}_i$, where we normalize them so that they have a well-defined large-N limit, i.e. $\mathcal{O}_i \sim N^0$. By a simple counting of powers of N that we do not review here (see e.g. [12]), it is easy to show that the connected correlator of m of these operators satisfies

$$\langle \mathcal{O}_1 \mathcal{O}_2 ... \mathcal{O}_m \rangle_C \sim N^{2-2m}. \tag{1.5}$$

Now let us use this to compute the variance of one of these operators:

$$\langle (\mathcal{O} - \langle \mathcal{O} \rangle)^2 \rangle = \langle \mathcal{O}\mathcal{O} \rangle_C \sim N^{-2} \tag{1.6}$$

Thus it appears that in the large-N limit, all operators are arbitrarily sharply peaked about their expectation values. This is the very definition of what it means to be "classical"; we conclude that regardless of the strength of the Yang-Mills coupling g_{YM}, a new classical limit emerges when $N \to \infty$. There is a useful analogy due to [12]; in the standard classical limit, as $\hbar \to 0$ we find that the functional integral of quantum mechanics is concentrated on just one field configuration, the usual classical solution. All observables are arbitrarily sharply peaked about their values on this classical solution, and once we find this classical solution by solving the equations of motion we can build a useful semi-classical approximation (if we so desire). It appears that as $N \to \infty$ something similar is happening in gauge theory: there should be some "gauge field configuration" that dominates some sort of functional integral, but we do not know what it is, nor do we have an algorithm for finding it.

Historically, this solution is called the "master field" and for many years its identity was a missing ingredient in our understanding of large-N gauge theory. Let us speculate briefly about what equations it might satisfy; they should be classical equations, but they should contain the information of essentially infinitely many degrees of freedom per four-dimensional spacetime point, as $N = \infty$. How might such information be organized?

1.2.2 The degrees of freedom of gravity

Let us now keep these thoughts in mind and turn to what appears to be a completely different question: in a theory of gravity and matter, how are the degrees of freedom encoded in space? This question can be answered at several levels. Let us begin at the most elementary level: if the gravitational coupling G_N is taken to be small, it is probably sensible to think of a theory of gravity and matter as an ordinary quantum field theory about a fixed background. Taking the theory to be massless for simplicity, we find that if we consider a region with volume V and energy E, its entropy scales like

$$S \sim Va, \tag{1.7}$$

where a depends on the energy density $\rho = \frac{E}{V}$ which does not scale with the volume. This is a standard and familiar result.

Let us now consider what happens when the gravitational coupling G_N is turned on. One of the great results of classical general relativity tells us that something very interesting now happens if we imagine making V small while holding E constant. Eventually the linear size characterizing V will be smaller than the Schwarzschild radius $r_s(E)$ appropriate to the energy E,

$$r_s(E) = \frac{2G_N E}{c^4} \tag{1.8}$$

and our system will collapse into a black hole. This system is very different from the one we started with, and one of the great results of *semi*-classical general relativity tells us that the counting of the entropy should now be done differently. The answer – the Bekenstein-Hawking entropy – turns out to be independent of the details of the theory, and is

$$S = \frac{A}{4G_N}\frac{c^3}{\hbar}, \tag{1.9}$$

where here A is the *area* of – not the volume within – the event horizon of the resulting black hole. This is completely contrary to any intuition we have from local quantum field theory, and we are reluctantly led to conclude that at high energies, the degrees of freedom are *not stored in a simple local way* in the spacetime. In fact, one is now tempted to say that in some deeper sense, a theory of gravity behaves like it has one less dimension than one might expect.

1.2.3 The punch line

On the one side, in large N four-dimensional gauge theory, we seek equations defining a "classical limit" that somehow contains infinitely more degrees of freedom than any standard theory. On the other hand, in classical gravity in five dimensions, we see that somehow the counting of gravitational degrees of freedom tells us that it is begging to be described as a conventional (i.e. non-gravitational) theory in *four* dimensions.

The punch line is clear:

The classical limit of $N \to \infty$ gauge theories is related to classical gravity in one higher dimension.

This is a preposterous statement, and of course we would not be making it if there were not a great deal of evidence that it were true. But what happens if N is no longer strictly infinite? One expects that configurations other than the master field will contribute on the gauge theory side–the theory is becoming "semi-classical", in that fluctuations about the master field will contribute. On the gravitational side, these fluctuations can be precisely mapped to traditional *quantum* fluctuations about a bulk gravitational spacetime. Presumably if we had a way (e.g. string theory) to sum up these quantum fluctuations, we would reconstruct the finite N gauge theory. In other words,

Certain finite N gauge theories are exactly equivalent to quantum gravity in one higher dimension.

This is the statement of the holographic correspondence. There are by now many explicit examples of the duality arising from string theory. The most well-studied example is that between maximally supersymmetric Yang-Mills theory with gauge group $SU(N)$ in four dimensions and quantum gravity (i.e. Type IIB string theory) on the product of a five-dimensional manifold called Anti-de Sitter space, or AdS_5 with a 5-sphere S^5. Maldacena was originally led to his celebrated conjecture about the equality of these two theories via a beautiful set of string-theoretical arguments [9] that we will not review here, but which lead to a precise mapping between the parameters of the two theories:

$$\frac{\lambda}{N^2} = g_s \qquad \left(\frac{R}{l_s}\right)^4 = 4\pi\lambda \tag{1.10}$$

Here λ is the Yang-Mills t'Hooft coupling $\lambda = g_{YM}^2 N$, R is the curvature radius of the bulk spacetime, l_s the string length, and g_s the string coupling. Notice that when N is large the string coupling, which controls bulk quantum gravitational effects, is small; thus, as claimed above, quantum effects in the bulk are $1/N^2$ effects in the gauge theory. Notice also that when λ is large the curvature of the gravitational description is small; thus we see the remarkable fact that

The classical gravitational description is good precisely when the gauge theory is strongly coupled.

This is the power of the duality, allowing us to solve strongly coupled quantum field theories using classical gravity.

1.3 Summary and contents of thesis

We pause now to briefly summarize what we have learned: large N gauge theories have a novel sort of classical limit that can be seen when the rank of the gauge group N is taken to be very large. For some of these theories, the classical limit thus

obtained turns out to be the usual classical limit of Einstein gravity, in one extra dimension.

In this simplest examples, the theory is defined on Anti de-Sitter space, whose metric takes the form

$$ds^2 = R^2 \frac{\eta_{\mu\nu} dx^\mu dx^\nu + dz^2}{z^2}. \tag{1.11}$$

We will take the viewpoint that this metric is in many ways the strongly coupled analog of the free field Lagrangian (1.1) that we started with; classical gravity about this background provides us a solvable system that is a holographic description of a strongly-coupled field theory. Just as we add terms such as (1.2) to (1.1) to obtain interesting physics, we will find various ways to mutilate (1.11) to describe physical phenomena of interest.

In the remainder of this section we briefly summarize the work that is done in this thesis. In Chapter 2 we provide a brief introduction to the the technology involved in performing calculations in holography, with a particular focus on real-time observables and applications to spinor fields [15]. In Chapter 3 we discuss hydrodynamics in the context of holography; placing the field theory at a finite temperature is dual to creating a black hole in the gravitational description. Thus one expects on general grounds that at long distances all such black holes should display hydrodynamic behavior, and indeed it has been known for many years that the horizon of a black hole behaves in many ways like a fluid. This is called the *membrane paradigm* of classical black hole mechanics [13], and holography may be thought of as a way to understand *why* it is true. We develop in detail the connection between the membrane paradigm and holography [14], and along the way we build a convenient formalism for computing real-time linear response on such backgrounds.

In Chapter 4 we turn our attention to charged black holes. A charged black hole at zero temperature contains an AdS_2 factor which drives a great deal of interesting low-energy physics. Previous work [16, 17, 18] has shown that fermionic perturbations of charged black hole reveal the existence of Fermi seas: these Fermi seas are not the weakly coupled Fermi liquids that can be found in solid-state physics textbooks, but rather display anomalous non-Fermi-liquid behavior that is of considerable physical interest, particularly in the context of the strange metals discussed above. In Chapter 5 we review these developments from the viewpoint of [19] to show how such non-Fermi liquid behavior arises from the near-horizon AdS_2 factor of the charged black hole. At some points in parameter space these non-Fermi liquids display properties somewhat similar to the electronic excitations of the real-life strange metals.

In Chapter 6 we compute the contribution to the resistivity arising from these holographic non-Fermi liquids [20]. As these fermions are a small ($O(1)$) part of a much larger ($O(N^2)$) system, to see their contribution to the conductivity we must calculate a $1/N^2$ correction; as described above, this involves calculating a quantum effect on the gravitational side, and we develop a considerable amount of technology to extract this effect. At the appropriate point in parameter space we find a resistivity that is linear in temperature, again one of the signatures of strange metallic behavior.

In Chapter 7 we discuss models of spontaneous symmetry breaking in holography; we realize ordered phases that break non-Abelian symmetries, with an eye to mod-

eling magnetism in strongly coupled systems [21]. The phase transition between the ordered and disordered phase can be driven to zero temperature by tuning couplings in the gravitational Lagrangian, and the resulting quantum phase transition is of the Berezinskii-Kosterlitz-Thouless type [22]. We explore the details of this transition and also demonstrate the existence of the expected Goldstone modes in the ordered phase of this model. In Chapter 8 we discuss the critical behavior at this quantum critical point, revealing novel behavior that we attempt to interpret.

A very brief concluding chapter provides some outlook. There are also two appendices: Appendix A discusses some exactly solvable spinor examples to illustrate the technology developed earlier, and Appendix B provides a pedagogical discussion of the Breitenlohner-Freedman bound, which plays an essential role in the quantum critical points discussed above.

Chapter 2

Calculations in AdS/CFT: a primer

2.1 Background

In this section we present a very brief review of the aspects of gauge/gravity duality that will be required for our discussion. Far more detailed expositions on AdS/CFT are available[1] The reader who is already familiar with the basic ideas of holography is encouraged to skip this chapter, and the reader who only wants to compute things can probably skip to the results (2.9) and (2.10).

As discussed above, holography (or gauge/gravity duality, or AdS/CFT) is the surprising statement that certain quantum field theories can be exactly equivalent to theories of quantum gravity that live in one extra dimension. This idea is obviously conceptually startling. However, recently an increasing amount of research has focused not on its philosophical implications but rather on its practical utility, which stems from the fact that it is a strong/weak duality: generally when the field theoretical side is strongly correlated, the gravitational description is weakly coupled and tractable. This suggests that complicated questions in strongly interacting many-body physics can be mapped to simple problems in classical gravity, i.e. to *geometry.*

We now present some details of the duality. In the most well-studied examples of the correspondence, gravity (and associated matter fields) propagating on a weakly curved Anti-de Sitter spacetime in $d+1$ dimensions (AdS_{d+1}) is mapped to a strongly coupled conformally invariant quantum field theory that lives in d dimensions (CFT_d). The relevant gravitational action now takes the form

$$S = \frac{1}{2\kappa^2}\int d^{d+1}x\,\sqrt{-g}\left(\mathcal{R} + \frac{d(d-1)}{R^2}\right) \tag{2.1}$$

Here R is the AdS radius, and is large (in appropriate units) when the dual field theory

[1]Here we summarize a few: the canonical early review is [23]. [24] focuses on supersymmetric aspects in $\mathcal{N} = 4$. The recent lectures [25] focus more on the physical conclusions that one can draw. [26] and [27] are an excellent introduction to the applications to many-body physics that are the focus of this thesis. [28] can be viewed as an introduction to heavy-ion physics and AdS/CFT both.

is strongly coupled. The simplest solution satisfying the field equations arising from (2.1) is pure Anti-de Sitter space, which takes the form

$$ds^2 = R^2 \left(\frac{dz^2 + \eta_{\mu\nu} dx^\mu dx^\nu}{z^2} \right) \tag{2.2}$$

Here the x^μ run over the coordinates of the field theory, and z is the extra "holographic" coordinate in the gravitational description. As the simplest and most symmetric solution on the gravitational side this geometry represents the *vacuum* of the dual field theory. Indeed, the vacuum of the CFT should be invariant under the conformal group in d-dimensions, which is precisely the same as the isometry group of AdS_{d+1}. We draw special attention to the following isometry:

$$z \to \lambda z \qquad x^\mu \to \lambda x^\mu \tag{2.3}$$

This is the isometry representing *scaling*; we see that as we scale the energy we must scale the holographic coordinate z as well. This is indicative of the fact that the holographic coordinate represents the "energy scale" at which we consider the theory in some way, with the UV at $z \to 0$ and the IR at $z \to \infty$. Thus the bulk *geometrizes the RG flow* of the field theory: we will make this more precise as we go along.

We would now like to study excitations about this state. Thus consider perturbing the CFT by a scalar operator $\mathcal{O}$, say by adding to the CFT Lagrangian a source term

$$\delta S_{CFT} = \int d^{d+1}x J(x)\mathcal{O}(x). \tag{2.4}$$

How do we study this on the gravity side? It turns out that for each (conformally primary) scalar operator $\mathcal{O}$ we have a scalar field ϕ in the bulk with mass m. In the simplest case the action is

$$S_\phi = -\frac{1}{2} \int d^{d+1}x \sqrt{-g} \left((\nabla\phi)^2 + m^2\phi^2 \right) \tag{2.5}$$

Now we note an important aspect of the spacetime (2.2); at $z = 0$ the spacetime contains a timelike boundary, on which we must prescribe boundary data to fully specify the evolution of bulk fields fluctuating on the geometry. By studying the equations of motion arising from the action above one can show that near the boundary a solution to the scalar wave equation has the expansion

$$\phi(z \to 0, x^\mu) \sim A(x) z^{\Delta_-} + B(x) z^{\Delta_+} \tag{2.6}$$

where the two exponents satisfy

$$\Delta_\pm = \frac{d}{2} \pm \nu_U \qquad \nu_U = \sqrt{\frac{d^2}{4} + m^2 R^2}. \tag{2.7}$$

As it turns out, Δ_+ is precisely the conformal dimension of the dual operator $\mathcal{O}$. We now state a relation that can be considered one of the fundamental identities of

AdS/CFT: the partition functions of the two sides of the duality are equal, and the CFT deformation (2.4) is represented on the gravity side by a boundary condition on the field $\phi(z, x^\mu)$ at the boundary, i.e: $A(x) = J(x)$. In equations we have

$$\left\langle \exp\left(\int d^{d+1}x J(x)\mathcal{O}(x)\right)\right\rangle_{CFT} = \exp\left(-S_{\text{grav}}\right)\Big|_{A(x)=J(x)}, \tag{2.8}$$

where on the right hand side we have replaced the quantum gravity partition function by its semi-classical limit: S_{grav} should be considered the on-shell action subject to the boundary condition $A(x) = J(x)$.

Note however that for a scalar field the bulk equations of motion are second order and thus the single boundary condition $A(x) = J(x)$ is not sufficient to completely specify the bulk solution. In general we will find an extra condition from the interior of the spacetime. One always finds that by demanding that the solution be *regular* everywhere in the interior in some way it is uniquely specified: this will fix the coefficient $B(x)$ in terms of $A(x)$. We now state (without derivation) the key results needed to use (2.8) to perform computations in the field theory:

1. By taking functional derivatives of a (carefully regulated) version of (2.8) one can show that the expectation value of the operator $\mathcal{O}(x)$ is

$$\langle \mathcal{O}(x)\rangle = 2\nu_U B(x). \tag{2.9}$$

   For example, if one finds a regular solution where $A = 0$ but $B \neq 0$, this implies that the operator $\mathcal{O}$ has spontaneously developed an expectation value, even in the absence of a source. Note that by studying the transformation of B under the scaling isometry (2.3) we can confirm the claim that the conformal dimension of $\mathcal{O}$ is Δ_+.

2. Relatedly, various two-point functions $\langle \mathcal{O}\mathcal{O}\rangle$ are related to the ratio $\frac{B}{A}$. In this work we will primarily be interested in the Lorentzian retarded Green's function $G_R(\omega, k)$; to find this, we should require that the the finite-frequency solution in the bulk be *infalling* at a horizon that will generically develop in the interior. This is the meaning of "regular" for a Lorentzian spacetime. The retarded correlator is then given by [42]

$$G_R(\omega, k) = 2\nu_U \frac{B(\omega, k)}{A(\omega, k)} \tag{2.10}$$

At a practical level, these two AdS/CFT results (and their generalizations to spinor fields) are all that we will need to perform computations in the rest of this thesis. We will justify these later in this chapter: for massless fields these relations are essentially equivalent to (2.24) and its analytic continuation, and the case of massive fields is treated in Appendix 2.B to this chapter. Note that while the factors of $2\nu_U$ in (2.9) and (2.10) can be important [63], we will generally omit them and be somewhat cavalier about overall prefactors in the rest of the text.

2.2 Real-time response

We now discuss in more detail the procedure for calculation of real-time response in AdS/CFT. A simple prescription for calculating retarded two-point functions in AdS/CFT was first proposed by Son and Starinets some years ago in [42]. This prescription, which was justified in different ways in the literature (see e.g. [43, 29, 66, 30, 31]), has been instrumental in extracting many important insights into strongly interacting many-body systems from AdS/CFT.

Here we review work in [14], where it was observed that the prescription of [42] could be reformulated in terms of boundary values of the canonical momenta of bulk fields by treating the AdS radial direction as "time". This reformulation has both conceptual and practical advantages; it expresses real-time response in terms of objects with intrinsic physical and geometric meaning. In this chapter we discuss this prescripstion and show that it follows simply from an analytic continuation of the original Euclidean formulation of AdS/CFT[2].

We then show that our formalism may be extended to spinors, which involve interesting subtleties as we are now dealing with a first order system. We work out an explicit prescription for calculating real-time retarded correlators of fermionic operators, which is important, e.g., for probing quasi-particle structure associated with Fermi surfaces from gravity [17, 16].

The plan of the next few sections is as follows. In section 2.2 we state and derive our reformulation of the real-time prescription for retarded Green's functions in AdS/CFT. In section 2.3 we work out in detail the application of this prescription to spinor fields in an asymptotic AdS spacetime. We conclude in section 2.4 with a brief summary. In Appendix 2.A to this chapter, we state our conventions for various Euclidean and retarded Green's functions, while Appendices 2.B and 2.C contain some technical details related to the main text. Finally, in Appendix A to this thesis we further illustrate the prescription using two exactly solvable examples: pure AdS and BTZ black hole.

We begin by first stating and then deriving our formulation of the real-time prescription for retarded Green's functions in AdS/CFT. For illustration, we consider a scalar operator $\mathcal{O}$ which is dual to a massless bulk scalar field ϕ. Massive modes contain extra divergences; while harmless, these complicate the discussion and are discussed in Appendix 2.B. The generalization to tensors is self-evident, and the generalization to spinors is discussed in detail in the next section.

To be specific, we will consider a scalar action

$$S = -\frac{1}{2}\int d^{d+1}x\,\sqrt{-g}\,(\partial\phi)^2 + \cdots \tag{2.11}$$

on a background spacetime metric of the form

$$ds^2 = -g_{tt}dt^2 + g_{rr}dr^2 + g_{ii}d\vec{x}^2 \equiv g_{rr}dr^2 + g_{\mu\nu}dx^\mu dx^\nu\ . \tag{2.12}$$

[2] A similar procedure was used in [66] to justify the prescription of [42]

The boundary is taken at $r = \infty$, where various components of the metric have the asymptotic behavior of AdS with unit radius,

$$g_{tt}, g^{rr}, g_{ii} \approx r^2, \qquad r \to \infty \ . \tag{2.13}$$

We will assume that the above metric has a horizon of some sort (to be more explicit below) in the interior.[3]

We also assume that the theory is translationally invariant in x^μ directions (i.e, all metric components depend on r only), and work in momentum space along these directions, e.g.

$$\phi(r, x^\mu) = \phi(r, k_\mu)\, e^{-i\omega t + i\vec{k}\cdot\vec{x}}, \qquad k_\mu = (-\omega, \vec{k}) \ . \tag{2.14}$$

We will frequently need to analytically continue to Euclidean signature via

$$t \to -i\tau, \qquad \omega \to i\omega_E, \qquad iS \to -S_E \tag{2.15}$$

where the Euclidean action S_E is given by

$$S_E = \frac{1}{2}\int d^{d+1}x\, \sqrt{g}\, (\partial\phi)^2 + \cdots \ . \tag{2.16}$$

2.2.1 Prescription

We begin by simply stating the prescription of [14] for computing the retarded correlator $G_R(k_\mu)$ for $\mathcal{O}$. In momentum space this reads:[4]

$$G_R(k_\mu) = \left(\lim_{r\to\infty} \frac{\Pi(r; k_\mu)|_{\phi_R}}{\phi_R(r, k_\mu)} \right)\Bigg|_{\phi_0=0} \tag{2.17}$$

where Π is the canonical momentum conjugate to ϕ with respect to a foliation in the r-direction. $\phi_R(r, k_\mu)$ is the solution to the equations of motion for ϕ which is in-falling at the horizon and satisfies the boundary condition $\lim_{r\to\infty} \phi_R(r, k_\mu) \to \phi_0(k_\mu)$. The notation $\Pi(r; k_\mu)|_{\phi_R}$ in equation (2.17) indicates that Π should be evaluated on the solution ϕ_R. Finally, the subscript $\phi_0 = 0$ means that in evaluating this ratio one should only take the part that is independent of ϕ_0; in an interacting bulk theory Π and ϕ_R will typically contain higher powers of ϕ_0 which are not relevant for two-point functions.

[3] In a spacetime which does not have a horizon (e.g. global AdS), i.e. completely regular in the interior, ϕ has a discrete spectrum. The corresponding boundary theory retarded function for $\mathcal{O}$ can then be written as a discrete sum of delta functions and thus does not have an interesting analytic structure.

[4] The reason we have (2.17) instead of $G_R(k_\mu) = \left(\lim_{r\to\infty} \frac{\delta\Pi|_{\phi_R}}{\delta\phi_0}\right)\Big|_{\phi_0=0}$ is due to subtleties in taking the limit $r \to \infty$. An example is the massive scalar case discussed in Appendix 2.B. Also, we found in [14] that the fact that all quantities in (2.17) remain meaningful in the bulk at arbitrary radius is helpful for a physical interpretation of this formula.

Note that (2.17) can also be equivalently (in fact more generally) written as

$$\langle \mathcal{O}(k_\mu) \rangle_{\phi_0} = \lim_{r\to\infty} \Pi(r; k_\mu)|_{\phi_R} \tag{2.18}$$

where $\langle \mathcal{O}(k_\mu) \rangle_{\phi_0}$ denotes the response of the system to external perturbations generated by adding $\int d^d x\, \phi_0(x)\mathcal{O}(x)$ to the boundary theory action. Equation (2.17) is the linearized limit of (2.18).[5]

An alert reader will immediately recognize that (2.18) is the exact Lorentzian analog of the standard prescription for boundary correlation functions in Euclidean signature as formulated in [10, 72]. Indeed we will now show that (2.17) and (2.18) (at the linearized level) can be derived from the original prescription of [10, 72] using a simple analytic continuation, even though they do not appear to follow directly from an action principle themselves.

2.2.2 Analytic continuation

First recall that a retarded correlator is analytic in the upper half complex-ω plane, and that the value of $G_R(\omega, \vec{k})$ along the upper imaginary ω-axis gives us the Euclidean correlator G_E, i.e.[6],

$$G_E(\omega_E, \vec{k}) = G_R(i\omega_E, \vec{k}) \qquad \omega_E > 0\ . \tag{2.19}$$

This expression applies both for finite and zero temperature, and both for bosonic and fermionic operators, with ω_E only taking discrete values at finite temperature. Equation (2.19) can now be inverted to obtain $G_R(\omega, \vec{k})$ as

$$G_R(\omega, \vec{k}) = G_E(\omega_E, \vec{k})\Big|_{\omega_E = -i(\omega + i\epsilon)}\ . \tag{2.20}$$

Note that at finite temperature ω_E only takes discrete values, and so the analytic continuation can be tricky. We will simply ignore this issue below, assuming that G_R is sufficiently well-behaved that such an analytic continuation is possible.

We now look at the central prescription of AdS/CFT in Euclidean signature [10, 72] (for both zero and finite temperature)

$$\left\langle \exp\left[\int d^d x\ \phi_0(x)\mathcal{O}(x)\right]\right\rangle_{\text{QFT}} = e^{-S_{\text{grav}}[\phi_0]} \tag{2.21}$$

[5] To see this more explicitly, it is helpful to recall the standard result from linear response theory that if one considers a system in equilibrium at $t \to -\infty$ and then perturbs its action with the term $\int d^d x\, \phi_0(x)\mathcal{O}(x)$, the one-point function of $\mathcal{O}$ in the presence of the source is given (to first order in ϕ_0) by

$$\langle \mathcal{O}(k_\mu) \rangle_{\phi_0} = G_R(k_\mu)\phi_0(k_\mu),$$

where G_R is the retarded correlator of $\mathcal{O}$.

[6] $G_E(\omega_E)$ for $\omega_E < 0$ is obtained from the advanced function. See Appendix 2.A for our conventions on the definitions of Euclidean and retarded functions.

where $S_{\rm grav}[\phi_0]$ is the bulk action for ϕ (which may include necessary boundary terms) evaluated at the classical Euclidean solution ϕ_E which is regular in the interior and satisfies boundary condition $\lim_{r\to\infty}\phi_E(r;x)\to\phi_0(x)$. From (2.21), one finds that one point function of $\mathcal{O}$ in the presence of the source ϕ_0 can be written as

$$\langle\mathcal{O}(x)\rangle_{\phi_0}=-\frac{\delta S_{\rm grav}}{\delta\phi_0(x)}=-\lim_{r\to\infty}\Pi_E(r,x)|_{\phi_E} \tag{2.22}$$

and its Fourier transform

$$\langle\mathcal{O}(\omega_E,\vec{k})\rangle_{\phi_0}=-\lim_{r\to\infty}\Pi_E(r,\omega_E,\vec{k})|_{\phi_E}\ . \tag{2.23}$$

In (2.22), Π_E is the canonical momentum for ϕ in Euclidean signature and should be evaluated at the classical solution ϕ_E. The second equality of (2.22) follows from the well known fact in classical mechanics that the derivative of an on-shell action with respect to the boundary value of a field is simply equal to the canonical momentum conjugate to the field, evaluated at the boundary. Note that in general the limit $r\to\infty$ in (2.23) is non-trivial and requires careful renormalization, which was developed systematically in [32, 33]. Similar cautionary remarks apply to other formulas below (in both Lorentzian and Euclidean signature).

At linear level in ϕ_0, one then finds that

$$G_E(\omega_E,\vec{k})=-\left(\lim_{r\to\infty}\frac{\Pi_E(r,\omega_E,\vec{k})|_{\phi_E}}{\phi_E(r,\omega_E,\vec{k})}\right)\Bigg|_{\phi_0=0} \tag{2.24}$$

In Euclidean signature, the above procedure is unambiguous as ϕ_E is unique (at least for sufficiently small ϕ_0); there will be only one solution that both satisfies the boundary conditions at infinity and is regular in the interior. This is not the case in Lorentzian signature, where in the interior one typically finds two oscillatory solutions, both of which are regular.

Once $G_E(\omega_E,\vec{k})$ is obtained, one can of course obtain G_R using (2.20). Here, we would like to argue that one can in fact obtain an intrinsic prescription for retarded functions by analytically continuing $\phi_E(r,\omega_E,\vec{k})$ directly in the bulk to Lorentzian signature[7]. More explicitly, introducing

$$\phi_R(\omega,\vec{k})=\phi_E(\omega_E,\vec{k})\Big|_{\omega_E=-i(\omega+i\epsilon)} \tag{2.25}$$

[7]A similar analytic continuation has been used earlier in [66] to justify the prescription of [42].

and then from (2.20) and (2.24), we obtain simply[8]

$$G_R(\omega, k_\mu) = -\lim_{r\to\infty} \frac{\Pi_E(r,\omega_E,\vec{k})|_{\phi_E}}{\phi_E(r,\omega_E,\vec{k})}\bigg|_{\omega_E=-i(\omega+i\epsilon)} = \lim_{r\to\infty} \frac{\Pi(r;\omega,\vec{k})|_{\phi_R}}{\phi_R(r,\omega,\vec{k})}, \tag{2.26}$$

which gives (2.17). Similarly, (2.23) becomes (2.18) under the same analytic continuation. To complete the derivation we still need to show that ϕ_R obtained in (2.25) satisfies the boundary conditions at the horizon and infinity as stated below (2.17). Since analytic continuation does not change the boundary conditions at infinity, we need only show that the function on the right-hand side of (2.25) satisfies the in-falling condition at the horizon. We do this explicitly by examining the behavior of ϕ_E near different types of horizons[9]:

- *Non-degenerate horizon*: consider a Euclidean black hole background of the form

$$ds^2 = f(r)d\tau^2 + \frac{1}{f(r)}dr^2 + a(r)^2 d\vec{x}^2 \tag{2.27}$$

where $f(r)$ has a simple zero at $r = r_0$, i.e. $f(r) \sim \frac{4\pi}{\beta}(r-r_0)$ and τ is periodic in β. From the wave equation of ϕ, one finds the following near-horizon solutions

$$\phi_+(r) \sim (r-r_0)^{+\frac{\omega_E\beta}{4\pi}} \qquad \text{or} \qquad \phi_-(r) \sim (r-r_0)^{-\frac{\omega_E\beta}{4\pi}}. \tag{2.28}$$

When the real part of $\omega_E > 0$ (which is always the case when evaluating a retarded correlator by (2.20)), $\phi_E \sim \phi_+$ and thus we find that

$$\phi_E(\omega_E,\vec{k})\Big|_{\omega_E=-i(\omega+i\epsilon)} \sim (r-r_0)^{-\frac{i\omega\beta}{4\pi}} \tag{2.29}$$

which is precisely the behavior of an in-falling wave, since from (2.14) it leads in coordinate space to a wave of the form $e^{-i\omega t}(r-r_0)^{-\frac{i\omega\beta}{4\pi}}$.

- *Degenerate horizon:* For a degenerate horizon (e.g. of an extremal black hole), we have a metric of the form (2.27) except that f now has a double pole at $r = r_0$, i.e. $f \sim c(r-r_0)^2$, where $c > 0$. The discussion is similar to that above except that the near-horizon solution can now be shown to take the form

$$\phi_E(\omega_E,\vec{k})\Big|_{\omega_E=-i(\omega+i\epsilon)} \sim e^{\frac{i\omega}{c(r-r_0)}}, \tag{2.30}$$

again corresponding to an in-falling wave.

[8]Note the relative minus sign between the first and second equality below is due to that in Euclidean signature $\Pi_E = \sqrt{g}g^{rr}\partial_r\phi$ (see (2.16)) and in Lorentzian signature $\Pi = -\sqrt{-g}g^{rr}\partial_r\phi$ (see (2.11)) with an extra minus sign.

[9]Note that the following discussion applies to any mass, as the mass term is never important at the horizon with a nonvanishing ω.

- *Poincaré horizon*: finally let us consider a Poincaré horizon of the form (near $z \to \infty$)

$$ds^2 = \frac{1}{z^2}\left[d\tau^2 + d\vec{x}^2 + dz^2\right] \tag{2.31}$$

Then the near horizon solutions for ϕ are given by

$$\phi_\pm \sim e^{\pm kz}, \qquad k = \sqrt{\omega_E^2 + \vec{k}^2}, \qquad z \to +\infty \tag{2.32}$$

Note that if we take the branch of the square root that is positive, then the regular solution $\phi_E \sim \phi_-$. We now perform the analytic continuation $\omega_E = -i(\omega + i\epsilon)$, under which the branch of the square root with positive real part becomes

$$k = \begin{cases} -i\sqrt{\omega^2 - \vec{k}^2} & \omega > |\vec{k}| \\ i\sqrt{\omega^2 - \vec{k}^2} & \omega < -|\vec{k}| \end{cases} \tag{2.33}$$

where we have assumed a timelike momentum $|\omega| > |\vec{k}|$ (as otherwise the problem is the same as in the Euclidean case). When plugged into $\phi_- \sim e^{-kz}$, Equation (2.33) again describes an in-falling wave for both signs of ω.

The key point here is that the $+i\epsilon$ in the analytic continuation (2.20) is important; it guarantees that the solution that was regular at the horizon in Euclidean signature becomes the solution that is in-falling at the horizon in Lorentzian signature.

Note that while the Euclidean prescription (2.21)–(2.24) for computing correlation functions follow from an action principle, this is not the case for the Lorentzian prescription (2.17) and (2.18), which cannot be obtained by taking functional derivatives of the on-shell Lorentzian action. While analytic continuation of a Euclidean solution yields a Lorentzian solution as in (2.25), analytic continuation of a Euclidean on-shell *action*–which necessarily involves an integral over the full spacetime manifold–does not necessarily yield the correct Lorentzian action. The Lorentzian manifold generically differs from the Euclidean one in many crucial aspects such as the topology, the number of boundaries, etc., making the implementation and interpretation of such a procedure much more subtle. On the other hand, the analytic continuation of the canonical momentum as in our prescription requires only a *local* analytic continuation on the boundary of the manifold and is thus much simpler.

2.2.3 Vector and tensor operators

Before concluding our discussion of bosonic operators, we point out that in this formalism the tensor structure of the real-time response follows naturally without needing to decompose the system mode by mode into a series of scalar wave equations. Let us imagine first a bulk vector field A_M with Maxwell action and gauge coupling g_{eff}; this is dual to a conserved current $\mathcal{J}^\mu$, and the expression (2.18) then becomes

$$\langle \mathcal{J}^\mu \rangle = -\lim_{r\to\infty} \frac{1}{g_{\text{eff}}^2}\sqrt{-g}F^{r\mu} \tag{2.34}$$

where the expression on the right-hand side is the momentum conjugate to A_μ. Similarly, if we consider the field theory stress tensor $T^{\mu\nu}$, we find that

$$\langle T^{\mu\nu} \rangle = \lim_{r\to\infty} \frac{\sqrt{-\gamma}}{16\pi G_N} \left(K^{\mu\nu} - \gamma^{\mu\nu} K^\lambda_\lambda \right), \tag{2.35}$$

correctly captures the real-time response of the system to metric perturbations. Here $\gamma_{\mu\nu}$ and $K_{\mu\nu}$ are the induced metric and extrinsic curvature on each constant-r slice, and the expression on the right-hand side is the Brown-York stress tensor [75, 74], i.e. precisely the momentum conjugate to a gravitational perturbation $h_{\mu\nu}$. The validity of these formulas even in real-time was a key element in the results relating AdS/CFT to the membrane paradigm in [14].

2.3 Retarded correlators for fermionic operators

In this section we generalize the prescription (2.17) and (2.18) to fermionic operators. We first consider the calculation of Euclidean functions in an asymptotic AdS geometry, reviewing (and slightly generalizing) the earlier results of [76, 77, 78]. We then discuss the prescription for real-time retarded correlators. In the next section we use the prescription to calculate retarded correlation functions for fermonic operators in field theories dual to the pure AdS and BTZ geometries, where closed-form expressions can be obtained.

We consider a boundary theory fermionic operator $\mathcal{O}$ which is dual to a spinor field ψ in the bulk[10]. We will suppress all spinor indices. Since we are interested in two point functions of $\mathcal{O}$, it is enough to consider the quadratic part of the action for ψ, which can be written as

$$S = \mathcal{N} \int d^{d+1}x \sqrt{-g}\, i(\bar{\psi}\Gamma^M D_M \psi - m\bar{\psi}\psi) + S_{\rm bd} \tag{2.36}$$

where $\bar{\psi} = \psi^\dagger \Gamma^t$ and

$$D_M = \partial_M + \frac{1}{4}\omega_{abM}\Gamma^{ab}\,. \tag{2.37}$$

$S_{\rm bd}$ denotes the boundary terms required to ensure that the total action has a well defined variational principle [78] and is briefly discussed in Appendix 3.E. In (2.36)–(2.37) $M, N \cdots$ denote abstract spacetime indices and $a, b, \cdots$ denote abstract tangent space indices. Gamma matrices with a specific index (like $\Gamma^t, \Gamma^r, \Gamma^i$ as opposed to those with an abstract index Γ^M) always correspond to those in the tangent frame. The boundary theory gamma matrices will be denoted by γ^μ. The background metric is taken to be (2.12) with the associated asymptotics. We will be working in momentum space with the Fourier transform of ψ denoted by $\psi(r, k_\mu)$. Finally, the action is normalized by a factor $\mathcal{N}$; we will ignore this factor in the following, as it simply contributes an overall factor in front of all boundary theory correlators, but one can

[10]Note that in this section $\mathcal{O}$ is fermionic whereas in Section 2.2 $\mathcal{O}$ was bosonic; we apologize for the abuse of notation.

show that its sign is fixed by bulk unitarity.[11]

The analytic continuation to Euclidean signature is as in (2.15) with also

$$\gamma^t \to -i\gamma^\tau, \qquad \Gamma^t \to -i\Gamma^\tau, \qquad \bar{\psi} \to -i\bar{\psi} \tag{2.38}$$

and thus the Euclidean action following from (2.36)

$$S_E = -\int d^{d+1}x\sqrt{g}\,(\bar{\psi}\Gamma^M \mathcal{D}_M\psi - m\bar{\psi}\psi) + S_{\rm bd}\ . \tag{2.39}$$

2.3.1 Euclidean correlators

We first review how the Euclidean prescription (2.21)–(2.24) works for a spinor operator, where we now have

$$\left\langle \exp\left[\int d^dx\ (\bar{\chi}_0\mathcal{O} + \bar{\mathcal{O}}\chi_0)\right]\right\rangle_{\rm QFT} = e^{-S_{\rm grav}[\chi_0,\bar{\chi}_0]}. \tag{2.40}$$

To find the right hand side of (2.40), we need to construct a ψ_E which is regular in the interior and satisfies the boundary condition $\lim_{r\to\infty}\psi_E = \chi_0$. Attempting to interpret this equality, we realize that the situation here is a bit more subtle than for a scalar field: ψ and χ_0 are spinors of different spacetime dimensions, and thus may have a different number of components. Also, the action for ψ contains only one derivative and imposing Dirichlet boundary conditions for such a first order system requires more care. It turns out that these two issues are intimately related.

To see this, it is convenient to decompose ψ in terms of eigenvalues of Γ^r, with

$$\psi = \psi_+ + \psi_-, \qquad \psi_\pm = \Gamma_\pm\psi, \qquad \Gamma_\pm = \frac{1}{2}(1 \pm \Gamma^r) \tag{2.41}$$

where from (2.39) we find the corresponding Euclidean canonical momentum[12] $\Pi_\pm$ (in r-slicing) conjugate to $\psi_\pm$ to be

$$\Pi_+ = -\sqrt{g}g_{rr}^{-\frac{1}{2}}\bar{\psi}_-, \qquad \Pi_- = \sqrt{g}g_{rr}^{-\frac{1}{2}}\bar{\psi}_+\ . \tag{2.42}$$

Thus we see that $\psi_\pm$ are conjugate to each other. If we supplied Dirichlet boundary conditions for both of them at infinity, then it would completely fix the solution everywhere; however this is obviously incorrect, as (generically) this solution would not be regular in the interior. Instead we should *begin* by demanding regularity in

[11] To see this, consider canonically quantizing the action (2.36) by imposing the equal-time anti-commutation relation $\{\psi(x), \pi(x')\} = i\delta^{(d)}(x,x')$, where here π is the momentum conjugate to ψ with respect to *time*. We find that $\pi = -i\mathcal{N}\sqrt{-g}\psi^\dagger$. If we now require that the anticommutator $\{\psi,\psi^\dagger\}$ be *positive*–a requirement in a Hilbert space with states of positive norm–then we find that this fixes the sign of $\mathcal{N}$ to be *negative*. Reinstating this factor of $\mathcal{N}$ in front of retarded correlators found in this paper results in positive spectral densities in the boundary theory, as required by boundary unitarity.

[12] For fermions we use only the Euclidean canonical momenta, and have thus omitted the subscript E

the interior; this then leaves us with the freedom to impose boundary conditions χ_0 for either ψ_+ or ψ_-, i.e. only for half of the components of ψ.

When the boundary theory dimension d is even, we can choose the bulk Gamma matrices

$$\Gamma^\mu = \gamma^\mu, \qquad \Gamma^r = \gamma^{d+1} \tag{2.43}$$

where γ^{d+1} is the analogue of γ^5 for $d = 4$. Thus from the d-dimensional point of view, the two components $\psi_\pm$ transform like d-dimensional Weyl spinors of opposite chirality. As the boundary value of one of $\psi_\pm$, χ_0 (and so also $\mathcal{O}$) is then a d-dimensional boundary spinor of definite chirality. Thus for d even a Dirac spinor ψ in the bulk is mapped to a chiral spinor $\mathcal{O}$ on the boundary.

When d is odd, it is convenient to work with the representation

$$\Gamma^r = \begin{pmatrix} 1 & 0 \\ 0 & -1 \end{pmatrix} \qquad \Gamma^\mu = \begin{pmatrix} 0 & \gamma^\mu \\ \gamma^\mu & 0 \end{pmatrix}, \tag{2.44}$$

which can be easily seen to satisfy the $d+1$ dimensional Clifford algebra. In this basis we can see that the two components $\psi_\pm$ each transform as a d-dimensional Dirac spinor; thus for d odd χ_0 and $\mathcal{O}$ are both Dirac spinors. In all dimensions the number of components of $\mathcal{O}$ is always half of that for ψ.

To decide on which of $\psi_\pm$ to impose Dirichlet boundary conditions, we must examine their asymptotic behavior at large r, which can be worked out by solving the Dirac equation for ψ in the region $r \to \infty$ (with metric given by (2.13)). This computation is performed in more detail in Appendix A.1 and here we discuss only the asymptotic behavior of ψ, which is given by

$$\psi_+(r,k) = A(k) r^{-\frac{d}{2}+m} + B(k) r^{-\frac{d}{2}-m-1}, \qquad \psi_- = C(k) r^{-\frac{d}{2}+m-1} + D(k) r^{-\frac{d}{2}-m}, \quad r \to \infty \tag{2.45}$$

Plugging this expansion back into the Dirac equation we find the following relations between the expansion coefficients

$$D = -\frac{i\gamma\cdot k}{k^2}(2m+1)B, \qquad C = \frac{i\gamma\cdot k}{2m-1}A, \qquad \gamma\cdot k = \gamma^\mu k_\mu, \quad k^2 = k_\mu k^\mu \ . \tag{2.46}$$

Using (2.42), we see that the corresponding canonical momenta behave as

$$\Pi_+ = -\bar{C} r^{\frac{d}{2}+m-1} - \bar{D} r^{\frac{d}{2}-m}, \qquad \Pi_- = \bar{A} r^{\frac{d}{2}+m} + \bar{B} r^{\frac{d}{2}-m-1}, \qquad r \to \infty \ . \tag{2.47}$$

Note that in deriving (2.46) we have used (2.43) or (2.44) for d even or odd.

Notice that as we take $m \to -m$, we simply exchange the role of $\psi_\pm$, with $A \leftrightarrow D$ and $B \leftrightarrow C$. We can thus restrict our attention to $m \geq 0$. Among all terms in (2.45), the term with coefficient A is dominant. We thus should the impose boundary conditions

$$A = \chi_0, \quad \text{i.e.} \quad \lim_{r\to\infty} r^{\frac{d}{2}-m}\psi_+ = \chi_0 \ . \tag{2.48}$$

Now taking a derivative with respect to χ_0 on both sides of (2.40), one finds that as

in (2.22), the response of $\bar{\mathcal{O}}$ is formally given by the conjugate momentum Π_+.[13] However, for general m, as in the case of a massive scalar discussed in Appendix 2.B, one should define the boundary limit carefully. In view of the second equation in (2.48), we thus find

$$\langle \bar{\mathcal{O}} \rangle_{\chi_0} = -\lim_{r\to\infty} r^{m-\frac{d}{2}} \Pi_+, \quad \text{i.e.} \quad \langle \bar{\mathcal{O}} \rangle_{\chi_0} = \bar{D} \ . \tag{2.49}$$

Note that in obtaining the second equation above we have extracted only the finite terms in the right hand side of the first equation[14]. This appears reasonable since the other term in Π_+, which is proportional to C, is locally related to the source A.

With this boundary condition on $\psi(r \to \infty)$ specified, the solution ψ_E to the equations of motion which is regular in the interior is then uniquely determined. From this we can extract the corresponding D; we will find that D and A are related by a matrix $\mathcal{S}$,

$$D(k) = \mathcal{S}(k) A(k) \tag{2.50}$$

then the boundary Euclidean two-point correlator is given by[15]

$$G_E(k_\mu) = \mathcal{S}(k_\mu)\gamma^\tau \ . \tag{2.53}$$

Sometimes it may be easier to solve for B in (2.45), in which case introducing a matrix $\mathcal{T}$

$$B = \mathcal{T} A \tag{2.54}$$

we then have from (2.46)

$$G_E(k_\mu) = -\frac{i}{k^2}(2m+1)(\gamma\cdot k)\,\mathcal{T}\,\gamma^\tau \ . \tag{2.55}$$

To conclude this subsection, we make some further remarks:

1. Using the standard scaling argument, the identification of the source and response in (2.48) and (2.49) implies that the scaling dimension Δ of $\mathcal{O}$ is related to m by

$$\Delta = \frac{d}{2} + m \tag{2.56}$$

which is consistent with results obtained in [76] for pure AdS.

2. In the case of a massive scalar (as discussed in Appendix 2.B), the $r \to \infty$ limit

[13] See Appendix 3.E for an explicit discussion of the variation of S_{grav}.

[14] Here we are assuming that divergent terms should be removed by holographic renormalization. It might be worth checking this more explicitly.

[15] Note that from (2.40),

$$\langle \mathcal{O}(x) \rangle = \int d^d y\, G_E(x-y)\,\gamma^\tau\,\chi_0(y) \tag{2.51}$$

which in momentum space becomes

$$\langle \mathcal{O}(k) \rangle = G_E(k)\,\gamma^\tau\,\chi_0(k) \tag{2.52}$$

The γ^τ factor is due to that $G_E \sim \langle \mathcal{O}\mathcal{O}^\dagger \rangle$ rather than $\langle \mathcal{O}\bar{\mathcal{O}} \rangle$.

in the ratio $\frac{\Pi}{\phi_E}$ is somewhat subtle since subdominant terms in Π and ϕ_E also contribute which changes the overall constant. This does not appear to happen to fermions.

3. When $0 \leq m < \frac{1}{2}$, all terms in $\psi_\pm$ are normalizable. We thus can choose either A or D as the source and treat the other as the corresponding response. Note that if we choose D as the source term then

$$\Delta = \frac{d}{2} - m, \quad \rightarrow \quad \frac{d-1}{2} < \Delta < \frac{d}{2} \tag{2.57}$$

In this range the double trace operator of $\mathcal{O}$ is a relevant perturbation. The partition functions for the two alternative ways to quantize the theory should be related by a Legendre transform as one is the conjugate momentum of the other [79].

4. For $m = \frac{1}{2}$, the two terms in ψ_- are degenerate. Instead one has

$$\psi_- = r^{-\frac{d}{2}-\frac{1}{2}}(C \log r + D) \tag{2.58}$$

The relations between A, C in (2.46) are now replaced by

$$C = (i\gamma \cdot k)A \, . \tag{2.59}$$

In this case the term proportional to A is not normalizable and should be treated as the source term.

5. For even d, if χ_0 has negative chirality, then we should be imposing boundary conditions on ψ_-, which in turn implies that the bulk mass term must be negative. An example illustrating this is shown in Appendix A.2 with the BTZ black hole.

2.3.2 Prescription for retarded correlators

Now we simply analytically continue ψ_E and (2.48)–(2.55) to Lorentzian signature, precisely as in the bosonic case with (2.25) and (2.20). We obtain the following prescription for computing retarded correlators for spinor operators:

1. Find a solution $\psi_R(r, k_\mu)$ to the Lorentzian equations of motion which is infalling at the horizon.

2. Expand $\psi_R(r, k_\mu)$ near $r \to \infty$ as

$$\psi_{R+} = Ar^{-\frac{d}{2}+m} + Br^{-\frac{d}{2}-m-1}, \qquad \psi_{R-} = Cr^{-\frac{d}{2}+m-1} + Dr^{-\frac{d}{2}-m}, \quad r \to \infty \tag{2.60}$$

where $\psi_{R\pm}$ are spinors of definite Γ^r eigenvalue as defined in (2.41).

3. Then $G_R(k_\mu)$ is obtained from the analytic continuation of (2.53) by

$$G_R(k_\mu) = i\mathcal{S}(k_\mu)\gamma^t = \frac{2m+1}{k^2}(\gamma\cdot k)\,\mathcal{T}\,\gamma^t \tag{2.61}$$

where $\gamma\cdot k = \gamma^\mu k_\mu$, $k^2 = k_\mu k^\mu$ and $\mathcal{S}$ and $\mathcal{T}$ are defined by the relations

$$D = \mathcal{S}A, \qquad B = \mathcal{T}A\ . \tag{2.62}$$

We end this section by noting that causality and unitarity of the boundary CFT impose two important properties on its real-time correlators. Causality implies that the retarded correlator must be analytic in the upper half of the complex ω plane; this is easily seen to be true for correlators calculated using the prescription above. Unitarity implies that the imaginary part of the diagonal elements of the matrix G_R is proportional to a spectral density and must be positive for all ω; as mentioned above, the overall sign of the correlator is proportional to the normalization of the Dirac action, and one can show that a sign consistent with bulk unitarity also results in positive spectral densities in the boundary theory.

2.4 Summary

In this chapter we reviewed the basic formalism for calculations in AdS/CFT. We had a particular focus on real-time applications; in particular, we showed that an intrinsic Lorentzian prescription for computing retarded Green functions from gravity can be obtained by analytic continuation from the corresponding problem in Euclidean signature. An important message here is that, even in Lorentzian signature, for any bulk field–whether bosonic or fermionic–the corresponding conjugate momentum contains the response of the dual operator. The field theory response can thus be expressed in terms of quantities with clear physical meaning in the bulk; as we shall see in the next chapter, this will make transparent the origin of phenomena such as the universality of transport coefficients.

We also explained in detail the issues that arise when attempting to find Lorentzian correlators of fermionic operators. In Appendix A we work out simple examples to illustrate the methods. In Chapter 5 we will review work by [16, 19] that uses these techniques to compute fermionic correlators in gravity backgrounds that are dual to finite-density states, with important and fascinating results.

2.A Definitions of correlators

We start by assuming that $\mathcal{O}$ is a hermitian bosonic operator; in that case our convention for the Euclidean correlator is

$$G_E(t,\vec{x}) = \langle T_E\mathcal{O}(x)\mathcal{O}(0)\rangle, \tag{2.63}$$

where T_E denotes Euclidean time ordering and at finite temperature the Euclidean time direction is taken to have period β.

Our conventions for the various realtime correlators are as follows, where ρ denotes the thermal density matrix:

$$G_R(t,\vec{x}) = i\theta(t)\,\mathrm{tr}(\rho[\mathcal{O}(t,\vec{x}),\mathcal{O}(0)]) \tag{2.64}$$
$$G_A(t,\vec{x}) = -i\theta(-t)\,\mathrm{tr}(\rho[\mathcal{O}(t,\vec{x}),\mathcal{O}(0)]) \tag{2.65}$$

Note that with this sign convention the imaginary part of G_R is equal to π multiplied by the spectral density, and thus is *positive* definite. Another common convention is to use the opposite sign for both G_R and G_A; in particular, this was used in our earlier work [14].

For $\mathcal{O}$ fermionic and complex we use the following conventions

$$G_E(t,\vec{x}) = \langle T_E \mathcal{O}(x)\mathcal{O}^\dagger(0)\rangle, \tag{2.66}$$
$$G_R(t,\vec{x}) = i\theta(t)\,\mathrm{tr}(\rho\{\mathcal{O}(t,\vec{x}),\mathcal{O}^\dagger(0)\}) \tag{2.67}$$
$$G_A(t,\vec{x}) = -i\theta(-t)\,\mathrm{tr}(\rho\{\mathcal{O}(t,\vec{x}),\mathcal{O}^\dagger(0)\}) \tag{2.68}$$

2.B Massive fields

For massive scalar fields, the boundary limit is more subtle due to various divergences. To be specific we consider a scalar action of the form

$$S = -\frac{1}{2}\int d^{d+1}x\sqrt{-g}\,\left((\partial\phi)^2 + m^2\phi^2\right) \tag{2.69}$$

with the background metric satisfying the standard asymptotic AdS behavior (2.13) near the boundary.

Then ϕ_R has the asymptotic behavior

$$\phi_R(r,k_\mu) \approx A(k_\mu)\,r^{\Delta-d} + B(k_\mu)\,r^{-\Delta}, \qquad r\to\infty \tag{2.70}$$

where

$$\Delta = \frac{d}{2} + \nu, \qquad \nu = \sqrt{m^2 + \frac{d^2}{4}} \tag{2.71}$$

Note now the field theory source should now be taken to be A, which differs by a power of r from the boundary value of ϕ. This implies that

$$\langle \mathcal{O}(k_\mu)\rangle_A = \lim_{r\to\infty} r^{\Delta-d}\Pi(r;k_\mu)\big|_{\phi_R}, \tag{2.72}$$

where as before $\Pi = -\sqrt{-g}g^{rr}\partial_r\phi$ is the canonical momentum to ϕ. Plugging in the near-boundary expansion (2.70), we see that Π has the asymptotic behavior

$$\Pi(r,k_\mu)\big|_{\phi_R} \approx -(\Delta-d)A(k_\mu)r^\Delta + \Delta B(k_\mu)r^{d-\Delta}, \tag{2.73}$$

and thus the extra power of r in (2.72) exactly cancels the power of r in front of the subleading solution B, so the final answer contains a finite part that is independent of r. Note nevertheless that some care must be taken in the limit [63], and the retarded Green function G_R should now be written as

$$G_R(k_\mu) = \lim_{r\to\infty} r^{2(\Delta-d)} \frac{\Pi(r,k_\mu)\big|_{\phi_R}}{\phi_R(r,k_\mu)} = (2\Delta - d)\frac{B(k_\mu)}{A(k_\mu)} \tag{2.74}$$

where one is instructed to extract only the finite piece on the right-hand side.

2.C Boundary terms for spinors

Here we consider various technical issues related to the variation of the Dirac action. In particular, we explain why the momentum conjugate to ψ_+ can truly be considered the response of the operator $\langle\bar{\mathcal{O}}\rangle$ dual to ψ; essentially this argument is due to [78] and we review it here for clarity. Throughout this section we assume $m > 0$; a similar argument holds for $m < 0$ with an interchange of $\psi_\pm$.

Consider the bulk Euclidean Dirac action

$$S_{\text{bulk}} = -\int d^{d+1}x\sqrt{g}\,(\bar{\psi}\Gamma^M\mathcal{D}_M\psi - m\bar{\psi}\psi) \tag{2.75}$$

From this action the momentum Π_+ conjugate to ψ_+ is

$$\Pi_+ = -\sqrt{gg^{rr}}\bar{\psi}_- \tag{2.76}$$

It appears that the momentum conjugate to $\bar{\psi}$ is identically zero; however we expect this momentum to contain information regarding the field theory operator $\mathcal{O}$, which certainly does not vanish in general. Upon an integration by parts, however, we can transfer the radial derivative from ψ to $\bar{\psi}$; in that case we find that the momentum conjugate to ψ_+ is 0, but the momentum $\bar{\Pi}_+$ conjugate to $\bar{\psi}_+$ is now

$$\bar{\Pi}_+ = -\sqrt{-gg^{rr}}\psi_- \tag{2.77}$$

Confusingly, however, it appears that the two expressions above cannot apply simultaneously, although our expectation from the field theory side is that neither of them should vanish. Clearly boundary terms in the action are playing an important role; we now explain precisely how to fix these boundary terms and what their effects are.

The portion of the action (2.75) containing radial derivatives can be written explicitly as

$$S_{\text{bulk}} \supset -\int d^{d+1}x\sqrt{gg^{rr}}(\bar{\psi}_-\partial_r\psi_+ - \bar{\psi}_+\partial_r\psi_-) \tag{2.78}$$

From this we can see that if we vary this action around a solution to the equations

of motion $\psi \to \psi + \delta\psi$; the variation works out to be

$$\delta S_{\text{bulk}} = \text{bulk term} - \int_{\partial\mathcal{M}} d^d x \sqrt{g g^{rr}} (\bar{\psi}_- \delta\psi_+ - \bar{\psi}_+ \delta\psi_-), \tag{2.79}$$

where the bulk term is proportional to the equations of motion and the boundary term follows from (2.78). Note that the on-shell action is thus a function of both ψ_+ and ψ_-; however, this is not correct. As mentioned in the text, if we impose infalling boundary conditions we are no longer free to choose ψ_-, and this information must be implemented in our variational principle. This is done by adding to our action the following boundary term

$$S_\partial = -\int_{\partial\mathcal{M}} d^d x \sqrt{g g^{rr}} \bar{\psi}_+ \psi_- \tag{2.80}$$

We now see that the variation of the full action is

$$\delta S_{\text{total}} = \delta(S_{\text{bulk}} + S_\partial) = -\int_{\partial\mathcal{M}} d^d x \sqrt{g g^{rr}} (\bar{\psi}_- \delta\psi_+ + \delta\bar{\psi}_+ \psi_-) \tag{2.81}$$

Thus the on-shell action no longer depends on ψ_-; also, note that we have[16]

$$\Pi_+ \equiv \frac{\delta S_{\text{total}}}{\delta\psi_+} = -\sqrt{g g^{rr}} \bar{\psi}_- \qquad \bar{\Pi}_+ \equiv \frac{\delta S_{\text{total}}}{\delta\bar{\psi}_+} = -\sqrt{g g^{rr}} \psi_-, \tag{2.82}$$

where we are now defining the conjugate momenta Π to be the on-shell variation of S_{total}. Thus we see that the naive relations (2.76) and (2.77) *do* indeed hold simultaneously when we use the correct boundary action. It is easy to see that if we had started with a different action related to (2.75) by only boundary terms we would have obtained a different value of S_∂ but the final answer (2.82) would have been the same. (It is shown in [78] that a symmetric splitting of the kinetic term in (2.75) results in the boundary term used in the original work with spinors in AdS/CFT [76, 77]).

[16]Note that the first expression refers to a derivative from the right and the second to a derivative from the left. For our application to the generating function of a QFT we use the same convention.

Chapter 3

Holographic hydrodynamics and the membrane paradigm

3.1 Hydrodynamics and horizons

We are now equipped with the formalism we need to perform real-time computations using holography. In this chapter we will apply this technology to discuss how universal features of interacting quantum field theories at finite temperature are mapped via gauge/gravity duality to universal features of black hole horizons. For example, any interacting quantum field theory at finite temperature should be described by hydrodynamics when viewed at sufficiently long length scales. For those with a gravity dual, the bulk geometry involves a black hole with a non-degenerate horizon, and the UV/IR connection then suggests that the field theory physics at long scales should be governed by the near-horizon portion of the dual geometry. In fact, classical general relativity tells us that there is a precise sense in which any black hole has a fictitious fluid living on its horizon, in the so-called "membrane paradigm" [13]. It is thus tempting to identify the membrane paradigm fluid on the horizon with the low-energy description of the strongly coupled field theory. This connection was first made by [34] and other related work includes [36, 35, 37]. See also [4] for a general review of the hydrodynamic limit in AdS/CFT and related references on the subject. The material in this chapter is largely taken from [14].

In this paper we aim to clarify this connection by comparing the linear response (to small external perturbations) of the horizon membrane fluid to that of the boundary theory fluid. Since in the hydrodynamic regime one is interested in conserved quantities (or Goldstone modes), which in turn correspond to massless modes in the bulk, we will concentrate only on massless bulk modes in this paper. These cover almost all interesting situations so far discussed in the literature. The only exception is the bulk viscosity, as it cannot be associated with a massless degree of freedom in the bulk; this is discussed further in Section 3.7.

We show here that that regardless of the specific model in question, the low-frequency limit[1] of linear response of the boundary theory fluid is indeed completely

[1]Here by low-frequency limit, we mean the lowest order term in the derivative expansions of

captured by that of the horizon fluid. In particular, this enables us to express a generic transport coefficient of the boundary theory solely in terms of geometric quantities evaluated at the event horizon of the black hole. For example, this gives a simple proof of the universality of the shear viscosity in terms of *the universality of the coupling of a transverse graviton.* We also give an explicit expression for the conductivity of an arbitrary conserved current in the dual theory.

When moving away from the low frequency limit, however, the behavior of the boundary fluid cannot be fully captured by the horizon fluid even within the derivative expansion: even at generic frequency and momenta, the horizon response always corresponds to that of the low frequency limit of the boundary theory. Thus away from the low frequency limit, the full geometry of the spacetime plays a role. To explore this we consider a fictitious membrane at each constant-radius hypersurface and introduce a linear response function for each of them. One can then derive a flow equation for the radius-dependent response function; at generic momenta this evolves nontrivially from the horizon to the boundary, where it determines the response of the dual field theory. As an application of the flow equation we consider hydrodynamic diffusion. We give a simple derivation of the diffusion constants for charge and momentum diffusions and illustrate the difference between the diffusion phenomena observed at the horizon and at the boundary.

The plan of this chapter is as follows. For the rest of this section, we introduce our conventions and notations for the gravity and field theory sides. In Section 3.2 we give a quick review of the classical black hole membrane paradigm. In Section 3.3 we express linear response in AdS/CFT in a language similar to that of the membrane paradigm. Section 3.4 applies this language to the evaluation of zero-frequency transport coefficients in AdS/CFT. Sections 3.5 and 3.6 are devoted to results at finite frequency, such as the flow equation and hydrodynamic diffusion. We conclude this chapter with a brief discussion in Section 3.7.

3.1.1 Gravity setup

On the gravity side, we will be examining very general black brane backgrounds, which we take to have the form

$$ds^2 = g_{rr}dr^2 + g_{\mu\nu}dx^\mu dx^\nu = -g_{tt}dt^2 + g_{rr}dr^2 + g_{ij}dx^i dx^j \ . \tag{3.1}$$

Indices $\{M,N\}$ run over the full $d+1$-dimensional bulk, $\{\mu,\nu\}$ over each d-dimensional constant-r slice, and $\{i,j\}$ over spatial coordinates. We assume the above metric has an event horizon at $r = r_0$, where g_{tt} has a first order zero and g_{rr} has a first order pole. We assume that all other metric components are finite (i.e. neither zero nor infinite) at the horizon.

We take the boundary at $r = \infty$ and assume that the metric asymptotes to a structure that supports a gauge-gravity duality. We assume that all metric components and position-dependent couplings depend on r only so that we have translational invariance in t and x^i directions. We also assume the full rotational symmetry between

frequency and spatial momenta.

x^i directions, i.e.

$$g_{ij} = g_{zz}\delta_{ij} \tag{3.2}$$

with z one of the spatial direction.

Note that the metric (3.1) does not have to be a spacetime metric, it could also be (for example) the induced metric on the worldvolume of a D-brane or a fundamental string in AdS.

We will often work in Fourier space on each constant-r slice. For example for a scalar field ϕ, we write

$$\phi(r, x^\mu) = \int \frac{d^d k}{(2\pi)^d} \phi(r, k_\mu)\, e^{ik_\mu x^\mu}, \qquad k_\mu = (-\omega, \vec{k}) \ . \tag{3.3}$$

For simplicity of notation, we will distinguish $\phi(r, x^\mu)$ from its Fourier transform $\phi(r, k_\mu)$ by its argument only.

3.1.2 Field theory setup

We will be relating these gravity backgrounds to quantum field theories taken at finite temperature. Consider a field theory containing an operator $\mathcal{O}$ with an external classical source ϕ_0. At the level of linear response theory the one-point function of $\mathcal{O}$ is linear in ϕ_0, and when expressed in Fourier space the proportionality constant is simply the thermal retarded correlator G^R of $\mathcal{O}$

$$\langle \mathcal{O}(\omega, \vec{k}) \rangle_{\text{QFT}} = -G^R(\omega, \vec{k}) \phi_0(\omega, \vec{k}) \tag{3.4}$$

where ω and $\vec{k}$ denote the frequency and spatial momentum respectively (see e.g. [38]). The low frequency limit of this correlator is of physical importance, as it defines a transport coefficient χ:

$$\chi = -\lim_{\omega \to 0} \lim_{\vec{k} \to 0} \frac{1}{\omega} \text{Im} G^R(\omega, \vec{k}) \ . \tag{3.5}$$

Note that this definition essentially means that if we apply a time varying source $\phi_0(t)$, then in the low frequency limit the response of the system is[2]

$$\langle \mathcal{O} \rangle_{\text{QFT}} = -\chi \partial_t \phi_0(t) \tag{3.6}$$

These transport coefficients are typically parameters in an effective low energy description (such as hydrodynamics or Langevin equations) and once specified they completely determine the macroscopic behavior of the medium. A well-known example is the shear viscosity η, for which one takes $\mathcal{O} = T_{xy}$, the off-diagonal component of the stress tensor. For DC conductivity σ one takes $\mathcal{O} = J_z$, where J_z is a component of the electric current. For quark diffusion constants characterizing the motion

[2]Note that the real part of G_R is even in ω and we set the zero frequency part of G_R to be zero since it gives rise to a contact term.

of a heavy quark moving in a quark-gluon plasma, $\mathcal{O}$ is given by the forces acting on the quark [39].

3.2 Classical black hole membrane paradigm

We begin our discussion with a brief review of the classical black hole membrane paradigm. Our treatment will not do sufficient justice to this elegant subject and will mostly follow the formulation of the paradigm put forth in [40]; for more detailed exposition see [13].

Imagine that we are observers hovering outside the horizon of a black hole. Since there is no (classical) way for the region inside the black hole to affect us, our effective action can be written as

$$S_{\text{eff}} = S_{\text{out}} + S_{\text{surf}} \tag{3.7}$$

where S_{out} involves an integration over the portion of spacetime outside the horizon and S_{surf} is a boundary term on the horizon, which can be determined by demanding that S_{eff} be stationary on a solution to the equations of motion. Physically, S_{surf} represents the influence that the black hole horizon has on the external universe. In practice, it is often more convenient to define S_{surf} on the "stretched horizon", which is a timelike surface of fixed r just outside the true horizon (see [41] for extended discussion). This is also more concrete, since no observer can hover at the genuine horizon: the stretched horizon acts as a cutoff for the spacetime outside the black hole.

3.2.1 Membrane conductivity

Let us consider a bulk $U(1)$ gauge field with standard Maxwell action (see Sec. 3.1.1 for our index conventions)

$$S_{\text{out}} = -\int_{r>r_0} d^{d+1}x\sqrt{-g}\frac{1}{4g_{d+1}^2(r)}F_{MN}F^{MN}\ , \tag{3.8}$$

where we have allowed a r-dependent gauge coupling g_{d+1}. The variation of this bulk action results in a boundary term at the horizon, which can only be canceled if

$$S_{\text{surf}} = \int_{\Sigma} d^dx\sqrt{-\gamma}\left(\frac{j^\mu}{\sqrt{-\gamma}}\right)A_\mu, \tag{3.9}$$

where j^μ is the conjugate momentum (with respect to r-foliation) of the field A^μ

$$j^\mu = -\frac{1}{g_{d+1}^2}\sqrt{-g}F^{r\mu} \tag{3.10}$$

and $\gamma_{\mu\nu}$ is the induced metric on the stretched horizon Σ. Equation (3.9) suggests that an observer hovering near the horizon will find that the horizon is carrying a

membrane current

$$J^{\nu}_{\rm mb} \equiv \left(\frac{j^{\nu}(r_0)}{\sqrt{-\gamma}}\right) = -\frac{1}{g^2_{d+1}}\sqrt{g_{rr}}F^{r\nu}(r_0) \ . \tag{3.11}$$

Note that the "Gauss's law" that we obtain by treating r as "time" becomes conservation of the currents $J^{\mu}_{\rm mb}$ and j^{μ} on any constant-r slice.

$$\partial_{\mu}J^{\mu}_{\rm mb} = \partial_{\mu}j^{\mu} = 0 \ . \tag{3.12}$$

While *a priori* the current $J^{i}_{\rm mb}$ (or j^{i}), which is determined by F^{ir}, and the electric field $E^{i} = F^{it}$ are independent variables, they are in fact proportional to each other at the horizon. This can be seen as follows. Since the horizon is a regular place for free in-falling observers, the electromagnetic field observed by them must be regular. This implies that near the horizon, A^{M} can only depend on r and t through their non-singular combination, the Eddington-Finklestein coordinate v defined by

$$dv = dt + \sqrt{\frac{g_{rr}}{g_{tt}}}dr \ . \tag{3.13}$$

This implies that

$$\partial_r A_i = \sqrt{\frac{g_{rr}}{g_{tt}}}\partial_t A_i \ , \quad r \to r_0 \tag{3.14}$$

and with gauge choice $A_r = 0$, we then have[3] (with $r \to r_0$)

$$F_{ri} = \sqrt{\frac{g_{rr}}{g_{tt}}}F_{ti} \quad \to \quad J^{i}_{\rm mb} = -\frac{1}{g^2_{d+1}}\sqrt{g^{tt}}F^{i}_{t} = \frac{1}{g^2_{d+1}}\hat{E}^{i} \tag{3.15}$$

Here $\hat{E}^{i}$ is an electric field measured in an orthonormal frame of a physical observer hovering just outside of the black hole. From (3.15), it is natural to interpret $J^{i}_{\rm mb}$ as the *response* of the horizon membrane to the electric field $\hat{E}^{i}$, leading to a membrane conductivity

$$\sigma_{\rm mb} = \frac{1}{g^2_{d+1}(r_0)} \ . \tag{3.16}$$

Note that (unlike those arising from conventional quantum field theories) this conductivity is frequency-independent and depends only on the gauge coupling at the horizon.

[3]This equation can be derived in a number of ways e.g. see [40] for a gauge-invariant derivation.

3.2.2 Scalar membrane and the shear viscosity of the membrane paradigm fluid

Now consider a massless bulk scalar field with action

$$S_{\text{out}} = -\frac{1}{2}\int_{r>r_0} d^{d+1}x\sqrt{-g}\,\frac{1}{q(r)}\,(\nabla\phi)^2, \tag{3.17}$$

where $q(r)$ can be considered an effective (r-dependent) scalar coupling. The boundary term on the horizon resulting from variation of this action requires the addition of a surface action at the horizon

$$S_{\text{surf}} = \int_\Sigma d^dx\sqrt{-\gamma}\left(\frac{\Pi(r_0,x)}{\sqrt{-\gamma}}\right)\phi(r_0,x) \tag{3.18}$$

where Π is again the momentum conjugate to ϕ with respect to a foliation in the r-direction,

$$\Pi = -\frac{\sqrt{-g}}{q(r)}\,g^{rr}\partial_r\phi\,. \tag{3.19}$$

Following the discussion of an electromagnetic field, equation (3.18) now implies that to an external observer the horizon appears to have a "membrane ϕ-charge" Π_{mb} given by

$$\Pi_{\text{mb}} \equiv \left(\frac{\Pi(r_0)}{\sqrt{-\gamma}}\right) = -\frac{\sqrt{g^{rr}}\partial_r\phi(r_0)}{q(r_0)} \tag{3.20}$$

Again, for a freely in-falling observer to find a nonsingular ϕ, near the horizon, ϕ should have the form $\phi(r,t,x_i) = \phi(v,x_i)$, where v is the Eddington-Finklestein coordinate (3.13). This implies $\partial_r\phi = \sqrt{\frac{g_{rr}}{g_{tt}}}\partial_t\phi$ and

$$\Pi_{\text{mb}} = -\frac{1}{q(r_0)}\sqrt{g^{tt}}\partial_t\phi(r_0) = -\frac{1}{q(r_0)}\partial_i\phi(r_0) \tag{3.21}$$

where in the last equality we have passed to an orthonormal basis. As in the electromagnetic case we can interpret Π_{mb} as the response of the horizon membrane induced by a local bulk field ϕ around the hole, leading to a membrane transport coefficient χ_{mb} (compare with (3.6))

$$\chi_{\text{mb}} = \frac{1}{q(r_0)} \tag{3.22}$$

We emphasize that in deriving (3.21) we did not take a low frequency or momentum limit; (3.22) is the full response for generic momenta and frequencies.

We can now apply this discussion to the computation of the shear viscosity of the horizon membrane by taking $\phi = h^y_x$, the off-diagonal component of the graviton. We assume that there is no spatial momentum in $x-y$ directions and that the background matter stress tensor does not mix with h^y_x. Then the graviton is transverse and its action is simply that of (3.17) with $q = 16\pi G_N$ where G_N is the bulk Newton's constant. Π_{mb} can now be interpreted as $(T_{\text{mb}})^x_y$, a component of the membrane

stress tensor. From (3.21) and (3.22) we thus conclude that [40, 13]

$$\eta_{\rm mb} = \frac{1}{16\pi G_N}, \quad \rightarrow \quad \frac{\eta_{\rm mb}}{s_{\rm mb}} = \frac{1}{4\pi} \tag{3.23}$$

where $s_{\rm mb} = 1/4G_N$ is (by definition) the entropy density per unit volume of the membrane fluid.

We see that the influence of the black hole on its surroundings can be taken into account by placing fictitious charges and currents on its horizon. Furthermore, these currents are related to applied fields in a very simple way, fixed completely by the condition of horizon regularity. This leads to simple expressions for transport coefficients such as $\eta_{\rm mb}$ and $\sigma_{\rm mb}$, although it is not immediately clear whether these coefficients are in any way related to those that we calculate from AdS/CFT.

3.3 Linear response in AdS/CFT: taking the membrane to the boundary

Let us now turn to the corresponding problem in AdS/CFT. The massless bulk field ϕ with action (3.17) is now dual to an operator $\mathcal{O}$ in the boundary theory. Recall that in *Euclidean* signature, the relation between the dual theory generating functional and the on-shell supergravity action[4] is given by

$$\left\langle \exp\left[-\int d^d x\, \phi_0 \mathcal{O}\right]\right\rangle_{\rm QFT} = e^{-S_{\rm grav}[\phi(r\to\infty)=\phi_0]}\,. \tag{3.24}$$

In other words, we must find a classical solution for ϕ that is regular in the bulk and asymptotes to a given value ϕ_0 at the boundary; derivatives of the on-shell gravity action with respect to this boundary value ϕ_0 will give us correlators for $\mathcal{O}$. Equation (3.24) implies that the one-point function in the presence of source ϕ_0 can be written as[5]

$$\langle \mathcal{O}(x^\mu)\rangle_{\phi_0} = \lim_{r\to\infty} \Pi(r, x^\mu) \tag{3.25}$$

where we have used the well known fact in classical mechanics that the derivative of an on-shell action with respect to the boundary value of a field is simply equal to the canonical momentum conjugate to the field, evaluated at the boundary.

As explained in the previous chapter, to generalize this to real-timee we evaluate (3.25) in Lorentzian signature, with the requirement that ϕ satisfy in-falling boundary conditions at the black hole horizon. In particulat, taking a Fourier transform of (3.25) and comparing with (3.4), we obtain a simple formula for the thermal retarded correlator G_R:

$$G_R(k_\mu) = -\lim_{r\to\infty} \frac{\Pi(r, k_\mu)}{\phi(r, k_\mu)}\,. \tag{3.26}$$

[4]In this paper we will only consider the gravity limit.

[5]Note that the limit on the right hand should be taken with some care. For example, for a massless field, one should take the part of Π which goes to $O(1)$ at infinity.

We believe (3.25) and (3.26) provide a more fundamental prescription, as they are expressed in terms of quantities of clear geometric and physical meaning[6]. We note that with a different choice of boundary conditions at the horizon (3.26) can also be used to calculate Feynman functions: this essentially follows from analytic continuation of (3.24) to Lorentzian signature[7]. It can also be immediately generalized to fields of higher spin or fields with more general action. For a vector field, $\mathcal{O}$ is replaced by a boundary current $\mathcal{J}^\mu$ and Π by j^μ defined in (3.10). For metric fluctuations $\mathcal{O}$ is replaced by the boundary stress tensor $\mathcal{T}^{\mu\nu}$ and Π by

$$T^{\mu\nu} = \frac{\sqrt{-\gamma}}{16\pi G_N}\left(K^{\mu\nu} - \gamma^{\mu\nu}K^\lambda_\lambda\right) \tag{3.27}$$

where $K_{\mu\nu}$ is the extrinsic curvature of a constant r-surface.

Comparing (3.25) with (3.20), we see that (3.25) expresses the AdS/CFT response in a language almost identical to that of the membrane paradigm, except that the "membrane" in question is no longer at the horizon but at the boundary $r \to \infty$. The object Π which was loosely interpreted as a "membrane response" is now *actually* the response of an operator $\mathcal{O}$ in the dual theory; in other words, if we move the membrane from the horizon to the boundary, membrane paradigm quantities become concrete gauge theory observables. Furthermore, as can be checked explicitly, the in-falling boundary condition for ϕ at the horizon is precisely the regularity condition discussed for the membrane paradigm, i.e. ϕ can only depend on r and t through the Eddington-Finklestein coordinate v (3.13). This is an expression of the physical statement that a local observer hovering at the horizon only sees things falling in, not coming out. An example illustrating this is given in Appendix 3.A.

3.4 Low frequency limit

In this section we first show that the field theory transport coefficient defined in (3.5) can be expressed solely in terms of quantities at the horizon. This immediately gives a general proof of the universality of shear viscosity. We then turn to a $U(1)$ vector field in the bulk and calculate the DC conductivity of the corresponding conserved boundary current.

[6]For a massive field in AdS, (3.25) and (3.26) become

$$\langle\mathcal{O}(k)\rangle = \lim_{r\to\infty} r^{\Delta-d}\Pi(r), \quad G_R(k_a) = \lim_{r\to\infty} r^{\Delta-d}\frac{\Pi(r)}{\phi_0(k_a)}$$

where Δ is the dimension of the corresponding operator $\mathcal{O}$.

[7]An important subtlety here is that the proper Euclidean continuation gives the so-called Hartle-Hawking vacuum and not the naive Schwarzschild vacuum.

3.4.1 General formula for transport coefficients

Using (3.26), equation (3.5) can now be written as

$$\chi = \lim_{k_\mu \to 0} \lim_{r \to \infty} \frac{\Pi(r, k_\mu)}{i\omega\phi(r, k_\mu)} \,. \tag{3.28}$$

To compute (3.28) we write the equations of motion for ϕ in a Hamiltonian form as

$$\Pi = -\frac{\sqrt{-g}}{q(r)} g^{rr} \partial_r \phi \tag{3.29}$$

$$\partial_r \Pi = \frac{\sqrt{-g}}{q(r)} g^{rr} g^{\mu\nu} k_\mu k_\nu \phi \,. \tag{3.30}$$

Note that in the low frequency limit (i.e. $k_\mu \to 0$, with $\omega\phi$ and Π fixed), equations (3.29) and (3.30) become trivial

$$\partial_r \Pi = 0 + \mathcal{O}(k_\mu \omega\phi) \qquad \partial_r(\omega\phi) = 0 + \mathcal{O}(\omega\Pi) \,. \tag{3.31}$$

Thus in the zero momentum limit the evolution in r is completely trivial and (3.28) can in fact be evaluated at any value of r! We will evaluate it the horizon where the in-falling boundary condition should be imposed. As we noted as the end of section 3.3, the in-falling boundary condition for ϕ at the horizon is in fact equivalent to the condition of horizon regularity in the membrane paradigm, which from (3.19)–(3.21) gives,

$$\Pi(r_0, k_\mu) = \frac{1}{q(r_0)} \sqrt{\frac{-g}{g_{rr} g_{tt}}}\bigg|_{r_0} i\omega\phi(r_0, k_\mu) \,. \tag{3.32}$$

We thus find the simple result

$$\chi = \frac{1}{q(r_0)} \sqrt{\frac{-g}{g_{rr} g_{tt}}}\bigg|_{r_0} = \frac{1}{q(r_0)} \frac{A}{V} \tag{3.33}$$

where A is the area of the horizon and V is the spatial volume of the boundary theory. Given that entropy density s of the boundary theory is given by $s = \frac{A}{4G_N V}$, χ can also be written as

$$\frac{\chi}{s} = \frac{4G_N}{q(r_0)} \,. \tag{3.34}$$

We find that the ratio χ/s is given by the ratio of the Newton constant G_N, which characterizes the gravitational coupling, to the effective coupling $q(r_0)$ for ϕ at the horizon. This is the result for the boundary fluid, but we see that it is closely related to the corresponding result for the horizon fluid, simply because the bulk evolution equations (3.29) and (3.30) are trivial in the low frequency limit. Note that (provided that some form of gauge-gravity duality exists so that (3.25) and (3.26) make sense) the precise asymptotic structure of the spacetime does not play an important role in our analysis.

Though we have used the example of a massless scalar field above, the discussion

clearly applies to components of more general tensor fields. Our treatment can be applied to very general effective actions of the form

$$S = -\frac{1}{2}\int \frac{d\omega d^{d-1}k}{(2\pi)^d} dr\sqrt{-g}\left[\frac{g^{rr}(\partial_r\phi)^2}{Q(r;\omega,\vec{k})} + P(r;\omega,\vec{k})\phi^2\right], \tag{3.35}$$

provided that the flow equations (3.31) remain trivial in the zero-momentum limit. This implies that Q should go to a nonzero constant at zero momentum and P must be at least quadratic in momenta, so a mass term would not be allowed. For (3.35) the corresponding transport coefficient is given by

$$\frac{\chi}{s} = \frac{4G_N}{Q(r_0, k_\mu = 0)} . \tag{3.36}$$

It is also straightforward to generalize the discussion to multiple coupled fields.

3.4.2 Universality of shear viscosity

The most obvious application of (3.33)–(3.34) is to the shear viscosity. For Einstein gravity coupled to matter fields, in the absence of a background off-diagonal component of the metric, the effective action for the transverse off-diagonal gravitons h^y_x, which is dual to $\mathcal{T}_{xy}$ in the boundary theory, is simply that of a massless scalar with effective coupling

$$q(r) = 16\pi G_N . \tag{3.37}$$

From (3.34) we thus find the celebrated result

$$\frac{\eta}{s} = \frac{1}{4\pi} \tag{3.38}$$

Note that the universality of (3.38) can now be attributed to the universality of the effective coupling (3.37) for a graviton h^y_x.

The proof here is very general, applying to all Einstein gravity duals known so far, including charged black holes dual to theories with chemical potential, the near-horizon region of general Dp-branes, and recently discovered geometries dual to non-relativistic CFTs [44].[8]

It is also useful to compare this proof to earlier calculations. By considering diffusive shear modes on the stretched horizon [34] derived a formula for the diffusion constant $\eta/(\epsilon + p)$ in terms of an integral from the horizon to the boundary, where ϵ and p are energy and pressure density. [46] showed that η/s is universal among a certain family of metrics by reducing the integral to a total derivative and then evaluating it at the horizon. A simpler proof along a similar line was given in [4].

[8] An interesting example that violates our assumptions but still satisfies (3.38) is the gravity dual to non-commutative $\mathcal{N} = 4$ plasma studied in [45]. This system has broken rotational invariance and a boundary stress tensor that is dual not to the bulk graviton but to a linear combination of graviton and B fields, and thus our analysis does not apply, though it would be interesting to see if it could be extended.

The proofs of [46, 4] do not include theories with nonzero chemical potentials which have been checked separately [50, 47, 48, 49, 51]. Note that there is no conflict with the integral formula of [34] and our result (3.34) since the diffusion constant $\eta/(\epsilon+p)$ involves a factor $\epsilon+p$ which generically cannot be expressed in terms of quantities at the horizon. Our proof is closer in spirit to the discussions in [52, 50, 53], which use the Kubo formula and are related to the universality of the absorption cross section of a minimally coupled scalar [54]. The treatment given here is more general and technically simpler. It also highlights the importance of the effective coupling at the horizon as the source of universality.

It has been conjectured [52] that the value of η/s in (3.38) is in fact a lower bound for all realistic matter. Equation (3.36) hints at how the bound could be violated. We need to find a theory whose "effective" gravitational coupling for the h^x_y polarization at the horizon is *stronger* than the universal value (3.37) for Einstein gravity. Gauss-Bonnet gravity as discussed in [55, 56] (see also [57]) is an example of this. There the effective action for h^y_x has the form of (3.35) with the effective coupling $Q(r)$ at the horizon satisfying (see 3.10 in [55])[9]

$$\frac{1}{Q(r_0)} = \frac{(1-4\lambda_{\rm GB})}{16\pi G_N} \ . \tag{3.39}$$

Thus for $\lambda_{\rm GB} > 0$ the graviton in this theory is more strongly coupled than that of Einstein gravity and the value of η/s dips below the value (3.38). This also indicates that for η/s to be arbitrarily small, the graviton has to be strongly coupled, which was indeed observed in the Gauss-Bonnet example [55].

Note that the formula (3.34) for the specific case of shear viscosity in higher derivative gravity theories has been conjectured recently in [58], where the authors also discuss the importance of the strength of the coupling for h^y_x and its relation to the violation of the viscosity bound.

3.4.3 Gauge fields and the DC conductivity

As another example of application of (3.34), we now turn to the DC conductivity. The bulk gauge field A_M in AdS is now dual to a conserved current $\mathcal{J}^\mu$ in the boundary theory. The action is given by (3.8), and the momentum conjugate to this gauge field is given by (3.10). From (3.26) and (3.25), the conductivity can be written as

$$\langle \mathcal{J}^i(k_\mu)\rangle_{\rm QFT} = j^i(r\to\infty)(k_\mu) \equiv \sigma^{ij}(k_\mu)F_{jt}(r\to\infty) \ . \tag{3.40}$$

[9] We note that while the formula (3.36) does not immediately apply to more general higher-derivative gravity theories such as the R^4 theory studied in [59] due to the presence of terms in the action that are higher than quadratic in derivatives, it is conceivable that with some effort the discussion may generalized to include that case as well.

Equation (3.40) defines AC conductivities which are related to the retarded Green function of the boundary current $\mathcal{J}^i$ by

$$\sigma^{ij}(k_\mu) = -\frac{G_R^{ij}(k_\mu)}{i\omega} \ . \tag{3.41}$$

The DC conductivity is obtained by the zero momentum limit of the above equations. Clearly at zero momentum due to rotational symmetry, $\sigma_{ij} = \sigma\delta_{ij}$ [10]. Below σ without an explicit argument always refers to the DC conductivity.

The in-falling boundary condition at the horizon, which translates into equation (3.15), gives us the ratio at the horizon :

$$j^i(r_0) = \frac{1}{g_{d+1}^2}\sqrt{\frac{-g}{g_{rr}g_{tt}}}g^{zz}\Big|_{r_0} F_{it}(r_0) \ . \tag{3.42}$$

It can be readily checked that in the zero momentum limit the bulk Maxwell equations give (see e.g. (3.90) and (3.92) of Appendix 3.B)

$$\partial_r j^i = 0 + \mathcal{O}(\omega F_{it}), \qquad \partial_r F_{it} = 0 + \mathcal{O}(\omega j^i) \tag{3.43}$$

implying that the relation (3.42) actually holds for all r. Combining (3.40) and (3.42), we see that the zero-frequency AdS/CFT conductivity is given by

$$\sigma = \frac{1}{g_{d+1}^2}\sqrt{\frac{-g}{g_{rr}g_{tt}}}g^{zz}\Big|_{r_0} \ . \tag{3.44}$$

One can also derive the above result by writing down an effective action for A_i in the gauge $A_r = 0$, in which case one finds an effective action of the form (3.17) with effective scalar coupling given by

$$\left(\frac{1}{q}\right)_{\text{EM}} = \frac{1}{g_{d+1}^2}g^{zz} \tag{3.45}$$

From (3.33), we again find (3.44). While the DC conductivities for various specific backgrounds have been found in the literature (see e.g. [62, 60, 61]), the general formula (3.44) appears to be new.

Now let us specialize to $d = 3$, (2+1)-dimensional field theories, in which case the metric dependence in (3.44) completely cancels and we find

$$\sigma = \frac{1}{g_4^2(r_0)} \ . \tag{3.46}$$

This formula was previously derived for $(2 + 1)$-dimensional CFTs (in which g_4 is necessarily constant) [62, 61]. We have now shown that it applies to any theory (conformal or not) with a gravity dual. This formula displays a sort of "bulk universality"

[10] Except in two spatial dimensions when we can also have an antisymmetric component proportional to ϵ^{ij}.

in that it appears very general from the gravity point of view but (unlike η/s) does not lead to any universality predictions from the field theory perspective, in this case because the bulk gauge coupling g_4^2 typically does not have a model-independent dual interpretation. We note however that if we restrict attention to CFTs, then g_4^2 *can* be related to the two-point function of the current at zero temperature, which has the form

$$\langle \mathcal{J}_\mu(x)\mathcal{J}_\nu(0)\rangle_{\rm CFT} = \frac{k}{x^4}\left[\delta_{\mu\nu} - 2\frac{x_\mu x_\nu}{x^2}\right] \tag{3.47}$$

with k given by $k = \frac{2}{\pi^2 g_4^2}$ [63]. We thus have the following general expression for the conductivity of any CFT_3 with a gravity dual[11]

$$\sigma = \frac{\pi^2 k}{2} \ . \tag{3.48}$$

The existence of such a relation is nontrivial. For related discussion see [61, 62].

For completeness, we also note that in $d = 3$, one can add to the Lagrangian (3.8) a theta term given by,

$$\frac{1}{4}\int d^4x\, \theta(r)\, \epsilon^{MNPQ} F_{MN} F_{PQ} \ , \tag{3.49}$$

where we have allowed the θ parameter to depend on r. With this addition, the canonical momentum with respect to a r-foliation for A_μ becomes

$$j^\mu = -\frac{1}{g_4^2(r)}\sqrt{-g}F^{r\mu} + \frac{\theta(r)}{2}\epsilon^{\mu\nu\lambda}F_{\nu\lambda} \ . \tag{3.50}$$

We immediately see that now σ^{ij} has an off-diagonal component (Hall conductivity) given by

$$\sigma^{12} = -\sigma^{21} = \theta(r \to \infty) \ . \tag{3.51}$$

This result is exact and (unlike the corresponding result for the diagonal conductivity) does not depend on conditions of horizon regularity or the low frequency limit. Note that if $\theta(r)$ is a nontrivial function (3.51) differs from the horizon response, which is $(\sigma_{\rm mb})^{12} = \theta(r_0)$.

For other dimensions the metric-dependence in (3.44) no longer cancels. Nevertheless we find that the dependence on the metric is essentially dictated by dimensional analysis, and one can still write the conductivity in a form similar to (3.46). We first rewrite (3.44) as

$$\sigma = \frac{1}{g_{d+1}^2}(g^{zz})^{\frac{d-3}{2}}\Big|_{r=r_0} \tag{3.52}$$

Now recall that in d-dimensions σ has mass dimension $d-3$ (so does $1/g_{d+1}^2$) and $(g^{zz}(r_0))^{\frac{1}{2}}$ is the conversion factor between a boundary length scale and the corre-

[11] In writing down both (3.46) and $k = \frac{2}{\pi^2 g_4^2}$ we have assumed a specific normalization for the boundary current $\mathcal{J}^\mu$. But Equation (3.48) is normalization independent.

sponding proper length at the horizon. Now suppose l is a characteristic scale in the boundary theory (e.g. the inverse temperature), then $l_{\rm hor} = (g^{zz})^{\frac{1}{2}} l$ is the corresponding proper length scale at the horizon. We can now write (3.52) as

$$\tilde{\sigma} = \frac{1}{\tilde{g}^2_{d+1}(r_0)}, \qquad \tilde{\sigma} = \sigma l^{d-3}, \quad \frac{1}{\tilde{g}^2_{d+1}(r_0)} = \frac{l^{d-3}_{\rm hor}}{g^2_{d+1}(r_0)} \ . \tag{3.53}$$

We have constructed the dimensionless conductivity $\tilde{\sigma}$ by rescaling σ by a boundary length scale l and similarly constructed the dimensionless horizon gauge coupling $\tilde{g}_{d+1}(r_0)$ by rescaling $g_{d+1}(r_0)$ by the corresponding horizon length scale $l_{\rm hor}$. Equation (3.53) now again shows "bulk universality" with a dimensionless conductivity solely determined by a dimensionless effective coupling constant. The non-universal metric dependence in (3.52) is hidden in the conversion factor between the length scales of the boundary and horizon.

As a concrete example, let us look at a CFT with a gravity dual given by AdS_{d+1} with $d \neq 3$, in which a black hole (with flat section) has the metric

$$ds^2 = \frac{r^2}{R^2}\left(-f(r)dt^2 + d\vec{x}_p^2\right) + \frac{R^2}{f(r)r^2}dr^2 \tag{3.54}$$

with $f(r) = 1 - (r_0/r)^d$. The Hawking temperature is given by $T = \frac{dr_0}{4\pi R^2}$. Applying (3.52) we find (as shown earlier in [61]) that

$$\sigma_{\rm CFT_d} = \frac{1}{g^2_{d+1}(r_0)}\left(\frac{r_0}{R}\right)^{d-3} \ . \tag{3.55}$$

The corresponding dimensionless conductivity and horizon coupling constant are $\tilde{\sigma}_{\rm CFT_d} = \sigma_{\rm CFT_d} T^{3-d}$ and $\frac{1}{\tilde{g}^2_{d+1}(r_0)} = \left(\frac{4\pi}{d}\right)^{d-3} \frac{R^{d-3}}{g^2_{d+1}(r_0)}$ respectively. Note that it is natural to define the dimensionless coupling constant at the horizon by normalizing it with the AdS curvature scale. The dimension-dependent prefactor $\left(\frac{4\pi}{d}\right)^{d-3}$ reflects the dimension-dependence of the conversion from a boundary length scale to that at the horizon.

To conclude this section, we see that a generic transport coefficient of an operator $\mathcal{O}$ dual to a massless mode in the bulk can be expressed in terms of geometric quantities at the horizon. We emphasize that our analysis depends critically on the existence of a non-degenerate horizon; e.g. for extremal black holes our results do not apply and the behavior of transport coefficients can be quite different. While here we have only discussed the shear viscosity and DC conductivity explicitly, there could be many other applications including e.g., the calculation of the quark diffusion coefficients κ_T and κ_L discussed in [39]. The understanding developed here should also make it easier to search for other transport coefficients that exhibit universality.

3.5 Flow from the horizon to the boundary

In the previous section we saw that in the low frequency limit the response of the boundary fluid is precisely captured by that of the horizon fluid in the membrane paradigm. This happened because the evolution of Π and $\partial_t\phi$ (or j^i and F_{ti} for a vector field) along the radial direction from the horizon to the boundary is trivial, and thus the AdS/CFT response depends only on the structure of the horizon. Note nonetheless that the natural definitions of the classical membrane paradigm currents $\Pi_{\rm mb}$ and $J^\mu_{\rm mb}$ differ from their AdS/CFT counterparts Π and j^μ by factors of $\sqrt{-\gamma}$, different index placements, etc. The differences are physically relevant; for example for $d \neq 3$, the boundary conductivity contains extra temperature-dependence, which should be contrasted with the perspective of a local observer at the horizon membrane who always observes that the conductivity is given by the inverse of the local coupling constant.

The membrane shear viscosity over entropy density ratio (3.23) does agree exactly with that of the boundary theory since $\eta_{\rm mb}$ and $s_{\rm mb}$ differ from the corresponding boundary theory quantity by a common factor which cancels in the ratio. This relation has been noted before [64, 36] and the connection between this and the AdS/CFT result is now clear. As is discussed in the conclusion to this paper, the connection between the membrane paradigm bulk viscosity and that of the dual theory is more subtle.

Away from the low frequency limit, the evolution (3.29)–(3.30) from the horizon to the boundary becomes nontrivial and depends on the full geometry. Indeed, the finite frequency/momentum response of an actual strongly coupled quantum field theory is expected to display complicated structure which simply does not exist in the frequency-independent classical membrane paradigm and should arise as we move outwards from the horizon.

To see this more explicitly, we consider a fictitious membrane at each constant radius along the radial direction and introduce a linear response function for each of them,

$$\bar{\chi}(r;k_\mu) = \frac{\Pi(r,k_\mu)}{i\omega\phi(r,k_\mu)} \,. \tag{3.56}$$

Note the above expression is defined for all r and k_μ. At $r \to \infty$, $\bar{\chi}(r\to\infty;k_\mu) = -\frac{G_R(k_\mu)}{i\omega}$, which is the finite momentum boundary response function, and at the horizon $r \to r_0$, $\bar{\chi}(r\to r_0;k_\mu) = \chi$, as a result of (3.32)–(3.33).

From (3.29) and (3.30), one can derive a flow equation for $\bar{\chi}(r;k_\mu)$ which governs its evolution from the horizon to the boundary

$$\partial_r\bar{\chi}(r) = i\omega\sqrt{\frac{g_{rr}}{g_{tt}}}\left[\frac{\bar{\chi}^2}{\Sigma_\phi(r)} - \Sigma_\phi(r)\left(1 - \frac{k^2}{\omega^2}\frac{g^{zz}}{g^{tt}}\right)\right] \tag{3.57}$$

where

$$\Sigma_\phi(r) = \frac{1}{q(r)}\sqrt{\frac{-g}{g_{rr}g_{tt}}}, \quad k^2 = \vec{k}\cdot\vec{k} \,. \tag{3.58}$$

The above equation makes manifest that as $k \to 0$ and $\omega \to 0$, $\bar{\chi}$ is independent of r. Furthermore as $r \to r_0$ in order for the solution to be regular the bracketed quantity in (3.57) must vanish, from which we recover

$$\bar{\chi}(r_0, k_\mu) = \Sigma_\phi(r_0) = \chi \tag{3.59}$$

where in the second equality we have used (3.33). It is important to emphasize that the full momentum response at the horizon $\bar{\chi}(r_0, k_\mu)$ automatically corresponds to only to the zero momentum limit of the boundary response, i.e. $\bar{\chi}(r_0, k_\mu) = \bar{\chi}(r \to \infty, k_\mu \to 0)$.

With "initial condition" (3.59) the flow equation (3.57) can then be integrated from the horizon to infinity to obtain the AdS/CFT response for all ω, k. The evolution to infinity represents a gradual incorporation of higher-momentum modes. It would be nice to find a precise connection between the flow equation (3.57) and the boundary RG flow, possibly in the framework of an exact RG equation [65]. Note that in general the solution to (3.57) will involve divergences as $r \to \infty$; these are the familiar UV divergences of the field theory and can be removed by the usual procedure of holographic renormalization.

We now turn to a $U(1)$ vector field. Without loss of generality, we can take the momentum to be along the z direction. The conductivities introduced in (3.40) and (3.41) then naturally separate into two groups, the longitudinal conductivity $\sigma_L(k_\mu) = \sigma^{zz}(k_\mu)$ along z direction, and the transverse conductivity $\sigma_T(k_\mu) = \sigma^{xx}(k_\mu)$ along spatial directions not z, i.e. $(x, y, ...)$. As for the scalar case, this motivates us to introduce longitudinal and transverse r-dependent "conductivities" respectively,

$$\bar{\sigma}_L(r; k_\mu) = \frac{j^z(r, k_\mu)}{F_{zt}(r, k_\mu)}, \qquad \bar{\sigma}_T(r; k_\mu) = \frac{j^x(r, k_\mu)}{F_{xt}(r, k_\mu)} \,. \tag{3.60}$$

$\bar{\sigma}_{L,T}(r \to \infty; k_\mu)$ are the boundary theory responses, and are related to the full retarded correlator $G_R^{\mu\nu}$ of $\mathcal{J}_\mu$ as in (3.41).

The Maxwell equations for the vector field in the bulk similarly separate into two groups: a "longitudinal" channel involving fluctuations along (t, z) and a "transverse" channel involving fluctuations along all other spatial directions. Using the Maxwell equations in the respective channel we can then derive the flow equation for $\bar{\sigma}_{L,T}$. Defining

$$\Sigma_A(r) = \frac{1}{g_{d+1}^2} \sqrt{\frac{-g}{g_{rr} g_{tt}}} g^{zz} \tag{3.61}$$

we show in Appendix 3.B that $\bar{\sigma}_L$ satisfies an equation of the form

$$\partial_r \bar{\sigma}_L = i\omega \sqrt{\frac{g_{rr}}{g_{tt}}} \left[\frac{\bar{\sigma}_L^2}{\Sigma_A(r)} \left(1 - \frac{k^2}{\omega^2} \frac{g^{zz}}{g^{tt}} \right) - \Sigma_A(r) \right] \,. \tag{3.62}$$

$\bar{\sigma}_T$ satisfies the same equation as (3.57), but with Σ_ϕ replaced by Σ_A. Regularity at

the horizon membrane again provides the initial data at the horizon

$$\bar{\sigma}_{T,L}(r_0, k_\mu) = \Sigma_A(r_0) = \sigma \ . \tag{3.63}$$

There is a curious relation between the flow equations for $\bar{\sigma}_L$ and $\bar{\sigma}_T$. It can be readily checked from (3.62) and (3.57) that the quantity $\frac{1}{\bar{\sigma}_L}$ satisfies an equation which is identical to that of $\bar{\sigma}_T$ after the replacement $\Sigma_A(r) \to \frac{1}{\Sigma_A(r)}$. This can be interpreted as a relation between the conductivities of two different theories, and is discussed in Appendix 3.C.

3.6 Diffusion at the boundary and at the horizon

In section 3.4 we showed that in the low frequency limit the linear response at the boundary is fully captured by the response of the horizon. In section 3.5 we showed that finite frequency/momentum response of the boundary cannot be captured by that at the horizon since the horizon response always corresponds to the low frequency limit of the boundary theory. In this section we examine linear response at the next order in the derivative expansion using the examples of diffusion of charge and momentum density. The discussion serves to highlight the differences between the diffusion at the horizon and the boundary. It also provides a straightforward application of the flow equations derived in the last section, which we use to give a simple derivation of the diffusion constant.

3.6.1 Charge diffusion

Consider disturbing the thermal equilibrium of the boundary theory by a small nonuniform perturbation of charge density varying along the z direction. The charge gradient generates a nonvanishing current $\mathcal{J}^z$ and eventually the charge diffuses away back into thermal equilibrium. To lowest order in the derivative expansion the diffusion process is governed by the dispersion relation

$$\omega = -iDk^2, \qquad k = k_z \tag{3.64}$$

where D is the diffusion constant. In the linear response regime (3.40)-(3.41), equation (3.64) appears as a pole in the retarded Green function G_R^{zz}, since there is a nonzero current $\mathcal{J}^z$ even in the absence of an external field.

To study the diffusion process from gravity we should thus examine the longitudinal channel in the regime $\omega \sim k^2$ and $\omega/T \ll 1, k/T \ll 1$. Assuming this scaling and taking $\bar{\sigma}_L \sim O(1)$, we obtain from (3.62)

$$\frac{\partial_r \bar{\sigma}_L}{\bar{\sigma}_L^2} = -\frac{ik^2}{\omega}\frac{\sqrt{g_{rr}g_{tt}}}{\Sigma_A g_{zz}} \ . \tag{3.65}$$

The solution to this equation with initial condition given by (3.42) is

$$\frac{1}{\bar{\sigma}_L(r)} = \frac{1}{\sigma} + i\frac{k^2}{\omega}\int_{r_0}^{r} dr' \frac{\sqrt{g_{rr}g_{tt}}g^{zz}}{\Sigma_A} \tag{3.66}$$

where we have used that the DC conductivity σ is given by $\sigma = \Sigma_A(r_0)$. Now recalling that $\sigma^{zz}(k_\mu) = \sigma_L(k_\mu) = \bar{\sigma}_L(r \to \infty, k_\mu)$ and using (3.41), we find that

$$G_R^{zz}(k_\mu) = \frac{\omega^2\sigma}{i\omega - Dk^2} \tag{3.67}$$

where the diffusion constant D is given by the integral

$$D = \sigma\int_{r_0}^{\infty} dr' \frac{g_{rr}g_{tt}}{\sqrt{-g}}g_{d+1}^2 \,. \tag{3.68}$$

Equation (3.68) is equivalent to the diffusion constant derived in [34, 36] once we substitute the explicit expression (3.44) for σ.

Note that the diffusion constant D (3.68) cannot be generically written in terms of horizon quantities. Now using the Einstein relation [12]

$$\Xi D = \sigma \tag{3.69}$$

where Ξ is the charge susceptibility, we find a general expression for Ξ,

$$\Xi = \left[\int_{r_0}^{\infty} dr' \frac{g_{rr}g_{tt}}{\sqrt{-g}}g_{d+1}^2\right]^{-1} \,. \tag{3.70}$$

In Appendix 3.D we give an alternative derivation of (3.70) for an arbitrary charged black brane; thus the logic of this section can also be viewed as a proof that any black brane obeys the Einstein relation.

Having derived the retarded Green function (3.67) in the diffusion regime, let us now find bulk solutions to the Maxwell equations that are dual to these diffusive modes in the gauge theory. This in particular will enable us to compare the explicit diffusion processes on the horizon membrane and at the boundary. For this purpose we again examine the longitudinal channel Maxwell equations (3.90) and (3.92) in the limit of small ω and k but finite $\omega \sim k^2$,

$$\partial_r j^z = \mathcal{O}(\omega F_{zt}), \tag{3.71}$$

$$\partial_r F_{zt} = \frac{ik^2}{\omega}\frac{g_{rr}g_{tt}g_{d+1}^2}{\sqrt{-g}}j^z + \mathcal{O}(\omega j^z) \,. \tag{3.72}$$

[12] Note that with the Einstein relation below (3.67) precisely has the form which one expects from hydrodynamics

$$G_{zz}^R = \frac{\omega^2\Xi D}{i\omega - Dk^2} \,.$$

The above equations can be immediately integrated to give

$$j^z(r) = j^z(r_0) = \text{const}, \tag{3.73}$$

$$F_{zt}(r) = F_{zt}(r_0)\left[1 + \sigma\frac{ik^2}{\omega}\int_{r_0}^{r} dr' \frac{g_{rr}g_{tt}g_{d+1}^2}{\sqrt{-g}}\right] \tag{3.74}$$

where we have used the boundary condition $j^z(r_0) = \sigma F_{zt}(r_0)$ at the horizon.

Since we are interested in a diffusion process we should be looking for gauge theory configurations where the applied electric field is zero. Requring $F_{zt}(r \to \infty) = 0$ enforces a relation between ω and k that is exactly the dispersion relation (3.64) with D given by (3.68). When this relation is satisfied, in the dual picture we see standard diffusion with no electric field and $\langle \mathcal{J}^z \rangle_{\text{QFT}}$ decaying with time.

This should be contrasted with the behavior observed at the horizon. As j^z is constant throughout the spacetime, an observer at the horizon membrane will also see a current evolving with precisely the same behavior as that at the boundary. Indeed, diffusive behavior on stretched horizons has been noted before [34, 35]. However, the electric field F_{zt} at the horizon is *not* zero; indeed, we know that at the horizon the electric field exactly tracks the current via the boundary condition (3.42):

$$j^i(r_0) = \sigma F_{it}(r_0)\ , \tag{3.75}$$

and thus cannot be zero. Thus a local observer at the horizon has a rather different interpretation; he sees a nonzero electric field that is decaying with time as it falls into the horizon, and this electric field directly induces a membrane current via the simple response (3.75). As emphasized before, (3.75) in fact exists for all ω, k; however if ω, k satisfy the diffusion relation (3.64) with (3.68) then the electric field perturbations will vanish at infinity and the boundary interpretation of this configuration will be diffusion.

3.6.2 Momentum diffusion

For momentum diffusion one considers in the boundary theory a small nonuniform perturbation in momentum density $\delta\mathcal{T}_{at}$ varying along the z direction, where a is any spatial direction x,y, etc. not equal to z. The diffusion current is given by $\delta\mathcal{T}_{az}$ and the diffusion constant D_s can be written in terms of boundary quantities as (for a recent review see [4])

$$D_s = \frac{\eta}{\epsilon + p} \tag{3.76}$$

where ϵ and p and energy and momentum density.

The gravity modes corresponding to these components are h_{at}, h_{az} which decouple from the other components in the gauge $h_{ar} = 0$. The corresponding bulk canonical momenta are $T^{a\mu}$ given by (3.27), now with $\mu = (z,t)$. As pointed out in [34], the quickest route to the bulk equations of motion in this channel is via a Kaluza-Klein reduction in the a direction. In this case the relevant modes h^a_μ ($\mu = (t,z)$) can be

considered components of a gauge field A_μ with a metric-dependent gauge coupling. The precise mapping is

$$h^a_\mu = A_\mu, \qquad T^\mu_a = j^\mu, \qquad \frac{1}{g^2_{d+1}(r)} = \frac{g_{xx}(r)}{16\pi G_N} \tag{3.77}$$

whose derivation we review in Appendix 3.E. We can now immediately take over all of the results of the previous section: e.g. the corresponding "DC conductivity" is given by the entropy density $\frac{s}{4\pi}$ and the retarded correlator of $\mathcal{T}^z_a$ with itself is given by the analog of (3.67)

$$G_R^{az,az} = \frac{s}{4\pi}\frac{\omega^2}{i\omega - D_s k^2} \tag{3.78}$$

with the diffusion constant D_s given by

$$D_s = \frac{\eta}{\epsilon + p} = 4G_N\, s \int_{r_0}^{\infty} dr' \frac{g_{rr}g_{tt}}{\sqrt{-g}g_{xx}} \tag{3.79}$$

This equation is again equivalent to that in [34]. From (3.79) and (3.38) we now derive a general formula for $\epsilon + p$,

$$\frac{1}{\epsilon + p} = 16\pi G_N \int_{r_0}^{\infty} dr' \frac{g_{rr}g_{tt}}{\sqrt{-g}g_{xx}}\ . \tag{3.80}$$

Note that the analog of the "electric field" is a gauge-invariant [13] combination $\mathcal{E}_z$ of metric coefficients

$$\mathcal{E}_z \equiv \partial_z(h^a_t) - \partial_t(h^a_z)\ . \tag{3.81}$$

We will not repeat here the analysis of last subsection. Everything can be carried over with a change of notation as described above. We do emphasize again that the diffusion process at the boundary is different from that on the horizon. An observer at the horizon will see that the horizon metric is deformed; this deformation is directly inducing a fluid flow on the membrane via the response $T^z_a(r_0) = \frac{s}{4\pi}\mathcal{E}_z$.

Finally, note that diffusive behavior is not specific to the examples considered. Given a general pair $(\Pi, \partial_t\phi)$, the essential ingredient in this analysis is the existence of a scaling limit for ω, k where the response Π is constant in r but the source $\partial_t\phi$ is not (see (3.73), (3.74)). This can be translated into a constraint on general effective actions such as (3.35): we would like a limit where $P(r; k_\mu)/\omega \to 0$ but $Q(r; \omega, k)\omega \to O(1)$. This allows us to construct a bulk solution where the source $\phi(r \to \infty)$ vanishes but $\Pi(r \to \infty)$ does not.

[13] The gauge transforms in this section are diffeomorphisms of the (r, t, z) sector; the effect of these on the h^a_μ perturbations is that of the $U(1)$ of the effective gauge field A_μ.

3.7 Conclusion and discussion

We have shown that there is a precise sense in which the long-wavelength limit of a boundary theory at finite temperature is determined by the horizon geometry of its gravity dual. We derived expressions for various transport coefficients in terms of components of the metric evaluated at the horizon; this sheds light on the origin of the universality of the shear viscosity and resulted in a general formula for the conductivity (3.44). At finite frequency/momentum, however, propagating the information from the horizon to the boundary requires solving a nontrivial flow equation which describes how the full AdS geometry encodes the higher momentum degrees of freedom of the boundary theory. The examples of charge and momentum diffusion provide illustrations of this flow in a very simple context.

Note that the relation between the membrane paradigm bulk viscosity (which is negative) and the bulk viscosity of a conformal fluid (which is exactly zero) is more subtle. Here the relevant degree of freedom h_i^i does not satisfy a simple equation like h_x^y. Instead, it enters in a nontrivial way into the Hamiltonian constraint of general relativity in the bulk and thus (in the absence of a background scalar profile) is not actually a propagating degree of freedom, leading to a vanishing bulk viscosity for conformal theories. If one turns on a nontrivial massive scalar background (corresponding to a deviation from conformality) then fluctuations of this field can mix with the graviton h_i^i, bringing it to life and allowing a nonzero bulk viscosity[14]. Thus a systematic study of bulk viscosity will involve fluctuations of massive fields. This will dramatically change the structure of flow equations such as (3.57); in particular, the flow will no longer be trivial even in the low frequency limit and it is likely that the membrane response will not adequately capture the low-frequency AdS/CFT response. Such issues significantly complicate the analysis, although recently a universal result for the bulk viscosity was obtained in [70]. The methods used there are somewhat different from those used here, and it would be interesting to understand the precise connection.

We close this chapter by noting that the classical membrane paradigm fluid can be seen to play a conceptually satisfying role in the holographic description of a strongly coupled field theory at finite temperature. We hope that it may be a practically useful role as well, both for identifying what quantities are expected to display universal behavior and as a technical tool for simplifying future hydrodynamic computations in gauge-gravity duality.

3.A In-falling boundary conditions and horizon regularity

Here we demonstrate using the example of a scalar field that the in-falling boundary condition used in standard AdS/CFT calculations is equivalent to the condition of horizon regularity used in the membrane paradigm. At the horizon $r \to r_0$, the metric

[14]For explicit calculations see [66, 67, 68, 69].

may be written

$$g_{tt} = c_0(r - r_0), \qquad g_{rr} = \frac{c_r}{r - r_0} \tag{3.82}$$

One finds that near the horizon the equation for ϕ is given by

$$\sqrt{\frac{c_0}{c_r}}(r - r_0)\partial_r \left(\sqrt{\frac{c_0}{c_r}}(r - r_0)\partial_r \phi \right) + \omega^2 \phi = 0 \tag{3.83}$$

which gives

$$\phi \propto e^{-i\omega(t \pm x)}, \qquad dx = \sqrt{\frac{g_{rr}}{g_{tt}}} dr \tag{3.84}$$

The in-falling boundary condition implies that we should take the positive sign in the exponent. In that case it is clear that the solution can be written only in terms of the Eddington-Finkelstein coordinate v defined in (3.13):

$$\phi \propto e^{-i\omega v}, \qquad dv = dt + \sqrt{\frac{g_{rr}}{g_{tt}}} dr \tag{3.85}$$

The fact that ϕ depends only on the nonsingular coordinate v at the horizon is precisely the condition of horizon regularity used in the membrane paradigm. Note if we integrate the definition of v in a small neighborhood of the horizon and use the formula for the inverse Hawking temperature $\beta = 4\pi\sqrt{\frac{c_r}{c_0}}$ we obtain

$$v = t + \frac{\beta}{4\pi} \ln(r - r_0) \rightarrow \phi \propto (r - r_0)^{-\frac{i\omega\beta}{4\pi}} e^{-i\omega t} \tag{3.86}$$

which is recognizable as the standard form of the in-falling boundary condition.

3.B Bulk Maxwell equations and flow equations for conductivities

Here we assemble the relevant components of the bulk Maxwell equations, given by the variation of the action

$$S = -\int d^{d+1}x \sqrt{-g} \frac{1}{4g_{d+1}^2(r)} F_{MN} F^{MN} \tag{3.87}$$

As before j^μ is the momentum conjugate to A_μ with respect to a foliation by constant-r slices (3.10):

$$j^\mu = -\frac{1}{g_{d+1}^2} \sqrt{-g} F^{r\mu} \tag{3.88}$$

Rather than working with the gauge potentials A_M, we will write all equations in terms of gauge-invariant objects such as $F_{\mu\nu}$ and j^μ; this involves the manipulation of a larger number of equations but makes the physical interpretation more transparent. We will also assume that the background configuration of the gauge field is trivial;

in principle fluctuations around a nontrivial gauge field background can couple to the metric or other fields and require a more detailed analysis. Note that in (3.87) $g_{d+1}^2(r)$ can be given by the background value of a nontrivial scalar field, as symmetry arguments guarantee that fluctuations of such a scalar will decouple from the Maxwell perturbations.

If we take the momentum to be along the z direction, these equations naturally separate into two groups; a "longitudinal" channel involving fluctuations along (t, z) and a "transverse" channel involving fluctuations along all spatial directions not z, i.e. $(x, y, ...)$. Defining $G = \sqrt{-g}/g_{d+1}^2$ for notational convenience, we find that the longitudinal channel is governed by two dynamical equations:

$$-\partial_r j^t - G g^{tt} g^{zz} \partial_z F_{zt} = 0 \tag{3.89}$$

$$-\partial_r j^z + G g^{tt} g^{zz} \partial_t F_{zt} = 0 \tag{3.90}$$

as well as the conservation of j^μ and the Bianchi identity:

$$\partial_t j^t + \partial_z j^z = 0 \tag{3.91}$$

$$-\frac{g_{rr} g_{zz}}{G} \partial_t j^z - \frac{g_{rr} g_{tt}}{G} \partial_z j^t + \partial_r F_{zt} = 0 \tag{3.92}$$

We would like to derive a flow equation for $\bar{\sigma}_L(r; k_\mu) \equiv j^z / F_{zt}$. We begin by taking a single derivative:

$$\partial_r \bar{\sigma}_L = \frac{\partial_r j^z}{F_{zt}} - \frac{j^z}{F_{zt}^2} \partial_r F_{zt} \tag{3.93}$$

We now use attack the right-hand side, using (3.91) to eliminate j^t in favor of j^z, (3.92) to eliminate $\partial_r F_{zt}$ in favor of j^z, and (3.89) to eliminate $\partial_r j^z$ in favor of F_{zt}. The final differential equation for $\bar{\sigma}_L$ is

$$\partial_r \bar{\sigma}_L = i\omega \sqrt{\frac{g_{rr}}{g_{tt}}} \left[\frac{\bar{\sigma}_L^2}{\Sigma_A(r)} \left(1 - \frac{k^2}{\omega^2} \frac{g^{zz}}{g^{tt}} \right) - \Sigma_A(r) \right], \tag{3.94}$$

where as in the text (3.61) we have defined $\Sigma_A(r) = \frac{1}{g_{d+1}^2} \sqrt{\frac{-g}{g_{rr} g_{tt}}} g^{zz}$.

Similarly, the transverse channel is governed by a dynamical equation and two constraints from the Bianchi identity.

$$-\partial_r j^y - G g^{tt} g^{yy} \partial_t F_{ty} + G g^{zz} g^{yy} \partial_z F_{zy} = 0 \tag{3.95}$$

$$\partial_r F_{yt} - \frac{g_{rr} g_{yy}}{G} \partial_t j^y = 0 \tag{3.96}$$

$$\partial_z F_{ty} + \partial_t F_{yz} = 0 \tag{3.97}$$

To find the flow equation for $\bar{\sigma}_T \equiv j^y / F_{yt}$ we follow a procedure directly analogous to that above, using (3.97) to eliminate F_{yz} in favor of F_{yt}, (3.95) to eliminate $\partial_r j^y$

in favor of F_{yt}, and (3.96) to eliminate $\partial_r F_{yt}$ in favor of j^y. The resulting equation is

$$\partial_r \bar{\sigma}_T = i\omega \sqrt{\frac{g_{rr}}{g_{tt}}} \left[\frac{\bar{\sigma}_T^2}{\Sigma_A(r)} - \Sigma_A(r) \left(1 - \frac{k^2}{\omega^2} \frac{g^{zz}}{g^{tt}} \right) \right] . \tag{3.98}$$

3.C A curious relation and electric-magnetic duality

Examination of (3.94) and (3.98) shows that the quantity $\frac{1}{\bar{\sigma}_L}$ satisfies an equation which is identical to that of $\bar{\sigma}_T$ after the replacement $\Sigma_A(r) \to \frac{1}{\Sigma_A(r)}$. Following analogous discussion to that around (3.52) and (3.53), one can also interpret $\Sigma_A(r)$ as an "effective dimensionless coupling constant" at each r-hypersurface. In other words, if we have two bulk theories $1, 2$ whose dimensionless couplings Σ_A^i are related by

$$\Sigma_A^1(r) = \frac{1}{\Sigma_A^2(r)} \tag{3.99}$$

then the respective conductivities of these two theories are related by

$$\sigma_T^1(k_\mu) = \frac{1}{\sigma_L^2(k_\mu)} \qquad \sigma_L^1(k_\mu) = \frac{1}{\sigma_T^2(k_\mu)} \tag{3.100}$$

This is a peculiar relation which we now explain, starting with the special case when $d = 3$ and g_4^2 is constant. Here $\Sigma_A = 1/g_4^2$ is independent of position and the inversion $\Sigma_A(r) \to 1/\Sigma_A(r)$ only involves an inversion of the coupling constant g_4^2. At the quadratic level in the supergravity action this coupling can be scaled out and does not affect the dynamics, and so (3.100) actually relates σ_L to σ_T in the same theory: $g_4^2 \sigma_T = 1/(g_4^2 \sigma_L)$. This symmetry of the equations of motion is actually a consequence of electric-magnetic duality in four bulk dimensional electromagnetism. Switching E and B is equivalent to interchanging longitudinal electric fields E_z for transverse currents j^x and vice-versa. This relates the two sides of the relations in (3.100); this connection has been emphasized previously in [62].

To understand why a similar relation might hold in higher dimension, we should note that the bulk dynamics can always be reduced to an effective four-dimensional system by dimensional reduction along all dimensions not equal to r, t, x, z. The kinetic term for the gauge field is then

$$S = \int d^d x \frac{1}{g_{d+1}^2(r)} \sqrt{-h} g_{xx}^{\frac{d-3}{2}} F_{ab} F^{ab}, \tag{3.101}$$

where a, b are in the four dimensional space parametrized by r, t, x, z and h_{ab} is the metric on this space. The equations of motion from this action are identical to those of four-dimensional electromagnetism with position-dependent gauge coupling

$$\frac{1}{g_4^2(r)} = \frac{1}{g_{d+1}^2(r)} g_{xx}^{\frac{d-3}{2}} = \Sigma_A \tag{3.102}$$

On the other hand this theory is dual by standard four-dimensional electric-magnetic duality to a theory with inverted gauge coupling $g_4^2(r)$. Thus if two $(d+1)$ dimensional bulk theories satisfy (3.99), then the effective four-dimensional dynamics of these two theories are related by electric-magnetic duality. This relation manifests itself in (3.100). For $d = 3$ and constant g_{d+1}^2 such an expression is thought to be related to a non-Abelian generalization of particle-vortex duality in the boundary theory [62]; it would be interesting to find a similar boundary interpretation for the $d \neq 3$ case (3.100).

3.D The Einstein relation for arbitrary charged black branes

In the text we computed independent expressions for σ and D, the conductivity and diffusion constant for an arbitrary conserved current in any field theory with a gravity dual. To complete our discussion we now compute the charge susceptibility Ξ for an arbitrary charged black brane.

The charge density of the dual theory is $\rho = j^t(r \to \infty)$ and the chemical potential is $\mu = A_t(r \to \infty)$. To evaluate the susceptibility we require ρ to linear order in μ, $\rho(T, \mu) \equiv \Xi(T)\mu$. We consider a static bulk field configuration depending only on r. Examining (3.89) and (3.90), we obtain

$$\partial_r j^t = 0 \tag{3.103}$$

$$\partial_r A_t = \frac{g_{rr} g_{tt}}{G} j^t \tag{3.104}$$

with the immediate solution

$$j^t(r) = \rho = \text{const} \tag{3.105}$$

$$A_t(r) = A_t(r_0) + \rho \int_{r_0}^{r} dr' \frac{g_{rr} g_{tt}}{G} \tag{3.106}$$

Horizon regularity requires $A_t(r_0) = 0$, giving us $\mu = A_t(r \to \infty) = \rho \Xi^{-1}$ with

$$\Xi = \left[\int_{r_0}^{\infty} dr' \frac{g_{rr} g_{tt} g_{d+1}^2}{\sqrt{-g}} \right]^{-1} \tag{3.107}$$

Comparing with (3.68) and (3.44), we see that the Einstein relation

$$\sigma = \Xi D \tag{3.108}$$

is indeed satisfied for any black brane.

3.E Dimensional reduction for gravitational shear mode

As emphasized in [34], the relevant equations for gravitational shear mode fluctuations can be mapped onto an electromagnetism problem. Consider a metric perturbation of the form

$$g_{a\nu}(r) \to g_{a\nu}(r) + g_{aa}(r)h^a_\nu(r,t,z) \tag{3.109}$$

where a is a spatial direction that is not equal to z. Compare this to the standard form of the metric used in a Kaluza-Klein reduction along the a direction:

$$ds^2 = g_{MN}dx^M dx^N = g_{\alpha\beta}dx^\alpha dx^\beta + g_{aa}(dx^a + A_\beta dx^\beta)^2 \tag{3.110}$$

where the indices α, β omit the a direction and A_β is an effective $(d-1)$ dimensional gauge field. This is exactly the form of the perturbation (3.109), provided we set $A_\beta = h^a_\beta$. However since nothing depends on the a direction, we can integrate out a from the Einstein-Hilbert action constructed from (3.110). Standard dimensional reduction formulae (see e.g. [71]) give us the kinetic term for A

$$S = -\frac{1}{16\pi G_N}\int dx^a \int d^{d-1}x\sqrt{-g}g_{aa}F_{\alpha\beta}F^{\alpha\beta} \tag{3.111}$$

where F is the field strength tensor of A, which in terms of metric perturbations is $F_{\alpha\beta} = \partial_\alpha h^a_\beta - \partial_\beta h^a_\alpha$. Here the determinant $\sqrt{-g}$ is that of the full d-dimensional metric. This action is of exactly the standard Maxwell form (3.87) with an effective coupling for the gauge field

$$\frac{1}{g^2_{d+1}} = \frac{1}{16\pi G_N}g_{xx} \tag{3.112}$$

as claimed in the text.

Chapter 4

The finite-density state in AdS/CFT

4.1 Some inspiration

In the previous chapters we first built the formalism and then studied the dynamics of the finite-temperature state in AdS/CFT. In this chapter we will change our focus to the finite-*density* state: we now seek to understand the dynamics of a finite density of strongly correlated excitations charged under a global symmetry. Before plunging into holography it is good to remind ourselves why there is actually a need to understand the dynamics of strongly-interacting systems at finite density by thinking about the dynamics of a *weakly*-interacting system at finite density – i.e. an ordinary metal.

For over fifty years our understanding of the low-temperature properties of metals has been based on Landau's theory of Fermi liquids. In Fermi liquid theory, the ground state of an interacting fermionic system is characterized by a Fermi surface in momentum space, and the low energy excitations are weakly interacting fermionic quasiparticles near the Fermi surface. This picture of well-defined quasiparticles close to the Fermi surface provides a powerful tool for obtaining low temperature properties of the system and has been very successful in explaining most metallic states observed in nature, from liquid ^3He to heavy fermion behavior in rare earth compounds.

Since the mid-eighties, however, there has been an accumulation of metallic materials whose thermodynamic and transport properties differ significantly from those predicted by Fermi liquid theory [92, 93]. A prime example of these so-called non-Fermi liquids is the strange metal phase of the high T_c cuprates, a funnel-shaped region in the phase diagram emanating from the optimal doping at $T = 0$, the understanding of which is believed to be essential for deciphering the mechanism for high T_c superconductivity. The anomalous behavior of the strange metal—perhaps most prominently the simple and robust linear temperature dependence of the resistivity—has resisted a satisfactory theoretical explanation for more than 20 years. While photoemission experiments in the strange metal phase do reveal a sharp Fermi surface in momentum space, various anomalous behavior including the "marginal Fermi liquid" [110] form of the spectral function and the linear-T resistivity imply that quasiparticle descrip-

tion breaks down for the low-energy excitations near the Fermi surface [110, 111]. Other non-Fermi liquids include heavy fermion systems near a quantum phase transition [85], where similar anomalous behavior to the strange metal has also been observed.

The strange metal behavior of high T_c cuprates and heavy fermion systems thus challenges us to formulate a low energy theory of an interacting fermionic system with a sharp surface but without quasiparticles. We will now demonstrate that essentially the simplest possible finite-density state that can be modeled in holography supports fermionic excitations that satisfy precisely these properties.

Note that while the underlying UV theories in which our models are embedded most likely have no relation with the UV description of the electronic system underlying the strange metal behavior of cuprates or a heavy fermion system, it is tantalizing that they share striking similarities in terms of infrared phenomena associated with a Fermi surface without quasiparticles. This points to a certain "universality" underlying the low energy behavior of these systems. The emergence of an infrared fixed point and the associated scaling phenomena, which dictate the electron scattering rates and transport, could provide important hints in formulating a low energy theory describing interacting fermionic systems with a sharp surface but no quasiparticles.

4.2 The Reissner-Nordstrom black brane

Recall that our primary interest is to study systems at a finite density (and temperature). More specifically, we would like to study field theory states carrying a charge under a $U(1)$ current that we will call $J^\mu(x)$; this current is dual to a bulk gauge field $A_M(z,x)$, and so the global $U(1)$ symmetry in the field theory is represented by a $U(1)$ *gauge* symmetry in the gravitational description.

To create a nonzero charge density ρ we should turn on a finite chemical potential μ for the current; this corresponds to perturbing the CFT by the operator

$$\delta S_{U(1)} = \mu \int d^4x \; J^t. \tag{4.1}$$

Note that both conformal and Lorentz symmetries are broken by the introduction of the chemical potential, $\mu \neq 0$; thus we now expect our field theory to have a nontrivial RG flow, and we expect it to be somehow *different* in the time and spatial directions.

We turn now to the study of this state from gravity. Analogously to the scalar case discussed above, the boundary value of the gauge field A_μ is equal to the value of the field theory source for J^μ: thus the perturbation (4.1) means that we should study a classical gravity solution where the gauge field $A_t(z)$ at the boundary takes some nonzero value $A_t(z \to 0) = \mu$. The relevant action is now (2.1) but with the addition of the Maxwell term for the gauge field,

$$S = \frac{1}{2\kappa^2} \int d^4x \, \sqrt{-g} \left[\mathcal{R} + \frac{6}{R^2} + \frac{R^2}{g_F^2} F_{MN} F^{MN} \right] . \tag{4.2}$$

g_F is a bulk gauge coupling; the factors of R in its definition combine with the dimensional Newton's constant κ^2 out front to make it dimensionless.

The solution that satisfies the relevant boundary condition is that of a charged Reissner-Nordstrom black hole[1] [89, 90]. Any field theory state at finite temperature is dual to a black hole in the bulk, and the charge carried by the black hole is directly related to the charge density of the field theory state. The ratio of the temperature T to the chemical potential μ is a dimensionless ratio characterizing the black hole; as we are mostly interested in zero-temperature physics we will focus on the case when $\frac{T}{\mu} = 0$, in which case the metric and background gauge field are given by

$$ds^2 = \frac{R^2}{z^2}(-f dt^2 + d\vec{x}^2) + \frac{R^2}{z^2}\frac{dz^2}{f} \tag{4.3}$$

with

$$A_t = \mu(1 - \mu_* z), \quad f = 1 + 3\mu_*^4 z^4 - 4\mu_*^3 z^3, \quad \mu_* \equiv \frac{\mu}{\sqrt{3}g_F} \tag{4.4}$$

Compare this to (2.2): the nontrivial function $f(z)$ indicates that the physics is changing with scale. The horizon of the black hole is at the radial coordinate $z_* \equiv \frac{1}{\mu_*}$ where $f(z_*) = 0$. Note that the chemical potential μ is the only scale of the system and provides the basic energy unit. For convenience we introduce the appropriately rescaled μ_*, which will be used often below as it avoids having the factor $\sqrt{3}g_F$ flying around.

Note now that for small $z \ll z_*$ we have $f \sim 1$, and the metric resembles that of pure AdS (2.2) with no chemical potential; this is telling us that physics at energy scales much larger than the chemical potential μ is simply that of the conformal vacuum, as expected. However at $z \sim z_*$ the geometry is very different: f has a double zero at the horizon $z = z_* \equiv \frac{1}{\mu_*}$, with

$$f(z) \approx 6\frac{(z_* - z)^2}{z_*^2} + \cdots, \quad z \to z_* \tag{4.5}$$

As a result the horizon is actually an infinite proper distance away. In fact, the near-horizon geometry factorizes into $\mathrm{AdS}_2 \times \mathbb{R}^2$:

$$ds^2 = \frac{R_2^2}{\zeta^2}(-dt^2 + d\zeta^2) + \mu_*^2 R^2 d\vec{x}^2 \qquad A = \frac{g_F}{\sqrt{12}\zeta}dt. \tag{4.6}$$

Here we have defined a new radial coordinate ζ and R_2 is the curvature radius of AdS_2,

$$\zeta \equiv \frac{z_*^2}{6(z_* - z)}, \qquad R_2 \equiv \frac{R}{\sqrt{6}}. \tag{4.7}$$

The metric (4.6) applies to the region $\frac{z_* - z}{z_*} \ll 1$ which translates into $\mu\zeta \gg 1$.

Note that if we are at a nonzero temperature, the function $f(z)$ will then develop a

[1]Here we say "black hole" even though the horizon is planar with topology $\mathbb{R}^2$; it would perhaps be more accurate to say "black brane."

first-order zero at some z_T, and for large temperatures this asymptotic AdS_2 structure will be lost. If we are interested in asymptotically small temperatures there is an alternative scaling limit in which we take $T \to 0$, $\frac{\omega}{T} = \text{const}$; this results in the AdS_2 identified above being replaced by an AdS_2 black hole [19].

As discussed in [19] the near-horizon AdS_2 region plays a crucial role in determining the low energy behavior of the boundary theory. At a heuristic level, as we increase ζ, because of the warp factor $1/\zeta^2$ before dt^2, the local proper time $d\tau = \frac{R_2 dt}{\zeta}$ is increasingly redshifted compared to the boundary time t. As a result, local bulk processes, say with a duration $\delta\tau$, happening at increasingly larger values of ζ corresponds to increasingly longer *time* $\delta t = \frac{\zeta}{R}\delta\tau$ processes in the boundary theory. Similarly a process with local proper energy δE translates into lower and lower energies $\delta\omega \sim \frac{\delta E R_2}{\zeta}$ in the boundary theory as ζ is increased. Note that there are no such dilatations in spatial directions and spatial momenta.

We now note that the metric (4.6) has a scaling isometry

$$t \to \lambda t, \qquad \zeta \to \lambda\zeta, \qquad \vec{x} \to \vec{x} \tag{4.8}$$

under which only the time coordinate scales (compare this to the relevant scaling symmetry for Lorentz-invariant AdS_4 (2.3) in which the spatial and time coordinates scale in the same way.) In fact the AdS_2 region is invariant under a full $SL(2,\mathbb{R})$ isometry group.

These features have led [19] to argue that at low energies the system is described by a (0+1)-dimensional CFT (from now on called the *IR CFT*) which is dual to $AdS_2 \times \mathbb{R}^2$. The IR CFT is $(0+1)$ dimensional as the nontrivial scaling behavior happens only in the time direction, with the $\mathbb{R}^2$ directions essentially becoming spectators.[2] It is crucial to note that this conformal invariance has nothing to do with the CFT_3 in the ultraviolet, whose conformal invariance was completely broken by the chemical potential. This new IR CFT is *emergent*, and appears to have to do with the collective motion of the large number of charged excitations sustaining the background charge density.

We stress that while we do not have an explicit Lagrangian description of this IR CFT, using our dual gravity description we can compute most observables. For example, consider the UV operator $\mathcal{O}$ discussed above. It is dual to a bulk field ϕ with mass m related to its UV conformal dimension by (2.7), and we now also allow it to have a charge q. We now expect its Fourier transform $\mathcal{O}_k(t)$ to match onto some operator $\Phi_k(t)$ in the IR CFT. Just as above, we can compute the conformal dimension δ_k of $\Phi_k(t)$ by studying classical solutions of ϕ in the AdS_2 geometry; we find the IR analog of (2.7) :

$$\delta_k = \frac{1}{2} + \nu_k \tag{4.9}$$

[2]Similar to the S^5 in $AdS_5 \times S^5$ for $\mathcal{N} = 4$ SYM theory.

with

$$\nu_k = \sqrt{m^2 R_2^2 - q_*^2 + \frac{1}{4} + \frac{k^2}{6\mu_*^2}}, \quad k = |\vec{k}|, \quad q_* = \frac{q g_F}{\sqrt{12}} . \tag{4.10}$$

Equation (4.10) has some interesting features. Firstly, the IR dimension depends on the momentum momentum k: as a result operators with larger k become less important in the IR. Note, however, this increase with momentum only becomes significant as $k \sim \mu$. For $k \ll \mu$, we can approximately treat δ_k as momentum independent. Secondly ν_k decreases with q, i.e. an operator with larger q will have more significant IR fluctuations (given the same vacuum dimension Δ). From the bulk point of view, this comes about from the coupling to the background electric field strength.

4.3 Low energy behavior of retarded Green functions

Let us now turn to the main observable that we will study; the retarded Green's function for an operator $\mathcal{O}$,

$$G_R(t, \vec{x}) \equiv i\theta(t) \operatorname{tr} \left(\rho [\mathcal{O}(t, \vec{x}), \mathcal{O}(0)]_\pm \right), \tag{4.11}$$

where ρ is the density matrix characterizing the ensemble and the notation $[,]_\pm$ refers to a commutator for scalars and an anticommutator for spinors. The retarded Green's function carries all of the real-time information about the response of the system: in particular, its imaginary part is proportional to the spectral density $A(\omega, k) = \frac{1}{\pi} \mathrm{Im}\, G_R(\omega, k)$. For real-life systems the spectral density of the electron operator can actually directly be measured in ARPES experiments, making the retarded Green's function a very important observable.

We now explicitly compute the low-energy retarded Green's function $G_R(\omega, k)$ for a scalar operator considered above. Basically our task is to understand how the expansion coefficients A, B in (2.10) behave at low frequencies; we expect the IR CFT identified above to play an important role in determining this low-energy behavior. Before embarking on this calculation we first simply state the final result. The reader who is impatient may take this result and move on to the next section:

$$G_R(\omega, \vec{k}) = \mu_*^{2\Delta - 3} \frac{b_+(\omega, k) + b_-(\omega, k) \mathcal{G}_k(\omega) \mu_*^{-2\nu_k}}{a_+(\omega, k) + a_-(\omega, k) \mathcal{G}_k(\omega) \mu_*^{-2\nu_k}} . \tag{4.12}$$

The various objects appearing in this formula deserve explanation. $\mathcal{G}_k(\omega)$ is the Green's function in the IR CFT for the IR operator Φ_k; it provides "universal" data that depends only on the IR CFT. Due to the emergent conformal invariance at zero temperatures it behaves as $\omega^{2\nu_k}$ with ν_k defined in (4.10). $a_\pm$ and $b_\pm$ are quantities that arise from the solving the equations of motion in the full UV region; the key fact here is that they are analytic in ω and have a smooth $\omega \to 0$ limit. They can be thought of as encoding the non-universal physics of the flow down from the UV to

the IR CFT.

We now present the derivation of this formula. We follow closely the discussion of [19] to which we refer readers for more details. The equation of motion (in momentum space) for ϕ in the charged black hole geometry (4.3) can be written as

$$z^4\partial_z\left(\frac{f}{z^2}\partial_z\phi\right)+z^2\left(\frac{(\omega+qA_t)^2}{f}-k^2\right)\phi-m^2R^2\phi=0\,. \tag{4.13}$$

Recall from (2.6) that near the AdS_4 boundary $\phi(z)$ has the standard asymptotic behavior $\phi(z\to 0)\sim Az^{3-\Delta_+}+Bz^{\Delta_+}$ and that the correlator we seek to compute can be written as

$$G_R(\omega,\vec{k})=\frac{B}{A} \tag{4.14}$$

provided that ϕ is an in-falling wave at the horizon.

We are interested in the behavior of G_R in the low frequency limit ($\omega\ll\mu$). However, we cannot directly perform a perturbative expansion in ω in (4.13) since the ω-dependent term becomes singular and dominates at the horizon where $f(z_*)\to 0$, no matter how small ω is. This is not just a technicality; physically this reflects the abundance of critical modes coming from the IR CFT and is of tremendous importance.

To deal with it, it is useful to isolate the near-horizon $AdS_2\times\mathbb{R}^2$ region (4.6) (which will be referred to as the IR region) from the rest of the black hole spacetime (which will be referred to as the UV region). In the IR AdS_2 region the ω dependence will be treated non-perturbatively. The crossover between the two regions happens near the boundary of AdS_2 with $\frac{1}{\mu}\ll\zeta\ll\frac{1}{\omega}$, where $\mu\zeta\sim\frac{z_*}{z_*-z}$ remains big so that we are still in the near-horizon region, but the ω-dependent term $z_*^2\frac{\omega^2}{f}\sim\omega^2\zeta^2$ in (4.13) becomes small. In the UV region we can treat the small ω limit using a standard perturbative expansion with the lowest order equation given by setting $\omega=0$ in (4.13).

So we start with a solution in the $AdS_2\times\mathbb{R}^2$ region and evolve it outwards, matching it to a solution in the UV region to determine the coefficients A and B. The scalar wave equation on the $AdS_2\times\mathbb{R}^2$ region (4.6) is

$$-\partial_\zeta^2\phi_{\vec{k}}+\frac{R_2^2m_k^2}{\zeta^2}\phi_{\vec{k}}=\left(\omega+\frac{q_*}{\zeta}\right)^2\phi_{\vec{k}}, \tag{4.15}$$

where $m_k^2=\frac{k^2}{\mu_*^2R^2}+m^2$ and $q_*=\frac{qq_F}{\sqrt{12}}$. As we are computing a retarded correlator we are looking for an *in-falling* solution at the black hole horizon. Expanding (4.15) near the black hole horizon, we find two solutions

$$\phi(\zeta\to\infty)\sim e^{\pm i\omega\zeta} \tag{4.16}$$

of which the positive root is the infalling solution. We now take this infalling solution and evolve it to the boundary of the AdS_2 region. The solutions to (4.15) now have the expansion near the AdS_2 boundary

$$\phi_{\vec{k}}(\zeta\to 0)\sim\alpha\zeta^{\frac{1}{2}+\nu_k}+\beta\zeta^{\frac{1}{2}-\nu_k} \tag{4.17}$$

where ν_k is defined in (4.10). Compare this to (2.6); it implies that the conformal dimension of the IR operator $\Phi_{\vec{k}}$ is $\delta_k = \frac{1}{2} + \nu_k$, as claimed in (4.9). However now recall that the ratio $\frac{\beta}{\alpha}$ is for an infalling solution by *definition* equal to the IR CFT Green's function for $\Phi_{\vec{k}}(t)$ in the IR CFT, by the IR analog of (4.14). Thus up to an overall constant we can write the above solution as

$$\phi(\zeta) = \zeta^{\frac{1}{2}-\nu_k} + \mathcal{G}_k(\omega)\zeta^{\frac{1}{2}+\nu_k}. \tag{4.18}$$

$\mathcal{G}_2(\omega)$ can be found explicitly by directly solving (4.15) and is recorded below in (4.27). Even without calculation we can see from conformal invariance that it must behave as $\mathcal{G}_2(\omega) \sim \omega^{2\nu_k}$.

We now need to continue evolution all the way to the asymptotically AdS_4 region to extract the coefficients A and B. We thus need to match the IR solution (4.18) to a solution in the UV region. Now that we are out of the dangerous IR region, to leading order we can set $\omega = 0$ in (4.13) in the UV region. The resulting equation has two independent solutions $\eta_\pm^{(0)}$ which can be specified by their behavior near $z \to z_*$ as

$$\eta_\pm^{(0)}(z) \to \left(\frac{6(z_* - z)}{z_*}\right)^{-\frac{1}{2}\pm\nu_k} = \left(\frac{\zeta}{z_*}\right)^{\frac{1}{2}\mp\nu_k}, \quad z \to z_* \tag{4.19}$$

with the corresponding asymptotic behavior as $z \to 0$ as

$$\eta_\pm^{(0)}(z) \approx a_\pm^{(0)}(k)\left(\frac{z}{z_*}\right)^{3-\Delta} + b_\pm^{(0)}(k)\left(\frac{z}{z_*}\right)^{\Delta}. \tag{4.20}$$

$a_\pm^{(0)}(k)$ and $b_\pm^{(0)}(k)$ thus defined are (dimensionless) functions of k which can be computed numerically.

In the overlapping region both (4.18) and (4.19) apply, which determines the full UV solution to be

$$\phi(z) = \eta_+^{(0)}(z) + \mathcal{G}_k(\omega) z_*^{2\nu_k}\eta_-^{(0)}(z). \tag{4.21}$$

Equation (4.21) can be generalized to higher orders in ω^3 (for details see [19])

$$\phi(z) = \eta_+(z) + \mathcal{G}_k(\omega) z_*^{2\nu_k}\eta_-(z) \tag{4.23}$$

where

$$\eta_\pm = \eta_\pm^{(0)} + \omega\eta_\pm^{(1)} + O(\omega^2) \tag{4.24}$$

are the two linearly independent perturbative solutions to the full UV region equation. Near $z = 0$, $\eta_\pm$ have the expansion of the form (4.20) with various coefficients $a_\pm^{(0)}, b_\pm^{(0)}$

[3]Note that for a neutral scalar with $q = 0$, equation (4.13) only depends on ω^2 and the expansion parameter in (4.24) and (4.25) should be ω^2, i.e.

$$a_+(k,\omega) = a_+^{(0)}(k) + \omega^2 a_+^{(2)}(k) + O(\omega^4) \tag{4.22}$$

replaced by $a_\pm, b_\pm$ which have an analytic ω-expansion such as

$$a_+(k,\omega) = a_+^{(0)}(k) + \omega a_+^{(1)}(k) + \cdots \ . \tag{4.25}$$

Note that since both the boundary conditions specifying $\eta_\pm$ (4.19) and the equation (4.13) are real, $a_\pm, b_\pm$ are real. From (4.23) and the expansion of $\eta_\pm$ near $z = 0$ we thus find the boundary theory Green's function to be

$$G_R(\omega,\vec{k}) = \mu_*^{2\Delta-3}\frac{b_+(\omega,k) + b_-(\omega,k)\mathcal{G}_k(\omega)\mu_*^{-2\nu_k}}{a_+(\omega,k) + a_-(\omega,k)\mathcal{G}_k(\omega)\mu_*^{-2\nu_k}} \ . \tag{4.26}$$

This is the result claimed above. The remaining task is to compute $\mathcal{G}_2(\omega)$; if we explicitly solve the relevant wave equations in the pure AdS_2 region we see that for a scalar it is given by [19]

$$\mathcal{G}_k(\omega) = \frac{\Gamma(-2\nu_k)}{\Gamma(2\nu_k)}\frac{\Gamma(\frac{1}{2}+\nu_k - iq_*)}{\Gamma(\frac{1}{2}-\nu_k - iq_*)}(-2i\omega)^{2\nu_k} \ . \tag{4.27}$$

This can be written as $\mathcal{G}_2(\omega) = c(k)\omega^{2\nu_k}$ where $c(k)$ has an imaginary part.

We conclude this discussion with some remarks:

1. The preceding discussion was all at zero temperature. At a small finite temperature we must replace the asymptotic AdS_2 geometry (4.6) with an AdS_2 black hole. The AdS_2 Green's function takes the form $\mathcal{G}_2(\omega) = T^{2\nu_k} f\left(\frac{\omega}{T}\right)$ where f is a scaling function that can be determined explicitly. The explicit formula for a charged scalar at finite temperature is [19, 91]

$$\mathcal{G}_2^{(T)}(\omega) = (4\pi T)^{2\nu_k}\frac{\Gamma(-2\nu_k)}{\Gamma(2\nu_k)}\frac{\Gamma(\frac{1}{2}+\nu_k - iq_*)}{\Gamma(\frac{1}{2}-\nu_k - iq_*)}\frac{\Gamma\left(\frac{1}{2}+\nu_k - i\frac{\omega}{2\pi T} + iq_*\right)}{\Gamma\left(\frac{1}{2}-\nu_k - i\frac{\omega}{2\pi T} + iq_*\right)} \ . \tag{4.28}$$

   In addition, there will also be analytic finite-T corrections to $a_\pm, b_\pm$, which can be treated perturbatively in T.

2. We also only considered a scalar. A precisely analogous calculation can be done for a Dirac spinor field in the bulk. Some of the details are different (and will be discussed in the section on fermions below) but at the end of the day the formula (4.26) still applies to each of the *eigenvalues* of the Green's function, which is now a matrix in spinor space. However a key point is that the corresponding IR CFT correlators are *different* for fermions and bosons, which we will discuss below.

4.4 Some physics: bosons v.s. fermions

Much of the rest of this thesis will be spent on the study of (4.26). It is now helpful to take a step back and ask precisely what sort of physics we are searching for. We seek

to understand the low-energy physics of these systems; to that end, let's sit at some generic value of k and study the spectral properties of (4.26) at a small frequency. The full imaginary part of the correlator comes from the AdS_2 part, and so we find

$$\mathrm{Im}\, G_R(\omega, k) \sim \mu_*^{2\Delta-3} \frac{a_+ b_- - a_- b_+}{a_+^2} \mathrm{Im}\, \mathcal{G}_2(\omega) + ... \sim \mathrm{Im}\,[c(k)]\, \omega^{2\nu_k} + ... \qquad (4.29)$$

It is interesting that we always find some nonzero spectral weight, at *any* k; this is a consequence of the AdS_2 IR CFT, which contributes gapless degrees of freedom at any momentum. This is quite different from the situation in more "ordinary" gapless systems, like a free massless boson or a Lorentz-invariant CFT, in which case one finds gapless degrees of freedom only about the specific *point* in momentum space $k = 0$. Note also the emergent scale invariance in ω.

To find more physics, however, we must search for more interesting structure in (4.26); we will find it in two special cases:

1. The coefficient $a_+(k)$ might *vanish*. This might happen at some special $k \equiv k_F$, or we might find some other way to tune it. This will lead to a pole in the retarded Green's function at zero frequency (note that $\mathcal{G}_2(\omega \to 0) = 0$). If we move slightly away from $k = k_F$ the pole will move off of the origin and into the complex ω plane.

2. The conformal dimension $\frac{1}{2} + \nu_k$ of the IR CFT operator might go imaginary. Recall that for a scalar the conformal dimension this dimension is given by

$$\nu_k = \sqrt{m^2 R_2^2 - q_*^2 + \frac{1}{4} + \frac{k^2}{6\mu_*^2}}, \quad k = |\vec{k}|, \quad q_* = \frac{q g_F}{\sqrt{12}} \qquad (4.30)$$

   and so for a sufficiently small mass or a sufficiently large charge we will find an imaginary ν_k. This is related to the violation of a Breitenlohner-Freedman bound [125] in the AdS_2 region. A complex conformal dimension seems peculiar, and it can be shown after some algebra (performed in some detail in Chapter 8) that this too leads to (an infinite number of) poles in the complex ω plane.

However, the interpretation of these two cases is very different depending on whether we are studying fermions or bosons. It is not difficult to show that if we are studying *fermions*, then the poles described above are always in the *lower half ω-plane*. The excitations represented by these poles are then decaying exponentially in time, and this means that they represent actual finite-lifetime excitations in the theory. Indeed we will interpret the first case described above, where there are singularities in a surface in k-space, as evidence for the existence of a Fermi surface, just as the case for a free Fermi liquid. We shall see that the existence of the AdS_2 region will introduce new effects, making it a non-Fermi liquid.

On the other hand, if we are studying bosons, then in the first case above the pole can move through to the *upper half ω-plane* as we vary k, and in the second case (imaginary ν_k) the infinite number of poles will always be in the upper-half

ω-plane. Poles in the upper-half plane of a retarded Green's function have a very different interpretation; they indicate a mode growing exponentially in time and thus an instability of the vacuum. In other words, the bulk scalar is trying to condense. When it is just on the verge of condensing it is a phase transition, and if we can arrange for this to happen at zero temperature (as we shall in Chapters 7 and 8) it is a *quantum phase transition.*

The demonstration that poles are in the upper-half plane for bosons and the lower-half plane for fermions is not difficult and is performed in [19]. While we do not repeat the computation here, we do stress that this follows from very general principles of the spectral properties of Green's functions for bosons and fermions. Although in the bulk we are dealing with classical equations of scalars and spinors and have not imposed any statistics, the self-consistency of AdS/CFT implies that the classical equations for bulk scalars and spinors should encode the *quantum statistics* of the boundary theory and we see that this is indeed the case.

Thus we see that the same formula (4.26) contains within it the both the physics of non-Fermi liquids and quantum phase transitions – two of the finite-density problems addressed in the introduction. The remainder of this thesis will study them each in turn.

Chapter 5

Holographic non-Fermi Liquids

5.1 Some philosophy: where is the Fermi surface?

In the previous section, we described a finite-density state with a rather simple holographic description (4.3). We know that it is a finite-density state by *construction*; we engineered it in the bulk to have a nontrivial gauge field configuration, which resulted in a nonzero value for the boundary theory charge density. However one may now ask some very natural questions about the field-theory interpretation of this state:

1. What sort of excitations are carrying the charge density? Are they bosons or fermions?

2. If they are fermions, does our system have a Fermi surface? How do we see it?

The answers to these questions are surprisingly tricky. Recall that we did not start with a precise string theory construction above; we simply postulated the existence of a $U(1)$ current in the dual field theory and assumed the very natural form for a *bulk* action (4.2). It is not at all clear from this bulk description what sorts of fundamental field theory excitations carry the charge. In known string theoretical constructions that could result in a four-dimensional action such as (4.2), we believe that at weak coupling there are both bosons and fermions charged under the relevant current. It is rather hard to say which of them will end up carrying the charge at strong coupling – this seems like a *very* complicated dynamical question – and thus it is hard to say whether or not we *expect* the system should have a Fermi surface.

On the other hand, it is precisely such dynamical questions that gravity should solve for us. So rather than worrying too much about what we expect we will take a very pragmatic approach: we will perform "photoemission" experiments on our black hole. This means that we will simply take a fermionic operator Ψ in the field theory and calculate its retarded response function $G_R(\omega, k)$ using the techniques detailed above. If the system has a Fermi surface, we should see its signature in *non-analytic behavior in $G_R(\omega, k)$ at a shell in momentum space $k = k_F$*. Without further ado, let us finally search for this potential Fermi surface.

5.2 Setup

Our fermionic operator $\Psi(x)$ is dual to a bulk spinor field $\psi(z,x)$. We will assume a standard Dirac action in the bulk,

$$S = -\int d^4x\sqrt{-g}\; i(\bar{\psi}\Gamma^M\mathcal{D}_M\psi - m\bar{\psi}\psi), \tag{5.1}$$

where the covariant derivative $\mathcal{D}_M$ contains couplings to both the background gauge field and the spin connection,

$$\mathcal{D}_M = \partial_M + \frac{1}{4}\omega_{abM}\Gamma^{ab} - iqA_M. \tag{5.2}$$

As expected, here q is the charge of Ψ under the $U(1)$ current J^μ. The asymptotic structure of solutions to (5.1) is different from the scalar case discussed above, essentially because it is a first order system with more components. Note that the bulk spinor ψ has four components; however it is dual to a boundary theory operator Ψ which has only two components, as expected for a three-dimensional field theory. We discuss how this comes about in Chapter 2.3, but the upshot is that the UV dimension Δ_+ of Ψ is related to the bulk mass by

$$\Delta_+ = \frac{3}{2} + mR, \tag{5.3}$$

and the boundary theory Green's function can be diagonalized to take the form

$$G_R(\omega,k) = \begin{pmatrix} G_1(\omega,k) & 0 \\ 0 & G_2(\omega,k) \end{pmatrix}, \tag{5.4}$$

where the momentum k has been taken to be along one of the spatial directions and both $G_{\alpha=1,2}$ are the ratio of appropriately defined boundary theory expansion coefficients A_α, B_α, as in (2.10)

$$G_\alpha = \frac{B_\alpha}{A_\alpha}. \tag{5.5}$$

The master formula (4.26) applies to both of the eigenvalues $G_{1,2}$, which will have different values for the prefactor in the AdS_2 Green's function and the UV expansion coefficients $a_\pm, b_\pm$. A useful relation (shown in [19]) is $G_1(\omega,k) = G_2(\omega,-k)$; this means that from now on with no loss of generality we can simply restrict to G_1; when we refer to G_R in the rest of this section this is what we mean.

Now by studying the behavior of the Dirac equation in the AdS_2 reason, we can find the dimension δ_k of the spinor operator in the IR CFT to be

$$\delta_k = \frac{1}{2} + \nu_k \qquad \nu_k = \sqrt{m^2R_2^2 - q_*^2 + \frac{k^2}{6\mu_*^2}}. \tag{5.6}$$

Note this is slightly different from the corresponding result for the charged scalar

(4.10). Similarly, the AdS_2 Green's function is also slightly different,

$$\mathcal{G}_2(\omega) = \frac{\Gamma(-2\nu_k)}{\Gamma(2\nu_k)}\frac{\Gamma(1+\nu_k-iq_*)}{\Gamma(1-\nu_k-iq_*)}\frac{\left(m+\frac{ikR}{\mu_*}\right)R_2 - iq_* - \nu_k}{\left(m+\frac{ikR}{\mu_*}\right)R_2 - iq_* + \nu_k}(-i\omega)^{2\nu_k} \equiv c(k)\omega^{2\nu} \ . \tag{5.7}$$

The prefactor differs from the scalar case, and indeed its precise structure *is* important for guaranteeing that the poles in the fermionic retarded correlator are always in the lower half plane. Together with the master formula (4.26) which we reproduce here for convenience:

$$G_R(\omega,\vec{k}) = \mu_*^{2\Delta-3}\frac{b_+(\omega,k)+b_-(\omega,k)\mathcal{G}_k(\omega)\mu_*^{-2\nu_k}}{a_+(\omega,k)+a_-(\omega,k)\mathcal{G}_k(\omega)\mu_*^{-2\nu_k}}, \tag{5.8}$$

we now have all the ingredients we need to search for Fermi surfaces.

5.3 $a_+ = 0$: Fermi surfaces

Recall that all of the UV coefficients $a_\pm, b_\pm$ in (5.8) are analytic in ω and k, i.e. we can consider expanding them as follows:

$$a_+(\omega,k) = a_+^{(0)}(k) + a_+^{(1)}(k)\omega + a_+^{(2)}(k)\omega^2 + ... \tag{5.9}$$

Imagine now that $a_+^{(0)}$ vanishes at some value of $k \equiv k_F$: we find $a_+^{(0)}(k_F) = 0$. Before proceeding let us understand what this means; recall that a_+ is the leading UV expansion coefficient of the infrared AdS_2 solution (4.19) that is *regular* in the deep interior of the spacetime. If $a_+(\omega = 0, k) = 0$ for some k, then this means that at this value of k the bulk Dirac equation has a zero-energy solution whose radial profile vanishes both in the deep interior (because we are looking at the + solution in (4.19)) and at the AdS_4 boundary (because the expansion coefficient $a = 0$). This is a normalizable fermion state that is bound to the black hole, and one might call it charged *fermionic hair*. One can verify numerically that several such bound-states exist.

To understand the signature of such bound states in the response function, let us now study the zero frequency behavior of $G_R(\omega, k)$ near $k \sim k_F$; we find simply

$$G_R(\omega = 0, k) \approx \frac{b_+^{(0)}(k_F)}{\partial_k a_+^{(0)}(k_F) k_\perp} \qquad k_\perp = k - k_F \tag{5.10}$$

At $k = k_F$ we have a pole in the Green's function; this is a zero-frequency singularity at a shell in k-space, and so is precisely the signature of a Fermi surface! Let us now turn on a small frequency ω near $k \sim k_F$. Keeping the first few terms in the relevant

expansion of (5.8), we find

$$G_R(\omega,k) \approx \frac{b_+^{(0)}(k_F)}{\partial_k a_+^{(0)}(k_F)k_\perp + \omega a_+^{(1)}(k_F) + a_-^{(0)}(k_F)\mathcal{G}_2(\omega)\mu_*^{-2\nu_{k_F}}} . \tag{5.11}$$

This expression can be written as

$$G_R(\omega,k) \approx \frac{h_1}{k_\perp - \frac{1}{v_F}\omega - \Sigma(\omega)} . \tag{5.12}$$

where we have defined $v_F \equiv -\frac{\partial_k a_+^{(0)}}{a_+^{(1)}}$, $h_1 \equiv \frac{b_+^{(0)}(k_F)}{\partial_k a_+^{(0)}(k_F)}$; these can be found numerically and are positive. This expression looks very much like the propagator for finite-frequency response near a Fermi surface. v_F looks just like a Fermi velocity and is determined from UV data.

However we see a new ingredient when we look at $\Sigma(\omega)$, which plays the role of a self-energy and is given by

$$\Sigma(\omega) = -\frac{a_-^{(0}}{\partial_k a_+^{(0)}(k_F)} \frac{\mathcal{G}_2(\omega)}{\mu_*^{2\nu_{k_F}}} \equiv hc(k)\left(\frac{\omega}{\mu_*}\right)^{2\nu_{k_F}} \tag{5.13}$$

Thus this self-energy is (up to a prefactor) equal to the AdS_2 Green's function. Note that the width of the quasiparticle is simply given by the imaginary part of the Green's function, $\Gamma = \mathrm{Im}\,\Sigma$. But recall now that for a standard Fermi liquid we always have $\Gamma_{FL} = \mathrm{Im}\,\Sigma_{FL}(\omega) \sim \omega^2$, following from basic kinematics of interactions about the Fermi surface. Here, however, we have

$$\Gamma = \mathrm{Im}\,\Sigma \sim \omega^{2\nu_{k_F}} . \tag{5.14}$$

Thus the width of the excitation now has a nontrivial scaling with ω; ν_{k_F} is a nontrivial number, determined from dynamics. In other words, (5.12) is the response function corresponding to a *non-Fermi liquid*; a system with a Fermi surface but whose excitations appear to *not* be Landau quasiparticles.

The dispersion of the pole representing this excitation is the solution to the equation

$$k_\perp - \frac{1}{v_F}\omega_c - \Sigma(\omega_c) = 0 \qquad \omega_c(k) = \omega_*(k) - i\Gamma(k) \tag{5.15}$$

in the complex plane, which we have split into real and imaginary parts ω_* and Γ. The physics turns out to be rather different depending on the value of ν_{k_F}, and we now study the different values in turn. For simplicity of notation in the rest of this section we will drop the subscript k_F: $\nu \equiv \nu_{k_F}$ *in this section only.*

5.3.1 $\nu > \frac{1}{2}$

If $\nu > \frac{1}{2}$, then the analytic linear-in-ω term in (5.12) dominates over the self-energy, which goes like $\omega^{2\nu}$. Thus the dispersion is essentially controlled by the balancing

between the first two terms in (5.15); note however that the sole contribution to the *imaginary* part of the pole comes from the complex self-energy. We find the following expression for the motion of the pole as $k_\perp$ is varied:

$$\omega_c(k_\perp) = v_F k_\perp - v_F hc(k_F) \left(\frac{v_F k_\perp}{\mu_*}\right)^{2\nu} \tag{5.16}$$

Thus we see that this is a linear dispersing quasiparticle $\omega_* = v_F k_\perp$, with width $\Gamma \sim \omega^{2\nu}$ that is always much smaller than the energy ω_*: as we approach the pole $\frac{\Gamma(k)}{\omega_*(k)} \sim k_\perp^{2\nu-1} \to 0$ as $k_\perp \to 0$. Furthermore the residue at the pole is always finite and given by

$$Z = -h_1 v_F \ . \tag{5.17}$$

This is then a stable quasiparticle. It is not *qualitatively* different from the excitations of a Fermi liquid, except that its width satisfies $\Gamma \sim \omega^{2\nu}$ rather than $\Gamma_{FL} \sim \omega^2$. Finally, note that in this range the IR CFT operator corresponding to the fermion has dimension $\delta = \frac{1}{2} + \nu > 1$ and so the operator is *irrelevant* in the AdS_2 sense.

5.3.2 $\nu < \frac{1}{2}$

If $\nu < \frac{1}{2}$, the situation is different. Now in (5.12) the non-analytic contribution from $\Sigma(\omega)$ always dominates over the analytic linear-in-ω correction, which we may completely neglect. The solution to (5.15) now takes the form

$$\omega_c = \mu_* \left(\frac{k_\perp}{hc(k_F)}\right)^{\frac{1}{2\nu}} \tag{5.18}$$

As $c(k_F)$ is complex this pole has both a real and imaginary part; however now they are both coming from the same place, i.e. the AdS_2 Green's function. As a result the dispersion is now nonlinear, $\omega_* \sim k_\perp^{\frac{1}{2\nu}}$. Importantly, the width Γ is now always comparable to the frequency ω_*, e.g. for $k_\perp > 0$ we have

$$\frac{\Gamma(k)}{\omega_*(k)} = -\tan\left(\frac{\arg(c(k_F))}{2\nu}\right) = \text{const} \tag{5.19}$$

A similar expression exists with a different angle for $k_\perp < 0$. Thus as we vary $k_\perp$ through 0, the pole moves along a straight line towards the origin, eventually bouncing off and retreating at another angle (but always in the lower-half plane). The residue at the pole is

$$Z = -\frac{\omega_c h_1}{2\nu k_\perp} \propto k_\perp^{\frac{1}{2\nu}-1}, \tag{5.20}$$

and so actually vanishes as we approach the Fermi surface $k_\perp = 0$. The fact that the width of the quasiparticle is always the same order as its energy and that the residue vanishes at the pole indicate that this is *not* a stable quasiparticle; thus we see that we have a concrete example of a system with a sharp Fermi surface, but with no quasiparticles! Note that in this regime the IR CFT operator corresponding to

the fermion has dimension $\delta = \frac{1}{2} + \nu < 1$, and so is *relevant* in the AdS_2 sense.

5.3.3 $\nu = \frac{1}{2}$: Marginal Fermi Liquid

We turn now to the threshold case between the two studied above. Here we see that the two terms (analytic and AdS_2) are both naively proportional to ω and are thus becoming degenerate. As is often the case when there is such a degeneracy, a logarithmic term in ω is generated. Basically both $a_+^{(1)}$ and $\mathcal{G}_2(\omega)$ have simple poles at $\nu = \frac{1}{2}$; the two divergences cancel and leave behind a finite $\omega \log \omega$ term with a real coefficient,

$$G_R(\omega, k) \approx \frac{h_1}{k_\perp + \tilde{c}_1 \frac{\omega}{\mu_*} \log \frac{\omega}{\mu_*} + c_1 \frac{\omega}{\mu_*}} \tag{5.21}$$

Here $\tilde{c}_1$ is real and c_1 is complex; for more details on the derivation of this formula see Section VI A of [19].

Remarkably, this is of precisely the form postulated in [110] for the response function of the "Marginal Fermi Liquid", a phenomenological model that well describes many properties of the optimally doped cuprates. Here this response function emerges from a first-principles holographic calculation (albeit only at the specially tuned value $\nu = \frac{1}{2}$). Note that here the quasiparticle width is suppressed compared to its energy, but only logarithmically $\Gamma \sim \frac{\omega_*}{\log(\omega_*)}$. Similarly, the quasiparticle residue scales like $Z \sim 1/\log(k_\perp)$ and so also vanishes logarithmically. This logarithmic suppression was the original motivation for the word "Marginal" in the name given in [110]; here we point out that at this point in parameter space the IR CFT operator has dimension $\delta = \frac{1}{2} + \nu = 1$, and so the word "Marginal" refers also to the IR CFT operator and is entirely appropriate. The potential physical applications of this $\nu = \frac{1}{2}$ point make it very interesting, although from our gravitational treatment so far we do not really have any way to single it out.

However, we are left now with a tantalizing question: we have found a system whose single-particle electronic density of states matches with that of the optimally doped cuprates. Is its resistivity also linear in T? To answer this, we will have to compute the contribution of these holographic non-Fermi liquids to the conductivity, a calculation which is the topic of the next chapter.

5.4 ν imaginary

Throughout this discussion we have concentrated on the parameter regime where ν_k (and so the conformal dimension of the IR CFT operator) is *real*. However we see from the formula for ν_k,

$$\nu_k = \sqrt{m^2 R^2 - q_*^2 + \frac{k^2}{6\mu_*^2}} \tag{5.22}$$

that if the charge of the scalar is sufficiently large and k^2 sufficiently small, ν_k can become *imaginary*. Basically we see that the background electric field acts through the spinor charge as an effective "negative mass", making it possible to violate the

Breitenlohner-Freedman bound in the AdS_2 region and resulting in an imaginary conformal dimension. This possibility was alluded to in Section 4.4 above, where it was explained that this leads to an infinite number of poles in the Green's function. This result and its meaning is discussed in substantially more detail in Chapter 7 on holographic quantum phase transitions below, but we mention again that for fermions all of these poles are in the lower-half ω-plane, and so represent quasinormal modes. In the scalar case these poles would have been in the upper-half ω-plane, representing a dynamical instability. For fermions the interpretation of these poles is somewhat more subtle, but we explain below how they do represent the existence of a different ground state at very low energies. First, however, we study the behavior of the Green's function in this region at low frequencies.

5.4.1 Oscillatory behavior

Let us define the imaginary conformal dimension to be

$$\nu_k = -i\lambda_k \qquad \lambda_k = \sqrt{q_*^2 - m^2R^2 - \frac{k^2}{6\mu_*^2}}. \tag{5.23}$$

We now find from (4.26) the leading small frequency behavior

$$G_R(\omega,k) = \mu_*^{2\Delta-3}\frac{b_+^{(0)} + b_-^{(0)}c(k)\left(\frac{\omega}{\mu_*}\right)^{-2i\lambda_k}}{a_+^{(0)} + a_-^{(0)}c(k)\left(\frac{\omega}{\mu_*}\right)^{-2i\lambda_k}}. \tag{5.24}$$

Note now that though the equations obeyed by the $\eta_\pm$ are real, the *boundary conditions* on $\eta_\pm$ have now become complex, and so $a_\pm, b_\pm$ can also be complex. In fact, since we have $\eta_+ = (\eta_-)^*$ at the horizon, we now also have

$$a_+ = (a_-)^* \qquad b_+ = (b_-)^*. \tag{5.25}$$

In particular, at $\omega = 0$ we now have $\mathrm{Im}\, G_R(\omega = 0, k) = \mathrm{Im}\frac{b_+^{(0)}}{a_+^{(0)}} \neq 0$, and thus we have gapless excitations even at precisely zero frequency. At finite frequency the result (5.24) is oscillatory; it is periodic in $\log\omega$ with a period given by $\tau_k = \frac{\pi}{\lambda_k}$, i.e. it is invariant under a *discrete* scale transformation

$$\omega \to e^{n\tau_k}\omega, \qquad n \in \mathbb{Z} \tag{5.26}$$

These features take on rather more significance in the scalar case studied in detail in Chapter 7. Here we simply note that careful study of (5.24) reveals an infinite number of exponentially separated poles in the lower half-plane; as (5.26) shows, there is an accumulation point at $\omega = 0$.

5.4.2 Backreaction and a new ground state

Here we study the implications of the existence of this region in more detail. An useful way to understand this is to study the effective potential for semiclassical charged particles moving in AdS_2 with a background electric field. This represents the same physics as the $mR_2 \to \infty$ limit of the wave equation calculations described above. It is not difficult to show that for $q_* > mR_2$ – when the effective AdS_2 dimension becomes imaginary – a well[1] appears in this effective potential, which becomes deeper as $q \to \infty$. For q the same sign as that of the black hole, this well represents physical particles that have been repelled from the black hole, and one expects that these states should actually be filled. Here we can understand the difference between bosons and fermions: for bosons we have an enormous number of quanta filling the lowest state of the well. This represents the scalar *field* developing a coherent background value and classically condensing. This phenomena is discussed in detail in Chapter 7.

For fermions the interpretation is slightly more subtle. Pauli exclusion now prevents a classical condensation, and the situation was first discussed in [109]. As $q \to \infty$ the well is deep enough that it can be treated via a local WKB approximation, in which we consider free fermions propagating on locally flat space. We now find that the background gauge potential creates a local Fermi surface at each point in the *bulk*. It was shown that the backreaction of the filled fermion states dramatically changes the geometry. Rather than having an infrared $AdS_2 \times \mathbb{R}^2$ sourced by the charge on the black hole, that charge is now carried by the fermions themselves, and the geometry becomes Lifshitz with a finite z.[2] The dynamic exponent z behaves as

$$z \sim (g_F q)^4 \frac{R_2^2}{\kappa^2} \tag{5.27}$$

where κ is the bulk gravitational coupling as in (2.1), q the charge of the fermions, and g_F the bulk gauge coupling. Note that as z has an inverse power of Newton's constant it scales as N^2 and so is very large; essentially this means that at finite energies the physics is very close to that of the AdS_2, but at energies that are exponentially small $E \sim \exp(-\alpha N^2)$ with $\alpha \sim \mathcal{O}(1)$ we will cross over to a regime that is controlled by the finite fermion density and has Lifshitz scaling. The black hole is gone; now we have a hovering density of fermions carrying a finite charge density. Note that it is only visible at exponentially small temperatures ($T \sim \exp(-\alpha N^2)$) and so at the moderately small temperatures imagined above all of the physics described above is unchanged.

This is dual to a genuinely different state of matter and has been studied in more detail in [120, 121, 122, 123]; see also [124]. In these works the couplings involved are assumed to have a different N^2 scaling to those used in these lectures, and so the Lifshitz physics discussed above can be pushed to $\mathcal{O}(1)$ energies. The resulting setup has been dubbed by [120] an "electron star". Note that in all of these systems

[1] If we study only AdS_2 it is not strictly a well as the UV end of it actually admits traveling waves (hence the oscillatory character of (5.24)), but if we consider UV completing this region with an AdS_4 it becomes a bona-fide well that can support localized states.

[2] Recall AdS_2 may formally be considered a limit of $z \to \infty$ Lifshitz.

the finite entropy density of the $AdS_2 \times \mathbb{R}^2$ is resolved by the Lifshitz geometry, and many of the mysterious properties of AdS_2 are replaced by the better-understood properties of weakly-interacting fermions at finite density (albeit moving in an extra holographic direction). For example, we can see magnetic oscillations at tree level in the bulk [121]. The finite temperature physics has been studied in [122, 123], revealing a phase transition back to an ordinary black hole at high temperatures. The interplay between these systems and the AdS_2-dominated non-Fermi liquids described in these lectures deserves to be better understood.

Chapter 6

Transport by holographic non-Fermi liquids

6.1 Introduction

In the previous chapter we reviewed work that showed that non-Fermi liquid behavior emerges naturally in the simplest finite-density state that can be described in AdS/CFT. The low energy behavior of these non-Fermi liquids was shown to be governed by a nontrivial infrared fixed point which exhibits nonanalytic scaling behavior only in the time direction. In particular, the nature of low energy excitations around the Fermi surface is found to be governed by the scaling dimension ν of the fermionic operator in the IR fixed point. For $\nu > \frac{1}{2}$ one finds a Fermi surface with well-defined quasiparticles while the scaling of the self-energy is in general different from that of the Fermi liquid. For $\nu \leq \frac{1}{2}$ one instead finds a Fermi surface without quasiparticles. For $\nu = \frac{1}{2}$ one recovers the "marginal Fermi liquid" (MFL) which has been used to describe the strange metal phase of cuprates.

In this chapter we generalize the discussion of fermionic spectral function to charge transport. We compute the contribution to low temperature optical and DC conductivities from such a non-Fermi liquid. We find that the optical and DC conductivities have a scaling form which is again characterized by the scaling dimension ν of the fermionic operators in the IR. The behavior of optical conductivity gives an independent confirmation of the absence of quaiparticles near the Fermi surface. In particular we find for $\nu = \frac{1}{2}$, which corresponds to MFL, the linear-T resistivity is again recovered.

The non-Fermi liquids disccussed above were found by calculating the fermionic response functions in the finite density state by solving Dirac equation in the black hole geometry (6.4). The Fermi surface has a size of order $O(N^0)$ and various argument in [16, 19] indicate that the fermionic charge density associated with a Fermi surface should also be of order $O(N^0)$. In contrast, the charge density carried by the black hole is given by the classical geometry, giving rise to a boundary theory density of order $\rho_0 \sim O(G_N^{-1}) \sim O(N^2)$. Thus in the large N limit, we will be studying a small part of a large system, with the background $O(N^2)$ charge density essentially

providing a bath for the much smaller $O(N^0)$ fermionic system we are interested in.

The optical conductivity of the system can be obtained from the Kubo formula

$$\sigma(\omega) = \frac{1}{i\omega}\langle J_x(\omega)J_x(-\omega)\rangle_{\text{retarded}} \tag{6.1}$$

where J_x is the current density for the global $U(1)$ in x direction at zero spatial momentum. The right hand side of (6.1) can be computed on the gravity side from the propagator of the gauge field A_x with endpoints on the boundary, as in Fig. 6-1. In a $1/N^2$ expansion, the leading contribution—of $O(N^2)$—comes from the background black hole geometry. This reflects the presence of the charged bath, and not the fermionic system in which we are interested. As discussed earlier, these fermions have a density of $O(N^0)$, and will give a contribution to σ of order $O(N^0)$. Thus to isolate their contribution we must perform a one-loop calculation on the gravity side as indicated in Fig. 6-1. Higher loop diagrams can be ignored since they are suppressed by higher powers in $1/N^2$. This one-loop calculation is similar in spirit to the one-loop calculations of the free energy in [94, 95, 96] where it was shown that the Fermi surface does exhibit quantum oscillations in a magnetic field.

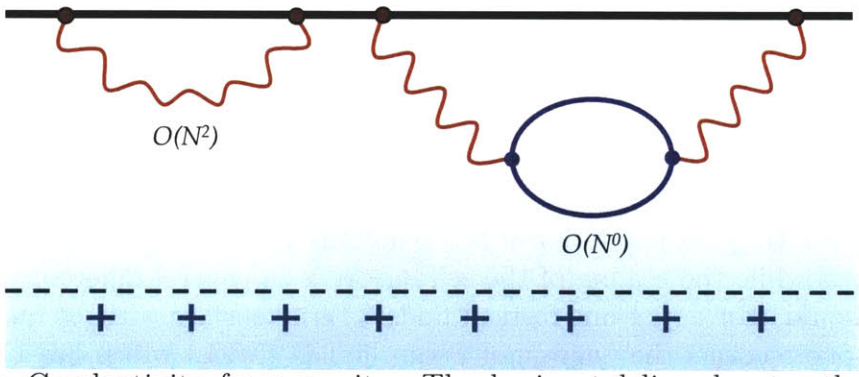

Figure 6-1: Conductivity from gravity. The horizontal line denotes the boundary spacetime, which has $d = 2 + 1$ dimensions, and the vertical axis denotes the radial direction r of the black hole, which is the direction extra to the boundary spacetime. The boundary lies at $r = \infty$. The current-current correlator in (6.23) can be obtained from the propagator of the gauge field A_x with endpoints on the boundary. Wavy lines correspond to gauge field propagators and the dark line denotes the bulk propagator for the ψ field. The left diagram is the tree-level propagator for A_x, while the right diagram includes the contribution from a loop of ψ quanta. The contribution from the Fermi surface associated with boundary fermionic operator $\mathcal{O}$ can be extracted from the diagram on the right.

The one-loop contribution to (6.23) from gravity contains many contributions and we are only interested in the part coming from the Fermi surface, which can be unambiguously extracted. This is possible because conductivity from independent channels is additive, and, as we will see, the contribution of the Fermi surface is *non-analytic* in temperature T as $T \to 0$. We emphasize that the behavior of interest to us is *not* the conductivity that one could measure most easily if one had an experimental

instantiation of this system and could hook up a battery to it. It is swamped by the contribution from the $\mathcal{O}(N^2)$ charge density, which however depends analytically on temperature. In the large-N limit which is well-described by classical gravity, these contributions appear at different orders in N and can be clearly distinguished. In cases where there are multiple Fermi surfaces, we will show that the 'primary' Fermi surface (this term was used in [19] to denote the one with the largest k_F) makes the dominant contribution to the conductivity.

We are now left with a vexing problem – calculations of one-loop Lorentzian processes in a black hole geometry are notoriously subtle. Should one integrate the interaction vertices over the full black hole geometry or only the region outside the black hole? How do we treat the horizon? How do we treat diagrams such as those indicated in Figure 6-2 in which a loop is cut in half by the horizon?

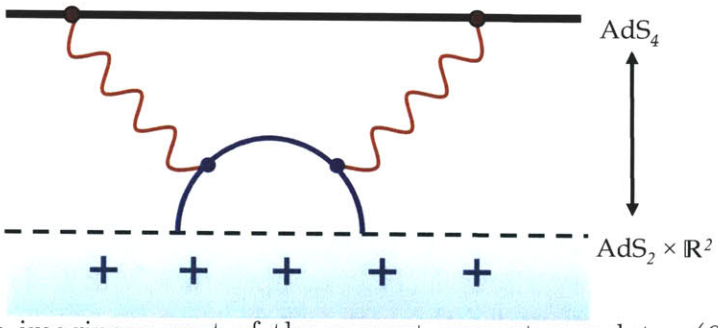

Figure 6-2: The imaginary part of the current-current correlator (6.23) receives its dominant contribution from diagrams in which the fermion loop goes into the horizon. This also gives us an intuitive picture: the dissipation of current is controlled by the decay of the particles running in the loop, which in the bulk occurs by falling into the black hole.

One standard strategy is to compute the corresponding correlation function in Euclidean signature, where these issues do not arise and then obtain the Lorentzian expression using analytic continuation (for $\Omega_l > 0$)

$$G_R^{(j)}(\Omega) = G_E^{(j)}(i\Omega_l = \Omega + i\epsilon) \tag{6.2}$$

where $G_R^{(j)}(\Omega)$ denotes the Lorentzian current correlation function on the right hand side of (6.23). This, however, requires precise knowledge of the Euclidean correlation function, which is not possible, given the complexity of the problem. We will adopt a hybrid approach. We first write down an integral expression for the two-point current correlation function $G_E^{(j)}(i\Omega_l)$ in Euclidean signature. We then perform analytic continuation (6.2) to Lorentzian signature *inside the integral*. This gives an intrinsic Lorentzian expression for the conductivity. The procedure can be considered as the generalization of the procedure discussed in [15] for tree-level amplitudes to one-loop. After analytic continuation, the kind of diagrams indicated in figure 6-2 are included unambiguously. In fact they are the dominant contribution to the dissipative part of the current-current correlation function, which gives us the resistivity.

Typical one-loop processess in quantum gravity also contain UV divergences. As

in [94, 153], we are computing a UV-safe quantity, and short-distance issues will not be relevant. In a QFT in flat spacetime, there is no UV divergence associated with temperature-dependent quantities: the temperature is an IR cutoff, UV divergences are independent of such an IR regulator. The temperature-dependence of high-energy effects is suppressed by $e^{-\beta E}$, so unless the density of such states grows faster than $e^{+\beta E}$, ∂_β must kill them. Further, we are interested in contributions to the conductivity which are non-analytic in temperature T at $T \to 0$. It will be clear from the structure of our calculation that such quantities will not depend on UV physics; thoroughly unsurprisingly, we will find that the UV completion of quantum gravity is not important in determining the low-temperature dependence of the resistivity of our strange metal phase.

6.1.1 Finite density state for CFT$_d$

In the remainder of this introduction we briefly review the physics of the finite density state, essentially generalizing the discussion of Chapter 4 to arbitrary dimension. To put the state at finite density we turn on a chemical potential μ for the $U(1)$ global symmetry. On the gravity side, such a finite density system is described by a charged black hole in $d+1$-dimensional anti-de Sitter spacetime (AdS$_{d+1}$) [90]. The conserved current J_μ of the boundary global $U(1)$ is mapped to a bulk $U(1)$ gauge field A_M. The black hole is charged under this gauge field, resulting in a nonzero classical background for the electrostatic potential $A_t(r)$. For definiteness we take the charge of the black hole to be positive. The action for a vector field A_M coupled to AdS$_{d+1}$ gravity can be written

$$S = \frac{1}{2\kappa^2}\int d^{d+1}x\,\sqrt{-g}\left[\mathcal{R} - \frac{d(d-1)}{R^2} - \frac{R^2}{g_F^2}F_{\mu\nu}F^{\mu\nu}\right] \tag{6.3}$$

which is asymptotically AdS with a nonzero chemical potential $A_t \overset{r\to\infty}{\approx} \mu$. The background is given by [89, 90]

$$ds^2 \equiv g_{MN}dx^M dx^N = \frac{r^2}{R^2}(-f dt^2 + d\vec{x}^2) + \frac{R^2}{r^2}\frac{dr^2}{f} \tag{6.4}$$

with

$$f = 1 + \frac{Q^2}{r^{2d-2}} - \frac{M}{r^d}, \qquad A_t = \mu\left(1 - \frac{r_0^{d-2}}{r^{d-2}}\right) . \tag{6.5}$$

r_0 is the horizon radius determined by the largest positive root of the redshift factor

$$f(r_0) = 0, \qquad \to \qquad M = r_0^d + \frac{Q^2}{r_0^{d-2}} \tag{6.6}$$

and

$$\mu \equiv \frac{g_F Q}{c_d R^2 r_0^{d-2}}, \qquad c_d \equiv \sqrt{\frac{2(d-2)}{d-1}} . \tag{6.7}$$

It is useful to parametrize the charge of the black hole by a length scale $r_\star$, defined by

$$Q \equiv \sqrt{\frac{d}{d-2}}\, r_*^{d-1} \,. \tag{6.8}$$

In terms of $r_\star$, the density, chemical potential and temperature of the boundary theory are

$$\rho = \frac{1}{\kappa^2}\left(\frac{r_*}{R}\right)^{d-1}\frac{1}{e_d}, \tag{6.9}$$

$$\mu = \frac{d(d-1)}{d-2}\frac{r_*}{R^2}\left(\frac{r_*}{r_0}\right)^{d-2} e_d, \tag{6.10}$$

$$T = \frac{d r_0}{4\pi R^2}\left(1 - \frac{r_*^{2d-2}}{r_0^{2d-2}}\right) \tag{6.11}$$

where we have introduced

$$e_d \equiv \frac{g_F}{\sqrt{2d(d-1)}} \,. \tag{6.12}$$

In the extremal limit $T \to 0$, the geometry near the horizon at $r = r_0$ is $AdS_2 \times \mathbb{R}^{d-1}$:

$$ds^2 = \frac{R_2^2}{\zeta^2}\left(-d\tau^2 + d\zeta^2\right) + \frac{r_*^2}{R^2} d\vec{x}^2 \tag{6.13}$$

with

$$A_\tau = \frac{e_d}{\zeta} \,. \tag{6.14}$$

The AdS_2 coordinates are related to the UV coordinates by

$$\zeta = \lambda \frac{R_2^2}{r - r_\star}, \quad \tau = \lambda t \tag{6.15}$$

where $\lambda \to 0$ is the scaling variable, which will drop out of all physical quantities. The curvature radius of AdS_2 given by

$$R_2 = \frac{1}{\sqrt{d(d-1)}} R \,. \tag{6.16}$$

We refer the reader to [19] for further details.

6.2 $O(N^2)$ conductivity

In this section we consider the leading-in-N^2 contribution to the conductivity[1]. Our motivation is twofold. Firstly, this represents a 'background' from which we need to extract the Fermi surface contribution; we will show that this contribution to the conductivity is analytic in T, unlike the Fermi surface contribution. Secondly, the

[1]This was also considered recently in [151, 112].

bulk propagators which determine this answer are building-blocks of the one-loop calculation required for the Fermi surface contribution.

6.2.1 Resistivity in clean systems

In a translation-invariant and boost-invariant system at finite charge density (without disorder or any other mechanism by which the charge-carriers can give away their momentum), the DC resistivity is zero. An applied electric field will accelerate the charges. This statement is well-known but we feel that some clarification will be useful. It can be understood as follows. Start with a uniform charge density at rest and in equilibrium, in a frame where

$$j^t \equiv \rho \neq 0, \quad T^{tt} = \epsilon \neq 0, \quad T^{ii} = P, \qquad j^i = 0, \quad \pi^i \equiv T^{ti} = 0 \ ; \tag{6.17}$$

ϵ is the energy density and P is the pressure. Boost[2] by a velocity u^i to a frame where

$$j^i = u^i \rho, \qquad \pi^i = u^i(\epsilon + P) \ . \tag{6.18}$$

This gives

$$j^i = \frac{\rho}{\epsilon + P} \pi^i \ , \tag{6.19}$$

which is effectively a constitutive relation. In a non-relativistic system, the enthalpy $\epsilon + P$ reduces to the mass of the particles. Combining this with conservation of momentum (Newton's law)

$$\partial_t \pi^i = \rho E^i \tag{6.20}$$

and Fourier transforming gives

$$j^i(\Omega) = \frac{i}{\Omega} \frac{\rho^2}{(\epsilon + P)} E^i(\omega) \tag{6.21}$$

and hence

$$\mathrm{Re}\, \sigma(\Omega) = \frac{\pi \rho^2}{\epsilon + P} \delta(\Omega) \tag{6.22}$$

plus, in general, dissipative contributions. Note that in systems where the relation $\vec{J} = \frac{\rho}{\epsilon + P} \vec{\pi}$ is an operator equation, momentum conservation implies that there are no dissipative contributions, and the conductivity is exactly given by (6.22).

Our treatment is somewhat heuristic, but a more careful hydrodynamic analysis that also takes into account the leading frequency dependence was performed in [116], where it was explicitly shown that the presence of impurities broadens this delta function into a Drude peak. We will find a similar delta function in the $O(N^2)$ contribution to the conductivity below. We stress that this delta function follows entirely from kinematics and is not of interest to us, as it represents a ballistic contribution to the conductivity that is not related to the non-Fermi-liquid $O(N^1)$ contribution, which

[2] We perform a small boost $u^i \ll c$, so we can use the Galilean transformation, even if the system is relativistic.

can be cleanly isolated from this term by its temperature dependence. It does *not* contain a delta function in Ω, as the Fermi surface current can dissipate by interacting with the $O(N^2)$ bath.

6.2.2 Retarded vector boundary to bulk propagator

To calculate the conductivity using the Kubo formula

$$\sigma(\omega) = \frac{1}{i\omega}\langle J_y(\omega)J_y(-\omega)\rangle_{\text{retarded}} \ , \tag{6.23}$$

we need to consider small fluctuations of the gauge field $\delta A_y \equiv a_y$ which is dual to J_y with a nonzero frequency Ω and $k = 0$. In the background of a charged black hole, such fluctuations of a_y mix with the vector fluctuations h_{ty} of the metric, as we discuss in detail in Appendix 6.B. After eliminating h_{ty} from the equations for a_y, we find that (see Appendix 6.B for details)

$$\partial_r\left(\sqrt{-g}g^{rr}g^{yy}\partial_r a_y\right) - \sqrt{-g}g^{yy}\left(m_{\text{eff}}^2 + g^{tt}\omega^2\right)a_y = 0 \tag{6.24}$$

where a_y acquires an r-dependent mass given by

$$m_{\text{eff}}^2 R_2^2 = 2\left(\frac{r_*}{r}\right)^{2d-2} \ . \tag{6.25}$$

The small frequency and small temperature (ω/T fixed) limit of the solution to this equation can be obtained by the matching technique of [19]; the calculation parallels closely that of [19]. The idea is to divide the geometry into two regions in each of which the equation can be solved approximately; at small frequency, these regions overlap and the approximate solutions can be matched. The *outer* (UV) region is defined by $r - r_\star > \omega R_2^2/\epsilon$ for some arbitrary matching point ϵ; in this region we can solve the equation in an ordinary Taylor expansion in ω (and, if desired, also in temperature T). The *inner* (IR) region is simply described by the near-horizon limit where the geometry is $AdS_2 \times \mathbb{R}^2$.

To compute the IR region quantities, we can study the gauge field propagating in the near-horizon metric, (6.13). The r-dependent effective mass term in (6.25) goes to a constant value $m_{\text{eff}}^2 R_2^2 = 2$ in the near horizon limit $r \to r_*$. The zeroth order IR region differential equation is the same as that of a scalar field in AdS_2 with this mass. The answer simplifies because the gauge field is not charged ($q = 0$) and has zero spatial momentum ($k = 0$). The QFT mode j^y to which the transverse gauge field couples thus flows to a scalar operator in the IR CFT whose retarded two point function we will denote $\mathcal{G}_y$. The effective mass determines the IR CFT scaling dimension for $a_y(k = 0)$ in the AdS_2 region (see (56) of [19]) to be $\Delta_{IR} = \frac{1}{2} + \nu$ with

$$\nu = \frac{1}{2}\sqrt{1 + 4\mathcal{C}R_2^2\left(\frac{R}{r_\star}\right)^{2d-2}} = \frac{3}{2}, \tag{6.26}$$

that is, the solutions behave near the UV end of the AdS_2 region like $a_y(\zeta) \sim \zeta^{\frac{1}{2}\pm\nu}$, where ζ is the AdS_2 coordinate introduced in (6.15). The integrality of the IR CFT dimension of the current operator should have a physical explanation. The value $\Delta_{IR}(j_y) = 2$ seems to be a very general result: it is not changed by including higher derivative couplings in the bulk [112], and it is also found in examples with near-horizon Lifshitz behavior [150]. It would be nice to understand what are the necessary conditions for this conclusion.

The retarded solution in the IR region behaves near the boundary of AdS_2 (the matching region) as

$$a_y \overset{\zeta\to 0}{\simeq} \zeta^{\frac{1}{2}-\nu} + \mathcal{G}_R \zeta^{\frac{1}{2}+\nu} \ . \tag{6.27}$$

The scalar IR CFT retarded Green's function $\mathcal{G}_R(\omega)$ (that is, the retarded two-point function of the operator dual to a scalar field propagating in AdS_2) was computed in Appendix D of [19] for arbitrary scaling dimension ν and charge q. The associated wave equation is exactly solvable. At temperature T, the result takes the form

$$\mathcal{G}_R(\omega) = (2\pi T)^{2\nu} \frac{\Gamma(-2\nu)\Gamma\left(\frac{1}{2}+\nu-\frac{i\omega}{2\pi T}+iqe_d\right)\Gamma\left(\frac{1}{2}+\nu-iqe_d\right)}{\Gamma(2\nu)\Gamma\left(\frac{1}{2}-\nu-\frac{i\omega}{2\pi T}+iqe_d\right)\Gamma\left(\frac{1}{2}-\nu-iqe_d\right)} \ . \tag{6.28}$$

To find the IR CFT Green's function appropriate to the vector field, we examine the $q = 0, k = 0, \nu \to 3/2$ limit of this expression (6.28), and we find a finite answer:

$$\mathcal{G}_y(\Omega) = \frac{i\Omega}{3}\left(\Omega^2 + (2\pi T)^2\right) \ . \tag{6.29}$$

We can then construct the bulk-to-boundary (retarded) propagator with boundary condition $a_y(r) \to 1$ at the AdS_{d+1} boundary. First we define zeroth-order outer-region functions $\eta^{(0)}_{y\pm}$ to be solutions of (6.24) which behave in the matching region like

$$\eta^{(0)}_{y\pm}(r) \overset{r\to r_\star}{\approx} \left(\frac{r-r_\star}{R_2^2}\right)^{-\frac{1}{2}\pm\frac{3}{2}} \ . \tag{6.30}$$

Then we can define two linearly-independent solutions in the outer region as series in T and ω

$$\eta_{y\pm}(r;\omega,T) = \sum_n^\infty \omega^n \eta^{(n)}_{y\pm}(r). \tag{6.31}$$

The quantities $\eta^{(n)}_{y\pm}$ also depend analytically on temperature T; for economy of notation, we leave implicit the expansion in T. In terms of their behavior at the boundary, we define

$$\eta^{(n)}_{y\pm} \overset{r\to\infty}{\approx} a^{(n)}_{y\pm} + b^{(n)}_{y\pm} r^{2-d} \ . \tag{6.32}$$

Matching to the behavior in the IR region (6.27), the desired bulk-to-boundary propagator is then

$$a_y(r) = \frac{\eta_{y+}(r) + \mathcal{G}_y \eta_{y-}(r)}{a_{y+} + \mathcal{G}_y a_{y-}} \ . \tag{6.33}$$

Note that $\eta_{y\pm}, a_{y\pm}$ are real and analytic in T, Ω. The leading order solution for the

$T = 0$ RN black hole was determined analytically in [151]; in particular

$$\eta^{(0)}_{y+} = \frac{r_0}{(d-2)R_2^2}\left(1 - \left(\frac{r_0}{r}\right)^{d-2}\right). \tag{6.34}$$

Useful relations arise from the constancy in r of the Wronskian

$$W[a_1, a_2] \equiv a_1\sqrt{g}g^{yy}g^{rr}\partial_r a_2 - a_2\sqrt{g}g^{yy}g^{rr}\partial_r a_1 \tag{6.35}$$

where $a_{1,2}$ are solutions to (6.24). In particular, equating $W[\eta^{(0)}_{y+}, \eta^{(0)}_{y-}]$ at boundary and horizon gives

$$\left(b^{(0)}_{y-}a^{(0)}_{y+} - a^{(0)}_{y-}b^{(0)}_{y+}\right) = \frac{2\nu}{d-2}r_\star^{d-3}R^2\ . \tag{6.36}$$

Note that this equation assumes the normalization of the gauge field specified in (6.30).

6.2.3 Tree-level conductivity

In this subsection we use the matching techniques of [19] to study the low-frequency and low-temperature conductivity at tree level in the RN black hole.

The $O(N^2)$ conductivity may be found from the expression

$$\sigma(\Omega) = \lim_{r\to\infty}\frac{2R^2}{g_F^2\kappa^2}\frac{\sqrt{-g}g^{yy}g^{rr}\partial_r a_y}{i\Omega a_y} \tag{6.37}$$

using the solution (6.33). Note that the mixing of the gauge field with the metric fluctuations complicates the derivation of this formula; for a clear discussion, see section 2.7 of [26]. The result is

$$\sigma(\Omega) = (2-d)\frac{2R^{3-d}}{g_F^2\kappa^2}\frac{b_{y+} + \mathcal{G}_y b_{y-}}{i\Omega\left(a_{y+} + \mathcal{G}_y a_{y-}\right)}\ . \tag{6.38}$$

Of course this expression is only useful in the small Ω, T limit, which we take now:

$$\sigma(\Omega) = (2-d)\frac{2R^2}{g_F^2\kappa^2}\left(\frac{b_{y+}}{i\Omega a_{y+}} + \frac{\mathcal{G}_y}{i\Omega}\frac{(b_{y-}a_{y+} - a_{y-}b_{y+})}{a_{y+}^2} + \ldots\right)\ . \tag{6.39}$$

The contribution from the IR CFT Green's function scales as T^2, Ω^2 for small temperatures and frequencies. In the imaginary part of σ, this contribution is therefore swamped by the analytic-in-T, Ω corrections to the UV-region quantities $a_y^\pm, b_y^\pm$ at small T; however it makes the leading contribution to the real part at $\Omega \neq 0$. We can use the analytic form of the leading-order solution $\eta^{(0)}_{y+}$ in equation (6.34) to obtain

$$\sigma(\Omega) \;=\; \frac{2R^{3-d}r_0^{d-2}}{g_F^2\kappa^2 i\Omega} - \frac{2(d-2)^2}{g_F^2\kappa^2}r_0^{d-5}R^{5-d}R_2^4\left(\Omega^2 + (2\pi T)^2\right) + \ldots$$

$$= \frac{\rho^2}{\epsilon+P}\frac{1}{i\Omega} - \mathcal{K}\left(\frac{d-2}{d(d-1)}\right)^{d-3}\left(\frac{\mu}{e_d}\right)^{d-5}\left(\Omega^2+(2\pi T)^2\right)+\ldots \quad (6.40)$$

The first term in (6.39) produces the requisite delta function at $\Omega = 0$ in the real part of the conductivity. For the specific case of the RN black hole, the coefficient of the resulting delta function in $\sigma(\Omega)$ agrees with the hydrodynamic answer $\frac{\rho^2}{\epsilon+P}$ (*q.v.* also formula (156) of [26]). In the second term, we used the Wronskian relation (6.36); the constant $\mathcal{K} \equiv \frac{2R^{d-1}}{g_F^2\kappa^2}$ can be interpreted in field theory terms: it is defined via the vacuum current-current correlator as

$$\langle j_x(\omega,k)j_x(-\omega,k)\rangle_{\mu=0,T=0} = \mathcal{K}\begin{cases} -iw^{d-2}, & \text{d odd} \\ w^{d-2}\ln w, & \text{d even} \end{cases} \quad (6.41)$$

where $w \equiv \sqrt{\omega^2-\vec{k}^2}$. Due to the inverse factor of κ^2 it essentially goes like a positive power of N^2, i.e. we may say that $\mathcal{K} \sim N^2$.

Thus the key point here is that the $O(N^2)$ part of the *dissipative* DC conductivity comes from the second term in (6.40)

$$\sigma(T) \sim N^2T^2 \quad (6.42)$$

It is interesting to note that the delta function in the conductivity is a direct result of the fact that the fluctuations of the bulk field a_y are *massive*, as is clear from the perturbation equation (6.24). This is not a breakdown of gauge-invariance; rather the gauge field acquired a mass through its mixing with the graviton. In the absence of such a mass term the radial equation of motion is trivial in the hydrodynamic limit (as was shown in Chapter 3) and there is no such delta function.

We also note that for a clean system such as this, there is no nontrivial heat conductivity or thermoelectric coefficient at $k = 0$, independent of the charge conduction. This is because momentum conservation is exact, and just as in the discussion of section 6.2.1, there can therefore be no dissipative part of these transport coefficients.

6.3 Outline of computation of $O(1)$ conductivity

As explained in the introduction, in order to obtain the contribution of a Fermi surface to the conductivity, we need to extend the tree-level gravity calculation of the previous section to the one-loop level with the corresponding bulk spinor field running in the loop. This one-loop calculation is rather complicated and is spelled out in detail in the next section. In this section we outline the main ingredients of the computation without going into details.

6.3.1 Cartoon description of the gravity calculation

In this subsection we will describe a toy version of the one-loop conductivity. We will assume that the *boundary theory* retarded Green's function of the dual operator has a Fermi-surface-like pole at $\omega = 0$ and $k = k_F$ of the kind described in Chapter 5. We will brutally neglect some "complications" (where the word here includes such niceties as spinor indices, matrix structures, gauge-graviton mixing, and a host of other important details) that turn out to be inessential in understanding the structure of the calculation.

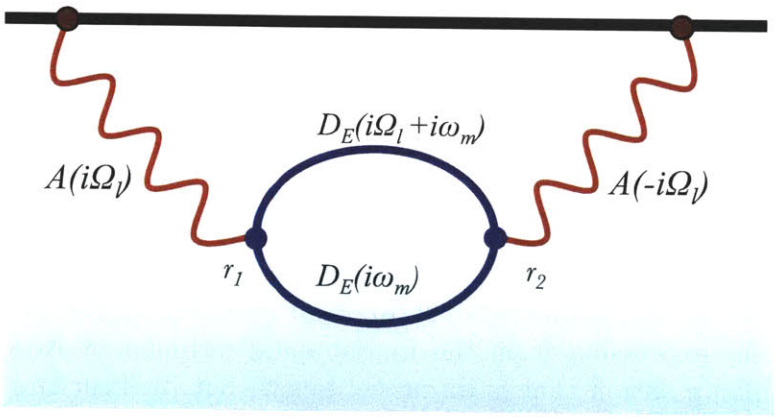

Figure 6-3: The bulk Feynman diagram by which the spinor contributes to the conductivity.

The important bulk Feynman diagram ('Witten diagram') is depicted in Figure 6.3.1. Note that it is structurally very similar to the particle-hole bubble which contributes to the Fermi liquid conductivity (see e.g. [152]): an external current source creates a fermion-antifermion pair, which then recombine. The DC conductivity is proportional to the imaginary part of the diagram when evaluated on real frequencies: we will show that in computing this imaginary part, the intermediate states are on-shell. The calculation differs from the standard Fermi liquid calculation in two important ways, which in some sense cancel each other out. The first, obvious difference is that the gravity amplitude involves integrals over the extra radial dimension of the bulk geometry. It turns out, however, that these integrals can be packaged into factors in the amplitude (called Λ below) that play the role of a corrected vertex. The second main difference is that actual vertex correction diagrams in the bulk are suppressed by further powers of N^{-2} and are therefore negligible, at least in the limit in which we work.

We now proceed to perform the computation. While it is more convenient to perform the tree-level calculation of the last section in the Lorentzian signature, for the one-loop calculation it is far simpler to work in Euclidean signature, where one avoids thorny conceptual issues regarding the choice of vacuum and whether interaction vertices should be integrated through the horizon or not. Our strategy is to first write down an integral expression for the Euclidean two-point function

function[3] $G_E(i\Omega_l)$ and then analytically continue to Lorentzian signature inside the integral (for $\Omega_l > 0$)

$$G_R(\Omega) = G_E(i\Omega_l = \Omega + i\epsilon) \tag{6.43}$$

The imaginary part of the Lorentzian gGreen's function will then give us the conductivity via the Kubo formula (6.23).

We now turn to the evaluation of the diagram in Figure 6.3.1, which works out to have the structure

$$\begin{aligned} G(i\Omega_l) &= -cT\sum_{i\omega_n}\int \frac{d^{d-1}k}{(2\pi)^{d-1}} dr_2 dr_2 \times \\ & D_E(r_1, r_2; i\Omega_l + i\omega_n, \vec{k}) K_A(r_1; i\Omega_l) D_E(r_2, r_1; i\Omega_l, \vec{k}) K_A(r_2; i\Omega_l) \end{aligned} \tag{6.44}$$

The ingredients here deserve further explanation. $D_E(r_1, r_2; i\Omega_l, k)$ is the spinor propagator in Euclidean space. $K_A(r; i\Omega_l)$ is the boundary-to-bulk propagator for the gauge field; it takes a gauge field source localized at the boundary and propagates it inward, computing its strength at a bulk radius r. c is an overall constant. The vertices have a great deal of matrix structure that we have suppressed, and the actual derivation of this expression from the fundamental formulas of AdS/CFT requires a little bit of manipulation that is discussed below, but its structure should appear plausible. The radial integrals dr should be understood as including the relevant metric factors to make the expression covariant.

We would now like to perform the Euclidean frequency sum. This is conveniently done using the spectral representation of the Euclidean green's function for the spinor,

$$D_E(r_1, r_2; i\omega_m, \vec{k}) = \int \frac{d\Omega}{(2\pi)} \frac{\rho(r_1, r_2; \Omega, \vec{k})}{i\omega_m - \Omega}, \tag{6.45}$$

where $\rho(r_1, r_2; \Omega, \vec{k})$ is the bulk-to-bulk spectral density. This object plays a very important role in our calculation. The derivation of this object for the spinor is discussed in detail in Appendix 6.A, but it is possible to understand its structure from the far simpler expression for a *scalar* field, to which we now turn.

6.3.2 Interlude: Bulk-to-bulk spectral density for a scalar field

Purely for illustrative purposes, we now discuss the bulk-to-bulk spectral density for a scalar field. This plays no role in our final calculation, but is instructive for understanding the structure of the bulk-to-bulk spectral density.

Note first that the bulk-to-bulk retarded propagator for the scalar is defined as

[3] We put the i in the argument of all Euclidean correlation functions to eventually make the analytic continuation to Lorentzian signature more natural.

follows. It satisfies the differential equation

$$\nabla_r^2 G_R(\omega, \vec{k}; r, r') = \frac{1}{\sqrt{-g}}\delta(r - r') \tag{6.46}$$

with boundary conditions such that it is normalizable at the boundary and ingoing at the horizon. This uniquely fixes the answer to be the following well-known expression:

$$G_R(\omega, \vec{k}; r, r') = \frac{\phi_\flat(r_>)\phi_{\text{in}}(r_<)}{W[\phi_\flat, \phi_{\text{in}}]} \tag{6.47}$$

where $r_>(r_<)$ are the greater (lesser) of r, r'. $W[\phi_1, \phi_2]$ denotes the Wronskian and is defined as

$$W[\phi_1, \phi_2] = \sqrt{-g}g^{rr}(\phi_1\partial_r\phi_2 - \phi_2\partial_r\phi_1) \tag{6.48}$$

Here we have defined solutions of the homogenous differential equation $\phi_\flat, \phi_{\text{in}}$ and for future reference $\phi_\sharp$ by the following boundary conditions

$$\phi_\sharp(r) \sim 1r^{\Delta-d} + 0r^{-\Delta}, \qquad \phi_\flat(r) \sim 0r^{\Delta-d} + 1r^{-\Delta} \tag{6.49}$$

and ϕ_{in} is purely infalling at the horizon. ϕ_{in} was studied carefully in [19]. Note that ϕ_{in} can be expressed in terms of $\phi_{\sharp,\flat}$ as follows:

$$\phi_{\text{in}}(r) = \phi_\sharp(r) + G_B\phi_\flat(r) \tag{6.50}$$

where G_B is the *boundary theory* (retarded) Green's function (recall this is the ratio of two UV expansion coefficients). We have chosen an overall normalization for the solution arbitrarily since it drops out from (6.47). One can check by explicit calculation that this propagator does indeed satisfy the defining equation (6.46).

Now the spectral density is typically defined as

$$\rho(r, r'; \omega, \vec{k}) = \text{Im}\, G_R(r, r'; \omega, \vec{k}) \tag{6.51}$$

To evaluate the imaginary part of (6.47), we note that that $\phi_{\sharp,\flat}$ are real, since they satisfy real boundary conditions and the equation of motion is real. Thus the full imaginary part comes from the $G_B(\omega, k)$, and we find

$$\rho(r, r'; \omega, k) = \frac{\phi_\flat(r)\phi_\flat(r')}{W_{\flat\sharp}}\rho_B(\omega, \vec{k}) \tag{6.52}$$

where $\rho_B = \text{Im}\, G_B(\omega, k)$ is the *boundary theory* spectral density. The Wronskian $W_{\sharp\flat}$ is independent of r and is determined by the boundary behavior of $\phi_{\sharp,\flat}$ to be a pure constant.

This formula can be somewhat surprising and we now pause to discuss it. The bulk-to-bulk spectral density *factorizes* in the radial direction; thus in some sense the density of states is largely determined by the analytic structure of the boundary theory spectral density $\rho_B(\omega, \vec{k})$ We will see that this means that despite the presence of the extra radial direction in the bulk, the essential form of one-loop calculations

in this framework will be determined by the boundary theory excitation spectrum, with all radial integrals simply determining the structure of interaction vertices that appear very similar to those in field theory.

The formula corresponding to (6.52) for the spinor is recorded in (6.145). It is rather similar but takes into account the matrix structure of the propagator; this will not be relevant for our current purposes and so we simply schematically write for the spinor

$$\rho(r,r';\omega,\vec{k}) = \psi(r)\rho_B(\omega,k)\overline{\psi(r')} \tag{6.53}$$

where $\psi(r)$ is a normalizable spinor wavefunction. We now return to the evaluation of the expression (6.44).

6.3.3 Performing radial integrals

We now use standard manipulations from finite-temperature field theory to rewrite the Matsubara sum in (6.44) in terms of an integral over Lorentzian spectral densities. These techniques are reviewed in Appendix 6.G; in particular, using (6.225) we find

$$\begin{aligned} G(i\Omega_l) &= -c\int \frac{d\omega_1}{2\pi}\frac{d\omega_2}{2\pi}\frac{d^{d-1}k}{(2\pi)^{d-1}}dr_1dr_2\frac{f(\omega_1)-f(\omega_2)}{\omega_1-\omega_2-i\Omega_l}\times & (6.54)\\ &\quad \rho(r_1,r_2;\omega,\vec{k})K_A(r_1;i\Omega_l)\rho(r_2,r_1;i\Omega_l,\vec{k})K_A(r_2;i\Omega_l), & (6.55)\end{aligned}$$

where $f(\omega)$ is the Fermi distribution $f(\omega) = \frac{1}{e^{\beta\omega}+1}$. Now we seek to evaluate the imaginary part of this diagram when evaluated on real frequencies; setting $i\Omega_l = \Omega + i\epsilon$ and taking the imaginary part, we find a contribution from the delta function

$$\mathrm{Im}\left(\frac{1}{\omega_1-\omega_2-\Omega-i\epsilon}\right) = \pi\delta(\omega_1-\omega_2-\Omega)\ . \tag{6.56}$$

If the other factors have imaginary parts they may contribute as well; we show later that their contribution is not important. We thus find the Lorentzian expression

$$\begin{aligned} \mathrm{Im}\,G(\Omega) &= -c\pi\int \frac{d\omega_1}{2\pi}\frac{d^{d-1}k}{(2\pi)^{d-1}}dr_1dr_2(f(\omega_1)-f(\omega_1-\Omega))\times & (6.57)\\ &\quad \rho(r_1,r_2;\omega_1,\vec{k})K_A(r_1;\Omega)\rho(r_2,r_1;\omega_1-\Omega,\vec{k})K_A(r_2;\Omega) & (6.58)\end{aligned}$$

Note that the propagators $K_A(r_1;\Omega)$ have now become Lorentzian objects that propagate infalling waves.

We now realize the true power of the spectral decomposition; the bulk-to-bulk propagator factorizes into a product of spinor wavefunctions, allowing us to do each radial integral *independently*. In this way all of the radial integrals can be repackaged into an effective vertex

$$\Lambda(\omega_1,\omega_2,\Omega) = \int dr\overline{\psi}(r;\omega_1)K_A(r;\Omega)\psi(r;\omega_2), \tag{6.59}$$

and we are left with the formula

$$\begin{aligned} \mathrm{Im}\, G(\Omega) &= -c\pi \int \frac{d\omega_1}{2\pi} \frac{d^{d-1}k}{(2\pi)^{d-1}} (f(\omega_1) - f(\omega_1 - \Omega)) \times \\ &\quad \rho_B(\omega_1, k)\Lambda(\omega_1, \omega_1 - \Omega, \Omega)\rho_B(\omega_1 - \Omega, k)\Lambda(\omega_1 - \Omega, \omega_1, \Omega) \end{aligned} \tag{6.60}$$

This formula involves only integrals over the *boundary* theory spectral densities; the radial integral over spinor and gauge field wavefunctions simply provides an exact derivation of the effective vertex Λ that determines how strongly these fluctuations couple to the external field theory current, as shown in Figure 6.3.3. A precise derivation of the effective vertex requires a complete solution to the bulk wave equations; however we will show later that it is smooth as its various arguments go to 0, which is all we shall require.

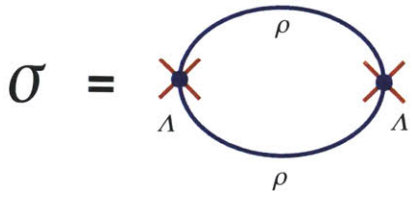

Figure 6-4: Final formula for conductivity; radial integrals only determine the effective vertex Λ, with exact propagator for boundary theory fermion running in loop.

6.3.4 DC conductivity

We would now like to extract a formula for the DC conductivity σ_{DC}. Taking the $\Omega \to 0$ limit and using the Kubo formula (6.23) we find

$$\sigma_{DC} = -\frac{c\pi S_{d-2}}{(2\pi)^{d-1}} \int \frac{d\omega}{2\pi} \frac{df}{d\omega} k^{d-2} dk \Lambda^2 \rho_B(\omega, k)^2 \tag{6.61}$$

This is precisely the usual formula for the conductivity from a Fermi liquid, except that our effective vertex is derived from a precise bulk calculation and – more importantly – the boundary theory spectral density is *not* that of a Fermi liquid. Rather, as described in Chapter 5, it takes the non-Fermi liquid form

$$\begin{aligned} \rho_B &= \frac{h_1 \mathrm{Im}\, \Sigma}{(k_\perp - \mathrm{Re}\,(\Sigma))^2 + \mathrm{Im}\,(\Sigma)^2} \qquad \Sigma = \frac{1}{v_F}\omega + h_2 \mathcal{G}_{k_F}(\omega) \\ &\mathrm{Im}\, \Sigma \sim T^{2\nu} g\left(\frac{\omega}{T}\right) \quad . \end{aligned} \tag{6.62}$$

We now track the leading temperature dependence of the conductivity as $T \to 0$. It is thus convenient to examine the behavior of the boundary spectral density $\rho_B(\omega, k)$

in the following scaling limit

$$T \to 0, \qquad \omega \to 0, \qquad x \equiv \frac{\omega}{T} = \text{finite} \quad . \tag{6.63}$$

This will be useful because the integral over frequency can be written as an integral over x. In the $T \to 0$ limit, to leading order in the T expansion we now have

$$\lim_{T\to 0} \rho_B^2 = \frac{\pi h_1^2}{2|\mathrm{Im}\,\Sigma|}\delta(k_\perp - \mathrm{Re}\,\Sigma) + \cdots \quad . \tag{6.64}$$

Plugging this into the expression (6.61) for σ_{DC}, the k-integral can now be done explicitly and we find that

$$\sigma_{DC} = \frac{cS_{d-2}}{(2\pi)^{d-1}} k_F^{d-2} \int \frac{d\omega}{2\pi} \frac{df}{d\omega} \frac{h_1^2}{\mathrm{Im}\,\Sigma} \Lambda^2 \tag{6.65}$$

To complete the story we need to determine the T-scaling of the effective vertex; this is done later in this text and it is shown that as $T, \omega \to 0$, Λ approaches a constant value. Thus we can now scale out all T-dependence in (6.65) by expressing the frequency integral in terms of the dimensionless frequency x. We have then

$$\sigma_{DC}(T \to 0) = \frac{cS_{d-2}}{(2\pi)^{d-1}} k_F^{d-2} T^{-2\nu} \left(\int dx \frac{df}{dx} \frac{1}{g(x)} \Lambda^2 \right) \tag{6.66}$$

where $g(x)$ was defined in (6.62) and the quantity in brackets is a pure number. Note that $\frac{df}{dx}$ is the derivative of the Fermi distribution and so is exponentially suppressed at large x, meaning that the integral is guaranteed to converge. The only T-dependence then comes from $\mathrm{Im}\,(\Sigma) \sim T^{2\nu}$, and thus we conclude that

$$\sigma_{DC}(T) = aT^{-2\nu} \tag{6.67}$$

with a a prefactor that can be calculated numerically. This is the central result of this chapter; the rest of this chapter is essentially devoted to the careful and technical calculations needed to justify various claims made in this section.

It is worth stating precisely what is different about the calculation we will now perform:

1. The careful treatment of spinor fields and associated indices will require some care.

2. The gauge field fluctuations on this background actually mix with the graviton fluctuations; thus the propagator K_A described above actually contains a graviton component. This is dual to the field-theoretical fact that pulling on a large charge density with an electric field causes energy as well as charge fluctuations. Thus the effective vertex Λ is rather more involved than the schematic form above.

6.4 Detailed computation: resistivity from a spinor field

We now perform the calculation performed above in detail, paying attention to all subtleties.

6.4.1 A general formula

We consider a free spinor field in the above spacetime with an action

$$S = -\int d^{d+1}x\sqrt{-g}\, i(\bar{\psi}\Gamma^M \mathcal{D}_M\psi - m\bar{\psi}\psi) = \int d^{d+1}\sqrt{-g}\,\mathcal{L} \tag{6.68}$$

where $\bar{\psi} = \psi^\dagger\Gamma^{\underline{t}}$ and

$$\mathcal{D}_M = \partial_M + \frac{1}{4}\omega_{abM}\Gamma^{ab} - iqA_M \tag{6.69}$$

The abstract spacetime indices are $M, N\cdots$ and the abstract tangent space indices are $a, b, \cdots$. The index with an underline denotes that in tangent space. Thus Γ^a to denote gamma matrices in the tangent frame and Γ^M those in curved coordinates. Note that

$$\Gamma^M = \Gamma^a e_a{}^M \ . \tag{6.70}$$

The background metric is given by

$$ds^2 = -g_{tt}dt^2 + g_{rr}dr^2 + g_{ii}dx_i^2 \tag{6.71}$$

We are interested in computing the one-loop correction to the retarded two-point function of the boundary vector current due to a bulk spinor field. In the presence of a background gauge field profile, the fluctuations of the bulk gauge field mix with those of the metric. Consider small perturbations in $a_j \equiv \delta A_j$ and $h_t^j = \delta g_t^j$. In Appendix 6.C we find that the corrections to the Dirac action are given at cubic order by

$$\delta S_3[a_j, h_t^j, \psi] = -i\sum_j \int d^{d+1}x\sqrt{-g}\bar{\psi}\left(-h_t^j\Gamma^t\partial_j + \frac{1}{8}g_{jj}\,\partial_r h_t^j\,\Gamma^{rtj} - iqa_j\Gamma^j\right)\psi \tag{6.72}$$

There are also quartic corrections (involving terms quadratic in bosonic fluctuations) which are given in Appendix 6.C. These terms give only subleading corrections, as we discuss in Appendix 6.E.

Now we go to Euclidean signature via

$$t = -i\tau \qquad \omega = i\omega_E \qquad A_t = iA_\tau \qquad iS = -S_E \tag{6.73}$$

It's helpful to keep in mind that ψ and $\psi^\dagger$ don't change under the continuation, and

we do not change $\Gamma^{\underline{t}}$. The Euclidean spinor action can then be written as

$$S_E = i\int d^{d+1}x\sqrt{g}\bar{\psi}\left(\Gamma^M D_M^{(0)} - m\right)\psi + \delta S_3 + \cdots \tag{6.74}$$

where δS_3 can be written in momentum space as

$$\begin{aligned}\delta S_3 = -T^2\sum_{\omega_m}\sum_{\Omega_l}\int\frac{d^{d-1}k}{(2\pi)^{d-1}}\int dr\sqrt{-g}\\ \times\bar{\psi}(r;i\omega_m+i\Omega_l,\vec{k})\,B(r;i\Omega_l,\vec{k})\,\psi(r;i\omega_m,\vec{k})\ .\end{aligned} \tag{6.75}$$

Here the kernel $B(r;i\Omega_l,\vec{k})$ contains all dependence on the gauge and metric fluctuations, which we have also Fourier expanded:

$$\begin{aligned}&B(r;i\Omega_l,\vec{k}) = \\ &-i\sum_j\left(-ik_j h_t^j(r;i\Omega_l)\Gamma^t + \frac{g_{jj}}{8}\partial_r h_t^j(r;i\Omega_l)\,\Gamma^{rtj} - iqa_j(r;i\Omega_l)\Gamma^j\right)\ .\end{aligned} \tag{6.76}$$

Note that since we are only interested in calculating the conductivity at zero spatial momentum, we have taken a_j and h_t^j to have zero spatial momentum.

We now evaluate the one-loop determinant by integrating out the fermion field. We seek the quadratic dependence on the gauge and gravition fields; the relevant term in the effective action is given by the Feynman diagram in Figure 6.3.1 and is

$$\begin{aligned}\Gamma[a_j,h_t^j] = -\frac{1}{2}T^2\sum_{\omega_m}\sum_{\Omega_l}\int\frac{d^{d-1}k}{(2\pi)^{d-1}}\int dr_1\sqrt{g(r_1)}dr_2\sqrt{g(r_2)}\\ \times\mathrm{tr}\left(D_E(r_1,r_2;i\omega_m+i\Omega_l,\vec{k})B(r_2;\Omega_l,\vec{k})\right.\\ \left.D_E(r_2,r_1;i\omega_m,\vec{k})B(r_1;-\Omega_l,\vec{k})\right)\end{aligned} \tag{6.77}$$

where the tr denotes the trace in spinor indices and $D_E(r_1,r_2;i\omega_m,\vec{k})$ denotes the bulk spinor propagator in the Euclidean signature. As always we suppress bulk spinor indicies. The bulk spinor propagator is discussed in some detail in Appendix 6.A. The single most important property that we use is its spectral decomposition

$$D_E(r_1,r_2;i\omega_m,\vec{k}) = \int\frac{d\omega}{2\pi}\frac{\rho(r_1,r_2;\omega,\vec{k})}{i\omega_m-\omega}, \tag{6.78}$$

where $\rho(r_1,r_2;\omega,\vec{k})$ is the bulk spectral function. As is shown in show in (6.145) of Appendix 6.A, the bulk spectral function can be written in terms of that of the boundary theory as

$$\rho(r,r';\omega,\vec{k}) = \psi_\alpha(r)\,\rho_B^{\alpha\gamma}(\omega,\vec{k})\,\overline{\psi_\gamma}(r') \tag{6.79}$$

where the boundary spectral function ρ_B is Hermitian and ψ is the normalizable

Lorentzian wave function for the free Dirac equation in the black hole geometry[4]. $\rho_B(\omega, k)$ is the boundary theory spectral density of the holographic non-Fermi liquid, and was discussed in detail in Chapter 5 of this thesis. Note that in (6.79) bulk spinor indices are suppressed and α, γ can be interpreted as the boundary spinor indices. In Appendix 6.A we give a detailed discussion of the relation between these indices.

Now introduce various momentum space Euclidean *boundary* to bulk propagators for the gauge field and graviton.

$$\begin{aligned} a_j(r; i\Omega_l) &= K_A(r; i\Omega_l) A_j(i\Omega_l), \\ h_t^j(r; i\Omega_l) &= K_h(r; i\Omega_l) A_j(i\Omega_l) \end{aligned} \tag{6.80}$$

where $A_j(i\Omega_l)$ is the source for the boundary conserved current in Euclidean signature. These are objects which propagate a gauge field source at the boundary to a gauge field or a metric fluctuation in the interior, and so should perhaps be called K_A^A and K_h^A; we drop the second 'A' label since we will never insert metric sources in this paper.

$K_A(r; i\Omega_l)$ and $K_h(r; i\Omega_l)$ go to zero (for any nonzero Ω_l) at the horizon and they do not depend on the index j due to rotational symmetry. K_h and K_A are not independent; in Appendix 6.B we show that

$$\partial_r K_h = -\frac{\mathcal{C}\sqrt{g_{rr} g_{tt}}}{h^{\frac{d+1}{2}}} K_A \tag{6.81}$$

where $\mathcal{C}$ is a constant satisfying $\mathcal{C} R_2^2 \left(\frac{R}{r_\star}\right)^{2d-2} = 2$.

Now using the definition of the propagators (6.80) we can write the kernel $B(r; i\Omega_l, \vec{k})$ in (6.76) in terms of a new object $Q^j(r;, i\Omega_l, \vec{k})$ that has the source explicitly extracted:

$$B(r; i\Omega_l, \vec{k}) = Q^j(r; i\Omega_l, \vec{k}) A_j(i\Omega_l) \tag{6.82}$$

where Q^j thus satisfies

$$Q^j(r; i\Omega_l, \vec{k}) = -i\left(-ik_j K_h(r; i\Omega_l)\Gamma^t + \frac{g_{jj}}{8}\partial_r K_h(r; i\Omega_l)\Gamma^{rtj} - iqK_A(r; i\Omega_l)\Gamma^j\right). \tag{6.83}$$

Plugging (6.82) into (6.77), we can now express the entire expression in terms of the boundary gauge field source $A_j(i\Omega_l)$. Taking two functional derivatives of this expression with respect to A_j, we find that the the boundary Euclidean current correlator can now be written as

$$\begin{aligned} G_E^{ij}(i\Omega_l) \;=\; & -T\sum_{\omega_m}\int \frac{d^{d-1}k}{(2\pi)^{d-1}} \int dr_1 \sqrt{g(r_1)} dr_2 \sqrt{g(r_2)} \\ & \times \mathrm{tr}\left(D_E(r_1, r_2; i\omega_m + i\Omega_l, \vec{k}) Q^i(r_2; i\Omega_l, \vec{k}) D_E(r_2, r_1; \omega_m, \vec{k}) Q^j(r_1; -i\Omega_l, \vec{k})\right) \end{aligned} \tag{6.84}$$

[4] For a precise definition of the normalizable Lorentzian wave function, see again Appendix 6.A. In this section, to avoid clutter, we will use the boldface font to denote the normalizable solution. The non-normalizable solution will not appear.

Note that all objects in here are entirely well-defined and self-contained; we now need only evaluate this expression.

To begin this process we first plug (6.78) into (6.84) and then perform the sum over ω_m using standard techniques that are reviewed in Appendix 6.G.1. We find that equation (6.84) can be further written as

$$\begin{aligned} G_E^{ij}(i\Omega_l) &= -\int \frac{d^{d-1}k}{(2\pi)^{d-1}} \int \frac{d\omega_1}{2\pi}\frac{d\omega_2}{2\pi} \int dr_1\sqrt{g(r_1)}dr_2\sqrt{g(r_2)}\, \frac{f(\omega_1)-f(\omega_2)}{\omega_1 - i\Omega_l - \omega_2} \\ &\quad \times \mathrm{tr}\left(\rho(r_1,r_2;\omega_1,\vec{k})Q^i(r_2;i\Omega_l,\vec{k})\rho(r_2,r_1;\omega_2,\vec{k})Q^j(r_1;-i\Omega_l,\vec{k})\right) \end{aligned} \tag{6.85}$$

where $\rho(r_1,r_2;\omega_1,\vec{k})$ is the bulk-to-bulk spinor spectral density. We have a convenient representation for it in (6.79); plugging this into (6.85) we find that

$$\begin{aligned} G_E^{ij}(i\Omega_l) &= -\int \frac{d^{d-1}k}{(2\pi)^{d-1}} \int \frac{d\omega_1}{2\pi}\frac{d\omega_2}{2\pi}\, \frac{f(\omega_1)-f(\omega_2)}{\omega_1 - i\Omega_l - \omega_2} \\ &\quad \times \rho_B^{\alpha\beta}(\omega_1,\vec{k})\,\Lambda^i_{\beta\gamma}(\omega_1,\omega_2,i\Omega_l,\vec{k})\,\rho_B^{\gamma\delta}(\omega_2,\vec{k})\,\Lambda^j_{\delta\alpha}(\omega_2,\omega_1,-i\Omega_l,\vec{k}) \end{aligned} \tag{6.86}$$

with

$$\Lambda^i_{\beta\gamma}(\omega_1,\omega_2,i\Omega_l,\vec{k}) = \int dr\sqrt{g}\,\overline{\psi_\beta}(r;\omega_1,\vec{k})\,Q^i(r;i\Omega_l;\vec{k})\,\psi_\gamma(r;\omega_2,\vec{k})\ . \tag{6.87}$$

Let us now pause for a moment to examine this expression. In the last series of manipulations we replaced the interior frequency sum with an integral over real Lorentzian frequencies; however by doing this we exploited the fact that the spectral density *factorizes* in r. This allowed us to absorb all radial integrals into Λ, which should be thought of as an effective vertex for the virtual spinor fluctuations. Now only the *boundary theory* spectral density ρ_B appears explicitly in the expression. This form for the expression is perhaps not surprising from a field-theoretical point of view; however it is interesting that we have an *exact* expression for the vertex, found by evaluating radial integrals over normalizable wave functions.

We now obtain the retarded Green function for the currents by starting with $G_E(i\Omega_l)$ for $\Omega_l > 0$ and analytically continuing $G_E(i\Omega_l)$ to Lorentzian signature via

$$G_R(\Omega) = G_E(i\Omega_l = \Omega + i\epsilon) \tag{6.88}$$

We will suppress the $i\epsilon$ in equations below for notational simplicity but it is crucial to keep it in mind. For simplicity of notations we will denote the Lorentzian analytic continuation of various quantities only by their argument, *e.g.*

$$K_A(r;i\Omega_l)|_{i\Omega_l=\Omega} \to K_A(r;\Omega) \tag{6.89}$$

We also make the analogous replacements also for K_h, Q^i and $\Lambda_{\alpha\beta}$. Note that $K_A(r;\Omega)$ and $K_h(r;\Omega)$ have now become *retarded* functions which are in-falling at the horizon and satisfy

$$K_A^*(r,\Omega) = K_A(r,-\Omega), \qquad K_h^*(r,\Omega) = K_h(r,-\Omega)\ . \tag{6.90}$$

It then can be readily checked that

$$Q_i^\dagger(r;\Omega,\vec{k}) = \Gamma^{\underline{t}} Q_i(r;-\Omega,\vec{k})\Gamma^{\underline{t}} \tag{6.91}$$

which further leads to

$$\Lambda^{i*}_{\beta\gamma}(\omega_1,\omega_2,\Omega,\vec{k}) = \Lambda^i_{\gamma\beta}(\omega_2,\omega_1,-\Omega,\vec{k}) \ . \tag{6.92}$$

Also note that in (6.86) both $\Lambda^i(\omega_1,\omega_2,\pm i\Omega_l,\vec{k})$ analytically continue to $\Lambda^i(\omega_1,\omega_2,\Omega,\vec{k})$.

We thus find that the retarded Green function for the currents can be written as

$$\begin{aligned} G_R^{ij}(\Omega) = -\int \frac{d^{d-1}k}{(2\pi)^{d-1}} \int \frac{d\omega_1}{2\pi}\frac{d\omega_2}{2\pi} \frac{f(\omega_1)-f(\omega_2)}{\omega_1-\Omega-\omega_2-i\epsilon} \\ \times \rho_B^{\alpha\beta}(\omega_1,\vec{k})\,\Lambda^i_{\beta\gamma}(\omega_1,\omega_2,\Omega)\,\rho_B^{\gamma\delta}(\omega_2,\vec{k})\,\Lambda^j_{\delta\alpha}(\omega_2,\omega_1,\Omega) \end{aligned} \tag{6.93}$$

where

$$\Lambda^i_{\beta\gamma}(\omega_1,\omega_2,\Omega,\vec{k}) = \int dr\sqrt{g}\,\overline{\psi_\beta}(r;\omega_1,\vec{k})\,Q^i(r;\Omega,\vec{k})\,\psi_\gamma(r;\omega_2,\vec{k}) \tag{6.94}$$

and

$$Q^j(r;\Omega,\vec{k}) = -i\left(-ik_jK_h(r;\Omega)\Gamma^t + \frac{g_{jj}}{8}\partial_r K_h(r;\Omega)\Gamma^{rtj} - iqK_A(r;\Omega)\Gamma^j\right) \ . \tag{6.95}$$

Note that (6.93) is now expressed in terms of intrinsic boundary quantities; Λ can be interpreted as an effective vertex. The complex, frequency-dependent conductivity is

$$\sigma^{ij}(\Omega) \equiv \frac{G_R^{ij}(\Omega)}{i\Omega} \ . \tag{6.96}$$

We now manipulate the expression for the effective vertex using a trick elaborated on in detail in Appendix 6.D. It is shown there that provided that Q^j is sandwiched between two on-shell spinors as it is in (6.94), one can replace it with

$$Q^j(r;\Omega,\vec{k}) \to -i\left(-\frac{k_j}{\Omega}\partial_r K_h(r;\Omega)\Gamma^r + \frac{g_{jj}}{8}\partial_r K_h(r;\Omega)\Gamma^{rtj} - iqK_A(r;\Omega)\Gamma^j\right) \tag{6.97}$$

This manipulation replaced the K_h with its radial derivative $\partial_r K_h$; the fact that this is possible implies that the expression is not sensitive to the constant mode in the radial profile of the graviton. This is actually a consequence of the Ward identity corresponding to momentum conservation in the boundary theory, and the manipulation performed above is explained in detail in Section 6.D. In any case, one can now use the relation between gauge and graviton propagators (6.81) to eliminate $\partial_r K_h$ in favor of K_A, leaving us with

$$Q^j(r;\Omega,\vec{k}) = -iK_A(r;\Omega)g_{jj}^{-\frac{1}{2}}\left(-iq\Gamma^{\underline{j}} + \mathcal{C}g_{jj}^{-\frac{d}{2}}\Gamma^{\underline{r}}\left(\frac{k_j}{\Omega}\sqrt{g_{tt}} - \frac{\sqrt{g_{jj}}}{8}\Gamma^{\underline{tj}}\right)\right) \tag{6.98}$$

This is the form of Q^j that will be used in the remainder of this calculation.

6.4.2 Angular integration

We will now use the spherical symmetry of the underlying system to perform the angular integration in (6.93). For this purpose we choose a reference direction, say, with $k_x = k \equiv |\vec{k}|$ and all other spatial components of $\vec{k}$ vanishing. We will denote this direction symbolically as $\theta = 0$ below. Then from the transformation properties of spinors it is easy to see that

$$\begin{aligned} \rho_B(\vec{k}) &= U(\theta)\rho_B(k, \theta = 0)U^\dagger(\theta), \\ \Lambda_i(\vec{k}) &= R_{ij}(\theta)U(\theta)\Lambda_j(k, \theta = 0)U^\dagger(\theta) \end{aligned} \tag{6.99}$$

where $R_{ij}(\theta)$ is the orthogonal matrix which rotate a vector $\vec{k}$ to $\theta = 0$ and U is the unitary matrix which does the same rotation on a spinor (i.e. in α, β space). The angular integral in (6.93) is reduced to

$$\frac{1}{(2\pi)^{d-1}} \int d^{d-2}\theta \, R_{ik}(\theta)R_{jl}(\theta) = C\delta_{ij}\delta_{kl} \tag{6.100}$$

where C is a normalization constant and $d^{d-2}\theta$ denotes the measure for angular integration. The conductivity can now be written as

$$\sigma^{ij}(\Omega) = \delta^{ij}\sigma(\Omega) \tag{6.101}$$

with

$$\begin{aligned} \sigma(\Omega) &= \frac{C}{i\Omega}\int_0^\infty dk k^{d-2} \int \frac{d\omega_1}{2\pi}\frac{d\omega_2}{2\pi}\frac{f(\omega_1) - f(\omega_2)}{\omega_1 - \Omega - \omega_2 - i\epsilon} \\ &\quad \times \sum_i \rho_B^{\alpha\beta}(\omega_1, k)\, \Lambda^i_{\beta\gamma}(\omega_1, \omega_2, \Omega, k)\, \rho_B^{\gamma\delta}(\omega_2, k)\, \Lambda^i_{\delta\alpha}(\omega_2, \omega_1, \Omega, k) \end{aligned} \tag{6.102}$$

where $\rho_B(\omega, k)$ and $\Lambda^i_{\delta\alpha}(\omega_2, \omega_1, \Omega, k)$ in (6.102) and in all expressions below should be understood as the corresponding quantities evaluated at $\theta = 0$ as in (6.99).

Equation (6.102) can now be further simplified in a basis in which ρ_B is diagonal, i.e. $\rho_B^{\alpha\beta} = \rho_B^\alpha \delta^{\alpha\beta}$, leading to

$$\sigma(\Omega) = -\frac{C}{i\Omega}\int_0^\infty dk k^{d-2} \int \frac{d\omega_1}{2\pi}\frac{d\omega_2}{2\pi}\frac{f(\omega_1) - f(\omega_2)}{\omega_1 - \Omega - \omega_2 - i\epsilon} \rho_B^\alpha(\omega_1, k)\, M_{\alpha\gamma}(\omega_1, \omega_2, \Omega, k)\, \rho_B^\gamma(\omega_2, k) \tag{6.103}$$

where (there is no summation over α, γ below)

$$M_{\alpha\gamma}(\omega_1, \omega_2, \Omega, k) = \sum_i \Lambda^i_{\alpha\gamma}(\omega_1, \omega_2, \Omega, k)\Lambda^i_{\gamma\alpha}(\omega_2, \omega_1, \Omega, k) \tag{6.104}$$

The above expression is very general, but we can simplify it slightly by using some explicit properties of the expression for ρ_B. We seek singular low-temperature behav-

ior in the conductivity, which will essentially arise from low-frequency singularities in ρ_B. At the holographic Fermi surfaces described in Chapter 5, at discrete momenta $k = k_F$, only *one* of the eigenvalues of ρ_B, say ρ_B^1, develops singular behavior. We see that we can extract the leading singularities in the $T \to 0$ limit by simply taking the term in (6.103) proportional to $(\rho_B^1)^2$. Thus (6.103) simplifies to

$$\sigma(\Omega) = -\frac{C}{i\Omega}\int_0^\infty dk k^{d-2}\int \frac{d\omega_1}{2\pi}\frac{d\omega_2}{2\pi}\frac{f(\omega_1)-f(\omega_2)}{\omega_1-\Omega-\omega_2-i\epsilon}\rho_B^1(\omega_1,k)\,M_{11}(\omega_1,\omega_2,\Omega,k)\,\rho_B^1(\omega_2,k) \tag{6.105}$$

and we will only need to calculate M_{11}. It is now convenient to finally write down an explicit basis of gamma matrices.

6.4.3 M_{11} in $d = 3$

For definiteness, let us now focus on $d = 3$ and choose the following basis of gamma matrices

$$\Gamma^{\underline{r}} = \begin{pmatrix} -\sigma^3 & 0 \\ 0 & -\sigma^3 \end{pmatrix}, \quad \Gamma^{\underline{t}} = \begin{pmatrix} i\sigma^1 & 0 \\ 0 & i\sigma^1 \end{pmatrix},$$
$$\Gamma^{\underline{x}} = \begin{pmatrix} -\sigma^2 & 0 \\ 0 & \sigma^2 \end{pmatrix}, \quad \Gamma^{\underline{y}} = \begin{pmatrix} 0 & \sigma^2 \\ \sigma^2 & 0 \end{pmatrix}. \tag{6.106}$$

and write

$$\Psi_1 = \begin{pmatrix} \Phi_1 \\ 0 \end{pmatrix}, \qquad \Psi_2 = \begin{pmatrix} 0 \\ \Phi_2 \end{pmatrix} \tag{6.107}$$

where $\Phi_{1,2}$ are two-component spinors. We then find that Λ^x (evaluated at $\theta = 0$) only has diagonal components while Λ^y only has off-diagonal components. From (6.104), we then find that

$$M_{11} = \Lambda^x_{11}(\omega_1,\omega_2,\Omega,k)\Lambda^x_{11}(\omega_2,\omega_1,\Omega,k)\,. \tag{6.108}$$

where

$$\Lambda^x_{11}(\omega_1,\omega_2,\Omega,k) = \int dr\sqrt{g_{rr}}\,K_A(\Omega)\Phi^T(\omega_1,k)\left(-Q_1\sigma^3+\frac{iQ_2}{\Omega}\sigma^2+Q_3\sigma^1\right)\Phi(\omega_2,k) \tag{6.109}$$

with

$$Q_1 = qg_{jj}^{-\frac{1}{2}}, \qquad Q_2 = Cg_{jj}^{-\frac{d+1}{2}}k\sqrt{g_{tt}}, \qquad Q_3 = \frac{1}{8}g_{jj}^{-\frac{d}{2}}C\,. \tag{6.110}$$

This is a complete and self-contained expression that can be evaluated numerically if the wave-functions $\Phi_{1,2}$ are known. We thus conclude that the dominant contribution to the conductivity from the Fermi surface is given by (6.105) with M_{11} given by (6.108) and (6.109).

6.4.4 Spinor DC conductivity

In this section we finally extract the DC conductivity from the expressions above. The DC conductivity can now be obtained by taking the real part in (6.103), and the $\Omega \to 0$ limit,

$$\begin{aligned}\sigma_{\rm DC} &= -\frac{C}{2}\sum_{\alpha,\gamma}\int_0^\infty dk k^{d-2}\int\frac{d\omega}{2\pi}\frac{\partial f(\omega)}{\partial\omega} \\ &\quad \rho_B^\alpha(\omega,k)\,{\rm Re}\,M_{\alpha\gamma}(\omega,k)\,\rho_B^\gamma(\omega,k)+\mathcal{S}. \end{aligned} \tag{6.111}$$

where

$$M(\omega,k)\equiv\lim_{\Omega\to 0}M(\omega+\Omega,\omega,\Omega,k)\ . \tag{6.112}$$

$\mathcal{S}$ corresponds to the part which contains ${\rm Im}M_{\alpha\beta}(\omega,k)$ and arises from taking the imaginary part of the gauge propagator. It is shown in Appendix 6.E that it is subleading in the low temperature limit compared with the term written explicitly in (6.111), so we will neglect it from now on.

Let us now look at the $\Omega\to 0$ limit of (6.112), for which the $\frac{1}{\Omega}$ term in (6.98) has to be treated with some care. Naively, it appears divergent; however, note that

$$\lim_{\Omega\to 0}\frac{1}{\Omega}\overline{\Psi_\beta}(r;\omega+\Omega,\vec{k})\Gamma^{\underline{r}}\Psi_\gamma(r;\omega,\vec{k})=\overline{\partial_\omega\Psi_\beta}(r;\omega,\vec{k})\,\Gamma^{\underline{r}}\Psi_\gamma(r;\omega,\vec{k}) \tag{6.113}$$

is finite because $\overline{\Psi_\beta}(r;\omega,\vec{k})\Gamma^{\underline{r}}\Psi_\gamma(r;\omega,\vec{k})=0$. We can now write down the final explicit expression for Λ^i which goes into (6.112) via (6.104)

$$\begin{aligned}\Lambda^j_{\beta\gamma}(\omega,\vec{k}) &\equiv \lim_{\Omega\to 0}\Lambda^i_{\beta\gamma}(\omega+\Omega,\omega,\Omega) \\ &= i\int dr\sqrt{\frac{g_{rr}}{h}}\,K_A(r;\Omega=0)\,\overline{\Psi_\beta}(r;\omega,\vec{k})\left(iq\Gamma^{\underline{j}}+\frac{C}{8}h^{-\frac{d-1}{2}}\Gamma^{\underline{rtj}}\right)\Psi_\gamma(r;\omega,\vec{k}) \\ &\quad -iCk_j\int dr\sqrt{\frac{g_{rr}g_{tt}}{h^{d+1}}}\,K_A(r;\Omega=0)\,\overline{\partial_\omega\Psi_\beta}(r;\omega,\vec{k})\,\Gamma^{\underline{r}}\Psi_\gamma(r;\omega,\vec{k}) \end{aligned} \tag{6.114}$$

In particular, in the limit (6.114) the Λ^x vertex is proportional to the identity in spinor space,

$$\Lambda^x_{\beta\gamma}(\omega,k) = \delta_{\beta\gamma}\Lambda_\beta. \tag{6.115}$$

where the overall amplitude is given by

$$\begin{aligned}\Lambda_\beta &= (-1)^\beta i\int dr\sqrt{\frac{g_{rr}}{h}}\,K_A(r;\Omega=0)\,\overline{\Phi_\beta}(r;\omega,k)\left(iq\sigma^2+\frac{C}{8}h^{-\frac{d-1}{2}}\right)\Phi_\beta(r;\omega,k) \\ &\quad +iCk\int dr\sqrt{\frac{g_{rr}g_{tt}}{h^{d+1}}}\,K_A(r;\Omega=0)\,\overline{\partial_\omega\Phi_\beta}(r;\omega,k)\,\sigma^3\,\Phi_\beta(r;\omega,k) \end{aligned} \tag{6.116}$$

Similarly, the Λ^y vertex can be explicitly calculated to be

$$\Lambda^y_{12} = i \int dr \sqrt{\frac{g_{rr}}{h}} K_A(r; \Omega = 0) \overline{\mathbf{\Phi}_1}(r; \omega, k) \left(iq\sigma^2 + \frac{\mathcal{C}}{8} h^{-\frac{d-1}{2}} \right) \mathbf{\Phi}_2(r; \omega, k) \ . \quad (6.117)$$

where $\bar{\mathbf{\Phi}} \equiv \mathbf{\Phi}^\dagger i\sigma^1$

As this was a somewhat lengthy calculation, let us briefly recap: after a great deal of calculation, we derived an explicit formula for the one-loop DC conductivity,

$$\sigma_{\rm DC} = -\frac{C}{2} \int_0^\infty dk k^{d-2} \int \frac{d\omega}{2\pi} \frac{\partial f(\omega)}{\partial \omega} \rho^1_B(\omega, k) \, \mathrm{Re}\, M_{11}(\omega, k) \, \rho^1_B(\omega, k) \quad (6.118)$$

To complete the story we should examine how Λ scales with T in the $T \to 0$ limit. Naively if we examine the structure of the objects making up Λ (and thus M) in (6.94), we see that we have a radial integral over a normalizable wavefunction, which one would expect to be finite and have a smooth (nonzero) limit as $T \to 0$. Indeed a more detailed analysis (carried out in Appendix 6.F) reveals that this is indeed the case, and we can view $M \sim T^0$. The remainder of the analysis is precisely that done earlier in Section 6.3.4, and results in

$$\sigma_{DC}(T) = aT^{-2\nu} \quad (6.119)$$

with a a prefactor that can be calculated numerically in terms of expressions given earlier in this paper. As mentioned earlier, this is the central result of this chapter.

6.5 Discussion and conclusions

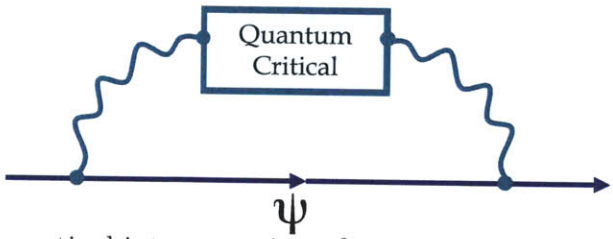

Figure 6-5: Field-theoretical interpretation of our results; the quantum critical sector in this example is provided by the AdS_2 region [19, 107].

Despite the complexity of the intermediate steps, the result that we find for the DC conductivity is very simple. One can package all radial integrals into effective vertices in a way that makes it manifest that the actual conductivity is completely determined by the lifetime of the one-particle excitations, as is clear from the formula (6.65). We should stress that from a field-theoretical point of view this result is *not* obvious, as the single-particle lifetime measures the time needed for the particle to decay, whereas the conductivity is sensitive to the *way* in which it decays.

For example, if the Fermi quasiparticles are coupled to a gapless boson (as is the case in many field-theoretical constructions of non-Fermi-liquids; see e.g. [92, 114,

115, 113, 117, 118, 119, 148, 149] and references therein), small-momentum scattering is strongly preferred because of the large phase space available to the gapless boson at small momenta. However, this small-momentum scattering does *not* degrade the current and so contributes differently to the conductivity than it does to the single-particle lifetime, meaning that the resistivity grows with temperature with a higher power than the single-particle scattering rate [149].

In our calculation, this does not happen. To understand why, note that in our gravity treatment the role played by the gapless boson in the above example is instead filled by the AdS_2 region. From a field theoretical point of view, in our model one could imagine coupling a normal Fermi liquid to a quantum critical sector providing these gapless modes, as in Figure 6-5 [19, 107]. This AdS_2 region provides a set of gapless modes to which the fermion can decay. In our bulk treatment this process has a nice geometric interpretation in terms of the fermion falling into the black hole, as in Figure 6-2. However, these modes are critical *for any momentum* (recall (4.29)), somewhat similar to that postulated for the bosonic fluctuation spectrum in the MFL description of the cuprates. Thus the phase space for scattering does not care about the momentum transfer, and the conductivity is determined by the one-particle lifetime.

In particular, this means that the result for the conductivity at the Marginal Fermi Liquid point $\nu = \frac{1}{2}$ – when the single-particle spectral function takes the MFL form – is consistent with a *linear resistivity*, just as is observed in the strange metals. The correlation between the single-particle spectral function and the collective behavior and transport properties is a strong and robust prediction of our framework. While it is fascinating that this set of results is self-consistent, we do stress that the marginal $\nu = \frac{1}{2}$ point is not special from our gravity treatment, and more work needs to be done to understand if there is a way to single it out in holography.

Finally, we note that it has been an open problem how to construct a framework for non-Fermi liquids. The gauge/gravity framework we are using provides a well-defined way to address physical questions in such a system. Although the underlying UV theories in which our models are embedded most likely have no relation with the UV description of the electronic system underlying the strange metal behavior of cuprates or a heavy fermion system, they do share striking similarities in terms of IR phenomena associated with a Fermi surface without quasiparticles. In particular, the emergence of an IR fixed point and the associated scaling phenomena, which dictate the electron scattering rates and transport, could in the most optimistic case provide a framework in which to explain the phenomenological success of the MFL description.

6.A Spinor bulk-to-bulk propagator

In this appendix we derive the spinor bulk-to-bulk propagator. For simplicity of exposition we focus on the case when the dimension d of the boundary theory is odd; the correspondence between bulk and boundary spinors is different when d is even, and though a parallel treatment can be done we shall not perform it here. We denote

by $\mathcal{N}$ the dimension of the bulk spinor representation; in the case that d is odd we have $\mathcal{N} = 2^{\frac{d+1}{2}}$. Our treatment will essentially apply to any asymptotically AdS spacetime with planar slicing and a horizon in the interior; the criterion of asymptotically AdS is important only in the precise choice of UV boundary conditions and can be easily modified if necessary.

We begin with the bulk spinor action in real-time:

$$S = \int d^d x dt \sqrt{-g} i\bar{\psi} \left(\Gamma^M D_M - m\right) \psi \tag{6.120}$$

where $\bar{\psi} \equiv \psi^\dagger \Gamma^{\underline{t}}$. From here we can derive the usual Dirac equation,

$$(\Gamma^M D_M - m)\psi = 0, \tag{6.121}$$

where the derivative D is understood to include both the spin connection and couplings to background gauge fields. We would like to derive the retarded bulk-to-bulk propagator, which satisfies the equation

$$(\Gamma^M D_M - m) G_R(r, r'; \omega, k) = \frac{i}{\sqrt{-g}} \delta(r - r'), \tag{6.122}$$

where we work in Fourier space in all directions but r. We begin by understanding some properties of the bulk tree-level solutions to the Dirac equation.

6.A.1 Bulk solutions

Infalling solutions to the spinor equation have been discussed in some detail in Chapter 2.3 of this thesis. A key point is that if r_0 denotes the radial coordinate of the horizon the infalling solutions satisfy

$$\psi_A^{in}(r \to r_0) \sim (r - r_0)^{-\frac{i\omega\beta}{4\pi}}, \tag{6.123}$$

with β the inverse Hawking temperature of the horizon. A slightly different boundary condition is used if we have a degenerate zero-temperature horizon. Now it is a fact that only *half* of the solutions to the Dirac equation are infalling; thus we have $\frac{\mathcal{N}}{2}$ infalling solutions which we denote by ψ_A^{in}, $A \in \left\{1..\frac{\mathcal{N}}{2}\right\}$. Clearly one can find outgoing solutions ψ_A^{out} by changing the sign in the exponent in (6.123).

We now discuss solutions at the AdS boundary. As discussed in a slightly less covariant manner in Chapter 2.3, for large r (i.e. with the AdS boundary at $r \to \infty$) we have purely normalizable Ψ and purely non-normalizable $\mathfrak{Y}$ solutions defined respectively by

$$\psi_\alpha(r \to \infty) \sim \zeta_\alpha^- r^{-mR - d/2} \tag{6.124}$$

$$\mathfrak{Y}_\alpha(r \to \infty) \sim \zeta_\alpha^+ r^{+mR - d/2} \quad . \tag{6.125}$$

The $\zeta_\alpha^\pm$ are eigenspinors of Γ^r,

$$(1 \mp \Gamma^{\underline{r}})\zeta_\alpha^\pm = 0 \ , \tag{6.126}$$

and we choose to normalize them so that

$$\zeta_\alpha^{\dagger\pm}\zeta_\beta^\pm = 1_{\alpha\beta} \ . \tag{6.127}$$

This leads to the following completeness relation,

$$\sum_\alpha \zeta_\alpha^\pm \zeta_\alpha^{\dagger\pm} = \frac{1}{2}(1 \mp \Gamma^{\underline{r}}) \ . \tag{6.128}$$

Once again, α runs from 1 to $\frac{\mathcal{N}}{2}$ (as the two different eigenspaces of $\Gamma^{\underline{r}}$ span the full spinor space.) It should be interpreted as the *boundary* theory spinor index.

Now we note that he combination of the $\boldsymbol{\psi}_\alpha$ and the $\mathfrak{Y}_\alpha$ form a complete basis of solutions, so we can expand any solution – and in particular the infalling solutions – in terms of them,

$$\psi_A^{in} = A_A^\alpha \mathfrak{Y}_\alpha + B_A^\alpha \boldsymbol{\psi}_\alpha \tag{6.129}$$

Here A and B are both $\frac{\mathcal{N}}{2} \times \frac{\mathcal{N}}{2}$ matrices that connect the infalling and boundary solutions. Note that the boundary theory spinor retarded Green's function G_B can now be written in a covariant way as

$$G_B^{\alpha\sigma} = iB_A^\alpha (A^{-1})_\beta^A (\gamma^t)^{\beta\sigma} \ . \tag{6.130}$$

with γ^t the boundary theory gamma matrix. This is the covariant generalization of (2.61) and will be useful in what follows. One can find the *advanced* boundary theory correlator by using outgoing solutions and their corresponding outgoing expansion coefficient matrices B, A in (6.130).

We now establish some relations amongst these solutions that we will call Wronskians. Note first that by using the Dirac equation (6.121) we can show that for *any* two radial solutions $\psi_1(r)$, $\psi_2(r)$ evaluated at the same frequency and momentum, the Wronskian $W[\psi_1, \psi_2]$ defined as

$$W[\psi_1, \psi_2] \equiv \sqrt{-g g^{rr}}\overline{\psi_1}(\omega, k)\Gamma^{\underline{r}}\psi_2(\omega, k) \tag{6.131}$$

is a *radial* invariant, i.e. $\partial_r W = 0$.

We now compute some Wronskians that we will need later. First, we compute the Wronskian between a normalizable and non-normalizable solution; as this is a radial invariant we can do this at infinity using (6.125) and (6.125). Note that all powers of r cancel and we find

$$W[\mathfrak{Y}_\alpha, \boldsymbol{\psi}_\beta] = (\zeta_\alpha^+)^\dagger \Gamma^{\underline{t}}\Gamma^{\underline{r}}\zeta_\beta^- = -(\zeta_\alpha^+)^\dagger \Gamma^{\underline{t}}\zeta_\beta^- = -(\gamma^t)_{\alpha\beta} \tag{6.132}$$

In the last equality we have made a choice on how to relate the $\zeta_\alpha^\pm$, which up till now never appeared in the same equation. This choice will simplify some equations later

and coincides with the natural choice using the concrete basis (2.44). Similarly, we find

$$W[\psi_\alpha, \mathfrak{Y}_\beta] = (\gamma^t)_{\alpha\beta} \tag{6.133}$$

Finally, let us compute the Wronskian between two normalizable solutions,

$$W[\psi_\alpha, \psi_\beta] = -r^{-2mR}(\zeta^-_\alpha)^\dagger \Gamma^{\underline{t}} \zeta^-_\beta = 0\,. \tag{6.134}$$

To understand the last equality imagine inserting a factor of $(1 - \Gamma^{\underline{r}})/2$ before the ζ^-_β; this is a projector and has no effect on the ζ^-_β, but if we anticommute it to the left it will be annihilated by the (ζ^-_α); thus we conclude that this Wronskian between two normalizable solutions is 0. Similar arguments show that $W[\mathfrak{Y}_\alpha, \mathfrak{Y}_\beta] = 0$.

6.A.2 Constructing the propagator

We are now ready to construct the bulk-to-bulk retarded propagator, which satisfies the equation

$$(\Gamma^M D_M - m) G_R(r, r'; \omega, k) = \frac{i}{\sqrt{-g}} \delta(r - r'), \tag{6.135}$$

together with the boundary conditions that as either argument r or $r' \to r_0$ the propagator should behave like an infalling wave (6.123), and similarly as r or $r' \to \infty$ the propagator should be normalizable as in (6.125). Note that the operator defined above acts only on the left index of the propagator (which is a matrix in spinor space) and on the argument r; if we can demonstrate that the propagator indeed satisfies this equation then it will also satisfy the corresponding equation with the differential operator acting from the right and as a function of r', by the equality of left and right inverses. Thus we will only explicitly show that the operator satisfies the equation in r.

With the benefit of hindsight, we now simply write down the answer for the bulk-to-bulk retarded propagator

$$G_R(r, r'; \omega, k) = \psi_\alpha(r) G_B^{\alpha\beta}(\omega, k) \overline{\psi_\beta}(r') + \begin{cases} i\mathfrak{Y}_\alpha(r)(\gamma^t)^{\alpha\beta}\overline{\psi_\beta}(r') & r < r' \\ i\psi_\alpha(r)(\gamma^t)^{\alpha\beta}\overline{\mathfrak{Y}_\beta}(r') & r > r' \end{cases} \tag{6.136}$$

We now set out to prove that this propagator has all of the properties required of it, very few of which are manifest in this form. We begin by staying away from the delta function at $r = r'$ and studying the case $r > r'$, where we have

$$G_R(r, r'; \omega, k) = \psi_\alpha(r) \left(G_B^{\alpha\beta}(\omega, k) \overline{\psi_\beta}(r') + i(\gamma^t)^{\alpha\beta} \overline{\mathfrak{Y}_\beta}(r') \right) \qquad r > r' \tag{6.137}$$

We see that this satisfies the defining equation (6.135) in r, as well as the boundary condition that the solution be normalizable as $r \to \infty$, as the dependence on r is simply that of the normalizable solution ψ_α.

We turn now to $r < r'$, where we have

$$G_R(r,r';\omega,k) = \left(\psi_\alpha(r)G_B^{\alpha\beta}(\omega,k) + i\mathfrak{Y}_\alpha(r)(\gamma^t)^{\alpha\beta}\right)\overline{\psi_\beta}(r') \qquad r < r' \tag{6.138}$$

Now using the definition of the G_B in (6.130) and the representation of the infalling wave (6.129) we see that this can be written as

$$G_R(r,r';\omega,k) = i\psi_A^{in}(r)(A^{-1})_\sigma^A(\gamma^t)^{\sigma\beta}\overline{\psi_\beta}(r') \tag{6.139}$$

Again, this satisfies both the defining equation (6.135) and the infalling boundary condition for $r < r'$, as the dependence on r is now simply that of the infalling solution.

We must now verify that the discontinuity across $r = r'$ is correct to result in the delta function seen in (6.135). To see this we integrate (6.135) across $r = r'$ to conclude that the required property is

$$\sqrt{-gg^{rr}}\Gamma^r(G_R(r+\epsilon,r) - G_R(r,r+\epsilon)) = i \tag{6.140}$$

Putting the form of (6.136) into this equation we see that we *need*

$$\sqrt{-gg^{rr}}\Gamma^r\left(\psi_\alpha(r)(\gamma^t)^{\alpha\beta}\overline{\mathfrak{Y}_\beta}(r) - \mathfrak{Y}_\alpha(r)(\gamma^t)^{\alpha\beta}\overline{\psi_\beta}(r)\right) = \mathbf{1}, \tag{6.141}$$

where the right hand side is an identity matrix in spinor space. This is thus an $\mathcal{N}\times\mathcal{N}$ matrix equation.

To show that it is satisfied we will take several Wronskians. Consider contracting both sides from the left with $\overline{\mathfrak{Y}_\sigma}(r)$. The right-hand side becomes just $\overline{\mathfrak{Y}_\sigma}$. The left-hand side then becomes a sum of two Wronskians; the Wronskian of $\mathfrak{Y}$ with itself vanishes, and we find then for left-hand side

$$W[\mathfrak{Y}_\sigma,\psi_\alpha](\gamma^t)^{\alpha\beta}\overline{\mathfrak{Y}_\beta} = -(\gamma^t)_{\sigma\alpha}(\gamma^t)^{\alpha\beta}\overline{\mathfrak{Y}_\beta} = \overline{\mathfrak{Y}_\sigma}, \tag{6.142}$$

where in the first equality we have used (6.132) and in the second we have used the d-dimensional Clifford algebra, $(\gamma^t)^2 = -\mathbf{1}$. This is then consistent with (6.141). Note that we can vary σ over any of its $\frac{\mathcal{N}}{2}$ values and there is a suppressed implicit bulk spinor index on both sides; thus we have actually established $\frac{\mathcal{N}^2}{2}$ relations.

To establish the remaining $\frac{\mathcal{N}^2}{2}$, consider acting with the left with $\overline{\psi_\sigma}$ to find

$$-W[\psi_\sigma,\mathfrak{Y}_\alpha](\gamma^t)^{\alpha\beta}\overline{\psi_\beta} = \overline{\psi_\sigma}, \tag{6.143}$$

by arguments identical to those above. This is an *independent* set of $\frac{\mathcal{N}^2}{2}$ equations; we conclude that the discontinuity is indeed correct for all $\mathcal{N}^2$ components and the form of the propagator proposed in (6.136) is indeed correct.

Finally, we would like to compute the bulk-to-bulk spectral density, which is the object actually used in our calculation. This is straightforwardly found; it is defined to be

$$\rho(r,r';\omega,k) = -i(G_R(r,r';\omega,k) - G_A(r,r';\omega,k)) \ . \tag{6.144}$$

The difference between the retarded and advanced propagator lies in the choice of boundary conditions at the horizon. In our expression the definitions of ψ and $\mathfrak{Y}$ are at the asymptotic UV boundary and know nothing of boundary conditions at the horizon; thus only the first term in (6.136) knows whether we are computing an advanced or a retarded correlator, and we find

$$\rho(r,r';\omega,k) = \psi_\alpha(r)\rho_B^{\alpha\beta}(\omega,k)\overline{\psi_\beta}(r') \tag{6.145}$$

where $\rho_B^{\alpha\beta}(\omega,k) = -i(G_B^{(R)}(\omega,k) - G_B^{(A)}(\omega,k))^{\alpha\beta}$ is the *boundary* theory spectral density. This is the expression used in (6.79).

6.B Mixing between graviton and vector field

In this section we construct the tree-level equations of motion for the coupled vector-graviton fluctuations about the charged black brane background. The action can be written in the usual form,

$$S = \frac{1}{2\kappa^2}\int d^{d+1}x\,\sqrt{-g}\left[\mathcal{R} - 2\Lambda - \frac{R^2}{g_F^2}F_{\mu\nu}F^{\mu\nu}\right] \tag{6.146}$$

with background metric given by

$$ds^2 = g_{tt}dt^2 + g_{rr}dr^2 + g_{ii}dx_i^2 \tag{6.147}$$

and a nonzero background profile $A_0(r)$. It is convenient to work with the radial background electric field $E_r = \partial_r A_0$, which satisfies the equation of motion

$$\partial_r(E_r\sqrt{-g}g^{tt}g^{rr}) = 0\ . \tag{6.148}$$

We will denote

$$\mathcal{Q} \equiv E_r\sqrt{-g}g^{tt}g^{rr} = \text{const}\ . \tag{6.149}$$

Now consider small fluctuations

$$A_M \to A_0\delta_{M0} + a_M, \qquad g_{MN} \to g_{MN} + h_{MN}\ . \tag{6.150}$$

We seek to determine the equations of motion for these fluctuations; we first use our gauge freedom to set

$$h_{rM} = a_r = 0\ . \tag{6.151}$$

At quadratic level in fluctuations the Maxwell action can now be written as

$$\begin{aligned} S_{EM} \;=\; -C_1\int d^{d+1}x\,\Big[&\frac{1}{2}E_r\left(\sqrt{-g}g^{tt}g^{rr} - \sqrt{-g}g^{tr}g^{tr}\right)_{(2)}E_r + \frac{1}{4}\sqrt{-g}f_{MN}f^{MN} \\ &+E_r(g^{tt}g^{rr}\sqrt{-g})_{(1)}f_{0r} - \mathcal{Q}\left(h_t^i f_{ir} + h_r^i f_{ti}\right)\Big] \end{aligned} \tag{6.152}$$

with

$$C_1 = \frac{2R^2}{g_F^2 \kappa^2}, \qquad f_{MN} = \partial_M a_N - \partial_N a_M \tag{6.153}$$

The canonical momentum for a_μ is then given by

$$\pi^i = \frac{1}{C_1}\frac{\delta S}{\delta \partial_r a_i} = -\sqrt{-g} g^{rr} g^{ii} f_{ri} - \mathcal{Q} h_t^i \tag{6.154}$$

$$\pi^t = \sqrt{-g} g^{rr} g^{rr} f_{0r} + \left(\sqrt{-g} g^{rr} g^{rr}\right)_{(1)} E_r \tag{6.155}$$

The equation for a_r is essentially the Gauss law constraint in the bulk and leads to the conservation of this canonical momentum,

$$\partial_\mu \pi^\mu = 0 \tag{6.156}$$

Finally, the dynamical equations for a_i are

$$-\partial_r \pi^\mu + \sqrt{-g}\partial_\nu f^{\nu\mu} = 0 \tag{6.157}$$

We turn now to the gravitational fluctuations. At this point it is helpful to specialize to the zero momentum limit, i.e. all fluctuations depend only on t and r. Now all spatial directions are the same, and so we pick one direction (calling it y) and focus only on h_α^y, with $\alpha = (t, r)$, and where the indices are raised by the background metric. We will then find a set of coupled equations for a_y and h_t^y(and a_r and h_r^y, which will be set to zero in the end). The relevant equations then become

$$\pi^y = -\sqrt{-g} g^{rr} g^{yy} a_y' - \mathcal{Q} h_t^y \tag{6.158}$$

$$\partial_r \pi^y + \sqrt{-g} g^{yy} g^{tt} \omega^2 a_y = 0 \tag{6.159}$$

$$\frac{C_1}{C_2}\mathcal{Q} a_y = \sqrt{-g} g_{yy} g^{rr} g^{tt} \partial_r h_t^y \tag{6.160}$$

Taking a derivative of the first equation with respect to r one can derive an equation for a_y alone

$$\partial_r(\sqrt{-g} g^{rr} g^{yy} a_y') + \left(\frac{C_1 \mathcal{Q}^2}{C_2}\frac{g_{rr} g_{tt}}{\sqrt{-g} g_{yy}} - \sqrt{-g} g^{yy} g^{tt} \omega^2\right) a_y = 0 \tag{6.161}$$

Note now that using

$$g_{tt} = -f r^2, \qquad g_{rr} = \frac{1}{r^2 f}, \qquad g_{ii} = r^2 \tag{6.162}$$

we find that (6.161) becomes

$$\partial_r \left(r^{d-1} f a_y'\right) - \left(\mathcal{C} r^{-d-1} - \frac{\omega^2 r^{d-5}}{f}\right) a_y = 0 \tag{6.163}$$

In the last expression we introduced the constant $\mathcal{C} \equiv \frac{C_1}{C_2}\mathcal{Q}^2$ and we set $R = 1$. We note that the combination $\mathcal{C} R_2^2 \left(\frac{R}{r_\star}\right)^{2d-2} = 2$.

Equation (6.160) implies a corresponding relation between the bulk-to-boundary propagators K_a, K_h of the metric and gauge field, which is important for our calculation:

$$\mathcal{C} K_a = \sqrt{-g} g_{yy} g^{rr} g^{tt} \partial_r K_h \ . \tag{6.164}$$

6.C Couplings of a spinor to graviton and vector field

In this section we determine the couplings of a spinor to graviton and gauge field fluctuations; these are necessary to construct the bulk vertex. We consider a free spinor field with the action

$$S = -\int d^{d+1}x \sqrt{-g}\, i(\bar{\psi}\Gamma^M \mathcal{D}_M \psi - m\bar{\psi}\psi) = \int d^{d+1}\sqrt{-g}\,\mathcal{L} \tag{6.165}$$

where $\bar{\psi} = \psi^\dagger \Gamma^{\underline{t}}$ and

$$\mathcal{D}_M = \partial_M + \frac{1}{4}\omega_{abM}\Gamma^{ab} - iqA_M \tag{6.166}$$

The abstract spacetime indices are $M, N \cdots$ and the abstract tangent space indices are $a, b, \cdots$. The index with an underline denotes that in tangent space. Thus Γ^a to denote gamma matrices in the tangent frame and Γ^M those in curved coordinates. Note that

$$\Gamma^M = \Gamma^a e_a{}^M \tag{6.167}$$

Note that the nonzero spin connections for (6.71) are given by ($h = g_{ii}$)

$$\omega_{\underline{tr}} = -f_0 e^{\underline{t}}, \quad \omega_{\underline{ir}} = f_1 e^{\underline{i}}, \quad e^{\underline{t}} = g_{tt}^{\frac{1}{2}} dt, \quad e^{\underline{i}} = h^{\frac{1}{2}} dx^i \tag{6.168}$$

with

$$f_0 \equiv \frac{1}{2}\frac{g_{tt}'}{g_{tt}}\sqrt{g^{rr}}, \qquad f_1 \equiv \frac{1}{2}\frac{h'}{h}\sqrt{g^{rr}} \tag{6.169}$$

We now consider a perturbed metric of the form

$$ds^2 = -\tilde{g}_{tt}dt^2 + h(dy + bdt)^2 + g_{rr}dr^2 + h dx_i^2 \tag{6.170}$$

with

$$b \equiv h_t^y, \qquad \tilde{g}_{tt} = g_{tt} + hb^2 \tag{6.171}$$

The new spin connections are given by

$$\omega_{\underline{ty}} = f_2 e^{\underline{r}} \tag{6.172}$$

$$\omega_{\underline{tr}} = -\tilde{f}_0 e^{\underline{t}} + f_2 e^{\underline{y}} \tag{6.173}$$

$$\omega_{\underline{yr}} = f_1 e^{\underline{y}} + f_2 e^{\underline{t}} \tag{6.174}$$

$$\omega_{\underline{ir}} = f_1 e^{\underline{i}} \tag{6.175}$$

with

$$f_2 \equiv \frac{1}{2}\sqrt{\frac{h}{g_{rr}\tilde{g}_{tt}}}b', \qquad \tilde{f}_0 \equiv \frac{1}{2}\frac{\tilde{g}'_{tt}}{\tilde{g}_{tt}}\sqrt{g^{rr}} \tag{6.176}$$

and

$$e^{\underline{t}} = \tilde{g}_{tt}^{\frac{1}{2}}dt, \quad e^{\underline{y}} = h^{\frac{1}{2}}(dy + bdt), \quad e^{\underline{r}} = g_{rr}^{\frac{1}{2}} \quad e^{\underline{i}} = h^{\frac{1}{2}}dx^i \tag{6.177}$$

Also note that

$$\Gamma^t = \tilde{g}_{tt}^{-\frac{1}{2}}\Gamma^{\underline{t}}, \qquad \Gamma^y = -\tilde{g}_{tt}^{-\frac{1}{2}}b\Gamma^{\underline{t}} + h^{-\frac{1}{2}}\Gamma^{\underline{y}} \tag{6.178}$$

We thus find the corrections to the Dirac action is given by (with $a \equiv a_y$): at cubic order

$$\delta\mathcal{L}_3 = -i\bar{\psi}\left(-g_{tt}^{-\frac{1}{2}}h_t^y\Gamma^{\underline{t}}\partial_y + \frac{1}{4}f_2\Gamma^{\underline{rty}} - ih^{-\frac{1}{2}}qa_y\Gamma^{\underline{y}}\right)\psi \quad . \tag{6.179}$$

In (6.179) we have restored the indices on $b \equiv h_t^y, a_y$ because they make the covariant nature of the expression manifest.

At quartic order there are both $b^2\psi^2$ and $ba\psi^2$ terms. For completeness we list them, although they are not required for our calculation. The couplings of the bulk spinor which are quadratic in the bosonic bulk modes (altogether, quartic in fluctuations) are

$$\mathcal{L}_4 = \sqrt{-g}i\bar{\psi}\left[\frac{hb^2}{2g_{tt}}\left(\Gamma^M\mathcal{D}_M - m\right)_{(0)} - \frac{b}{\sqrt{g_{tt}}}\Gamma^{\underline{t}}\left(\frac{hb}{2g_{tt}}D_t - iqa\right) + \frac{1}{4}\Gamma^{\underline{r}}\left(\tilde{f}_0\right)_{(2)}\right]\psi \tag{6.180}$$

where

$$\left(\tilde{f}_0\right)_{(2)} = \frac{1}{2}\sqrt{g^{rr}}\partial_r\left(\frac{hb^2}{g_{tt}}\right) \ . \tag{6.181}$$

6.D Ward Identities in the bulk and boundary

6.D.1 Generalities

Here we review how the Ward identities of the boundary field theory are inherited from the corresponding local gauge symmetries in the bulk. In this section only we will work in Euclidean signature for simplicity of notation, and we consider a very general field theory with a stress tensor $T^{\mu\nu}$ and real operator $\mathcal{O}$. These are dual in the bulk to the metric g_{MN} and a real scalar field ϕ, and we denote with a subscript

0 the boundary values of these fields (*e.g.* $\phi(r \to \infty) = \phi_0$). The central relation of gauge-gravity duality applied to this system reads

$$\left\langle \exp\left[\int d^d x \left(\frac{1}{2} T^\nu_\mu g^\mu_{0\nu} + \phi_0 \mathcal{O}\right)\right]\right\rangle = Z[g^\mu_{0\nu}, \phi_0],, \tag{6.182}$$

where the left hand side is the field theory generating functional and Z denotes the partition function of the bulk gravity theory as a functional of the boundary values of the bulk fields. For concreteness we take the background metric to be diagonal and depend only on r.

Consider now the variation of the metric and other bulk fields under an infinitesimal diffeomorphism ξ_M

$$\delta_\xi g_{MN} = \nabla_M \xi_N + \nabla_N \xi_M \qquad \delta_\xi \phi = \xi^M \partial_M \phi \tag{6.183}$$

We restrict attention to diffeomorphisms along the field theory directions with $\xi_r = 0$. We find

$$\delta_\xi g_{\mu\nu} = \partial_\mu \xi_\nu + \partial_\nu \xi_\mu \qquad \delta_\xi g_{r\mu} = \partial_r \xi_\mu - \frac{g'_{\mu\mu}}{g_{\mu\mu}} \xi_\mu \tag{6.184}$$

It is standard to work in the gauge $g_{r\mu} = 0$. This choice does not completely fix the gauge. It only fixes the radial profile of the gauge transformation to be $\xi_\mu(r, x) = g_{\mu\mu}(r)\zeta_\mu(x)$, with $\zeta_\mu(x)$ an unrestricted function of the field theory coordinates. It is important to note that these unfixed gauge transformations do not vanish at the boundary: instead they shift the boundary value of the bulk scalar field and the "one up, one down" metric fluctuations in a simple way, with no extra factors of g_{xx}:

$$\delta_\xi g^\mu_{0\nu} = \eta^{\mu\rho}(\partial_\rho \zeta_\nu + \partial_\nu \zeta_\rho) \qquad \delta_\xi \phi_0 = \eta^{\mu\rho} \zeta_\mu \partial_\rho \phi_0, \tag{6.185}$$

where in this and the following expressions we raise and lower indices using the flat field theory metric $\eta^{\mu\nu}$.

Now the bulk gravity partition function $Z[g^\mu_{0\nu}, \phi_0]$ should be invariant under this transformation. This gives us the following relation

$$-2\partial_\nu \frac{\delta Z}{\delta g^\mu_{0\nu}(x)} + \frac{\delta Z}{\delta \phi(x)} \partial_\mu \phi(x) = 0. \tag{6.186}$$

Let us now understand the implications of this on the field theory generating functional in (6.182) by computing an example correlation function

$$\langle \partial_\mu T^\mu_\nu(x) \mathcal{O}(y) \rangle = \partial_\mu \frac{\delta^2 Z}{\delta g^\mu_{0\nu}(x) \delta \phi_0(y)}\bigg|_{g^\nu_{0\mu} = \phi_0 = 0} \tag{6.187}$$

The right hand side of this expression can be easily found by taking a functional derivative of (6.186) with respect to $\phi_0(y)$. Using the fact that $\delta Z / \delta \phi_0 = \langle \mathcal{O} \rangle$ when

all sources are set to 0 we find

$$\langle \partial_\nu T^\nu_\mu(x)\mathcal{O}(y)\rangle = -\partial_\mu\langle\mathcal{O}(x)\rangle\delta^{(d)}(x-y), \tag{6.188}$$

which is precisely the Ward identity associated with momentum conservation, arising as expected from bulk diffeomorphism invariance. The lesson here is that every unfixed bulk gauge transformation will result in a constraint on boundary theory correlation functions.

6.D.2 Momentum conservation at one loop

Let us now understand the implications for this in our calculation. We are computing correlation functions of the spatial components of the boundary theory current j^i at zero spatial momentum $\vec{k} = 0$ and nonzero frequency ω. In a background with nonzero charge density, we expect fluctuations of j^i to mix with those of the stress tensor T^{it}; however at zero spatial momentum correlation functions of T^{it} are very constrained.

To understand this consider the (Lorentzian signature) Fourier transform of (6.188). Taking the frequency to be Ω, we find

$$\Omega\langle T^t_i(\Omega)\mathcal{O}(-\Omega)\rangle = 0, \tag{6.189}$$

where we have used the fact that we are at zero spatial momentum and our background has translational invariance, causing the right-hand side of (6.188) to vanish. Thus if $\vec{k} = 0$ any correlator of T^{it} must vanish if $\Omega \neq 0$ and so must be proportional to $\delta(\Omega)$. This is nothing but the statement that momentum cannot relax. This confirms the statement made in Section 6.2.1 about the nonexistence of dissipative thermal conductivity in translation-invariant systems.

In our bulk one-loop calculation this will be enforced by invariance of the partition function under the following unfixed gauge transformation, constructed to leave g_{ri} unchanged precisely as in the example above:

$$\delta h_{it}(r,t) = g_{ii}(r)\partial_t\zeta_i(t) \quad \rightarrow \quad \delta h_{it}(r;\Omega) = -i\Omega g_{ii}(r)\zeta_i(\Omega) \ . \tag{6.190}$$

Note that in Fourier space this corresponds to a constant (in r) shift in the variable $h^i_t(r;\Omega)$. In our formalism the bulk wavefunctions of the graviton and gauge field are determined as in (6.80)

$$a_j(r;\Omega) = K_A(r;\Omega)A_j(\Omega), \qquad h^j_t(r;\Omega) = K_h(r;\Omega)A_j(\Omega) \tag{6.191}$$

where K_A and K_h are bulk-to-boundary propagators and $A_j(\Omega)$ is the source for the boundary conserved current (and thus corresponds to the boundary value of a_j). We see that the gauge transform (6.190) can be taken to be a constant shift $K_h(r;\Omega) \rightarrow K_h(r;\Omega) + f(\Omega)$; thus for the boundary theory Ward identity to be satisfied it is critical that such a shift leaves everything invariant. Note that such a shift essentially corresponds in quantum field theory to the emission of a "lightlike"

graviton $f(\Omega)$, with polarization along its "momentum" (which here is purely in the time direction, as $f(\Omega)$ does not depend on r). We expect the emission of such a graviton to be constrained by the *bulk* Ward identity associated with diffeomorphism invariance, which will thus guarantee the *boundary* Ward identity.

We now proceed to show explicitly how this happens in our formalism. The graviton wavefunction enters our expression in the on-shell effective vertex Λ:

$$\Lambda^i_{\beta\gamma}(\Omega,\omega,\vec{k}) = \int dr \sqrt{g_{rr}}\overline{\Psi_\beta}(r;\omega+\Omega,\vec{k})Q^i(r;\Omega,\vec{k})\Psi_\gamma(r;\omega,\vec{k}) \tag{6.192}$$

where Q^i from (6.83) is a function of the gauge field and graviton bulk to boundary propagators

$$\begin{aligned} Q^j(r;\Omega,\vec{k}) = -i\big(&-ik_jK_h(r;\Omega)\Gamma^t \\ &+\frac{g_{xx}}{8}\partial_rK_h(r;\Omega)\Gamma^{rtj} - iqK_A(r;\Omega)\Gamma^j\Big), \end{aligned} \tag{6.193}$$

Only the first term in the expression does not seem invariant, and we will focus our attention on this term. To proceed we will need the on-shell equations of motion for Ψ

$$\left(\sqrt{g^{rr}}\Gamma^{\underline{r}}\partial_r + i\sqrt{g^{ii}}K_\mu\Gamma^{\underline{\mu}} - m\right)\Psi = 0 \quad . \tag{6.194}$$

Consider now the matrix structure of the problematic coupling in Λ,

$$\overline{\Psi_\beta}(r;\omega+\Omega)\Gamma^t\Psi_\gamma(r;\omega) = \overline{\Psi_\beta}(r;\omega+\Omega)\Gamma^t\frac{i(\omega+\Omega-\omega)}{i\Omega}\Psi_\gamma(r;\omega), \tag{6.195}$$

where we have inserted a factor of 1 in a somewhat convoluted way in terms of ω and Ω. The reason for this becomes clear when we use the Dirac equation (6.194) to act with $\Gamma^t(\omega+\Omega)$ on the spinor $\bar{\Psi}_b(\Omega+\omega)$ on the left and with $\Gamma^t\omega$ on $\Psi_c(\omega)$ on the right. Most terms cancel, leaving

$$\overline{\Psi_\beta}(r;\omega+\Omega)\Gamma^t\Psi_\gamma(r;\omega) = \frac{i}{\Omega}\sqrt{g^{rr}}\partial_r\left(\overline{\Psi_\beta}(r;\omega+\Omega)\Gamma^{\underline{r}}\Psi_\gamma(r;\omega)\right). \tag{6.196}$$

We now use this identity in (6.192) and integrate by parts. We can drop both boundary terms: the term at infinity vanishes since the Ψ are normalizable, and the term at the horizon vanishes because the graviton wavefunction h^i_t must vanish there. We find for the relevant term,

$$\Lambda^i_{\beta\gamma}(\Omega,\omega,\vec{k}) = \int dr\ \overline{\Psi_\beta}(r;\omega+\Omega)\frac{ik_i}{\Omega}\partial_rK_h(r;\omega)\Gamma^{\underline{r}}\Psi_\gamma(r;\omega) + ... \tag{6.197}$$

It is clear from this expression that the spinor couples only to the radial derivative of the graviton, and a constant shift in K_h has no effect. In this expression, invariance under (6.190) and thus the boundary Ward identity are manifest. It is convenient to

encode this information by rewriting Q as

$$Q^j(r;\Omega,\vec{k}) = -i\Big(-\frac{k_j}{\Omega}\partial_r K_h(r;\Omega)\Gamma^r \\ +\frac{g_{xx}}{8}\partial_r K_h(r;\Omega)\Gamma^{rtj} - iqK_A(r;\Omega)\Gamma^j\Big), \tag{6.198}$$

where it is important to note that this expression is equivalent to the original (6.194) only when it is sandwiched between two on-shell spinors as in our expression for Λ.

6.E Other contributions to the conductivity at one loop

The majority of this paper has focused on the the $1/N$ contribution to the imaginary part of a photon self-energy from cutting across a spinor loop. However, at this order in $1/N$ this is *not* the only contribution to the the propagator. Quartic couplings involving the graviton (schematically, terms like $h^2\bar{\psi}\psi$ and $hA\bar{\psi}\psi$ in the Lagrangian) give rise to seagull diagrams that we have not evaluated. Even in the spinor bubble that we have focused on, there are extra contributions to the imaginary part of the photon self-energy from cutting not across the spinor loop but across the photon propagator itself, which already contains an imaginary part since it is essentially a retarded propagator on a black hole background.

In this section we justify our neglect of these diagrams by showing that their contributions to the DC conductivity are analytic in temperature. One can see heuristically how this comes about by noticing that the interesting frequency dependence of these diagrams comes not from the spinors that we are interested in, but from the tree-level gauge field and graviton propagators, which are analytic in temperature.

6.E.1 Seagull diagrams

All seagull diagrams are analytic in temperature. This is because they contain only one spinor propagator, and we need two spinor propagators to create a non-analyticity. To see this, we first write the schematic form of a seagull diagram S with external Euclidean frequency Ω_l:

$$S^{ij}(\Omega_l) = T\sum_{i\omega_m}\int\frac{d^{d-1}k}{(2\pi)^{d-1}}dr_1\sqrt{g(r_1)}\,\mathrm{tr} \\ \Big(P^j(r_1;-i\Omega_l,\vec{k})D_E(r_1,r_1;i\omega_m,\vec{k})P^i(r_1;i\Omega_l,\vec{k})\Big). \tag{6.199}$$

Here P^i contains the information of the graviton or gauge field propagators and vertex and is deliberately left vague. It is shown in equation (6.229) in Appendix 6.G that the Matsubara sum can be rewritten in terms of an integral over the bulk spectral

density

$$T\sum_{i\omega_m} D_E(r_1, r_2; i\omega_m, \vec{k}) = \int \frac{d\Omega}{2\pi} \tanh\left(\frac{\beta\Omega}{2}\right) \rho(r_1, r_2; \Omega, \vec{k}) \tag{6.200}$$

Now as before we recall that the bulk spectral density has a simple relation to the boundary spectral density ρ_B in terms of bulk normalizable wave functions $\psi_a(r)$: $\rho(\omega; r, r') = \psi_\alpha(r)\, \rho_B^{\alpha\beta}\, \overline{\psi_\beta}(r')$. Near the Fermi surface, the eigenvalues of the boundary spectral density matrix take the form (6.62). As we take $T \to 0$, the spectral density reduces to a delta function with support on the quasiparticle dispersion:

$$\lim_{T\to 0} \rho_B(\omega, k) = \pi\delta\left(k_\perp - \mathrm{Re}\,\Sigma\right). \tag{6.201}$$

Putting this relation and (6.229) into (6.200), we see that the seagull diagram appears completely analytic in T.

This should be contrasted with the behavior of the *square* of the spectral density. This quantity appears if we have more than one internal spinor line, and in the same limit behaves as

$$\lim_{T\to 0} \rho_B(\omega, k)^2 = \frac{\pi}{2\mathrm{Im}\,\Sigma}\delta(k_\perp - \mathrm{Re}\,\Sigma) \tag{6.202}$$

Note the overall factor of $1/\mathrm{Im}\,\Sigma$ outside this delta function; this behaves as $T^{-2\nu}$ and is the ultimate origin of the observed non-analyticity in the conductivity. It is clear from (6.201) that no such non-analyticity exists if we have only a single factor of ρ_B. Each factor of ρ_B comes from a bulk spinor propagator; thus if we have only one internal spinor line (as is the case for the seagull) the diagram will necessarily be analytic in T.

6.E.2 Other contributions from the spinor loop

The spinor bubble (Figure 6.3.1) is the diagram on which we have focused most of our attention. We recall the expression for its contribution to the boundary correlator (6.93),

$$\begin{aligned} G_R^{ij}(\Omega) = \int \frac{d^{d-1}k}{(2\pi)^{d-1}} \int \frac{d\omega_1}{2\pi}\frac{d\omega_2}{2\pi} \frac{f(\omega_1) - f(\omega_2)}{\omega_1 - \Omega - \omega_2 - i\epsilon} \\ \times \rho_B^{\alpha\beta}(\omega_1, \vec{k})\, \Lambda_{\beta\gamma}(\omega_1, \omega_2, \Omega)\, \rho_B^{\gamma\delta}(\omega_2, \vec{k})\, \Lambda_{\delta\alpha}(\omega_2, \omega_1, -\Omega). \end{aligned} \tag{6.203}$$

The DC conductivity is $1/\Omega$ times the imaginary part of this expression evaluated at $\Omega = 0$. The body of this paper focuses on computing the contribution from the imaginary part of the spinor loop. There is however another contribution even at generic values of $k \neq k_F$. This arises from the fact that the vertex Λ contains a factor of the bulk-to-boundary gauge field propagator at real frequency Ω, which has an imaginary part proportional to $i\Omega$ (coming essentially from incoming boundary conditions at the horizon). This can multiply the real part of the spinor loop at $\Omega = 0$ to give a finite contribution to the DC conductivity. In this section we show

that this contribution is analytic in T.

We want to calculate the real part of the spinor loop; thus we should simply set $\epsilon \to 0$ and compute the integrals. As before we will simply ignore the matrix structure of the $\rho_B^{\alpha\beta}$. Let us now perform the k integral first, *i.e.* we extract out the following part of the expression:

$$I(\omega_1, \omega_2) \equiv \int \frac{d^{d-1}k}{(2\pi)^{d-1}} \rho_B(\omega_1, \vec{k}) \rho_B(\omega_2, \vec{k})$$
$$\rho_B(\omega, \vec{k}) = \frac{\mathrm{Im}\,\Sigma(\omega)}{(k_\perp - \mathrm{Re}\,\Sigma(\omega))^2 + \mathrm{Im}\,\Sigma(\omega)^2} \tag{6.204}$$

We can perform this integral by contours in the complex $k_\perp$ plane to find

$$I(\omega_1, \omega_2) = \pi \int \frac{d\Omega_k}{(2\pi)^{d-1}}\, \mathrm{Im}\, \frac{1}{\Sigma(\omega_1) - \Sigma(\omega_2)^\star}. \tag{6.205}$$

Note that when evaluating the *imaginary* part of this bubble (as in the main text) we find a delta function which forces us to sit on-shell, i.e. $\omega_1 = \omega_2$ and this integral $I \sim 1/\mathrm{Im}\,\Sigma(\omega) \sim T^{-2\nu}$. Now, on the other hand, we will not sit on this point but instead integrate *through* it, softening the singularity. The dangerous part of the integral thus comes from $\omega_1 \sim \omega_2$; to extract this we define $\Delta = \omega_2 - \omega_1$ and use $\mathrm{Re}\,\Sigma(\omega) = \frac{1}{v_F}\omega + T^{2\nu} g\left(\frac{\omega}{T}\right)$ to find for our starting expression

$$G_R^{ij}(\Omega) \sim \int d\omega_2 d\Delta \frac{2\mathrm{Im}\,\Sigma(\omega_2)}{(2\mathrm{Im}\,\Sigma(\omega_2))^2 + \frac{1}{v_F^2}\Delta^2} \frac{df}{d\omega}(\omega_2) \frac{\Delta}{\Delta + \Omega} + \ldots \tag{6.206}$$

where we are interested in the $\Delta \to 0$ singularity and so have expanded everything in powers of Δ, neglecting higher order terms in both Δ and T and ignoring overall factors from Λ. Note that even at $\Omega = 0$, we do not find any divergence; the integral through $\Delta = 0$ gives an expression that is T^0. We conclude that the real part of the spinor loop–and thus the contribution from cutting across the gauge field propagator–is analytic in T.

6.E.3 Oscillatory region contribution

We return to the expression (6.105) for the conductivity as an integral over k. In the previous sections we have studied the temperature-dependence of the region of k near a Fermi surface at k_F. Here we ask whether the "oscillatory region" (values of k such that particle production occurs in the AdS_2 region of the geometry) make significant contributions to the conductivity. We will find that their contribution is finite at $T = 0$, and hence subleading compared to the $T^{-2\nu}$ behavior of a Fermi surface. We will not worry about numerical factors here.

For simplicity, we study the real part of the conductivity, and neglect the contri-

butions discussed in the previous parts of this Appendix:

$$\sigma(\Omega) = \frac{1}{\Omega}\int (d\vec{k}) \int \frac{d\omega}{2\pi} \left(f(\Omega+\omega) - f(\omega)\right) \times \rho(\omega+\Omega,k)\rho(\omega,k)\Lambda(\omega,\omega+\Omega)\Lambda(\omega+\Omega,\omega) \quad . \tag{6.207}$$

At zero temperature, the difference of Fermi factors in (6.207) has support only in $\omega \in [-\omega, 0]$. At small Ω (and in particular in the DC limit), we may therefore use the small-frequency approximation of [19]. In this approximation, the fermion spectral density in the oscillatory region may be written

$$\rho_{\rm osc}(\omega,k) = {\rm Im}\, \frac{e^{i\theta}|c|\omega^{i\lambda}+1}{e^{i\theta'}|c|\omega^{i\lambda}+1} \quad . \tag{6.208}$$

Recall that $c\omega^{i\lambda}$ is the IR CFT Green's function (the IR CFT dimension is imaginary) at $T=0$. $e^{i\theta,\theta'}$ are scattering phases constructed from the UV data. This expression is valid in the oscillatory regime $k < k_{\rm osc} = \sqrt{q^2 e_d^2 - m_k^2 R_2^2}$ (see eqn (68) of [19]). The important point now is that as a function of ω, the object (6.208) is *bounded*. In fact, it can be bounded uniformly in k (*i.e.* we can find a constant $\mathring{A}$ such that $\mathring{A} > \rho_{\rm osc}(\omega,k)$ for all $k < k_{\rm osc}$). Numerical evidence for this statement is figure 7 of [16].

The same is true of the factors $\Lambda(\omega,\Omega+\omega)$ in (6.207). This is because in the oscillatory regime, the solutions ψ (appearing in Λ) in the matching region are unit-amplitude waves.

So

$$\sigma_{osc}(\Omega) = \frac{1}{\Omega}\mathcal{I} \tag{6.209}$$

where

$$\mathcal{I} \equiv \int_{-\Omega}^{0} d\omega \left(\int dk \rho\rho\Lambda\Lambda\right) \quad . \tag{6.210}$$

$\mathcal{I}$ is the integral of a product of bounded functions over an interval of width Ω, and hence

$$\mathcal{I} < \mathcal{C}\Omega \tag{6.211}$$

for some constant $\mathcal{C}$. Hence the conductivity at small frequency and zero temperature

$$\sigma_{osc}(\Omega) < \mathcal{C} \tag{6.212}$$

is finite.

6.F Temperature scaling of effective vertex

In this section we study the temperature dependence of the effective vertex (6.94). For this purpose it is convenient to separate the radial integral into the UV and IR region,

$$\Lambda = \Lambda_{UV} + \Lambda_{IR} \quad . \tag{6.213}$$

To find the T-scaling of Λ we note the following ingredients:

1. Using the notation of [19], we can write $\mathbf{\Phi}$ as

$$\mathbf{\Phi}(k) = \frac{1}{W}(a_-\eta_+ - a_+\eta_-) \tag{6.214}$$

where W is independent of r. Note that for $k_\perp = \mathrm{Re}\,\Sigma \to 0$, $a_+ \propto \mathrm{Re}\,\Sigma$. Then it is easy to check that both terms in (6.116) scale as $O(T^0)$, implying

$$\Lambda_{UV} \sim O(T^0) \quad . \tag{6.215}$$

2. The inner region wave functions are conveniently expressed in terms of the rescaled coordinate

$$\zeta = \frac{TR_2^2}{r - r_*} \tag{6.216}$$

thus

$$g_{tt} \propto T^2, \quad dr \propto T, \qquad g_{rr} \propto T^{-2} \tag{6.217}$$

and in the $T \to 0$ limit

$$K_A(r) \to TK_A(\zeta), \quad \mathbf{\Phi}(k_\perp = \mathrm{Re}\,\Sigma) \propto T^\nu,$$

$$\partial_\omega \mathbf{\Phi}(k_\perp = \mathrm{Re}\,\Sigma) \propto T^{\nu-1} \quad . \tag{6.218}$$

From the above scalings we thus conclude that in the inner region both terms in (6.116) scale with T respectively as

$$\Lambda_{IR} \sim T^{2\nu+1} \quad . \tag{6.219}$$

From (6.215) and (6.219) we conclude that Λ_{UV} dominates, and therefore

$$\Lambda^2 \propto O(T^0) \qquad \Rightarrow \qquad \sigma_{\mathrm{DC}} \propto T^{-2\nu} \quad . \tag{6.220}$$

6.G Some useful formulas

Here we compile some standard and useful identities that are used in the main text.

6.G.1 How to do Matsubara sums

Consider the Euclidean correlation function

$$D_i^E(\omega_n) = \int \frac{d\omega}{2\pi} \frac{\rho_i(\omega)}{i\omega_n + \omega}, \tag{6.221}$$

and the frequency sum

$$\begin{aligned} S(\Omega_l) &\equiv T\sum_{\omega_m} D_1^E(\omega_m+\Omega_l)D_2^E(\omega_m) \\ &= T\sum_{\omega_m}\int \frac{d\omega_1}{2\pi}\frac{d\omega_2}{2\pi}\frac{\rho_1(\omega_1)}{i(\omega_m+\Omega_l)-\omega_1}\frac{\rho_2(\omega_2)}{i\omega_m-\omega_2}, \end{aligned} \tag{6.222}$$

where $\omega_m = \frac{2\pi m}{\beta}$ with m a half integer (an integer) for fermions (bosons), while $\Omega_l = \frac{2\pi l}{\beta}$ with l an integer. Note the identity

$$T\sum_{\omega_m}\frac{1}{i(\omega_m+\Omega_l)-\omega_1}\frac{1}{i\omega_m-\omega_2} = \pm\frac{f(\omega_1)-f(\omega_2)}{\omega_1-i\Omega_l-\omega_2} \tag{6.223}$$

with

$$f(\omega) = \frac{1}{e^{\beta\omega}\pm 1} \tag{6.224}$$

where the upper (lower) sign is for fermion (boson). We then find that

$$S(\Omega_l) = \pm\int \frac{d\omega_1}{2\pi}\frac{d\omega_2}{2\pi}\frac{f(\omega_1)-f(\omega_2)}{\omega_1-i\Omega_l-\omega_2}\,\rho_1(\omega_1)\,\rho_2(\omega_2) \tag{6.225}$$

We now apply this kind of technique for the spinor bulk-to-bulk propagator. We recall that the spinor Euclidean propagator admits the spectral decomposition

$$D_E(r_1,r_2;i\omega_m,\vec{k}) = \int\frac{d\Omega}{(2\pi)}\frac{\rho(r_1,r_2;\Omega,\vec{k})}{i\omega_m-\Omega}, \tag{6.226}$$

A standard trick is to rewrite the sum over fermionic Matsubara frequencies as a contour integral

$$T\sum_{i\omega_m}\to\frac{1}{2\pi i}\int_C d\omega\frac{1}{2}\tanh\left(\frac{\beta\omega}{2}\right) \tag{6.227}$$

where we take the contour C to encircle all the poles. A convenient deformation of the contour is to make it into two lines, one running left to right just above the real axis and the other running right to left just below. In the fermionic case this encircles all the poles. Using (6.226) we can now compute various sums, e.g.

$$\begin{aligned} &T\sum_{i\omega_m} D_E(r_1,r_2;i\omega_m,\vec{k}) = \\ &\frac{1}{2\pi i}\int\frac{d\Omega}{2\pi}\int_{-\infty}^{\infty}d\omega\frac{1}{2}\tanh\left(\frac{\beta\omega}{2}\right)\rho(r_1,r_2;\Omega,\vec{k}) \\ \times\ &\left[\frac{1}{\omega+i\epsilon-\Omega}-\frac{1}{\omega-i\epsilon-\Omega}\right] \end{aligned} \tag{6.228}$$

The bracketed factor reduces to a delta function, and we find eventually

$$T\sum_{i\omega_m} D_E(r_1,r_2;i\omega_m,\vec{k}) = \rho\int\frac{d\Omega}{2\pi}\tanh\left(\frac{\beta\Omega}{2}\right)\rho(r_1,r_2;\Omega,\vec{k}) \tag{6.229}$$

6.G.2 Useful integrals

Throughout our calculation we often need to integrate over a spectral density near a Fermi surface, integrals that often take the form

$$I_n(a) = \int dx\left(\frac{a}{x^2+a^2}\right)^n \tag{6.230}$$

where a is a small parameter usually related to the temperature. We generally only care about the small-a dependence, which is conveniently extracted by using the fact that

$$\int_{-\infty}^{\infty} dx\left(\frac{a}{x^2+a^2}\right)^n = a^{1-n}\sqrt{\pi}\frac{\Gamma\left(n-\frac{1}{2}\right)}{\Gamma(n)} \tag{6.231}$$

and noticing that for any $x \neq 0$, the integrand vanishes at $a = 0$, we see that as we take $a \to 0$, all of these functions become delta functions.

$$\lim_{a\to 0}\left(\frac{a}{x^2+a^2}\right)^n = a^{1-n}\sqrt{\pi}\frac{\Gamma\left(n-\frac{1}{2}\right)}{\Gamma(n)}\delta(x) \tag{6.232}$$

The values of n that are relevant to us are

$$\lim_{a\to 0}\left(\frac{a}{x^2+a^2}\right) = \pi\delta(x) \qquad \lim_{a\to 0}\left(\frac{a}{x^2+a^2}\right)^2 = \frac{\pi}{2a}\delta(x) \tag{6.233}$$

This is a rather nice way of saying that in the low-temperature ($a \to 0$) limit, only things on the Fermi surface matter.

Chapter 7

A holographic model of symmetry breaking

7.1 Introduction

In the previous chapters of this thesis we studied a finite-density state via holography. Importantly, this finite-density state broke no (global) symmetries; indeed the only global symmetry in our model was the $U(1)$ current under which the finite density was charged, and throughout our discussion we assumed that this $U(1)$ was unbroken even at arbitrarily low temperatures.

However upon some thought this situation may seem somewhat unnatural. The microscopic field-theoretical physics of our system is not well-understood, but due to the supersymmetry of the most well-understood models one expects that there should exist some bosonic excitations that are charged under every global $U(1)$ current. If we now turn on a chemical potential then one expects that these charged bosons would condense and break the symmetry. Experience with strongly correlated finite-density systems would in fact lead us to expect a wealth of low-temperature ordered phases, corresponding to the various symmetries that may be broken.

What would this look like in a holographic setup? On the field theory side we have the condensation of a scalar operator charged under some symmetry. On the gravity side, we would then expect a bulk scalar *field* that is charged under some *gauge* symmetry to condense, developing a nontrivial radial profile. This would Higgs the gauge symmetry in the bulk, corresponding to the breaking of the global symmetry in the boundary theory. We expect this to happen at sufficiently low temperatures, meaning that as we lower the temperature of our previously studied black hole horizons they should be unstable towards developing normalizable scalar field configurations.

In the context of black hole physics, this would seem to be precisely the sort of phenomena that is ruled out by no-hair theorems, which state that black holes cannot grow the sort of scalar hair that we have just described. Importantly, however, these no-hair theorems do not apply to asymptotically AdS spacetimes, as first realized by [99] and subsequently developed in detail by [100, 101]. Indeed, the Reissner-Nordstrom black hole studied above is unstable towards developing charged scalar

hair, resulting in a new kind of hairy black hole called a *holographic superconductor*, in which a $U(1)$ symmetry is broken by strong dynamics that results in the condensation of a charged operator; for a review see [102, 103].

In fact, our treatment in Chapter 4 already allows us to see the signature of this scalar instability. Recall that at precisely zero temperature the near-horizon region of the Reissner-Nordstrom black hole can be described by an $AdS_2 \times \mathbb{R}^2$ region. The conformal dimension of a scalar operator in the infrared conformal symmetry described by the AdS_2 region was calculated in (4.9) and can be written as

$$\delta = \frac{1}{2} + \sqrt{\frac{\Delta(\Delta - d)}{d(d-1)} - \frac{q^2}{2d(d-1)} + \frac{1}{4}} \,. \tag{7.1}$$

where d is the dimension of the dual field theory, q the charge of the scalar operator, Δ its dimension under the UV conformal symmetry (which has been broken by the finite density), and in this chapter we have set the bulk gauge coupling $g_F \to 1$. This determines the onset of an instability: if δ becomes complex, the system is unstable[1]. Due to the term proportional to $-q^2$ in (7.1), even an operator which is irrelevant in the UV can be unstable in the IR if q is sufficiently large.

Particularly interesting is the fact that the instability can be made to vanish at *zero temperature* by adjusting the various couplings appearing in (7.1) to tune δ from being imaginary to being real. This is then a qualitative change in the nature of the ground state at zero temperature and so is a *quantum* phase transition. Turning aside from holography for a moment, we see that quantum phase transitions naturally occur in strongly correlated many-body systems, which often contain competing interactions and the concomitant competing orders. When the transition is continuous, or first order with weak discontinuities, it gives rise to fluctuations that are both quantum and collective [82, 83, 84]. Such quantum criticality serves as a mechanism for some of the most interesting phenomena in condensed matter physics, especially in itinerant electronic systems [85, 87]. Among these are the breakdown of Fermi liquid theory and the emergence of unconventional superconductivity.

Quantum criticality is traditionally formulated within the Landau paradigm of phase transitions. The critical theory expresses the fluctuations of the order parameter, a coarse-grained classical variable manifesting the breaking of a global symmetry, in $d+z$ dimensions [82]; here d is the spatial dimension, and z the dynamic exponent. More recent developments [86, 88], however, have pointed to new types of quantum critical points. New modes, which are inherently quantum and are beyond order-parameter fluctuations, emerge as part of the quantum critical excitations. Quantum criticality is hence considerably richer and more delicate than its thermal classical counterpart. In turn, new methods are needed to search for, study, and characterize strongly coupled quantum critical systems, and it is for this reason that we turn to

[1] In the bulk, a complex δ is a violation of the AdS_2 BF bound and corresponds to an infinitely oscillating bulk field near the horizon and hence an instability, as pointed out in [108]. It is also possible to have an instability even if the conformal dimension is real, as found by dialing double-trace deformations in [105]; while the finite-temperature physics is similar in both cases, the zero-temperature quantum phase transition is wildly different from that discussed here.

holography.

In this and the next chapter we will study phenomena associated this transition in detail. In this chapter our focus will be on the condensation of a scalar that is neutral under the $U(1)$ representing electric charge but is charged in the adjoint of an extra global $SU(2)$ symmetry. This is the same symmetry-breaking pattern as that of antiferromagnetic order, which we now review.

7.1.1 Gravity formulation of a magnetic system

In the low energy limit of an electronic system, spin-orbit couplings become suppressed and spin rotations are decoupled from spacetime rotations. Thus spin rotations remain a symmetry even though the rotational symmetries may be broken by a lattice or other effects. The low energy theory is then characterized by an $SU(2)$ global symmetry which describes the spin rotation and a $U(1)$ symmetry describing the charge. This $SU(2)$ symmetry is of course only approximate and will be broken at high energies. However, if one is only interested in universality classes describing only low energy behavior (which does not involve spin-orbit couplings), this high energy breaking will be irrelevant and one might as well replace it by a UV completion in which the dynamics have an $SU(2)$ symmetry that is exact at all energies.

Using the standard AdS/CFT dictionary, the conserved currents $j^a_\mu, a = 1, 2, 3$ for $SU(2)$ spin symmetry and J^μ for $U(1)$ charge should be dual to bulk gauge fields making up a $SU(2)_{\text{spin}} \times U(1)_{\text{charge}}$ gauge group in the bulk. For simplicity, in our bulk description we will consider a theory in which this $SU(2) \times U(1)$ symmetry is exact to all energies. Modeling spin-orbit couplings and understanding how to take into account the relation with spacetime symmetries are interesting questions which will be left for future study (see also recent discussion in [107]).

We will be interested in studying the gravity dual of an "antiferromagnetic" phase in a continuum limit. In such a limit the background value of the spin density is zero, but there exists a staggered spin order parameter $\Phi^a, a = 1, 2, 3$ which transforms as a triplet under spin rotations. Its background value spontaneously breaks $SU(2)$ to the $U(1)$ subgroup corresponding to rotations about a single axis. This leads us to introduce a real scalar field ϕ^a transforming as a triplet under $SU(2)_{\text{spin}}$ (and neutral under $U(1)_{\text{charge}}$) as the corresponding bulk field. A phase with vanishing $SU(2)$ gauge fields but with a normalizable $\phi^a \neq 0$ in one direction can then be interpreted as an antiferromagnetic (AFM) phase, or a spin density wave (SDW) phase in an itinerant-electron context. A "ferromagnet" would have nonzero $SU(2)$ gauge fields, corresponding to a nonzero background spin density in the field theory; we also study this by applying a source analogous to an external magnetic field.

Note that the spirit of this discussion is parallel to that of holographic superconductors in that the gravity description captures the macroscopic dynamics of the order parameter and the symmetry breaking pattern, but does not explain its microscopic origin.

7.1.2 Quantum phase transitions in holographic models of symmetry breaking

To describe the AFM order and its transition, we proceed in a way analogous to the superconducting case. The magnetic case considered here involves a neutral order parameter. Indeed, with the exception of superconductivity, most ordering phenomena in condensed matter systems involve a neutral order parameter; other examples include charge density wave order and Pomeranchuck instability. We are therefore led to consider holographic phase transitions involving condensation of a neutral scalar field in a finite density system. Here we again consider a charged black hole which is dual to a boundary conformal theory at a finite chemical potential μ for a $U(1)$ charge.

Setting $q = 0$ in (7.1) one finds that δ becomes complex if

$$\max\left(\frac{d-2}{2}, d-\Delta_c\right) < \Delta < \Delta_c \equiv \frac{d+\sqrt{d}}{2} \tag{7.2}$$

where $\frac{d-2}{2}$ corresponds to the unitarity bound on a scalar operator in d spacetime dimensions. On the gravity side this regime is where a scalar field ϕ satisfies the Breitenlohner-Freedman (BF) bound [125] of AdS_{d+1} but violates the BF bound of the near horizon AdS_2 region, as was recognized first in [101]. An elementary discussion of the physics of the BF bound is provided in Appendix B.

In this chapter we construct the phase diagram for the condensation of such a neutral scalar field in the $T - \Delta$ (equivalently, the $T - m^2$, see Eq. (18)) plane. For all Δ in the range (7.2) there exists a critical temperature T_c below which the neutral scalar field condenses. The phase transition is second order with mean field exponents. For the standard quantization[2] in AdS_{d+1}, we find that T_c decreases with an increasing Δ and approaches zero at Δ_c.

Thus if we allow ourselves to vary Δ through Δ_c, we find a quantum phase transition, as was previously noticed in [101, 108] in the charged case. Within the context of a specific boundary field theory varying the UV conformal dimension Δ seems somewhat artificial: however the physics here is actually controlled by the effective mass of the scalar in the near horizon AdS_2 region, and we later discuss several concrete ways to achieve this. Interestingly, the quantum phase transition at Δ_c is not described by mean field exponents, but is instead of the Berezinskii-Kosterlitz-Thouless (BKT) type [22] with an exponentially generated scale. More explicitly, for $\Delta \sim \Delta_c$, at $T = 0$, there exists an IR scale

$$\Lambda_{IR} \sim \mu \exp\left(-\frac{C}{\sqrt{\Delta_c - \Delta}}\right), \quad C = \pi\sqrt{\frac{d(d-1)}{2\Delta_c - d}} \tag{7.3}$$

below which new physics appears (or in other words, the condensate becomes significant). From the point of view of the near horizon geometry AdS_2, this behavior can

[2]The story for alternative quantization is more involved, see discussion in sec. 7.2 for details.

be understood from the discussion in [104, 126] which argues that for a scalar field in AdS with a mass square below the BF bound, such an exponential scale should generally be generated.[3] An explicit holographic model realizing this phenomenon was also recently constructed in [127, 128]

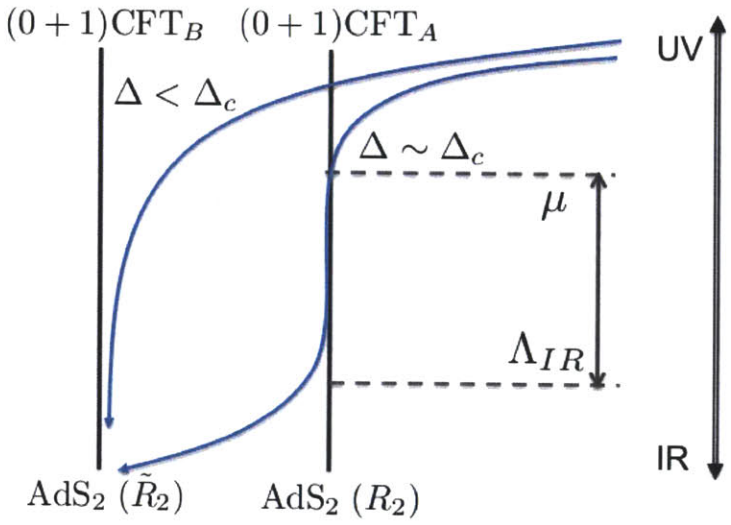

Figure 7-1: A cartoon picture for the flow of the system induced by the condensation of a neutral scalar field. The CFT_A refers to the $(0+1)$-dimensional IR CFT of the uncondensed system, described geometrically by an AdS_2 factor with radius R_2. When the dimension Δ of the operator is close to the quantum critical value Δ_c, the system stays near this IR CFT for an exponentially long scale, before flowing to the new fixed point, $(0+1)$ CFT_B, described by an AdS_2 factor with a different radius $\tilde{R}_2$.

Below the IR scale Λ_{IR} we show that the system in fact flows to a new IR fixed point which is controlled by a $(0+1)$-dimensional CFT, dual to an AdS_2 with a different cosmological constant determined by the condensed vacuum of the neutral scalar field. In Fig. 7-1 we give a cartoon picture of this flow.

The nature of the ordered phase can also be characterized in terms of its collective modes. The condensate breaks the global $SU(2) \to U(1)$: we show that the gapless spin waves expected from such a breaking arise naturally in the gravity description, and that they obey the proper dispersion relations.

The main focus of this current chapter is on the condensation of a neutral scalar; however it is clear that one can immediately apply the above discussion to condensation of *charged* scalar operators which give rise to the well-studied holographic

[3] At the BF bound an IR and UV fixed point, which corresponds to standard and alternative quantization respectively, collide and move to the complex plane, in analogue with the BKT transition. Note that in our case the standard and alternative quantization described here refer to those in AdS_2.

superconductors. Equation (7.1) implies that dialing Δ one finds a quantum critical point at Δ_c given by the larger root of (for standard quantization)

$$\frac{\Delta_c(\Delta_c - d)}{d(d-1)} - \frac{q^2}{2d(d-1)} + \frac{1}{4} = 0 \ . \tag{7.4}$$

Again for Δ close to Δ_c the system will linger around the IR fixed point of the uncondensed phase for an exponentially large scale (7.3) before settling into new fixed points. In this case the gravity description of the IR fixed points have been worked out before for $d = 3$ in [129, 130, 131, 132] (see also [135]). The stucture of the phase diagram will in general depend on the detailed form of the action, and non-minimal couplings such as those typically found in stringy embeddings (e.g. see [131, 132, 133, 134]) will change the results. It was found in [129] that for minimally coupled scalar actions and potentials similar to ours and for q small the system flows to a Lifshitz fixed point with a dynamic exponent $z \sim \frac{1}{q^2}$, while for larger values of q the system flows to another AdS_4 with a different cosmological constant. Combined with the discussion above for the condensation of a neutral scalar field we thus find a unifying picture for the quantum phase transitions for both charged and neutral order parameters as presented in Fig. 7-2. Note that AdS_2 can be considered as describing a d-dimensional theory with a dynamic exponent $z = \infty$, while AdS_4 a theory with $z = 1$.

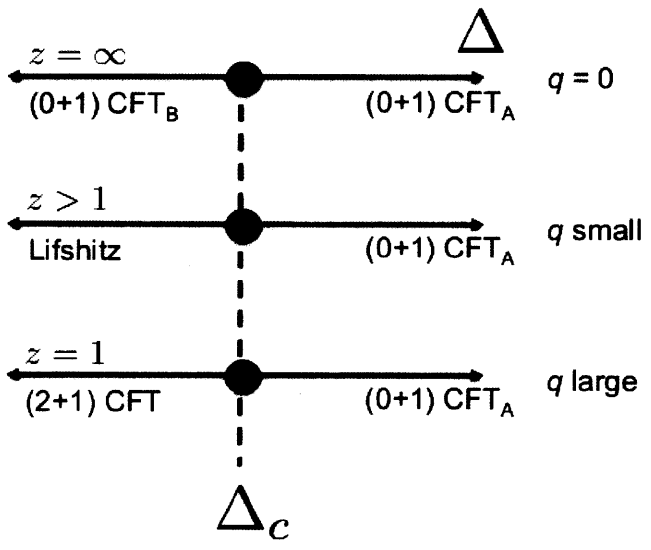

Figure 7-2: Tuning the UV dimension of the order parameter we find quantum phase transitions between a (0+1) dimensional IR CFT corresponding to AdS_2 in the unbroken phase and various types of symmetry-breaking phases. The type of symmetry-broken phase depends on the charge q of the order parameter.

Note that in our above discussion we have imagined the existence of an "experimental knob" which can be used to adjust the UV scaling dimension Δ of an operator.

It is important to note that we do this purely for convenience, and the nature of our discussion is completely insensitive to the precise realization of such a knob. The most useful knob will likely depend on the UV geometry into which this AdS_2 is embedded. For example, if one is studying a holographic superconductor an external magnetic field will also allow one to tune the IR scaling dimension. A similar UV realization is provided in a D3/D5 brane construction in [127], where a precisely analogous transition is studied. For convenience in the remainder of this paper we will simply imagine that we are free to tune the bulk mass and thus directly the UV dimension of the scalar. In Sec. 7.4.1 we give a simple model illustrating how this may be achieved.

A rough plan of the chapter is as follows. In the next section we describe a holographic phase transition corresponding to the condensation of a neutral scalar order parameter in a finite density system in a probe approximation. In section 7.3 we discuss some qualitative features of the effects of backreaction and the zero temperature limit of our solution. In section 7.4 we discuss the quantum phase transition that we find by tuning the UV conformal dimension. In section 7.5 we embed the scalar solution discussed in sec. 7.2 into an $SU(2)$ system describing the spin rotational symmetry. We proceed to study the spin waves from spontaneous breaking of the spin symmetry in the antiferromagnetic phase. In a probe limit we are able to isolate the spin wave excitations directly in the bulk and find their dispersion relations. We do not construct a spontaneous ferromagnet; however in section 7.6 we do show that if one considers aligning the "spins" with an external magnetic field then techniques similar to those in section 7.5 can be used to find a spin wave which has a quadratic dispersion relation, in line with field theoretical expectations. We conclude in section 2.4 with a discussion of further directions.

7.2 Condensation of a neutral order parameter at a finite density

In this section we provide a gravity dual description of the condensation of a neutral scalar field in a charged AdS black hole geometry which describes the onset of a real order parameter in the boundary theory at a finite density. We begin our analysis by studying the transition at a finite temperature. While our discussion applies to any spacetime dimension, for definiteness we will consider a $(2+1)$-dimensional boundary theory.

7.2.1 Setup

To put the system at a finite density we turn on a chemical potential μ for the $U(1)_{\text{charge}}$ in the boundary. This is described on the gravity side by a charged black hole with a nonzero electric field for the corresponding $U(1)$ gauge field B_M. The action for B_M coupled to AdS gravity can be written as

$$S = \frac{1}{2\kappa^2}\int d^4x\sqrt{-g}\left[\mathcal{R} + \frac{6}{R^2} - R^2 G_{MN}G^{MN}\right] \tag{7.5}$$

with $G_{MN} = \partial_M B_N - \partial_N B_M$ and R is the curvature radius of AdS. The equations of motion following from (7.5) are solved by the geometry of a charged black hole [89, 90],

$$\frac{ds^2}{R^2} \equiv g_{MN} dx^M dx^N = r^2(-f dt^2 + d\vec{x}^2) + \frac{1}{r^2}\frac{dr^2}{f} \tag{7.6}$$

with

$$f = 1 + \frac{3\eta}{r^4} - \frac{1+3\eta}{r^3}, \qquad B_t = \mu\left(1 - \frac{1}{r}\right) \tag{7.7}$$

where we have rescaled the coordinates so that the horizon is at $r = 1$ and all coordinates are dimensionless (see Appendix 7.A.1 for more details). The chemical potential and temperature are given by

$$\mu \equiv \sqrt{3}\eta^{\frac{1}{2}}, \qquad T = \frac{3}{4\pi}(1-\eta) \ . \tag{7.8}$$

η is a parameter between 0 and 1, where $\eta = 1$ corresponds to the extremal black hole with $T = 0$ and $\eta = 0$ corresponds to a finite temperature system with zero chemical potential (and charge density).[4] In the zero temperature limit, the near horizon geometry reduces to $AdS_2 \times \mathbb{R}^2$ with the curvature radius of the AdS_2 region related to that of the UV AdS_4 by

$$R_2 = \frac{R}{\sqrt{6}} \ . \tag{7.9}$$

As discussed in [101, 19], a neutral scalar field χ can develop an instability if the mass square of the scalar violates the near-horizon AdS_2 Breitenlohner-Freedman (BF) bound, while still satisfying the AdS_4 BF bound, i.e. [5]

$$-\frac{9}{4} < m^2R^2 < -\frac{3}{2} \ . \tag{7.11}$$

where the lower limit is the BF bound in AdS_4, the upper limit is the BF bound for the near horizon AdS_2 region, and we have used (7.9) to convert from AdS_2 to AdS_4 radii.

Once this condition is met, the scalar will want to condense near the horizon but will be stable at infinity. The condensed solution will involve a nontrivial radial profile for the scalar; we will see that at low temperatures the scalar will probe the extreme values of its potential and nonlinearities in the potential will be important. We choose to study a nonlinear Mexican hat potential with the Lagrangian for χ

[4] Note that since we are considering a conformal theory, only the dimensionless ratio $\frac{\mu}{T}$ is physically relevant, and it is clear that as η is varied from 0 to 1, $\frac{\mu}{T}$ takes all values from 0 to ∞.

[5] For general d boundary theory dimensions, equation (7.10) becomes

$$-\frac{d^2}{4} < m^2R^2 < -\frac{d(d-1)}{4} \ . \tag{7.10}$$

given by

$$\mathcal{L}_\chi = \frac{1}{2\kappa^2\lambda}\left[-\frac{1}{2}(\partial\chi)^2 - V(\chi)\right] \tag{7.12}$$

with

$$V(\chi) = \frac{1}{4R^2}\left(\chi^2 + m^2R^2\right)^2 - \frac{m^4R^2}{4}\,. \tag{7.13}$$

Here m^2 is the effective mass near the point $\chi = 0$, and should be chosen to satisfy the condition (7.11) (in particular, it is *negative*). λ is a coupling constant and we have chosen the constant in (7.12) so that at $\chi = 0$, there is no net contribution to the cosmological constant. The precise form of the potential in (7.13) is not important for our discussion below, provided that it does have a minimum and satisfies the condition (7.11)[6].

At zero temperature, we expect the scalar to condense until the value at the horizon reaches some point near the bottom of the Mexican hat, at which point the "effective AdS_2 mass" will again satisfy the AdS_2 BF bound and condensation will halt. At finite temperature, we expect a phase transition at some temperature T_c below which χ condenses. Note that at the classical level the coefficient of the χ^4 term is arbitrary, as it can be absorbed into λ in (7.12) via a rescaling of χ.

7.2.2 Phase diagram

We now seek the endpoint of the instability, i.e a nontrivial scalar profile for χ. We first consider the finite temperature case and take λ to be parametrically large so that we can ignore the backreaction of χ to the background geometry. We will discuss the backreaction in section 7.3 and there we argue that this approximation is good even at zero temperature.

The equation of motion for $\chi(r)$ is given by

$$\frac{1}{r^2}\partial_r\left(r^4 f\partial_r\chi\right) - \chi(\chi^2 + m^2R^2) = 0. \tag{7.14}$$

We are interested in a solution which is regular at the horizon and normalizable at the boundary, which can be found numerically.

We first consider the asymptotic behavior for χ near the horizon and the boundary. We require the solution to be regular at the horizon, i.e. to have the expansion

$$\chi(r) = \chi_h + \chi_h'(r-1) + \cdots\,, \qquad r \approx 1 \tag{7.15}$$

At finite temperature the factor f in (7.14) has a first order zero at the horizon, i.e. $f(r) = 4\pi T(r-1) + \cdots$. Demanding that (7.14) be nonsingular then leads to a

[6]The condensed phase $q = 0$ solutions without the stabilizing χ^4 term in the potential were studied in [101, 130]; at nonzero temperature these are similar to ours, but in the low temperature limit the structure described in Section 7.3 – which depends critically on the existence of a minimum to the potential – is not shared by those examples.

condition linking the near-horizon value of χ to its derivative:

$$\chi_h' = \frac{1}{4\pi T}\chi_h(\chi_h^2 + m^2R^2) \ . \tag{7.16}$$

A choice of χ_h fixes also χ_h' and thus completely specifies the solution.

Near the boundary $r \to \infty$, the linearized equation of (7.14) gives the standard asymptotic behavior

$$\chi(r) \approx Ar^{\Delta-3} + Br^{-\Delta}, \qquad r \to \infty \tag{7.17}$$

with Δ given by

$$\Delta = \frac{3}{2} + \sqrt{m^2R^2 + \frac{9}{4}} \ . \tag{7.18}$$

In the standard quantization A has the interpretation of the source[7] while B gives the response $\langle\Phi\rangle_A$ of the order parameter Φ dual to χ in the presence of source A. Note that the mass range (7.11) lies within the range $-\frac{9}{4} < m^2R^2 < -\frac{5}{4}$ for which an alternative quantization exists, in which the roles of A and B are exchanged [79]. The conformal dimension of Φ (i.e. the "dimension" of fluctuations about the point $\chi = 0$) is given by Δ (standard quantization) and $3 - \Delta$ (alternative quantization) respectively.

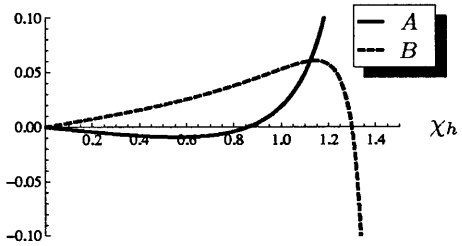

(a) A and B as a function of the horizon value of the scalar field χ_h.

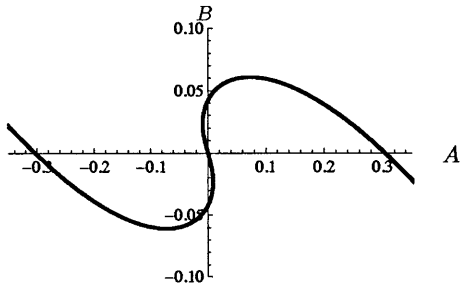

(b) B as a function of A: different points on the curve correspond to different values of χ_h.

Figure 7-3: The constants A and B determine the behavior of the scalar profile asymptotically. This is a representative plot where we scan the case $m^2R^2 = -2.1$ and $T = 0.00024$ (with $T/T_c = 0.22$) by varying χ_h. There is symmetry breaking if $A = 0$ $B \neq 0$ in the normal quantization or if $A \neq 0$ $B = 0$ in the alternative quantization.

The condensed phase for standard quantization is characterized by a normalizable nontrivial solution with $A = 0$, and then B gives the expectation value of the order parameter Φ. For the alternative quantization we look instead for a solution with $B = 0$, and A then gives the expectation value. The task before us now is to pick

[7]For example, in section 7.5 we interpret χ as corresponding to the staggered magnetization, in which case A can be interpreted as the staggered magnetic field.

a value for χ_h, and then numerically integrate the radial evolution equation to the boundary. As expected for a sufficiently low temperature, we find a nontrivial scalar hair solution, which means that there will exist a χ_h for which A or B vanishes, as shown in Figure 7-3.

For the standard quantization we find a continuous phase transition for all values of m^2 falling into the range (7.11); there is a nontrivial profile for χ for T smaller than some temperature T_c and none for T greater. In particular, as we increase m^2, the critical temperature T_c decreases to zero as the upper bound in (7.11) is approached. Precisely at the critical value $m_c^2 R^2 = -\frac{3}{2}$, we find a quantum phase transition: the physics in the vicinity of this point is discussed in Sec. 7.4. The phase diagram for standard quantization is plotted in Fig. 7-4.

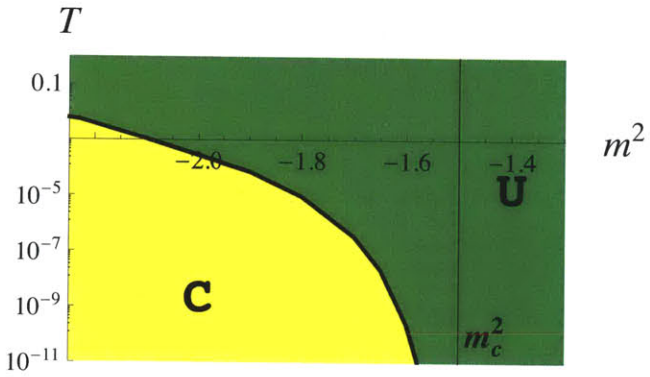

Figure 7-4: Phase diagram for the standard quantization. Note logarithmic scale for T. C denotes the condensed phase and U the uncondensed phase. $T_c \to 0$ as $m^2 \to m_c^2$, leading to a quantum critical point.

For the alternative quantization, the phase structure in the vicinity of the quantum critical point at $m^2 = m_c^2$ is the same as in the standard quantization. However the global structure of the phase diagram is somewhat different; in particular the specific value of the mass $m^2R^2 = -\frac{27}{16}$ plays an important role. This value of the mass corresponds to the UV scaling dimension for which the first nonlinear (i.e. arising from the ϕ^4 term in the potential) correction to the near-boundary asymptotics becomes degenerate with the term proportional to B. For $m^2R^2 < -\frac{27}{16}$ the phase structure is as described above, but for $m^2R^2 > -\frac{27}{16}$ one finds a new condensed phase in the *high temperature* regime. In particular, the critical temperature T_{c2} appears to increase with m^2. These solutions appear to be closely related to the thermodynamically unstable scalar hair solutions constructed in [136, 137], which studied uncharged black holes and thus correspond to the high-temperature limit of our construction. As these new phases appear to involve UV physics and are not related to the low temperature quantum-critical behavior that is the focus of this work, we defer an in-depth study of these phases and the critical value $m^2R^2 = -\frac{27}{16}$ to later work.

7.2.3 Critical exponents

A continuous phase transition can be characterized by various critical exponents: in the normal quantization with A the source and $B \sim \langle\Phi\rangle$ the expectation value we have the following behavior close to T_c:

1. The expectation value $\langle\Phi\rangle \propto (T_c - T)^\beta$ with mean field value $\beta = \frac{1}{2}$.
2. The specific heat: $C \propto |T_c - T|^{-\alpha}$ with mean field value $\alpha = 0$.
3. Zero field susceptibility: $\frac{\partial\langle\Phi\rangle}{\partial A}|_{A=0} \propto |T - T_c|^{-\gamma}$ with mean field value $\gamma = 1$.
4. Precisely at $T = T_c$, $\langle\Phi\rangle \sim A^{\frac{1}{\delta}}$ with mean field value $\delta = 3$

There are also other exponents associated with correlation functions at finite spatial or time separation which we will leave for future study. For our phase transition we find that all of the above exponents are precisely those of mean field theory. See Fig. 7-5 for numerical fits of exponent β and δ.

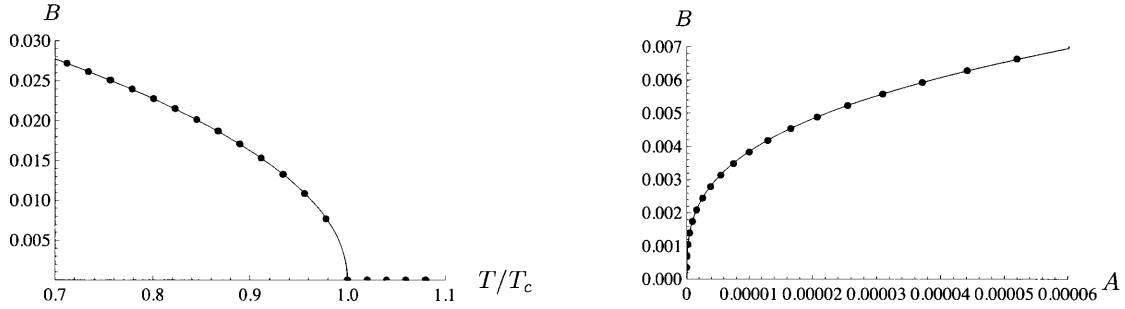

Figure 7-5: *Top:* Plot for exponent β, defined as $B \sim (T_c - T)^\beta$. $\beta = 0.49 \pm 0.03$ from numerical fit, compared with $\beta_{\text{mean field}} = \frac{1}{2}$. *Bottom:* Plot for exponent δ, defined as $B \sim A^{\frac{1}{\delta}}$ at T_c. $\delta = 3.03 \pm 0.05$ from numerical fit, compared with $\delta_{\text{mean field}} = 3$.

The existence of mean field exponents in this classical gravity analysis is not surprising[8] and can be translated into the statement that A and B are analytic functions of the horizon field χ_h. This follows from the fact that χ is regular at the horizon and the black hole geometry is smooth; we will find a rather different situation at $T = 0$ in the next section.

We now sketch the relevant arguments for finite-T. As argued above, for small χ_h we can expand A as

$$A \approx a_1(T)\chi_h + a_2(T)\chi_h^3 + \cdots \tag{7.19}$$

and similarly for B. Note that both A and B must both be odd functions of χ_h, due to the $\chi \to -\chi$ symmetry. At T_c, a new zero of A should be generated at $\chi_h = 0$ and move to a finite value of χ_h as T is further lowered.[9] Thus near T_c we should have

[8]Mean field exponents also appear in the phase transition associated with a charged scalar field in the holographic superconductor story [101, 139].

[9]In fact given $\chi \to -\chi$ symmetry, a pair of zeros are generated and move to opposite directions.

$a_1(T) = a(T - T_c)$ and $a_2(T) = b + \cdots$ with a and b having the same sign for $T > T_c$. For $T < T_c$, then A has a zero for χ_h taking a value χ_A given by

$$\chi_A = \sqrt{-\frac{a_1(T)}{a_2(T)}} \propto (T_c - T)^{\frac{1}{2}} \to 0. \tag{7.20}$$

Using χ_A as the initial value at the horizon gives the solution for the condensed phase. Assuming that B is still linear in χ_h near $\chi_h = 0$, we thus find that

$$B(\chi_A) \propto \chi_A \propto (T_c - T)^{\frac{1}{2}} \tag{7.21}$$

which gives us the critical exponent $\beta = \frac{1}{2}$. Turning now to the susceptibility, we find

$$\left.\frac{dB}{dA}\right|_{A=0} = \left.\frac{dB}{d\chi_h}\frac{d\chi_h}{dA}\right|_{A=0} \sim (T - T_c)^{-1}, \tag{7.22}$$

leading to $\gamma = 1$. Furthermore, precisely at $T = T_c$, $A \sim a\chi_h^3$ and B stays linear near $\chi_h = 0$. Thus we find that at $T = T_c$,

$$B(\chi_h) \propto \chi_h \propto A^{\frac{1}{3}} \tag{7.23}$$

which gives the critical exponent $\delta = 3$. One can also compute the free energy using holographic renormalization and indeed find mean field exponent $F \propto -(T_c - T)^2$ for $T < T_c$. In particular, the analytic expansion (7.19) for A and B in terms of χ_h guarantees that F has the Landau-Ginsburg form.

Note that the gravity analysis can be extended to all spacetime dimensions with the same mean field scalings. Presumably this has to do with the fact we are working in the large N limit, which suppresses fluctuations. This is also consistent with picture obtained in [19] in which the scalar instability essentially follows from a RPA type analysis. We expect that a $1/N$ computation involving quantum corrections in the bulk will reveal corrections to these mean-field exponents.

7.3 Backreaction and the zero temperature limit

In the usual studies of holographic superconductors, the scalar is charged under a $U(1)$ and so the usual probe approximation involves treating the scalar and $U(1)$ gauge field as negligible perturbations to the background metric. In these models lowering the temperature essentially means increasing the ratio μ/T; thus at sufficiently low temperatures the gauge field (and thus also the condensed scalar) will necessarily backreact strongly on the geometry, causing a breakdown of the probe approximation. The zero temperature limit of the backreacted geometries have been constructed [129, 130, 131, 132] and typically depend on the details of the couplings and charge of the scalar. One recurring theme is that at zero temperature the charges that was previously carried by the black hole is now completely sucked out of the hole and into its scalar hair. Once the black hole horizon is relieved of the burden of carrying a

large charge, it is usually replaced by a degenerate horizon with vanishing entropy.

In our model the situation is different. We always include the backreaction of the gauge field on the metric, as we start from the beginning with the charged black hole solution; it is consistent to solve for a scalar profile on this fixed background only because the scalar is uncharged and so its contribution to the backreaction can be cleanly suppressed by taking λ large.

In this section we will discuss the backreacted solution in the IR at zero temperature and argue that even if backreaction is included its effects are rather benign and do not change any qualitative conclusions. This is essentially because all of the charge must stay in the black hole itself, greatly constraining its near-horizon form.

First, we note that Gauss's law states that

$$\partial_r \left(\sqrt{-g} g^{rr} g^{tt} \partial_r A_t\right) = 0 \;\rightarrow\; g_{xx}\sqrt{g^{rr}g^{tt}}\partial_r A_t = \text{const} \,. \tag{7.24}$$

Thus if the electric field is nonsingular at the horizon, g_{xx} must be finite there: this is simply saying that the $\mathbb{R}^2$ at the horizon cannot degenerate as it has a nonzero electric field flux through it. We then expect that the near-horizon geometry factorizes into the form $\mathcal{M}_2 \times \mathbb{R}^2$, where $\mathcal{M}_2$ is some 2d manifold involving (t, r). Now consider the trace of the Einstein equation arising from the variation of (7.5) plus (7.12); the $U(1)$ field strength does not contribute to this equation as it is classically scale invariant, and we find:

$$\mathcal{R} + \frac{12}{R^2} = \frac{1}{2\lambda}\left[(\nabla\chi)^2 + 4V(\chi)\right], \tag{7.25}$$

where $\mathcal{R}$ is the Ricci scalar of the geometry and comes purely from the $\mathcal{M}_2$ factor. Now let us further assume that in the near-horizon region χ asymptotes to some constant value χ_h (we will show this to be consistent shortly). We then find that $\mathcal{M}_2$ has constant negative curvature, and thus must be AdS_2[10] with radius $\tilde{R}_2$ satisfying

$$\frac{1}{\tilde{R}_2^2} = \frac{1}{R_2^2} - \frac{1}{\lambda}V(\chi) \tag{7.26}$$

where R_2 is the curvature radius of the original AdS_2 near horizon geometry of the extremal charged black hole. Note that since $V(\chi_h) < 0$, $\tilde{R}_2 < R_2$. Thus we see that the backreacted IR geometry is very similar to the unperturbed geometry, except that its AdS_2 factor has a radius that is corrected by the presence of the near-horizon scalar potential.

Let us now study the scalar equation of motion (7.14) near the backreacted AdS_2 horizon:

$$\frac{1}{r^2}\partial_r(r^4\tilde{f}\partial_r\chi) = R^2\frac{dV}{d\chi} \tag{7.27}$$

where $\tilde{f}$ is the warp factor for the backreacted geometry and at zero temperature has a double zero at the horizon r_0; expanding near the horizon we see that regularity at

[10] More precisely, it could also be an AdS_2 black hole; the true zero temperature solution corresponds however to pure AdS_2.

the horizon requires

$$\frac{dV}{d\chi}(\chi(r=r_0))=0\ . \tag{7.28}$$

Thus we see that at the horizon χ will sit at the bottom of its potential. To understand how this AdS_2 region matches onto the asymptotic geometry, we expand $\chi=\chi_h+\delta(r)$ where χ_h is the bottom of the potential $V(\chi)$. Now working in the AdS_2 region and linearizing (7.27) near χ_h we find that δ obeys the standard AdS_2 wave equation:

$$\partial_r((r-r_0)^2\partial_r\delta)-\tilde{R}_2^2V''(\chi_h)\delta=0, \tag{7.29}$$

whose solutions are

$$\delta=\alpha(r-r_0)^{-\frac{1}{2}+\nu}+\beta(r-r_0)^{-\frac{1}{2}-\nu} \tag{7.30}$$

with

$$\nu=\sqrt{\frac{1}{4}+\tilde{R}_2^2V''(\chi_h)}, \tag{7.31}$$

Now we would like χ to approach χ_h as we approach the horizon; this means that we should not take the β solution above, as it invariably blows up as $r\to r_0$. Note that for the α solution to also not blow up, we need $-\frac{1}{2}+\nu>0$ and thus $V''(\chi_h)>0$. To stabilize the AdS_2 region we must truly be sitting at a *minimum* of the potential at the horizon. In this case the solution

$$\chi(r)=\chi_h+\alpha(r-r_0)^{-\frac{1}{2}+\nu} \tag{7.32}$$

can be interpreted as an *irrelevant* deformation of the new AdS_2 IR CFT that we are flowing to[11]. The value of the coefficient α is not fixed at this linearized level and must be determined by matching to the UV solution.

We have not solved for the fully backreacted geometry but have used this method to find a normalizable scalar solution on the $T=0$ charged black hole geometry using the above exponents. Our results match smoothly onto the $T\to 0$ limit of the profiles calculated using the finite temperature matching procedure discussed in Section 7.2. When λ is large we do not expect the inclusion of the backreaction to qualitatively change any of these results given the change of the cosmological constant is small.

It is instructive to compare this to the situation for charged holographic superconductors [129]. In this case for large charge it is found that the IR geometry flows to an AdS_4, while for sufficiently small charge it flows to a Lifshitz geometry, with exponent z satisfying

$$q^2\sim\frac{1}{z}, \tag{7.33}$$

at very small q (see Eq.(81) in [129]). We see that our AdS_2 solution corresponds to $z=\infty$ at $q=0$; increasing the charge we have a Lifshitz solution with finite z, and finally increasing further we find $z=1$ for AdS_4.

[11]Similar considerations are used in [129] to determine when an emergent AdS_4 can exist.

7.4 A quantum phase transition from classical gravity

We recall from the discussion in sec. 7.2.2 that when $m_c^2 R^2 \equiv -\frac{3}{2}$, the critical temperature approaches zero: thus we should obtain a "quantum phase transition" at zero temperature as m^2 is varied from above m_c^2 to below. In this section we consider the behavior near the quantum critical point from the condensed side. Our treatment in this chapter while demonstrate the basic physics, and more precise calculations near the critical point are performed in Chapter 8.

The accessibility of this quantum critical point depends on having the ability to tune the IR dimension of the field χ in some way. The simplest possible way is by directly tuning the mass, and before proceeding we pause briefly to explain how this may be possible in a simple bulk realization. A similar mechanism is discussed for uncharged black holes in AdS in [98].

7.4.1 Tuning across the quantum critical point

Imagine that the scalar χ contains a coupling to another scalar field ψ,

$$S_\chi \supset \int d^{d+1}x \sqrt{-g}\, F(\psi)\chi^2 \tag{7.34}$$

where $F(\psi)$ is some function whose detailed form will not be important for us. Now consider turning on a constant source h for ψ at the boundary, i.e. we require the boundary value of ψ to approach h. In the boundary theory language this corresponds to adding a term

$$\int d^d x\, h\, \mathcal{O}(x) \tag{7.35}$$

to the action with $\mathcal{O}$ the boundary operator dual to ψ. The source induces a nontrivial bulk solution for ψ, which in turn contributes to the action of χ as a mass term, shifting the effective m^2. However the new effective mass will typically be radially dependent; we require it to be nonzero at the AdS_2 horizon. If we write the IR dimension (7.1) of ψ as

$$\delta_\psi = \frac{1}{2} + \nu_\psi \tag{7.36}$$

then the asymptotics of ψ in the near horizon AdS_2 region are

$$\psi \sim (r - r_0)^{-\frac{1}{2} \pm \nu_\psi} \,. \tag{7.37}$$

For ψ to be regular at the horizon we need to choose the + sign in the exponent. So if $\nu_\psi = \frac{1}{2}$ then ψ approaches a constant at the horizon, and turning on a source h for ψ will change the effective IR mass of the field χ. From (7.1), ν_ψ is $\frac{1}{2}$ if ψ is dual to an operator with UV dimension $\Delta = d$, i.e. it is massless in the bulk. Thus whenever the UV CFT has such an operator with a nontrivial OPE with the order parameter operator Φ, we expect to be able to tune the system through the quantum critical

point by varying h in (7.35), i.e. there exists a critical value h_c of h at which we expect a quantum phase transition. It would be interesting to understand this mechanism further. Also note that for type II theories in an asymptotic AdS geometry, a natural candidate for ψ is the dilaton.

7.4.2 BKT scaling behavior and Efimov states

For $m^2 < m_c^2$, the BF bound of the near horizon region AdS_2 region is violated. It has been argued in [126] that for a general AdS gravity dual with mass slightly below the BF bound conformality is lost and an IR scale Λ_{IR} is generated exponentially as

$$\Lambda_{IR} \sim \mu \exp\left(-\frac{\pi}{\sqrt{m_c^2 R_2^2 - m^2 R_2^2}}\right) . \tag{7.38}$$

where μ represents some UV scale that in our case is the chemical potential. This exponential behavior is characteristic of the Berezinskii-Kosterlitz-Thouless (BKT) phase transition. One expects that this IR scale controls the physics near the quantum phase transition. In particular, the critical temperature T_c and the value of the condensate $\langle\Phi\rangle$ should be related to this scale. Here we present a reformulation of the arguments of [126] that demonstrates the behavior of T_c and $\langle\Phi\rangle$ explicitly.

We parameterize the AdS_2 region of the uncondensed geometry as

$$\frac{ds_2^2}{R_2^2} = \frac{-dt^2 + dz^2}{z^2}. \tag{7.39}$$

The linearized equation for the scalar about the point $\chi = 0$ is then

$$-\frac{d^2}{dz^2}\chi + \frac{R_2^2(m^2 - m_c^2) - 1/4}{z^2}\chi = \omega^2\chi, \tag{7.40}$$

where we have assumed time dependence $e^{-i\omega t}$. This is essentially a Schrodinger equation with "energy" ω^2: the existence of a negative energy bound state indicates a mode growing exponentially in time and hence an instability, and it is a well-known fact that if z can take values from 0 to ∞ then such negative-energy bound states exist when $m^2 < m_c^2$, leading to the BF bound.

In our problem, however, z does not take values on the whole half-line. At some small UV value z_{UV} we should match onto the asymptotic UV geometry. We will now show that if we also choose an appropriate infrared cutoff z_{IR} then even when m^2 is below the BF bound (7.40) will have no bound states. To understand this, let us assume for simplicity that χ satisfies Dirichlet boundary conditions $\chi(z_{IR,UV}) = 0$[12] and consider the zero energy $\omega = 0$ solutions to (7.40). We find that the solution is

[12]Note that more general boundary conditions simply result in slight changes in the value of z_{IR} and z_{UV}

oscillatory (see also discussion in [104])

$$\chi(z) = \sqrt{z}\sin\left[R_2\sqrt{m_c^2 - m^2}\log\frac{z}{z_{UV}}\right], \tag{7.41}$$

and importantly, the zero energy solution satisfies the boundary condition only when

$$\log\frac{z_{IR}}{z_{UV}} = \frac{\pi}{R_2\sqrt{m_c^2 - m^2}} \tag{7.42}$$

Essentially we must fit a single half-period of the oscillatory wave function inside. This wave function has no nodes; thus if z_{IR} satisfies this condition, then the lowest energy state has zero energy and there is no instability. Decreasing the distance between z_{IR} and z_{UV} will only increase the energy of the ground state. On the other hand, if we *increase* this distance–if z_{IR} is too high–then the ground state will have *negative* energy, indicating an instability.

Now in our problem z_{IR} can be provided by a small finite temperature, which ends the geometry with a horizon at some large value z_h. We thus find that if $z_h > z_{IR}$ as defined above, there will be an instability that can be resolved only by condensation of the scalar. The critical temperature T_c is thus given by

$$T_c \sim \frac{1}{z_h} \sim \mu\exp\left[-\frac{\pi}{R_2\sqrt{m_c^2 - m^2}}\right] \tag{7.43}$$

where $\mu \sim \exp[z_{UV}]$ is some UV scale. We have been able to confirm this numerically, including the prefactor in the exponent (see Fig. 7-6).

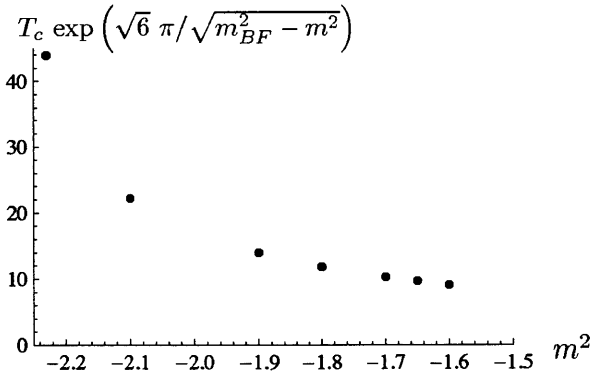

Figure 7-6: The exponential dependence of T_c as a function of $\sqrt{m_c^2 - m^2}R_2$. Here we have compensated for the expected theoretical behavior of T_c and plotted the resulting function versus m^2; we see that as $m^2 \to m_c^2$ the values approach a constant, verifying our prediction.

What if $T < T_c$? Now the IR cutoff cannot be provided by the horizon, and must instead be provided by nonlinearities associated with the scalar potential, which will become important near z_{IR}. We then expect that the condensate $\langle\Phi\rangle$ should itself exhibit similar exponential scaling as (7.43), as was found explicitly in a similar

context in [127]. We present here a simple way to understand this result. Note that for m^2 only slightly below m_c^2 the IR theory is basically the original conformal IR CFT for an exponential hierarchy of scales. In this IR CFT, χ is unstable and has dimension given by

$$\delta = \frac{1}{2} + i\sqrt{m_c^2 R_2^2 - m^2 R_2^2} \approx \frac{1}{2} \tag{7.44}$$

Since χ has dimension $\frac{1}{2}$, it should transform under a scaling transformation as

$$\chi(\lambda z) = \lambda^{\frac{1}{2}} \chi(z) \tag{7.45}$$

We expect that $\langle \Phi \rangle$ should be simply related to the value of $\chi(z)$ at the UV matching value z_{UV}, as essentially only linear UV evolution will be required to relate them, and thus

$$\langle \Phi \rangle \sim \chi(z_{UV}) \tag{7.46}$$

Similarly, the value of ϕ in the deep IR will be determined by nonlinearities, which we expect to result in

$$\chi(z_{IR}) \sim O(1) \tag{7.47}$$

We thus find from (7.45) that

$$\chi(z_{IR}) = \sqrt{\frac{z_{IR}}{z_{UV}}} \chi(z_{UV}) \tag{7.48}$$

which results upon evolution through the UV region to the AdS_4 boundary in

$$\langle \Phi \rangle \sim \sqrt{\frac{z_{UV}}{z_{IR}}} \sim \Lambda_{IR} \exp\left[-\frac{\pi}{2R_2\sqrt{m_c^2 - m^2}} \right]. \tag{7.49}$$

Note that the exponent for $\langle \Phi \rangle$ is half that obtained for T_c. In the intermediate conformal regime χ scales as a dimension $1/2$ operator and the temperature scales as dimension 1: this is the origin of the factor of two difference in the exponents above. Eventually in the far IR nonlinearities become important and a scale is generated, but the theory is not gapped; provided that the scalar potential has a minimum, as described in Section 7.3 it instead flows to a different AdS_2 fixed point, and the IR scale manifests itself only as an irrelevant perturbation (7.32) along which we flow to this new fixed point.

It is possible to perform a more explicit calculation of (7.49), following the techniques used in [127] where similar scaling is obtained in an AdS_2 that arises from a D3/D5 brane construction. From such a treatment it is clear that there should exist an infinite tower of "Efimov states" that correspond to allowing oscillatory solutions such as (7.41) to move through more periods before matching to the IR solution. These have $\langle \Phi \rangle \sim \left[-\frac{n\pi}{2R_2\sqrt{m_c^2 - m^2}} \right]$ with n a positive integer . We have been able to find the first two of these states numerically (see fig. 7-7); as explained in [127] the relevant wavefunctions have more nodes with increasing n and so the $n = 1$ state is

energetically favored.

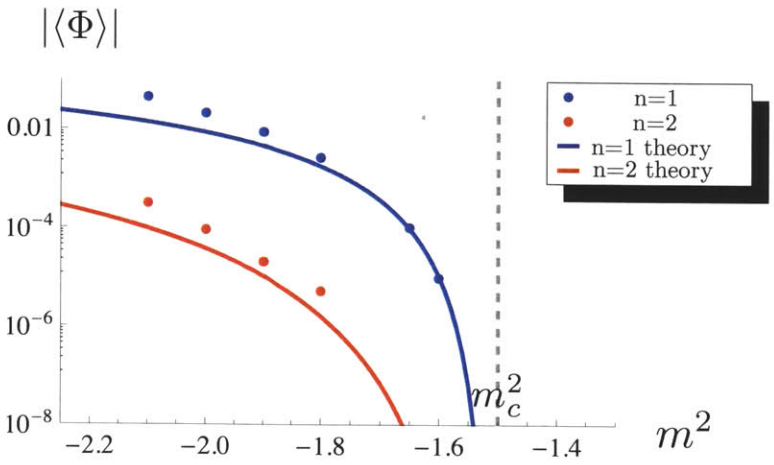

Figure 7-7: Efimov states: for comparison we plot expected results from the analytic arguments described in the text. Agreement can be seen at this level but numerical difficulties prevent us from probing this region more carefully.

To conclude this subsection we note that turning on any finite temperature the phase transition becomes that of the mean field, since the physics depended in a smooth way on the horizon value of the scalar χ_h. At zero temperature since the horizon is degenerate we expect the boundary values of χ to depend on the initial value α at the horizon in equation (7.32). It would be interesting to understand this better.

7.4.3 Quantum critical points for holographic superconductors

Finally, note that the scaling behavior (7.43) and (7.49) also applies to the condensate of a charged scalar, which results in the well-studied holographic superconductor.[13] In such a case the coupling to the background electric field is important; also one now has the possibility of supplying an external magnetic field H for $U(1)_{\text{charge}}$[14] The effect of the electric field on the conformal dimension is shown in (7.1), and the generalization of this formula to include the effect of the magnetic field is (see Appendix 7.A for a derivation),

$$\delta = \frac{1}{2} + \sqrt{\frac{m^2R^2}{6} + (6|bq| - q^2)\frac{\sqrt{1+12b^2}-1}{72b^2} + \frac{1}{4}} \tag{7.50}$$

[13]Similar exponential dependence of the critical temperature in such a case has been observed by Faulkner and Roberts.

[14] Note that this magnetic field is an external field strength for $U(1)_{\text{charge}}$ and has absolutely nothing to do with the "magnetic" field associated with the antiferromagnetic ordering discussed later in this paper, which would correspond to a chemical potential for the $SU(2)$ gauge field A_t^a.

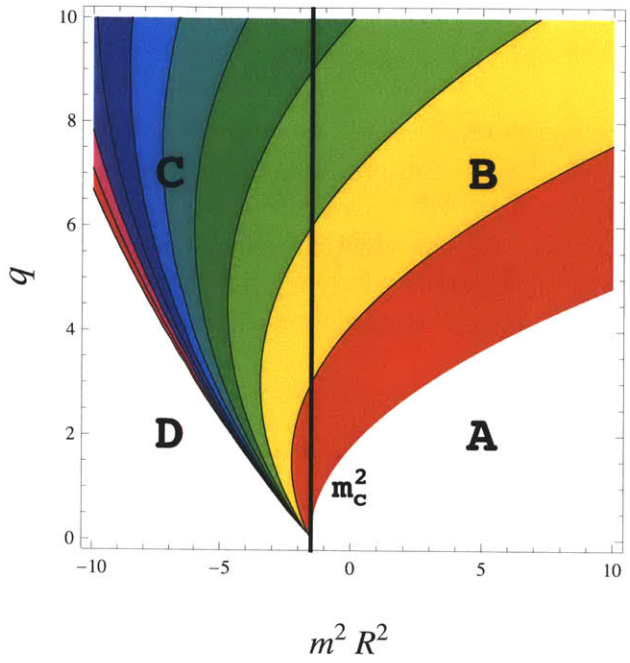

Figure 7-8: Contour plot of the critical magnetic field in the m^2, q plane. The color indicates the value of H_c, with more purple indicating a higher field. In region A the IR dimension even with $H = 0$ is real and there is no condensate. In regions B and C there exists a finite magnetic field H_c above which the condensate is destroyed. However H_c diverges as we move to the left and is infinite on the boundary between regions C and D. In region D even an infinitely strong magnetic field will not stop the condensation. This is understandable: everywhere to the the left of the line $m^2 = m_c^2$ the scalar has a sufficiently negative mass that it would have condensed even if it was uncharged and so it is perhaps not unexpected that a magnetic field cannot halt this condensation. In region C again the scalar would have condensed even if it was uncharged, but here the charge is high enough that a sufficiently strong magnetic field can stop the condensation.

where $b \equiv \frac{H}{\mu_B^2}$ is dimensionless ratio between the boundary magnetic field H and chemical potential[15]. Again the quantum phase transition will happen when δ becomes complex. It is clear from here that there is a different critical mass m_c^2 than in the neutral case; alternatively, one can now imagine tuning the magnetic field through a critical value H_c, which is again found by setting the expression inside the square root of (7.50) to zero. For $H > H_c$ there will be no condensate, and for H slightly less than H_c one will find similar non-analytic behavior as above as a function of the deviation of H from H_c. The explicit expression for H_c is rather complicated and is given in (7.160).

We plot the critical values H_c in the $q - m^2$ plane in Fig. 7-8. Note in particular that the expression in (7.50) containing b saturates at a finite value $\frac{|q|}{2\sqrt{3}}$ as $b \to \infty$.

[15] μ_B is the dimensional version of the dimensionless chemical potential μ we were using earlier, see Appendix 7.A.1 for further explanation.

Thus if

$$m^2R^2 + \sqrt{3}|q| < -\frac{3}{2} \tag{7.51}$$

no matter how large the magnetic field is, a condensate cannot be prevented. This is region D in Fig. 7-8. This is understandable: everywhere in this region the scalar mass is below the neutral AdS_2 BF bound $m^2R^2 = -\frac{3}{2}$ and so it would have condensed even if it was uncharged. As the electric field is in some sense not responsible for the instability, it may make sense that a magnetic field cannot halt it. It will be interesting to find field theoretical models with this feature.

7.5 Antiferromagnetism and spin waves

We have understood in detail the mechanism by which a neutral scalar field can condense in a finite-density geometry. We would now like to employ this new understanding to holographically model symmetry breaking with such a neutral order parameter. One immediate example is antiferromagnetic order: as explained in the introduction, in the low-energy limit of interest to us spin rotations may be thought of as a global $SU(2)$ symmetry. Antiferromagnetic ordering then corresponds to a spontaneous breaking $SU(2) \to U(1)$, where the unbroken direction corresponds to rotations about a single axis. In such a system the background value of the spin density remains zero, but there is a neutral order parameter Φ^a that corresponds to the staggered magnetism.

In this section we construct the bulk dual of the operator Φ^a: we embed the neutral scalar field χ discussed in sec. 7.2–7.4 into part of an $SU(2)$ triplet scalar field ϕ^a charged under the $SU(2)$ bulk gauge field corresponding to the global spin $SU(2)$ symmetry of a boundary theory. The phase transition discussed earlier then becomes a transition to an antiferromagnetic (AFM) phase.

Note that while we use the word "antiferromagnetic" there is no sense in which the microscopic degrees of freedom of our system consist of spins that are anti-aligned on a bipartite lattice. We use the term to describe only the symmetry breaking pattern described above, realized in a manner that manifestly requires a finite density for symmetry breaking. We do feel that if indeed gravity duals could be constructed top-down for such systems they would likely contain ingredients similar to those in our description.

7.5.1 Embedding of χ

More explicitly, we can consider the following action

$$S = S_{\text{grav}} + S_{\text{matter}} \tag{7.52}$$

with

$$S_{\text{grav}} = \frac{1}{2\kappa^2}\int d^4x\sqrt{-g}\left(\mathcal{R} + \frac{6}{R^2}\right) \tag{7.53}$$

where R is the curvature radius of AdS_4. The relevant part of the bulk Lagrangian for matter fields is then given by

$$\begin{aligned}\frac{2\kappa^2}{R^2}\mathcal{L}_{\text{matter}} &= -\frac{1}{4g_A^2}F^a_{MN}F^{MNa} - G_{MN}G^{MN} \\ &\quad -\frac{1}{\lambda}\left(\frac{1}{2}(D\phi^a)^2 - V(\phi^a)\right)\end{aligned} \tag{7.54}$$

with

$$\begin{aligned}F^a_{MN} &= \partial_M A^a_N - \partial_N A^a_M + \epsilon^{abc}A^b_M A^c_N, \\ G_{MN} &= \partial_M B_N - \partial_N B_M,\end{aligned} \tag{7.55}$$

and

$$D_M\phi^a = \partial_M\phi^a + \epsilon^{abc}A^b_M\phi^c\ . \tag{7.56}$$

We will take the potential V to have the double well form of (7.12)

$$V(\phi^a) = \frac{1}{2}m^2\vec{\phi}\cdot\vec{\phi} + \frac{1}{4}(\vec{\phi}\cdot\vec{\phi})^2\ . \tag{7.57}$$

We again put the system at a finite density by turning on a chemical potential for the $U(1)_{\text{charge}}$, with a background metric given by (7.6). We note that in this background all $SU(2)$ gauge fields are inactive. This highlights an important difference between this setup and the usual $U(1)$ holographic superconductor; in the Abelian case there is a background chemical potential μ for the $U(1)$ charge; this does not break the $U(1)$ but does interact via the bulk equations of motion with the charged scalar order parameter, causing it to condense for a suitable choice of mass and charge. This is distinctly different from the $SU(2)$ case studied here; specifying a chemical potential for the $SU(2)$ would involve picking a direction μ^a in the $SU(2)$ space, corresponding to an *explicit* breaking of the symmetry. This is analogous to applying an external magnetic field. We study this explicit breaking in sec. 7.6 and for now focus on the spontaneous breaking of $SU(2)$.

When m^2 falls in the range (7.11), the background (7.6) becomes unstable towards condensation of the scalar ϕ^a, which will then *spontaneously* break the $SU(2)$ to a $U(1)$ subgroup. More explicitly, consider the following ansatz

$$\phi^a_0 = \left(0, 0, \frac{\chi(r)}{R}\right), \qquad A^a_M = 0 \tag{7.58}$$

which can be readily checked by examining the equations of motion as being self-consistent, if we ignore the backreaction to the background geometry. We note in particular that one can consistently set the $SU(2)$ gauge field to 0. This is because of the non-Abelian nature of the interactions of the gauge field and scalar, e.g. $f^{abc}\phi_b A_c$ etc. which clearly vanish if all objects point only in one direction in the $SU(2)$ space.

Plugging (7.58) into the equations of motion following from (7.54) we precisely find (7.14) and our previous discussion of the phase transition in sec. 7.2–7.4 can be

taken over completely. Note that if we consider a finite λ and turn on backreaction, the profile for the $U(1)$ gauge field in (7.6) and the background metric will be modified, but one can still set the $SU(2)$ gauge field to zero.

7.5.2 Spin waves

To characterize the ordered phase, we study in this section perturbations around the symmetry breaking solution (7.58) with a nonzero order parameter ϕ^a but zero background gauge field A^a_M. We show that the system has two linearly dispersing gapless modes, corresponding in the field theory to the two Goldstone modes arising from the spontaneous breaking of the global $SU(2)$ symmetry, and that their velocity is given by the expression expected from the standard field theory for a quantum antiferromagnet. From the bulk point of view, low-frequency rotations of the order parameter in the broken symmetry directions will source bulk gauge field fluctuations, which we will find to be normalizable at the AdS boundary if they obey a specific dispersion[16].

Our analysis for the remainder of this section will not depend at all on the details of the metric or scalar profile (except that it is normalizable). We will work in a general boundary spacetime with a bulk black brane metric given by

$$ds^2 \equiv g_{MN}dx^M dx^N = g_{tt}dt^2 + g_{rr}dr^2 + g_{xx}d\vec{x}^2 \tag{7.59}$$

We work at finite temperature with g_{tt} (g_{rr}) having a first order zero (pole) at the horizon $r = r_0$.

Let us begin by understanding *why* from the gravity point of view there should exist a gapless mode. Consider a global $SU(2)$ gauge rotation of the background order parameter $\phi^a_0(r)$, at $\omega = 0$ and $k = 0$.

$$\delta\phi^a_i(r) = \epsilon\tau^i_{ab}\phi^b_0(r) \tag{7.60}$$

where $\tau^i, i = 1, 2$ is a generator along one of the broken directions so that $\delta\phi^a$ is nonzero and ϵ is a constant. This small perturbation will obviously be a solution to the bulk gravity equations of motion; it is in fact a normalizable solution at the AdS boundary, precisely because ϕ^a_0 is normalizable. This appears somewhat trivial—but note that this is exactly a gapless mode, as it is a normalizable solution that exists in the limit $\omega \to 0$. Now consider a *local* $SU(2)$ gauge rotation with the gauge parameter ϵ having a small frequency and momentum in the x-direction, i.e. $\epsilon(t, x) \propto e^{-i\omega t+ikx}$. The perturbation to the scalar takes the same form (7.60), but now we have extra perturbations to the gauge fields

$$\delta A^i_t = -i\omega\epsilon \qquad \delta A^i_x = ik\epsilon\ . \tag{7.61}$$

These are *not* normalizable at infinity, and thus this pure gauge transform is no longer

[16]Methods similar to those used here may be used to obtain analytic control over the hydrodynamics of the U(1) holographic superconductor [146].

a normalizable solution. Thus at any nonzero ω and k to find a normalizable mode we must move off of the pure gauge solution and actually solve the dynamical equations of motion. The existence of the the global solution (7.60) guarantees that we as we take $\omega, k \to 0$ we will find a gapless solution, but the dynamical bulk equations of motion will show that it will be normalizable only when a certain dispersion relation $\omega(k)$ is satisfied.

Pions in the bulk

The previous discussion has convinced us that the existence of the gapless mode is intimately related to our ability to perform global rotations on the order parameter, i.e. to *bulk* Goldstone modes. Let us thus parametrize fluctuations of ϕ in terms of bulk Goldstone fields (or "pions") $\pi^i(r,t,x)$ as follows:

$$\phi(r,x) = \exp(i\pi^i(r,t,x)\tau^i)\phi_0(r) \tag{7.62}$$

where $\phi_0(r)$ is the background solution and as before τ^i are the broken symmetry generators. We now work out the bulk quadratic action of the π^i to be[17]

$$S(\pi) = -\frac{R^2}{2\kappa^2}\int d^4x \frac{1}{2\lambda}\sqrt{-g}g^{MN}(\partial_M\pi^i - A_M^i)(\partial_N\pi^j - A_M^j)h_{ij} \tag{7.63}$$

Here h_{ij} can be viewed as a metric on the Goldstone boson space, given by

$$h_{ij}(r) = \frac{1}{2}\phi_0^\dagger(r)\{\tau_i,\tau_j\}\phi_0(r) = \frac{\chi^2}{R^2}\delta_{ij} \tag{7.64}$$

Thus the two Goldstone modes decouple. Below we will focus on one of them and drop the index i for notational simplicity.

The equation of motion for π is then

$$\partial_M\left(\chi^2\sqrt{-g}g^{MN}(\partial_N\pi - A_N)\right) = 0 \tag{7.65}$$

It is clear that in the limit $\omega, k \to 0$, a constant pion profile $\pi(r) = \pi_0$ and vanishing gauge field $A = 0$ provide a solution to the equations of motion. This is the gauge transform discussed earlier.

Let us now briefly detour to discuss the asymptotic behavior of the pion field. Carrying out the standard analysis and using the fact that the background solution is normalizable[18]: $\chi(r) \sim r^{-\Delta}$ for large r, we find that as $r \to \infty$.

$$\pi(r) \approx B + Ar^{-d+2\Delta}, \qquad r \to \infty \tag{7.66}$$

To understand this it is useful to remember that fluctuations in the original field $\delta\phi(r)$ are related to π as $\delta\phi(r) = \pi(r)^i\tau^i\phi_0(r) \sim \pi(r)r^{-\Delta}$. Comparing this to the

[17] In writing this expression we have assumed that the background gauge field is zero; thus we have neglected intrinsically non-Abelian terms of the form $f^{abc}\pi_b A_c$ which all arise at higher order.

[18] We restrict ourselves to the ordinary quantization for this section.

asymptotic behavior of the scalar (7.17) we see that the *constant* piece B of π at infinity is actually *normalizable*, while the piece A is not normalizable and should be viewed as the source for the pion field.[19]

Yang-Mills equations

Fluctuations of π will excite the non-Abelian gauge field $A^a_M(r,t,x)$, whose linearized equations are

$$\frac{1}{\tilde{g}_A^2}\nabla_M F^{MN} + \chi^2 g^{NP}(\partial_P \pi - A_P) = 0 \ . \tag{7.67}$$

Again we have suppressed the index i which labels the broken generators, since at the linearized level different directions decouple. We have absorbed various factors into a rescaled gauge coupling

$$\frac{1}{\tilde{g}_A^2} = \frac{R^2\lambda}{g_A^2}, \tag{7.68}$$

which controls the strength of the effects of the scalar sector on the gauge field. We could of course always choose a unitary gauge to get rid of the Goldstone boson π—but to make the connection to boundary Goldstone modes more obvious we will not do this and instead choose the gauge $A_r = 0$. It is convenient as in [14] to work with the momenta J^μ conjugate to the bulk gauge field A_μ, defined as[20]

$$J^\mu \equiv \frac{1}{\tilde{g}_A^2}\sqrt{-g}F^{\mu r} = -\frac{1}{\tilde{g}_A^2}\sqrt{-g}g^{rr}g^{\mu\nu}\partial_r A_\nu \ . \tag{7.69}$$

The value of the bulk field J^μ at the AdS boundary $r \to \infty$ is equal to the expectation value of the field theory current $\langle \mathcal{J}^\mu \rangle_{\rm QFT}$.

The $N = r$ component of the Maxwell equations (7.67) can now be written

$$\partial_\mu J^\mu = -\sqrt{-g}g^{rr}\chi^2(r)\partial_r \pi \ . \tag{7.70}$$

If the symmetry is unbroken then $\chi = 0$ and this is nothing but the conservation of current. Let us now consider evaluating this expression at the AdS boundary. Comparing (7.70) to the asymptotic behavior of π in (7.66) we see that the entire right-hand side of this expression is proportional (with no extra factors of r) to the coefficient A in the near-boundary expansion of π, i.e. to the source for the Goldstone boson field. This is simply the usual field theory Ward identity, which says that in the absence of a Goldstone source the field theory current is conserved.

The other nontrivial equations from (7.67) are those in t and x directions with

[19] It is amusing to note that computing the momentum conjugate to π precisely extracts out the *source* in this case, in exactly the same way that it extracts out the vev in the more familiar case of a standard massless scalar.

[20] For convenience of discussion here we have chosen a different normalization for the currents below.

nonzero $A_x(r,t,x)$ and $A_t(r,t,x)$ only, given by

$$-\partial_r J^t + \frac{1}{\tilde{g}_A^2}\nabla_x F^{xt} + \sqrt{-g}g^{tt}\chi^2(\partial_t\pi - A_t) = 0 \tag{7.71}$$

$$-\partial_r J^x + \frac{1}{\tilde{g}_A^2}\nabla_t F^{tx} + \sqrt{-g}g^{xx}\chi^2(\partial_x\pi - A_x) = 0\ . \tag{7.72}$$

Equations (7.65) and (7.70)–(7.72) are the full set of equations for this system.

Boundary Goldstone modes and their spin wave velocity

We will now solve the above equations in the hydrodynamic limit to show explicitly the existence of a Goldstone mode, i.e. a normalizable solution to (7.65) and (7.70)–(7.72) that is infalling (or regular) at the horizon and exists in the limit of small ω or k. We work in Fourier space

$$\pi = \pi(r)e^{-i\omega t+ikx} \qquad A_{t,x} = A_{t,x}(r)e^{-i\omega t+ikx} \tag{7.73}$$

Recall that at precisely 0 frequency and momentum we already know a solution to these equations: a constant pion profile $\pi(r) = \pi_0$ and $A = 0$. We now expand around this solution in powers of ω and k. To lowest order we simply solve the *forced* equations for A given by (7.71) and (7.72) with the forcing term provided by the zeroth-order solution for π, meaning that

$$A_t(r) \sim \mathcal{O}(\omega\pi_0), \qquad A_x(r) \sim \mathcal{O}(\pi_0 k). \tag{7.74}$$

The first correction to $\pi(r)$ enters through (7.65) and involves one extra field theory derivative, and thus we see that

$$\pi(r) = \pi_0 + \pi_1(r) \qquad \pi_1(r) \sim \mathcal{O}(\pi_0\omega^2, \pi_0 k^2) \tag{7.75}$$

The solution we want for A is both infalling at the black hole horizon and normalizable at the boundary; such a solution is nontrivial because of the forcing term[21] and is given by:

$$A_t = -i\omega\pi_0\left(1 - a_t(r)\right), \quad A_x = ik\pi_0\left(1 - a_x(r)\right) \tag{7.76}$$

where a_t and a_x are defined to be infalling at the horizon and satisfy the homogenous part (and zero frequency) part of (7.71) and (7.72):

$$\frac{1}{\tilde{g}_A^2}\partial_r(\sqrt{-g}g^{rr}g^{tt}\partial_r a_t) - \sqrt{-g}g^{tt}\chi^2 a_t = 0 \tag{7.77}$$

$$\frac{1}{\tilde{g}_A^2}\partial_r(\sqrt{-g}g^{rr}g^{xx}\partial_r a_x) - \sqrt{-g}g^{xx}\chi^2 a_x = 0 \tag{7.78}$$

[21] Of course as the force π_0 vanishes the only solution that is infalling and normalizable becomes the trivial one $A = 0$.

To ensure that A_t and A_x in (7.76) are normalizable we also require that

$$a_t(\infty) = 1, \qquad a_x(\infty) = 1 \ . \tag{7.79}$$

The corresponding equations for the pion profile are

$$\pi_1 = \omega^2 \pi_0 C^t(r) + k^2 \pi_0 C^x(r), \tag{7.80}$$

where the dynamical equations for C^t and C^x can be written from (7.65) as expressions for the radial independence of two objects α^t and α^x:

$$\partial_r \alpha^x = 0, \ \alpha^x \equiv -\sqrt{-g}\chi^2 g^{rr}\partial_r C^x + \frac{1}{\tilde{g}_A^2}\sqrt{-g}g^{rr}g^{xx}\partial_r a_x \tag{7.81}$$

$$\partial_r \alpha^t = 0, \ \alpha^t \equiv \sqrt{-g}\chi^2 g^{rr}\partial_r C^t - \frac{1}{\tilde{g}_A^2}\sqrt{-g}g^{rr}g^{tt}\partial_r a_t \tag{7.82}$$

The precise form of these equations turns out to not be important: the crucial fact is that $C^{t,x}$ are essentially driven by $a_{t,x}$, and so we can find solutions to them that are also infalling and normalizable–where normalizable in this case means that the term $\chi^2 \partial_r C^{x,t}$ vanishes at infinity (as explained in the discussion around (7.66)).

So far it appears that we have found a solution that is both infalling and normalizable, for *all* small frequency and momenta. This should not be possible, and indeed we have yet to impose the constraint (7.70). We find then the relation

$$\omega^2 = v_s^2 k^2 \qquad v_s^2 = \frac{\alpha_x}{\alpha_t} \ . \tag{7.83}$$

This is consistent only because of the radial independence of α_x and α_t, which away from the boundary involves fluctuations of the pion field. Thus we have shown that there exists a normalizable infalling mode provided that ω, k obey a linear relation. This is our main result.

It is convenient to evaluate (7.81) and (7.82) at $r = \infty$, where the terms depending on $C^{t,x}$ do not contribute, which leads to

$$\alpha_x = \frac{1}{\tilde{g}_A^2} \lim_{r\to\infty} \sqrt{-g}g^{rr}g^{xx}\partial_r a_x, \tag{7.84}$$

$$\alpha_t = -\frac{1}{\tilde{g}_A^2} \lim_{r\to\infty} \sqrt{-g}g^{rr}g^{tt}\partial_r a_t \ . \tag{7.85}$$

Note that this is equivalent to the statement that at the boundary the right-hand side of (7.70) vanishes—in the absence of a Goldstone boson source the current is conserved. Recall that a_t, a_x obey the zero frequency and unitary gauge infalling wave equations. It was shown in [14] that on such a field configuration at infinity the ratio of the current $J_{x,t} \sim \partial_r a_{x,t}$ to the field $a_{x,t}$ (which are unity in this case from (7.79)) itself is simply the field theory Green's function for the current. We thus

conclude that

$$\alpha_x = \lambda R^2 G_{xx}(\omega = 0, k = 0), \tag{7.86}$$
$$\alpha_t = -\lambda R^2 G_{tt}(\omega = 0, k = 0) \tag{7.87}$$

where

$$G_{\mu\nu}(\omega, k) = \langle j_\mu(\omega, k) j_\nu(-\omega, k) \rangle_{\text{retarded}} \tag{7.88}$$

are momentum space retarded Green function of the spin current j_μ along a symmetry broken direction. We thus find that the spin velocity v_s can be written as

$$v_s = \left(\frac{G_{xx}(\omega = 0, k = 0)}{-G_{tt}(\omega = 0, k = 0)} \right)^{1/2} . \tag{7.89}$$

This is the expected expression for an antiferromagnet. In particular, recognizing that [142, 143, 141]

$$\rho_s = G_{xx}(\omega = 0, k = 0), \qquad \chi_\perp = -G_{tt}(\omega = 0, k = 0) \tag{7.90}$$

where ρ_s is the spin stiffness and $\chi_\perp$ transverse magnetic susceptibility, we recover the standard expression

$$v_s = \sqrt{\frac{\rho_s}{\chi_\perp}} . \tag{7.91}$$

Note that equation (7.76) has a simple boundary theory interpretation: $j_\mu \propto \partial_\mu \pi_0$, as expected for the superfluid part of the current density. In our probe analysis, there is no normal component. Also note that our analysis above gives a nice correspondence between the Higgs mechanism in the bulk and the dynamics of Goldstone modes in the boundary theory.

7.5.3 Evaluation of spin wave velocity

We now evaluate G_{xx} and G_{tt} to find the spin velocity. It is convenient to derive a flow equation for them as in [14]. We start with a_x; examining the near-horizon behavior of equation (7.77) we see that for the solution to be nonsingular we need

$$\frac{\partial_r a_x}{a_x} = \frac{\tilde{g}_A^2 \chi^2}{4\pi T} \tag{7.92}$$

where T is the temperature. Introducing

$$\mathcal{G}_x(r) = \frac{1}{\tilde{g}_A^2} \frac{\sqrt{-g} g^{rr} g^{xx} \partial_r a_x}{a_x} \tag{7.93}$$

from (7.78) we find $\mathcal{G}_x$ satisfies the flow equation

$$\partial_r \mathcal{G}_x(r) = \sqrt{-g} g^{xx} \chi^2 - \frac{\tilde{g}_A^2 \mathcal{G}_x^2(r)}{\sqrt{-g} g^{rr} g^{xx}} \tag{7.94}$$

This equation should be integrated from the horizon (where from (7.92) we have $\mathcal{G}_x(r_h) = 0$) to the AdS boundary, where it is equal to the Green's function $G_{xx}(\omega = 0, k = 0)$.

Similarly to above, for a_t we introduce

$$\mathcal{H}_t(r) = \frac{\tilde{g}_A^2 a_t}{\sqrt{-g} g^{rr} g^{tt} \partial_r a_t} \tag{7.95}$$

This is convenient, as at the horizon $a_t = 0$. The corresponding flow equation for $\mathcal{H}_t$ is

$$\partial_r \mathcal{H}_t(r) = \frac{\tilde{g}_A^2}{\sqrt{-g} g^{rr} g^{tt}} - \mathcal{H}_t^2(r) \sqrt{-g} g^{tt} \chi^2 \tag{7.96}$$

and it should be integrated from the horizon, where the relevant boundary condition is $\mathcal{H}_t(r_h) = 0$, to infinity. In terms of (7.93) and (7.95) the spin wave velocity (7.89) can be written as

$$v_s = (-\mathcal{G}_x(\infty)\mathcal{H}_t(\infty))^{\frac{1}{2}} \ . \tag{7.97}$$

Evaluation of this requires knowledge of the scalar profile and can only be done numerically; some representative plots are shown in fig. 7-9.

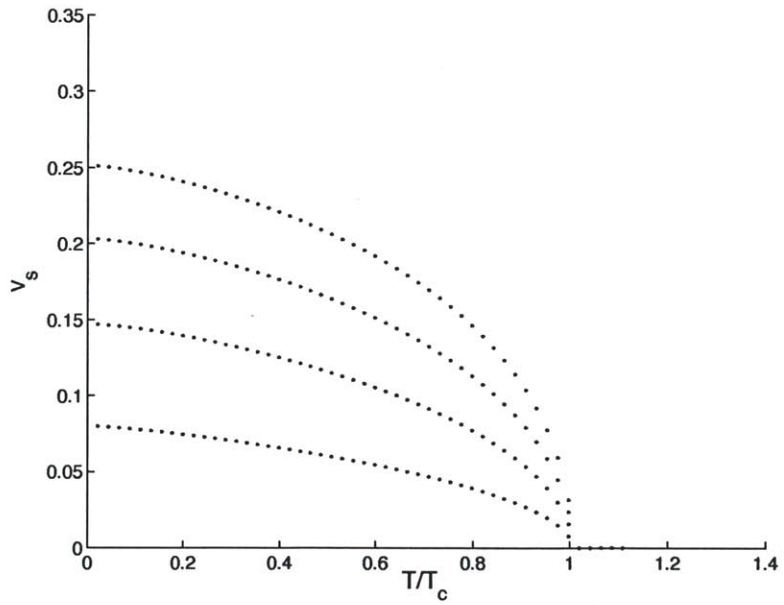

Figure 7-9: Spin wave velocity as a function of T/T_c for various values of the rescaled gauge coupling $\tilde{g}_A$: $\tilde{g}_A$ is varied from 1 (lowest curve) in unit increments to 4 (highest curve).

It is interesting to see what happens near the phase transition, where we have some analytic control; here we have $\chi^2 \sim (T - T_c)$ from earlier results; now examining the flow equations we see that $\mathcal{H}_t(\infty)$ remains finite in this limit, and is in fact given (up

to corrections analytic in $(T - T_c)$) by

$$-\mathcal{H}_t = -\int_{r_0}^{\infty} \frac{\tilde{g}_A^2}{\sqrt{-g} g^{rr} g^{tt}} = \frac{1}{\Xi} \tag{7.98}$$

where Ξ is the spin susceptibility in the unbroken phase. The second equality in (7.98) follows from the $U(1)$ analysis in Appendix D of [14]. On the other hand for $\mathcal{G}_x$ we find from (7.94) that near the transition $\mathcal{G}_x \sim (T - T_c)$. Thus the nonlinear term in the evolution can be neglected, leading to

$$\mathcal{G}_x(\infty) = \int_{r_0}^{\infty} dr \sqrt{-g} g^{xx} \chi^2 \ . \tag{7.99}$$

We find then near T_c

$$v_s^2 = \frac{1}{\Xi} \int_{r_0}^{\infty} dr \sqrt{-g} g^{xx} \chi^2 \propto (T - T_c) \ . \tag{7.100}$$

Note that above T_c, $\rho_s = G_{xx}(\omega = 0, k = 0)$ becomes identically zero. It would be interesting to extend this analysis to understand what happens to the spin wave velocity at zero temperature near the quantum critical transition.

7.6 External "magnetic fields" and forced ferromagnetic magnons

We have constructed a gravity description of the spontaneous breaking of an $SU(2)$ symmetry–analogous to the Neel phase in a spin system–and displayed the associated spin waves. In this section we turn briefly to a ferromagnet. A ferromagnet can be understood as a system undergoing spontaneous symmetry breaking in which the broken vacuum is charged under the unbroken generator. The spin waves in this case possess a quadratic dispersion $\omega \sim k^2$.

This setup is not straightforward to realize in holography–the spontaneous generation of a nonzero spin density means that essentially one now wants the *unbroken* non-Abelian gauge field *itself* to condense, without supplying any external chemical potentials. We leave this for future work.

In this section we consider something simpler–imagine applying an external magnetic field H to a sample containing spins, forcing them to align along the direction of the field. In our setup this corresponds to picking a direction in the $SU(2)$ space – we will pick the 3 direction – and supplying a chemical potential $\mu \sim H$ for the gauge field in that direction (in this section only μ refers to the chemical potential for the non-Abelian gauge field; we will set the $U(1)$ chemical potential to 0 here, as it does not play an essential role). It is interesting to note that this model has been studied before: it is precisely the "normal phase" of the holographic p-wave superconductor studied by [140], but our interpretation is different: in particular in those models a $U(1)$ subgroup of the $SU(2)$ is usually taken to be electric charge, which

is quite different from our approach. We will show that small fluctuations around such a configuration exhibit spin waves whose dispersion is not gapless, but whose dependence on momentum is indeed quadratic.

7.6.1 Gravity setup

We consider a generic spacetime metric (7.59) and a nontrivial non-Abelian gauge field profile

$$A_t^3(r) = \mu\alpha(r) \qquad \alpha(r \to \infty) = 1 \qquad \alpha(r_0) = 0, \tag{7.101}$$

with all other matter fields turned off. In particular the scalar ϕ^a is uncondensed and will play no role. We will also set the gauge coupling g_A to 1 as when the scalar is inactive g_A plays no role in the classical dynamics that follows. The profile $\alpha(r)$ solves the equation

$$\frac{1}{\sqrt{-g}}\partial_r\left(\sqrt{-g}g^{rr}g^{tt}\partial_r\alpha(r)\right) = 0 \tag{7.102}$$

$$\Rightarrow \quad J^{3t} \equiv -\sqrt{-g}g^{rr}g^{tt}\partial_r A_t^3 = \text{const} \tag{7.103}$$

where as above J^{3t} is the canonical momentum conjugate to A_t^3 and gives the expectation value of the spin density j^{3t} in the boundary theory as $\langle j^{3t}\rangle = J^{3t}(r=\infty)$. For simplicity, we will ignore the backreaction to the background metric, requiring that both μ and J^{3t} are small when expressed in units of the temperature. Note that μ and $\mathcal{J}^{3t}$ are related by the spin susceptibility Ξ

$$\langle j^{3t}\rangle = \mu\Xi, \tag{7.104}$$

with Ξ given by (7.98).

We will now slightly perturb this solution. We do not expect to find a gapless mode, as we have an "external magnetic field"; however at $k = 0$ we do expect to find a normalizable mode with $\omega = \mu$. To see the existence of this mode consider performing a gauge transform on the background (7.101) with infinitesimal gauge parameter Λ^a:

$$\delta A_M^a = \epsilon^{abc}\Lambda^c A_M^b + \partial_M\Lambda^a \tag{7.105}$$

It is convenient to work with the linear combinations

$$A^{\pm} = A^1 \pm iA^2, \tag{7.106}$$

as these are charge eigenstates under the rotations in the 3 direction for which we have supplied a chemical potential. If we assume a time dependence of the form $e^{-i\omega t}$ for Λ^+ we find the resulting A_t^+ can be written as

$$A_t^+ = \Lambda(A_t^3 - \omega)e^{-i\omega t} \tag{7.107}$$

where Λ is an overall (complex) constant. This perturbation is generically not normalizable at the AdS boundary; however if we demand that A_t^+ vanish at $r \to \infty$

then this fixes the frequency and we find

$$\omega = \mu, \qquad A_t^+(t,r) = \Lambda\mu(\alpha(r)-1)e^{-i\mu t} \equiv \Lambda A_{t0}(r)e^{-i\mu t} \tag{7.108}$$

Thus there is a normalizable mode at $\omega = \mu$ with the specified radial profile $A_{t0}(r) = \mu(\alpha(r)-1)$[22]. We will now turn on a small k to see how this mode evolves; as expected for a system with a background spin density, we will find that the frequency has a quadratic dependence on k.

7.6.2 Dispersion relation for the ferromagnetic magnon

To do this, we will need the full bulk Yang-Mills equations:

$$\frac{1}{\sqrt{-g}}\partial_M\left(\sqrt{-g}F^{aMN}\right) + \epsilon^{abc}A_M^b F^{cMN} = 0\,. \tag{7.109}$$

The presence of the background gauge potential A_t^3 can be conveniently taken into account by defining a gauge-covariant partial time derivative d_t that acts in the $\pm$ basis as

$$d_t A_{t,x}^+ = (\partial_t + iA_t^3)A_{t,x}^+\,. \tag{7.110}$$

We give all fields a spacetime dependence $e^{-i\mu t}e^{-i\Omega t+ikx}$. Here $\Omega \equiv \omega - \mu$ will parametrize deviation from the $\omega = \mu$ solution found above. The relevant equations of motion are those in (7.109) for $N = (r,t,x)$. We will work again with the bulk canonical momenta, defined as before:

$$J^{+t} \equiv -\sqrt{-g}F^{+rt} = -\sqrt{-g}g^{tt}g^{rr}\partial_r A_t^+, \tag{7.111}$$

$$J^{+x} \equiv -\sqrt{-g}F^{+rx} = -\sqrt{-g}g^{xx}g^{rr}\partial_r A_x^+\,. \tag{7.112}$$

We first examine the $N = r$ component of (7.109), which can be written as

$$d_t J^{+t} + \partial_x J^{+x} = iJ^{3t}A_t^+. \tag{7.113}$$

This equation is a bulk constraint that reduces on the boundary to the non-Abelian conservation of current. The remaining dynamical equations are

$$\frac{1}{\sqrt{-g}}\partial_r J^{+t} + \partial_x F^{+xt} = 0 \tag{7.114}$$

$$\frac{1}{\sqrt{-g}}\partial_r J^{+x} + d_t F^{+tx} = 0 \tag{7.115}$$

Only one of the components of the field strength tensor is affected by the gauge field background:

$$F_{xt}^+ = \partial_x A_t^+ - d_t A_x^+ = ikA_t^+ - (i\mu(\alpha-1) - i\Omega)A_x^+\,. \tag{7.116}$$

[22]The existence of such a mode was observed before in [140] in the context of conductivity of a p-wave superconductor.

We now want to perturb around the $\omega = \mu$ solution found above. We thus turn on a small k-dependence in (7.108) and consider a perturbation of the form

$$A_t^+ = e^{-i\mu t} e^{-i\Omega t + ikx} \left(A_{t0}(r) + A_{t1}(r; w, k) + \cdots \right) \tag{7.117}$$

where $A_{t0}(r) \sim (\alpha(r) - 1)$ is the previously found profile in (7.108). Recall that $\Omega \equiv \omega - \mu$ parametrizes departure from μ and will be the small parameter in the expansions that follow. A nonzero A_t^+ will also excite an A_x^+ which we take to have the form

$$A_x^+ = A_x^+(r; \Omega, k) e^{-i\mu t} e^{-i\Omega t + ikx} \, . \tag{7.118}$$

The other components of the gauge fields can be consistently set to zero except for $A_{t,x}^-$, which are related to $A_{t,x}^+$ by complex conjugation.

To obtain the magnon dispersion relation we will expand the above equations to lowest order in the Ω and k expansion and look for solutions that are both infalling (or regular) at the horizon and normalizable at the AdS boundary. These equations will have the same structure as in the antiferromagnetic case above; we will find second-order radial equations for A_x^+ and the correction A_{t1} that are forced by the known solution A_{t0}.

More explicitly, plugging (7.117) and (7.118) into (7.114)–(7.115), and expanding them in powers of Ω and k, we find that

$$A_x^+(r) \sim O(k), \qquad A_{t0} \sim O(k^2) \tag{7.119}$$

We thus introduce the following

$$A_x^+(r) = k \left(1 - \frac{a_x(r)}{a_x(\infty)} \right), \qquad A_{t1}(r) = k^2 a_{t1}(r), \tag{7.120}$$

Here by construction A_x^+ is normalizable, and from (7.115) we find that $a_x(r)$ satisfies the homogenous equation

$$\frac{1}{\sqrt{-g}} \partial_r \left(\sqrt{-g} g^{rr} g^{xx} \partial_r a_x \right) - \mu^2 (\alpha - 1)^2 g^{tt} g^{xx} a_x = 0. \tag{7.121}$$

There is a forced radial equation for the correction to A_{t1} profile $a_{t1}(r)$, but we will not need to solve it explicitly to find the dispersion, analogous to the antiferromagnetic case where the correction to the pion profile was not explicitly needed.

$$\frac{1}{\sqrt{-g}} \partial_r \left(\sqrt{-g} g^{rr} g^{tt} \partial_r a_{t1} \right) = \mu (\alpha - 1) g^{tt} g^{xx} a_x \, . \tag{7.122}$$

It is of course critical to note that an infalling and normalizable solution to this equation can always be found.

We now impose the constraint arising from the conservation of current (7.113). Again it is simplest to evaluate it at the AdS boundary first; here the right-hand side of (7.113) vanishes (as by construction we are looking at a normalizable solution with

$A_t^+(\infty) = 0$). We find the dispersion relation

$$\Omega = \omega - \mu = \left(\frac{1}{J^{3t}} \lim_{r\to\infty} \frac{\sqrt{-g} g^{rr} g^{xx} \partial_r a_x}{a_x(\infty)} \right) k^2 \tag{7.123}$$

This is the desired dispersion relation.

Let us briefly understand the physical origin of the differences from the linear and gapless dispersion found in the antiferromagnetic case. The dispersion is not linear because the background value of J^{3t} is finite in the $\omega \to 0$ limit, unlike in the antiferromagnetic case where it is proportional to ω: this means that we are now balancing a term of order ω against one of order k^2, rather than a term of order ω^2. The mode is not gapless because at infinity the gauge-covariant derivative $d_t = \partial_t + iA_t^3 \to -i\omega + i\mu$, resulting in a shift in ω. These considerations lead us to expect that if one were able to create a situation with a nonzero J^{3t} in the absence of a background chemical potential – i.e. a true spontaneous ferromagnet – one would find precisely the gapless quadratic dispersion of the standard ferromagnetic magnon.

Note that we can interpret the expression (7.123) in terms of field theory quantities. Again using expressions from [14], we can rewrite the ratio of $\partial_r a_x$ to a_x in terms of a field theory correlator to find

$$\Omega = \left(\frac{G^R(\omega = \mu, k = 0)}{J_3^t} \right) k^2, \tag{7.124}$$

with

$$G^R(\omega, k) = \left\langle j_x^+(\omega, k) j_x^-(-\omega, k) \right\rangle_{\text{retarded}} \tag{7.125}$$

i.e. G^R_{xx} is the field theory retarded correlator for j_x^+ evaluated at the nonzero frequency $\omega = \mu$. The prefactor of the quadratic dispersion is consistent with the expected result for a ferromagnet [144].

We now evaluate the constraint (7.113) at arbitrary r. Now the right-hand side no longer vanishes, and we find

$$\Omega = \omega - \mu = \gamma k^2, \tag{7.126}$$

where

$$\gamma = -\frac{1}{J^{3t}} \left(\mu(\alpha - 1)\sqrt{-g} g^{rr} g^{tt} \partial_r a_{t1}(r) - \frac{\sqrt{-g} g^{rr} g^{xx} \partial_r a_x(r)}{a_x(\infty)} \right) + a_{t1}(r) \,. \tag{7.127}$$

It can readily checked from (7.121) and (7.122) that γ is independent of r, and evaluated at $r \to \infty$ we find that γ reduces to the expression in (7.123). Again, even though we did not need to explicitly solve for $a_{t1}(r)$ to find the dispersion, its fluctuations are essential to make sure that the constraint from non-Abelian current conversation is upheld at all points in the bulk.

7.6.3 Evaluation of dispersion

We now turn to the evaluation of the dispersion γ. This bears a large formal similarity to the evaluation of conductivities studied in [14]. We consider the following "transport coefficient" defined at all values of r:

$$\sigma(r;\mu) = -\frac{\sqrt{-g}g^{rr}g^{xx}\partial_r a_x(r)}{i\mu a_x(r)} \tag{7.128}$$

The motivation behind this name will soon be made clear. Q is simply related to the boundary value of this object:

$$\gamma = -\frac{i\sigma(r\to\infty;\mu)}{\Xi} \tag{7.129}$$

where we have used (7.104). From (7.121), we find that σ obeys a simple radial evolution equation,

$$\partial_r\sigma = i\mu\sqrt{\frac{g_{rr}}{-g_{tt}}}\left(\frac{\sigma^2}{\Sigma} - \Sigma(\alpha-1)^2\right), \tag{7.130}$$

with

$$\Sigma(r) \equiv \sqrt{\frac{-g}{-g_{rr}g_{tt}}}g^{xx}(r) \tag{7.131}$$

and at the horizon the value of σ is fixed by the infalling boundary condition to be $\sigma(r_h;\mu) = \Sigma(r_h)$ (this is explained in detail in [14]).

Before considering general μ, let us consider the limit $\mu \to 0$, in which case $\partial_r\sigma = 0$, σ becomes constant in r, and is in fact equal to the normal (Abelian) DC conductivity σ_{DC} of a $U(1)$ current on this background. Thus we find for the "magnon" dispersion (7.123)

$$\omega = -ik^2\frac{\sigma_{DC}}{\Xi} \tag{7.132}$$

This relation is not surprising; when taking μ to 0 we are removing all non-Abelian effects and returning to the zero density system, and (7.132) simply describes the diffusion in the longitudinal channel of a $U(1)$ current. The diffusion constant is seen to be $\frac{\sigma_{DC}}{\Xi}$, as is required by the Einstein relation.

For generic μ we must evaluate this expression numerically. In this section alone for simplicity we work with the normal AdS-Schwarzschild metric in coordinates with η set to 0. We do not require the RN metric here; even in the absence of a net $U(1)$ charge, one can imagine polarizing thermally excited "spins" with an external magnetic field. We do not expect inclusion of a $U(1)$ charge to qualitatively change the results. We work in units where both σ_{DC} and Ξ have been set to 1. The results of the numerical evaluation are shown in Figures 7-10 and 7-11 as a function of μ/T.

Perhaps the most obvious feature of these diagrams is the γ has a large imaginary part, corresponding to a strong dissipation. This is due to the fact that we are evaluating our bulk equations as a perturbation about a nonzero frequency $\omega = \mu$; these waves are infalling at the black horizon and result in a large dissipation. We

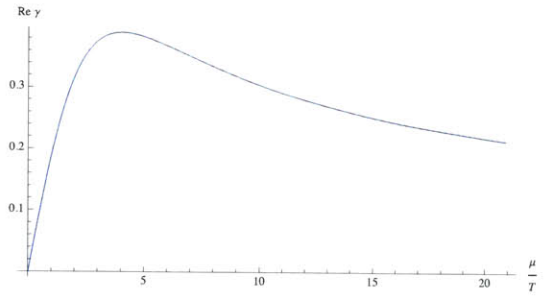

(a) $\mathrm{Re}\,\gamma$

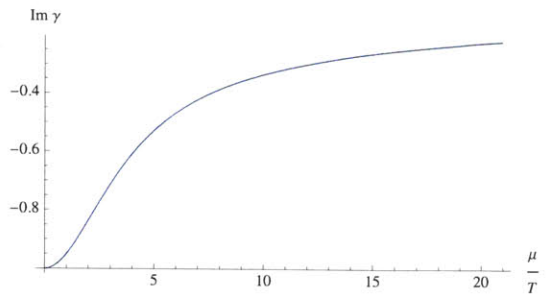

(b) $\mathrm{Im}\,\gamma$

Figure 7-10: The real and imaginary parts of γ are shown as a function of μ/T. Note as $\mu \to 0$, $\gamma \to -i$ as required by the Einstein relation.

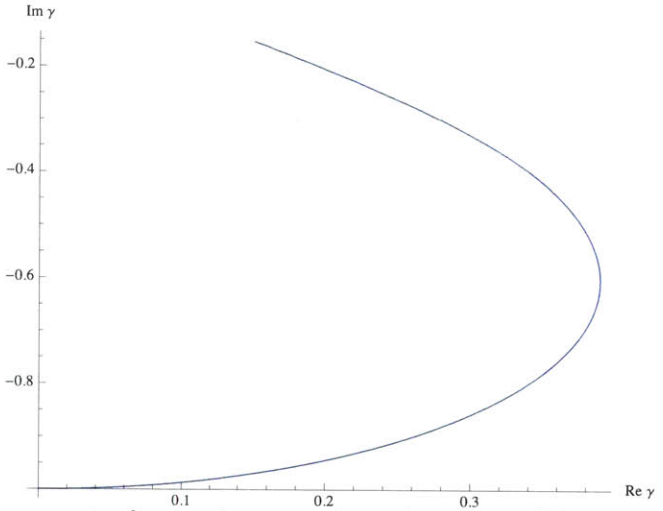

Figure 7-11: Movement of γ in the complex plane as μ/T is varied from 0 to 40.

expect that if we were able to construct a true spontaneous ferromagnet with $\mu = 0$ then our bulk equations would be evaluated at $\omega = 0$ and γ would then be both real and gapless.

As mentioned earlier, this model is the normal phase of the holographic p-wave superconductor of [140]. According to their discussion, at sufficiently large $\frac{\mu}{T}$ (roughly $\frac{\mu}{T} \sim 15.9$ in our units) this system becomes unstable towards a condensate of the vector fields $A^{1,2}_{x,y}$. It would be interesting to understand further such a condensate – in our language, a persistent spin current – from the magnetic point of view taken in this paper.

7.7 Conclusion

In this chapter we studied holographic phase transitions associated with condensation of a neutral order parameter, both at finite temperature and at the associated quantum critical point. We also considered the embedding of the neutral order parameter into the staggered magnetization for an antiferromagnetic phase. We show that at

the macroscopic level one recovers the expected features of the antiferromagnetic phases including existence of two gapless spin waves and their dispersion relations.[23] A similar discussion in a forced ferromagnetic phase reveals spin waves with quadratic dispersion relations which again agrees with field theoretical expectations.

One might be surprised at some aspects of this transition; in particular, note that we have an ordered phase in a $(2+1)$-dimensional *field*-theory at finite temperature. This appears to be in conflict with the Coleman-Mermin-Wagner theorem [145], which states that fluctuations of the Goldstone mode should destroy ordered phases in (2+1) dimensions at finite temperature. It seems clear that this is an artifact of the large-N approximation, which has the effect of freezing fluctuations. The resolution of this problem is discussed (in the context of a broken $U(1)$ symmetry) in [146], where the bulk mode that corresponds to the Goldstone mode of the boundary theory is constructed. This mode is precisely analogous to the spin waves constructed in this chapter. It is shown there that the quantum fluctuations of this bulk mode do indeed restore the symmetry over distances that are exponentially large in $1/N^2$.

Now while we studied the ordered phase in detail we did not yet discuss extensively the nature of the quantum critical point. In the vicinity of the critical point one expects to find extra gapless modes. As the quantum critical point is of a somewhat novel nature one also expects the gapless modes to be somewhat special, and it is to a discussion of this critical behavior that we turn in the next chapter.

7.A Effect of magnetic field on IR conformal dimension

In this appendix we outline the derivation of (7.50) demonstrating the effect of a background magnetic field on the IR conformal dimension of a charged scalar field.

7.A.1 Dyonic black hole

We will need to consider the effect of the magnetic field on the geometry. Turning on such an external boundary magnetic field for the $U(1)$ current dual to the bulk gauge B_M in (7.5), the corresponding bulk geometry becomes that of a dyonic black hole with both electric and magnetic charges,

$$ds^2 \equiv g_{MN}dx^M dx^N = \frac{r^2}{R^2}(-f dt^2 + d\vec{x}^2) + \frac{R^2}{r^2}\frac{dr^2}{f} \tag{7.133}$$

with

$$f = 1 + \frac{Q^2+P^2}{r^4} - \frac{M}{r^3} \tag{7.134}$$

$$B_t = \mu_B\left(1 - \frac{r_0}{r}\right), \quad B_x = -\frac{P}{R^4}y, \quad \mu_B \equiv \frac{Q}{R^2 r_0}. \tag{7.135}$$

[23] As discussed earlier these features only depend on symmetry breaking pattern and not details of the microscopic theory.

r_0 is the horizon radius determined by the largest positive root of the redshift factor

$$f(r_0) = 0, \qquad \rightarrow \qquad M = r_0^3 + \frac{Q^2 + P^2}{r_0} \,. \tag{7.136}$$

The geometry (7.133) describes the boundary theory at a finite density with the charge density ρ, energy density ϵ, entropy density s, respectively given by

$$\rho = 2\frac{Q}{\kappa^2 R^2 g_F}, \quad \epsilon = \frac{M}{\kappa^2\ R^4}, \quad s = \frac{2\pi}{\kappa^2}\left(\frac{r_0}{R}\right)^2 \,. \tag{7.137}$$

The external magnetic field H and temperature T are

$$H = \frac{P}{R^4}, \quad T = \frac{3r_0}{4\pi R^2}\left(1 - \frac{Q^2 + P^2}{3r_0^4}\right) \,. \tag{7.138}$$

μ_B in (7.135) corresponds to the chemical potential of the boundary system.

It is convenient to work with dimensionless quantities by introducing

$$Q = \mu r_0^2, \qquad P = h r_0^2 \tag{7.139}$$

and rescaling coordinates as

$$r \to r r_0, \quad (t, \vec{x}) \to \frac{R^2}{r_0}(t, \vec{x}) \tag{7.140}$$

after which equation (7.133) becomes

$$\frac{ds^2}{R^2} = r^2(-f dt^2 + d\vec{x}^2) + \frac{1}{r^2}\frac{dr^2}{f} \tag{7.141}$$

with

$$f = 1 + \frac{3\eta}{r^4} - \frac{1 + 3\eta}{r^3}, \quad B_t = \mu\left(1 - \frac{1}{r}\right), \quad B_x = -hy \tag{7.142}$$

and

$$3\eta \equiv \mu^2 + h^2 \,. \tag{7.143}$$

Setting $h = 0$ above one recovers the metric (7.6) used in the main text.

We will be interested in the system at zero temperature, for which

$$Q^2 + P^2 = 3r_0^4 \quad \text{or} \quad \mu^2 + h^2 = 3 \tag{7.144}$$

and the near horizon region becomes $\mathrm{AdS}_2 \times \mathbb{R}^2$ with curvature radius

$$R_2 = \frac{R}{\sqrt{6}} \,. \tag{7.145}$$

Note that in the zero temperature limit, due to conformal invariance of the underlying

vacuum theory the physically relevant quantity is the dimensionless ratio

$$b \equiv \frac{H}{\mu_B^2} = \frac{h}{\mu^2} \,. \tag{7.146}$$

Using the second relation in (7.144) we can then express bulk quantities like h (and thus μ) in terms of b,

$$h = \frac{\sqrt{1+12b^2}-1}{2b} \,. \tag{7.147}$$

7.A.2 Scalar operator dimension in the IR

Now consider a scalar field in AdS_4 of charge q and mass m, with an action

$$S = -\int d^4x\sqrt{-g}\,\left[(D_M\phi)^* D^M\phi + m^2\phi^*\phi\right], \tag{7.148}$$

where the gauge-covariant derivative satisfies

$$D_M\phi = (\partial_M - iqB_M)\phi \,. \tag{7.149}$$

Note that the action (7.148) depends on q only through

$$\mu_q \equiv \mu q \,, \quad h_q \equiv hq \tag{7.150}$$

which are the effective chemical potential and effective magnetic field for a field of charge q.

This problem is now similar to a Landau-level analysis from elementary quantum mechanics. After separation of variables using

$$\phi = e^{-i\omega t + ikx} Y(y) X(r) \,, \tag{7.151}$$

we find that the equations of motion can be written as

$$\begin{aligned} -\frac{1}{\sqrt{-g}}\partial_r(\sqrt{-g}g^{rr}\partial_r X) + \left(-g^{ii}u^2 + m^2 + g^{ii}\lambda^2\right) X = 0 \\ -\partial_y^2 Y + \left(v^2 - \lambda^2\right) Y = 0 \end{aligned} \tag{7.152}$$

with

$$v(y) \equiv k + h_q y, \quad u(r) \equiv \sqrt{\frac{g_{ii}}{-g_{tt}}}\left(\omega + \mu_q\left(1 - \frac{1}{r}\right)\right) \,. \tag{7.153}$$

One then finds that

$$Y_n(y) = e^{\frac{-\xi^2}{2}} H_n(\xi), \qquad \xi \equiv \sqrt{|h_q|}\,\left(y + \frac{k}{h_q}\right) \tag{7.154}$$

with H_n the usual Hermite polynomials. $X(r)$ is a radial profile that satisfies the

scalar wave equation with zero magnetic field $h = 0$, except that the momentum k on each constant-r slice has been discretized into Landau levels:

$$k^2 \to 2\,|h_q|\left(n+\frac{1}{2}\right), \qquad n = 0, 1, \cdots \tag{7.155}$$

A similar discussion can be applied to the AdS_2 region, where one finds that each Landau level has an effective mass given by

$$m_n^2 = m^2 + 2\,|h_q|\left(n+\frac{1}{2}\right)\frac{1}{R^2}\,. \tag{7.156}$$

The rest then follows exactly from the analysis in [19], and the IR dimension for ϕ is given by

$$\delta_n^{(B)} = \frac{1}{2} + \nu_n^{(B)} \tag{7.157}$$

with

$$\nu_n^{(B)} = \sqrt{m_n^2 R_2^2 - \frac{\mu^2 q^2}{36} + \frac{1}{4}}\,. \tag{7.158}$$

Let us examine a bit more closely the $n = 0$ mode, which is the most likely to condense,

$$\nu_0^{(B)} = \sqrt{\frac{m^2R^2}{6} + (6|bq| - q^2)\frac{\sqrt{1+12b^2}-1}{72b^2} + \frac{1}{4}} \tag{7.159}$$

where we used (7.147) to express h and μ in terms of the dimensionless boundary quantity b (7.146). Also note that $m^2R^2 = \Delta(\Delta - 3)$. This is the result (7.50) in the main text. The critical magnetic field b_c can be found by setting the quantity inside the square root to 0, and is

$$b_c = |q|\,\frac{D\left[1+\frac{1}{\sqrt{3}}\sqrt{q^2-2m^2R^2}\right] - 2q^2}{D^2 - 12q^2} \tag{7.160}$$

where

$$D \equiv \left(3 + 2m^2R^2\right) \tag{7.161}$$

is a quantity that goes to 0 when the scalar mass is precisely at the neutral AdS_2 BF bound.

It is interesting that the expression in (7.159) containing b saturates at a value $\frac{|q|}{2\sqrt{3}}$ as $b \to \infty$. Thus if

$$m^2R^2 + \sqrt{3}|q| < -\frac{3}{2} \tag{7.162}$$

no matter how large the magnetic field is, a condensate cannot be prevented. This is rather surprising and is discussed further in the main text.

Chapter 8

A bifurcating quantum critical point

8.1 Introduction

In the previous chapter we studied a very simple model, a neutral scalar field propagating on the finite density Reissner-Nordstrom black brane background. The action of the scalar was taken to be

$$S_\phi = \frac{1}{\lambda}\int d^4x\sqrt{-g}\left(-\frac{1}{2}(\nabla\phi)^2 - V(\phi)\right), \tag{8.1}$$

where $V(\phi)$ is a double-well potential, with fluctuations about $\phi = 0$ having a negative mass-squared $m^2 < 0$. These fluctuations have a dimension in the IR AdS_2 region given by the standard formula

$$\delta_k = \frac{1}{2} + \nu_k \qquad \nu_k = \sqrt{u + \frac{k^2}{6\mu_*^2}}, \qquad u \equiv m^2R_2^2 + \frac{1}{4}\,. \tag{8.2}$$

Here we have defined a parameter u. It was shown that if $u < 0$ then the $k = 0$ mode of the scalar develops an imaginary conformal dimension, indicating an instability towards condensation. In the previous chapter we discussed the condensed phase in some detail, focusing in particular on the case when the scalar was charged in the adjoint of a global $SU(2)$ symmetry. If $u > 0$ then the Reissner-Nordstrom black hole is stable, even at zero temperature[1] and thus $u = 0$ defines a quantum critical point.

In this section we study the critical behavior near the quantum critical point. We will discover novel behavior, including a susceptibility that does not diverge at the critical point, but instead *bifurcates*, attempting to go imaginary as we approach $u = 0$. It is this novel behavior that prompts us to call this a "bifurcating" quantum critical point.

We compute the susceptibility $\chi(\omega, \vec{k})$ using the matching techniques discussed in

[1]Here by "stable", we mean with respect to condensation of this particular scalar field; certainly it can have other instabilities that we are not considering here.

Chapter 4; for convenience, we reproduce the key expression for the zero-temperature retarded correlator here,

$$\chi(\omega,\vec{k}) = G_R(\omega,\vec{k}) = \mu_*^{2\nu_U}\frac{b_+(k,\omega)+b_-(k,\omega)\mathcal{G}_k(\omega)\mu_*^{-2\nu_k}}{a_+(k,\omega)+a_-(k,\omega)\mathcal{G}_k(\omega)\mu_*^{-2\nu_k}} \tag{8.3}$$

where ν_k is defined above and ν_U is its UV counterpart in the asymptotic AdS_4 region, i.e. if Δ is the UV conformal dimension of the operator in standard quantization we have

$$\Delta = \frac{3}{2}+\nu_U \qquad \nu_U = \sqrt{\frac{9}{4}+m^2R^2} \tag{8.4}$$

We shall require the analytic properties of the functions $a_\pm(\omega,k)$ and $b_\pm(\omega,k)$, which are reviewed in Appendix 8.A. The explicit expression for the AdS_2 Green's function for a neutral scalar is also reproduced below:

$$\mathcal{G}_k(\omega) = \frac{\Gamma(-2\nu_k)}{\Gamma(2\nu_k)}\frac{\Gamma(\frac{1}{2}+\nu_k-iq_*)}{\Gamma(\frac{1}{2}-\nu_k-iq_*)}(-2i\omega)^{2\nu_k}\ . \tag{8.5}$$

8.2 Zero temperature: from uncondensed side

We begin by approaching the quantum phase transition at zero temperature from the uncondensed side. To study the behavior near the critical point $u=0$ we study the implications of taking $\nu_k \to 0$ in (8.3), i.e. both k^2/μ^2 and u are small.

8.2.1 Static properties

We first study the critical behavior of the static susceptibility by setting $\omega \to 0$ in (8.3) and taking $u \to 0$ from the uncondensed side $u > 0$. From equation (8.77) we find that for small ν_k,

$$\chi(k) = \mu_*^{2\nu_U}\frac{\beta+\nu_k\tilde{\beta}}{\alpha+\nu_k\tilde{\alpha}} + O(\nu_k^2,k^2) \tag{8.6}$$

where $\alpha,\beta,\tilde{\alpha},\tilde{\beta}$ are numerical constants. Setting $k=0$ we find the zero momentum susceptibility is given by

$$\chi = \mu_*^{2\nu_U}\frac{\beta+\sqrt{u}\tilde{\beta}}{\alpha+\sqrt{u}\tilde{\alpha}}\ . \tag{8.7}$$

As already mentioned earlier, at the critical point the static susceptibility remains finite, given by

$$\chi|_{u\to 0_+} = \chi_0 \equiv \mu_*^{2\nu_U}\frac{\beta}{\alpha}\ . \tag{8.8}$$

which is in sharp contrast with the critical behavior from the Landau paradigm where one expects that the uniform susceptibility always diverges approaching a critical point. Due to the square root appearing in (8.7), χ has a branch point at $u=0$ and bifurcates into the complex plane for $u<0$. Of course, when $u<0$, eq. (8.7) can no

longer be used, but the fact that it becomes complex can be considered an indication of instability. Furthermore, taking a derivative with respect to u we find that

$$\partial_u \chi = \mu_*^{2\nu_U} \frac{\alpha\tilde{\beta} - \beta\tilde{\alpha}}{2\alpha^2} \frac{1}{\sqrt{u}} = -\mu_*^{2\nu_U} \frac{1}{4\nu_U \alpha^2} \frac{1}{\sqrt{u}} \to \infty, \qquad u \to 0 \tag{8.9}$$

where we have used (8.81) in the second equality. Thus even though $\chi(u)$ is finite at $u = 0$, it develops a cusp there, as shown in Fig. 8-1. It will turn out convenient to introduce a quantity

$$\chi_* \equiv \mu_*^{2\nu_U} \frac{1}{4\nu_U \alpha^2} = \chi_0 \frac{1}{4\nu_U \alpha\beta} \tag{8.10}$$

and then (8.9) becomes

$$\partial_u \chi = -\frac{\chi_*}{\sqrt{u}} \,. \tag{8.11}$$

Similarly, taking derivative over k^2 in (8.6) and then setting $k = 0$, we find that

$$\partial_{k^2} \chi(\vec{k})\big|_{k=0} = -\frac{\chi_*}{6\mu_*^2 \sqrt{u}}, \qquad u \to 0 \,. \tag{8.12}$$

Note that this divergence is related to the fact for any $u > 0$, $\chi(\vec{k})$ is analytic in k^2, but not at $u = 0$, where $\nu_k \propto k$.

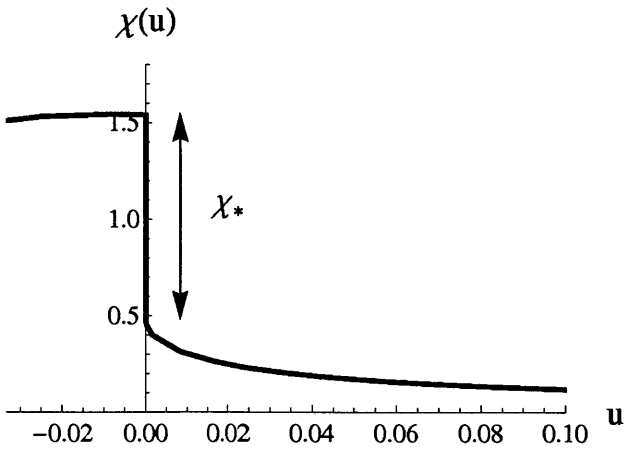

Figure 8-1: A plot of $\chi(u)$ as a function of u. We also include the behavior on the $u < 0$ side to be worked out in Sec. 8.3. Note that while there is a cusp in χ approaching the critical point from the uncondensed side ($u > 0$), there is no cusp approaching the critical point from the condensed side ($u < 0$). From both sides the susceptibility is finite at the critical point, but it tends to a different value on each side.

The above non-analytic behavior at $k = 0$ should have important consequences when we Fourier transform $\chi(\vec{k})$ to coordinate space. Indeed, by Fourier transforming $\chi(k)$ to coordinate space we find (for details see discussion around (8.107) in

Appendix 8.C) asymptotically at large x,

$$G(x) \equiv \int \frac{d^2k}{(2\pi)^2}\chi(\vec{k})e^{ikx} \approx \frac{\chi_*\sqrt{u}}{\pi x^2}\exp\left(-\frac{x}{\xi}\right) , \tag{8.13}$$

where the correlation length ξ is given by

$$\xi = \frac{1}{\sqrt{6}\mu_*\sqrt{u}} . \tag{8.14}$$

Thus as $u \to 0$ the correlation length ξ diverges as $u^{-\frac{1}{2}}$, which is the same as in a free theory.

Note however that there is additional suppression by factors of $\sqrt{u}$ in the numerator of this expression; this suggests that the actual power law falloff at the critical point is not the one found from setting $u \to 0$ above, but is rather faster. Indeed performing the integral at precisely $u = 0$ we find from (8.112),

$$G(x)\big|_{u=0} \sim \mu_*^{2\Delta-1}\frac{1}{(\mu_* x)^3} \tag{8.15}$$

with a different exponent $\sim x^{-3}$.

8.2.2 Dynamical properties

We now turn to the critical behavior of the susceptibility (8.3) at a nonzero ω near the critical point on the uncondensed side $u > 0$. We must now take extreme care the $\nu_k \to 0$ limit, as the factor $\left(\frac{\omega}{\mu_*}\right)^{2\nu_k}$ in the AdS_2 Green function (8.5) behaves differently depending on the order in which we take the $\nu_k \to 0$ and $\omega \to 0$ limits. For example, the Taylor expansion of such a term in small ν_k involves terms of the form $\nu_k \log(\omega/\mu_*)$. In the small ω limit, the resulting large logarithms will appear to invalidate the small ν_k expansion.

To proceed, we note first that the expression (8.3) together with the explicit expression for the AdS_2 Green's function (8.5) can be written

$$\chi(\omega,\vec{k}) = \mu_*^{2\nu_U}\left(\frac{b_+\Gamma(\nu_k)\left(\frac{-i\omega}{2\mu_*}\right)^{-\nu_k} + b_-\Gamma(-\nu_k)\left(\frac{-i\omega}{2\mu_*}\right)^{\nu_k}}{a_+\Gamma(\nu_k)\left(\frac{-i\omega}{2\mu_*}\right)^{-\nu_k} + a_-\Gamma(-\nu_k)\left(\frac{-i\omega}{2\mu_*}\right)^{\nu_k}}\right) . \tag{8.16}$$

Now from the discussion at the beginning of Appendix 8.A, we can write

$$a_\pm = a(\pm\nu_k; k^2, \omega), \quad b_\pm = b(\pm\nu_k; k^2, \omega) \tag{8.17}$$

where $a(\nu; k^2, \omega)$ and $b(\nu; k^2, \omega)$ are some functions analytic in all its variables. Us-

ing (8.17), we can now further rewrite (8.16) as

$$\chi(\omega,\vec{k}) = \mu_*^{2\nu_U}\frac{f_b(\nu_k)-f_b(-\nu_k)}{f_a(\nu_k)-f_a(-\nu_k)} \tag{8.18}$$

where[2]

$$f_b(\nu) \equiv b(\nu)\nu\Gamma(\nu)\left(\frac{-i\omega}{2\mu_*}\right)^{-\nu} \tag{8.19}$$

and similarly for $f_a(\nu)$. The point of this rewriting is to illustrate that if $f_{a,b}(\nu)$ have nonsingular Taylor expansions in ν – which is the case for any finite ω – then if we expand numerator and denominator in ν all the terms that are odd in ν will cancel, and thus $\chi(\omega,\vec{k})$ contains only *even* powers of ν_k, i.e. $\chi(\omega,\vec{k}) = \chi(\omega,u,k^2)$ and for any nonzero ω, $\chi(\omega,\vec{k})$ is *analytic* at $u=0$ and $k^2=0$. There is no non-analyticity of the sort that can be found in (8.6). In particular the expression for $\chi(\omega,\vec{k})$ approaching $u=0$ for the condensed side can be simply obtained by analytically continuing (8.18) to $u<0$. This should be expected since for a given ω, as we take $u\to 0_-$, it should always be the case that ω is much larger than the scale where the physics of condensate sets in, which should go to zero with u. Thus the physics of the condensate is not visible at a given nonzero ω. We will see in next section that the same thing happens at finite temperature.

Now expanding the gamma functions and $a_\pm, b_\pm$ in (8.16) to leading order in ν_k, but keeping the full dependence on ω, we find that

$$\chi(\omega,\vec{k}) = \chi_0\frac{\sinh\left(\nu_k\log\left(\frac{-i\omega}{\omega_b}\right)\right)}{\sinh\left(\nu_k\log\left(\frac{-i\omega}{\omega_a}\right)\right)} + \cdots \tag{8.20}$$

where the energy scales $\omega_{a,b}$ are given by

$$\omega_a = 2\mu_*\exp\left(\frac{\tilde{\alpha}}{\alpha}-\gamma_E\right), \quad \omega_b = 2\mu_*\exp\left(\frac{\tilde{\beta}}{\beta}-\gamma_E\right), \tag{8.21}$$

where γ_E is the Euler-Mascheroni constant, and χ_0 is the uniform susceptibility at the critical point given earlier in (8.8). Considering $\nu_k\to 0$ in (8.20) with a fixed ω, we then find

$$\chi(\omega,\vec{k}) = \chi_0\frac{\log\left(\frac{\omega}{\omega_b}\right)-i\frac{\pi}{2}}{\log\left(\frac{\omega}{\omega_a}\right)-i\frac{\pi}{2}} + O(u,k^2) \tag{8.22}$$

where the corrections are analytic in both u and k^2. Note that both the above expression and (8.20) have a pole at $\omega = i\omega_a$ in the upper half ω-plane. But this should not concern us as our expressions are only valid for $\omega \ll \mu_* \sim \omega_a$. Further

[2] Note that $\Gamma(\nu\to 0)\sim\frac{1}{\nu}-\gamma+\mathcal{O}(\nu)$, necessitating the extra factor of ν in the definition of $f_{a,b}(\nu)$ to obtain a nonsingular Taylor expansion.

taking the $\omega \to 0$ limit in (8.22) then gives

$$\begin{aligned}\chi(\omega,\vec{k}) &= \chi_0\left(1+\frac{1}{2\nu_U\alpha\beta}\frac{1}{\log\omega}+\frac{i\pi}{4\nu_U\alpha\beta}\frac{1}{(\log\omega)^2}+\cdots\right)\\ &= \chi_0+\frac{2\chi_*}{\log\omega}+\frac{i\pi\chi_*}{(\log\omega)^2}+\cdots\end{aligned} \tag{8.23}$$

where we have kept the leading nontrivial ω-dependence in both real and imaginary parts and used (8.10).

Equations (8.22) and (8.23) give the leading order expression at nonzero u (for both signs, as $\chi(\omega,k)$ is analytic at $u=0$ at a nonzero ω) and k^2 as far as $\nu_k \log\frac{\omega}{\omega_{a,b}}$ remains small. They break down when ω becomes exponentially small in $\frac{1}{\nu}$,

$$\omega \sim \Lambda_{\rm CO}, \quad \Lambda_{\rm CO} \sim \mu_* e^{-\frac{1}{\sqrt{u}}} . \tag{8.24}$$

In the regime of (8.24), the susceptibility (8.20) crosses over to

$$\chi(\omega\to 0,\vec{k}) = \chi_0 - 2\nu_k\chi_* - 4\nu_k\chi_*\left(\frac{-i\omega}{2\mu_*}\right)^{2\nu_k}+\cdots \tag{8.25}$$

which is the low energy behavior (4.29) for the uncondensed phase and is also consistent with (8.6). As always, there are perturbative corrections in ω that we have not included.

8.3 Zero temperature: from the condensed side

When $u<0$, the IR scaling dimension of $\mathcal{O}_{\vec{k}}$ becomes complex for sufficiently small k as $\nu_k = \sqrt{u+\frac{k^2}{6\mu_*^2}} = -i\lambda_k$ is now pure imaginary.[3] For a given nonzero ω and $|u|$ sufficiently small, as discussed after (8.18) the corresponding expression for $\chi(k,\omega)$ can be obtained from (8.20) by simply taking u to be negative, after which we find

$$\chi(\omega,\vec{k}) = \chi_0\frac{\sin\left(\lambda_k\log\left(\frac{-i\omega}{\omega_b}\right)\right)}{\sin\left(\lambda_k\log\left(\frac{-i\omega}{\omega_a}\right)\right)}+\cdots . \tag{8.26}$$

While (8.20) is valid to arbitrarily small ω, equation (8.26) has poles in the *upper* half frequency plane (for $k=0$) at[4]

$$\omega_n = i\omega_a\exp\left(-\frac{n\pi}{\sqrt{-u}}\right) \equiv i\Lambda_n,, \qquad n=1,2\cdots \tag{8.27}$$

[3]Note that the choice of the branch of the square root does not matter as (8.20) is a function of ν_k^2.

[4]Note that (8.26) also have poles for non-positive integer n. But at these values ω is either of order or much larger than the chemical potential μ to which our analysis do not apply.

with

$$\Lambda_n \sim \mu \exp\left(-\frac{n\pi}{\sqrt{-u}}\right) . \tag{8.28}$$

In particular, we expect (8.26) to break down for $\omega \sim \Lambda_1$, the largest among (8.28), and at which scale the physics of condensate should set in. This is indeed consistent with an earlier analysis of classical gravity solutions in [21, 127] where it was found that $\mathcal{O}$ develops an expectation value of order

$$\frac{\langle \mathcal{O} \rangle}{\mu^\Delta} \sim \left(\frac{\Lambda_1}{\mu}\right)^{\frac{1}{2}} . \tag{8.29}$$

The exponent $\frac{1}{2}$ in (8.29) is the scaling dimension of $\mathcal{O}$ in the eCFT$_1$ for $u = 0$, while Δ is its scaling dimension in the vacuum. It was also found in [21, 127] there are an infinite number of excited condensed states with a dynamically generated scale given by Λ_n and $\langle \mathcal{O} \rangle \sim \Lambda_n^{\frac{1}{2}}$, respectively. Thus the pole series in (8.27) in fact signals a geometric series of condensed states. This tower of condensed states with geometrically spaced expectation values is reminiscent of Efimov states [154]. The largest expectation value is for the first state $n = 1$, which is in fact the energetically favored vacuum. We now perform a detailed calculation to determine the full nonlinear response curve near the critical point. The reader who is only interested in the final result may skip to (8.43).

8.3.1 Construction of nonlinear bulk solution

As discussed in [21, 127], for the lowest $n = 1$ state there is a new exponentially generated scale

$$\Lambda_{IR} \sim \mu \exp\left(-\frac{\pi}{\sqrt{-u}}\right) \tag{8.30}$$

and when the AdS_2 radial coordinate ζ satisfies $\Lambda_{IR}\zeta \gg 1$ (i.e. deep in the AdS_2 region), ϕ becomes of order $O(1)$. Thus at zero temperature, no matter how close one is to the critical point and even though the vacuum expectation value of the condensed operator is very small near the critical point, the nonlinear dynamics of ϕ and the backreaction to the bulk geometry will be needed deep in the AdS_2 region. Nevertheless, we will find that a great deal of information can be obtained even without detailed analysis of the nonlinear equations and backreaction. For illustration purpose, as in [21] we will consider an action for ϕ of the form

$$\mathcal{L}_\phi = \frac{1}{\lambda}\left[-\frac{1}{2}(\partial\phi)^2 - V(\phi)\right] \tag{8.31}$$

where g is a coupling constant. The precise form of the potential $V(\phi)$ is not important for our discussion below except that $V(0) = 0$, $V''(0) = m^2$ and it has a minimum at some $\phi_0 \neq 0$. To be close to $u = 0$ critical point on the condensed side, we will thus take m^2 to be slightly below the critical value and so $u = (m^2 - m_c^2)R_2^2 < 0$.

We will now proceed to compute the response of the system to a static, uniform external source. Thus we consider equation of motion following from (8.31) with ϕ depending on radial coordinate only. The analysis is a slight generalization of that in [126, 127, 21]. To describe the behavior of the bulk solution describing a condensed phase, we separate the spacetime into three regions:

1. IR region I: $\zeta > \Lambda_{IR}^{-1}$. Here the nonlinear effect of the scalar potential is important and the value of ϕ is of O(1). We note that the boundary condition at the horizon is given by
$$\phi(\zeta \to \infty) = \phi_0 \tag{8.32}$$
where ϕ_0 is the minimum of the potential $V(\phi)$. Thus as $\zeta \to \infty$, the spacetime metric approaches $\widetilde{AdS}_2 \times \mathbb{R}^2$ where $\widetilde{AdS}_2$ has a different curvature radius from the near-horizon AdS_2 region of the condensed phase,
$$\frac{1}{\tilde{R}_2^2} = \frac{1}{R_2^2} - \frac{V(\phi_0)}{g} . \tag{8.33}$$

2. IR region II: AdS_2 region with $\zeta < \Lambda_{IR}^{-1}$ (but still $\mu\zeta \gg 1$ so that the AdS_2 scaling is appropriate). In this region the value of ϕ is small, and we can treat it linearly and neglect its backreaction on the geometry. Here ϕ has a well-defined but complex conformal dimension in $eCFT_1$ dual to the original AdS_2 (with $k = 0$) :
$$\delta_\pm = \frac{1}{2} \pm i\sqrt{-u}, \qquad -u \ll 1 \tag{8.34}$$
and general solution to linearized equation can be written as $a\zeta^{\delta_+} + b\zeta^{\delta_-}$.

3. UV region: the rest of the black hole spacetime. Again in this region linear analysis suffices.

Note that the IR region II is not guaranteed to exist *a priori*, but will be justified by the results, i.e. (8.30) (right now Λ_{IR} should be considered just as a parameter we introduce to distinguish IR region I and II).

We will solve the nonlinear equation following from (8.31) starting in IR region I and moving towards the boundary of the spacetime. Note that the horizon boundary condition (8.32) fixes one of the integration constants in the second-order equation for ϕ. As we move outwards, the scalar becomes smaller and smaller until around $\zeta \sim \Lambda_{IR}^{-1}$, where we can neglect its backreaction on the geometry and treat it linearly. Note that the solution to the nonlinear equation in IR region I should be insensitive to the precise value of m^2 (which is the mass square near $\phi = 0$) and thus when $|u| \ll 1$, we could set u to 0 in solving it. This implies that, near Λ_{IR}^{-1}, it should be a good approximation to solve the linearized equation (around $\phi = 0$) with $u = 0$, and

a general solution can be written as[5]

$$\phi(\zeta) = \gamma\sqrt{\frac{\zeta}{\zeta_*}}\log\frac{\zeta}{\zeta_*} + O(\sqrt{-u}) \tag{8.35}$$

where $\gamma \sim O(1)$ and $\zeta_* \sim \Lambda_{IR}^{-1}$ are integration constants.

In the limit of no backreaction (e.g. $g \to \infty$ in (8.33)), it can be readily checked that the full nonlinear problem in AdS_2 region has an AdS_2 scaling symmetry under which both the IR boundary condition (8.32) and the equations of motion are invariant. Recall that the horizon boundary condition (8.32) fixed only one of the two integration constants, leaving a one-parameter family of acceptable solutions. We conclude that in this case because of the scaling symmetry this family is parametrized by ζ_*, and the number γ must be fixed by (8.32) to be an $O(1)$ constant (as there are no small parameters in the nonlinear analysis). If we allow backreaction then these statements are no longer strictly true, in that as we traverse the remaining one-parameter family of solutions we will likely move through a nontrivial trajectory in the (γ, ζ_*) space. This should be kept in mind; however in the remainder of the analysis for simplicity we will assume that backreaction is small and so we can assume that γ is fixed by (8.32) and the remaining solutions are parametrized by ζ_*.

Now from (8.34) the most general solution to the linearized equation in IR region II can be written as

$$\phi(\zeta) = d_1\sqrt{\frac{\zeta}{\zeta_*}}\cos\left[\sqrt{-u}\log\frac{\zeta}{\zeta_*} + d_2\right] \tag{8.36}$$

where we have chosen ζ_* as a reference point and d_1, d_2 are numerical integration constants. For $\zeta \sim \zeta_*$, expanding (8.36) in $\sqrt{-u}$ and comparing with (8.35) we conclude that $d_1 \sim \frac{1}{\sqrt{-u}}$ and $d_2 = \frac{\pi}{2} + O(-u)$ and (8.36) can be written as

$$\phi(\zeta) = \frac{\gamma}{\sqrt{-u}}\sqrt{\frac{\zeta}{\zeta_*}}\sin\left(\sqrt{-u}\log\frac{\zeta}{\zeta_*}\right) . \tag{8.37}$$

It is important to emphasize that the $\sqrt{-u}\log\frac{\zeta}{\zeta_*}$ term may not be small, as ζ may vary over exponentially large distance in $1/\sqrt{-u}$.

Finally we now consider matching (8.37) to the solution in the UV region near $\mu\zeta \sim O(1)$ with identification $\zeta = \frac{z_*^2}{6(z_*-z)}$. This is exactly the same as the linear matching problems discussed in Chapter 4 and so we will be brief. In terms of the basis of solutions introduced in (4.20) we can write ϕ as

$$\phi(z) = \frac{\gamma}{\sqrt{-u}}\sqrt{\frac{z_*}{\zeta_*}}\frac{1}{2i}\left(e^{-i\sqrt{-u}\log\frac{\zeta_*}{z_*}}\eta_+^{(0)} - e^{i\sqrt{-u}\log\frac{\zeta_*}{z_*}}\eta_-^{(0)}\right) . \tag{8.38}$$

[5]Note at $u = 0$, the two exponents in (8.34) become degenerate and the independent solutions to the linear equation become $\zeta^{\frac{1}{2}}$ and $\zeta^{\frac{1}{2}}\log\zeta$ respectively.

Using the expansion (4.20) and the following definitions and properties of $a_\pm, b_\pm$:

$$a_+ = |a_+|e^{i\theta_a}, \qquad b_+ = |b_+|e^{i\theta_b}, \qquad a_- = a_+^*, \qquad b_- = b_+^* \tag{8.39}$$

we then conclude that the coefficients A and B are given by

$$\begin{aligned} A &= -z_*^{3-\Delta}\frac{\gamma}{\sqrt{-u}}|a_+|\sqrt{\frac{z_*}{\zeta_*}}\sin\left(\sqrt{-u}\log\frac{\zeta_*}{z_*} - \theta_a\right), \\ B &= -z_*^{-\Delta}\frac{\gamma}{\sqrt{-u}}|b_+|\sqrt{\frac{z_*}{\zeta_*}}\sin\left(\sqrt{-u}\log\frac{\zeta_*}{z_*} - \theta_b\right). \end{aligned} \tag{8.40}$$

Recall that ζ_* parametrizes movement through the solution space; as we vary ζ_*, we see that we trace out a *spiral* in the (A, B) plane, the implications of which are discussed below. See fig. 8-2. Note that no matter how small we consider A or B to be, the curve continues to spiral and nonlinear dynamics remains important–this is because the scalar in the deep interior is always of $O(1)$.

For the case of the double-well potential:

$$V(\phi) = \frac{1}{4R^2}\left(\phi^2 + m^2R^2\right)^2 - \frac{m^4R^2}{4}. \tag{8.41}$$

there is a $\phi \to -\phi$ symmetry which results in the symmetry $A,\ B \to -A,\ -B$ of fig. 8-2. For this potential in the limit of no backreaction we find $\gamma = 0.6$.

8.3.2 Efimov spiral

We now briefly discuss the physics of the structure constructed above; if we now take $\sqrt{-u} \to 0$ in the solution constructed above, we find

$$|a_+| = \alpha, \qquad |b_+| = \beta, \qquad \theta_a = -\sqrt{-u}\frac{\tilde{\alpha}}{\alpha}, \qquad \theta_b = -\sqrt{-u}\frac{\tilde{\beta}}{\beta} \tag{8.42}$$

giving us the nonlinear response curves

$$\begin{aligned} A &= z_*^{3-\Delta}\frac{\gamma}{\sqrt{-u}}\alpha\sqrt{\frac{z_*}{\zeta_*}}\sin\left(\sqrt{-u}\log\frac{\zeta_*}{z_*} + \sqrt{-u}\frac{\tilde{\alpha}}{\alpha}\right), \\ B &= z_*^{-\Delta}\frac{\gamma}{\sqrt{-u}}\beta\sqrt{\frac{z_*}{\zeta_*}}\sin\left(\sqrt{-u}\log\frac{\zeta_*}{z_*} + \sqrt{-u}\frac{\tilde{\beta}}{\beta}\right). \end{aligned} \tag{8.43}$$

where A and B denote the source and expectation value for $\mathcal{O}$ respectively, where γ is a $O(1)$ constant that is determined by nonlinear dynamics. ζ_*^{-1} is a dynamical energy scale which parametrizes movement through the solution space; as we vary ζ_*, we trace out a *spiral* in the (A, B) plane. See fig. 8-2. Since we are considering a system with a Z_2 symmetry $\mathcal{O} \to -\mathcal{O}$, in fig. 8-2 there is also a mirror spiral obtained from (8.43) by taking $(A, B) \to -(A, B)$.

The tower of "Efimov" states is obtained by setting the source $A = 0$, which leads

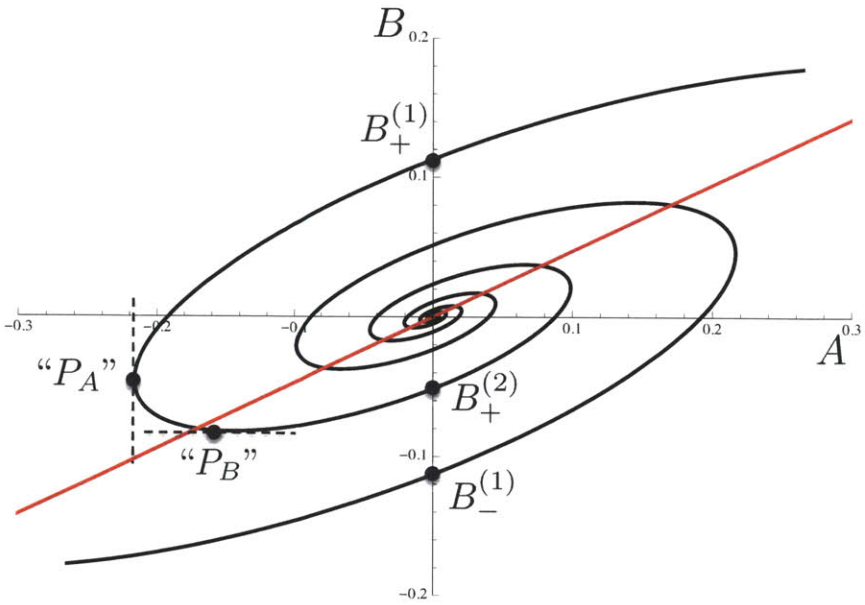

Figure 8-2: The Efimov spiral indicated above. The normalizable solutions in the standard quantization are given by the intersections of the spiral with respect to the B-axis, with $B_\pm^{(1)}$ the ground states and $B_\pm^{(2)}$ the first excited states, etc. Similarly those for alternative quantization are given by intersections with the A-axis. The red line indicates the linear susceptibility on the uncondensed side. For ease of representation a nonlinear mapping has been performed along the the major and minor axes of the spiral; while the zeros of A and B are preserved by this mapping the location of divergences and zeros of $\frac{dB}{dA}$ are *not* (hence the quotation marks in the location of "P_A" and "P_B", which are only for illustrative purposes).

to

$$\zeta_* = \zeta_n \equiv z_* e^{\frac{n\pi}{\sqrt{-u}} - \frac{\tilde{\alpha}}{\alpha}}, \qquad n = 1, 2, \cdots \tag{8.44}$$

which when plugged into the expression for B in (8.43) gives

$$\langle \mathcal{O} \rangle \propto |B| = \mu_*^\Delta \frac{\gamma}{2\nu_U \alpha} e^{-\frac{n\pi}{2\sqrt{-u}} + \frac{\tilde{\alpha}}{2\alpha}} \sim \mu_*^\Delta \exp\left(-n \frac{\pi}{2\sqrt{-u}}\right) \tag{8.45}$$

where we have used (8.81). These are the values at which the spiral intersects with the vertical axis, with that for the $n = 1$ state corresponding to the outermost intersection. Note that $\zeta_n \sim \Lambda_n^{-1}$ and equation (8.45) is consistent with the discussion below (8.29).

As $\sqrt{-u} \to 0$, from (8.43), A and B are becoming in phase, and the spiral is being squeezed into a straight line, with limiting slope

$$\left.\frac{B}{A}\right|_{\sqrt{-u}\to 0} = \mu_*^{2\Delta - 3} \frac{\beta}{\alpha} = \chi_0 \ . \tag{8.46}$$

This slope agrees with the value found from linear response approaching the critical point from the other side (8.8). This is however *not* the relevant slope for the susceptibility, which should be given by

$$\chi_L = \left.\frac{dB}{dA}\right|_{A=0} \tag{8.47}$$

which in the usual models of spontaneous symmetry breaking, corresponds to the longitudinal susceptibility. From (8.43) we find

$$\chi_L = \mu_*^{2\nu_U}\frac{\beta}{\alpha}\left(1+\frac{\tilde{\alpha}\beta-\alpha\tilde{\beta}}{2\alpha\beta}\right)+\mathcal{O}(u) = \chi_0+\chi_*+\mathcal{O}(u) \tag{8.48}$$

where we have used (8.81) and (8.10). Essentially, even though the spiral is squished into a straight line as we approach the transition, each *intersection* of the spiral with the $A=0$ axis has a different slope than the limiting slope of the entire spiral. Note that this result is independent of n and in particular applies to $n=1$, the ground state. Since χ_0 is the value at $u=0$ from the uncondensed side, we thus find a jump in the value of the uniform susceptibility in crossing $u=0$. The difference has precisely the same coefficient as the divergent terms in (8.9), and also appears elsewhere such as (8.23).

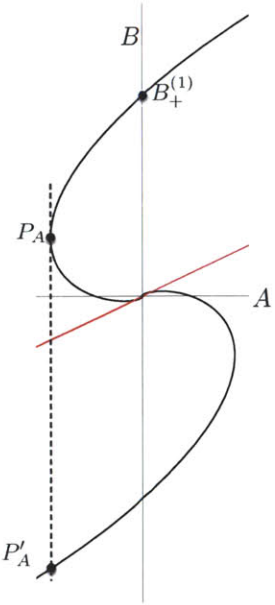

Figure 8-3: A zoomed in version of Figure 8-2, where there has been no nonlinear mapping and so the location of P_A is faithfully reproduced. As described in the text, at P_A the system becomes locally unstable and relaxes to P'_A. Appearances to the contrary, the spiral continues to wind around infinitely many times as it approaches the origin, a fact that is difficult to see without the nonlinear mapping.

We now elaborate a bit more on the interpretation of various parts of the spirals in Fig. 8-2. Let us start with the ground state[6] $B_+^{(1)}$, and first follow the spiral to the right, i.e. we apply an external source A in the *same* direction as the condensate. This will increase B according to (8.47) and (8.48). Note that near the critical point $B_+^{(1)}$ is exponentially small; thus as we increase A further, we will eventually reach a regime where the forced response is much larger than the condensate $B \gg B_+^{(1)}$ but is still much smaller than 1, $B \ll 1$. One thus expects that here the system should not care about the (exponentially small) condensate and the response should simply be given by that of the uncondensed state, i.e. the linear response line given by χ_0. Thus the spiral will approach a straight line parallel to the red straight line in the figure.

Now consider applying A in the opposite direction to the condensate. As the Z_2 symmetry was *spontaneously* broken, we now expect that $B_-^{(1)}$ should be the global minimum and $B_+^{(1)}$ should be only locally stable. Nevertheless, we can choose to stay in the "super-cooled" state given by $B_+^{(1)}$ and stay on the response curve given by following the spiral at $B_+^{(1)}$ to the left, where now the source acts to *reduce* B. The response curve in the region between $B_+^{(1)}$ and P_A is nonlinear as the effect of the condensate is important. At P_A the susceptibility $\frac{dB}{dA} \to +\infty$. At P_A the state that we are on becomes genuinely (i.e. even *locally*) unstable and if we continue to increase $|A|$, then the system will relax to the point P'_A, as shown in Figure 8-3. on the other branch of the spiral starting from $B_-^{(1)}$. Note that

$$\frac{B(P_A)}{B_+^{(1)}} \sim O(1) \tag{8.49}$$

where by $O(1)$ we mean that the ratio is independent of the small parameter $\sqrt{-u}$.

To complete the story let us now consider starting from the first excited state $B_+^{(2)}$ and again apply the external source along the direction of the condensate, which now corresponds to following the spiral to the left. Near $B_+^{(2)}$, the response is again controlled by (8.48), but again when $1 \gg |B| \gg |B_+^{(2)}|$, the system will forget that it is in a condensed state and the response will again be controlled by χ_0. The response curve will once again be parallel to the linear response line until we reach the region near P_B, where the response has now become exponentially large compared with the value at $B_+^{(2)}$, i.e. it is now comparable to the value of $|B_+^{(1)}|$:

$$\frac{|B(P_B)|}{B_+^{(1)}} \sim O(1), \quad \left|\frac{B(P_B)}{B_+^{(2)}}\right| \sim O\left(e^{\frac{\pi}{\sqrt{-u}}}\right) . \tag{8.50}$$

Near P_B the nonlinear effects due to the condensate again become important. In the region between P_A and P_B the susceptibility has the wrong sign and thus the system becomes locally thermodynamically unstable. It seems likely that if the source A is increased in an attempt to probe this region the system will instead move to a

[6]Equivalently we can also start with its Z_2 image $B_-^{(1)}$.

corresponding point P_B' on the other branch of the spiral. Also note that even though $B_+^{(2)}$ is an excited state and so not a global minimum of the free energy, it does appear to be locally thermodynamically stable.

The discussion above also gives a physical explanation as to why as $u \to 0_-$ the whole spiral is squished into a straight line with slope given by (8.8): the vast majority of the spiral (e.g. the exponentially large region between $B_+^{(2)}$ and P_B) must become parallel to such a straight line.

The existence of a tower of "Efimov" states with geometrically spaced expectation values may be considered a consequence of spontaneous breaking of the discrete scaling symmetry of the system. With an imaginary scaling exponent, (8.26) exhibits a discrete scaling symmetry with (for $k = 0$)

$$\omega \to e^{\frac{2\pi}{\sqrt{-u}}}\omega \tag{8.51}$$

which is, however, broken by the condensate.[7] The tower of "Efimov" states may then be considered the "Goldstone orbit" for this broken discrete symmetry.

We would also like to point out that $\partial_u \chi_L$ and $\partial_{k^2}\chi_L$ do not diverge at the critical point, unlike the case from the uncondensed side. Hence we do not get a cusp approaching the critical point from the condensed side. This is due to the fact that the small u corrections to (8.48) are all analytic, which can be checked by explicit calculation to the next nontrivial order.

8.3.3 Free energy across the quantum phase transition

The fact the order parameter (8.45) is continuous (to an infinite number of derivatives) across the transition implies that the free energy is also continuous (to an infinite number of derivatives). We outline the arguments here. The free energy is simply the (appropriately renormalized) Euclidean action of the scalar field configuration. We can divide the radial integral into two parts, the UV part and the IR AdS_2 part. It is clear that the contribution from the UV portion of the geometry will scale like $\phi^2 \sim \langle \mathcal{O} \rangle^2 \sim \exp\left[-\frac{\pi}{\sqrt{-u}}\right]$, since the scalar is small there and so a quadratic approximation to the action is sufficient.

To make a crude estimate of the IR contribution, where $\phi \sim O(1)$ and so nonlinearities in the scalar potential are important, let us ignore backreaction and imagine that in the IR the scalar is simply a domain wall: for $\zeta > \Lambda_{IR}^{-1}$ it sits at the bottom of its potential $\phi(\zeta) = \phi_0$ and that for $\zeta < \Lambda_{IR}^{-1}$ it is simply 0. Then we find for the Euclidean action[8] an expression of the form

$$S_E \sim V(\phi_0) \int_{\infty}^{\Lambda_{IR}^{-1}} d\zeta \sqrt{g} \sim \Lambda_{IR} \tag{8.52}$$

[7]Note that for the $n = 1$ state, since the physics of the condensate sets in already at Λ_1, the range of validity for (8.26) is not wide enough for the discrete scaling symmetry to be manifest.

[8]As we are at zero temperature the Euclidean time is not a compact direction, and so all expressions for the Euclidean action contain a factor extensive in time that we are not explicitly writing out.

which again scales as $S_E \sim \Lambda_{IR} \sim \exp\left[-\frac{\pi}{\sqrt{-u}}\right]$. Note what has happened: even though the scalar is of $O(1)$ in the deep IR and so contributes to the potential in a large way, the infinite redshift deep in the AdS_2 horizon suppresses this contribution to the free energy, making it comparable to the UV part. A more careful calculation also reveals that the free energy is indeed negative compared to the uncondensed state. We thus conclude that

$$F \sim -\exp\left[-\frac{\pi}{\sqrt{-u}}\right] \tag{8.53}$$

and that the free energy is also continuous across the transition to an infinite number of derivatives, reminiscent of a transition of the Berezinskii-Kosterlitz-Thouless type.

8.4 Thermal aspects

We now look at the critical behavior near the bifurcating critical point at a finite temperature. Our starting point is the expression for the finite-temperature susceptibility, which we reproduce below for convenience:

$$\chi(\omega,\vec{k},T) = \frac{b_+(k,\omega,T) + b_-(k,\omega,T)\mathcal{G}_k^{(T)}(\omega)\mu_*^{-2\nu_k}}{a_+(k,\omega,T) + a_-(k,\omega,T)\mathcal{G}_k^{(T)}(\omega)\mu_*^{-2\nu_k}}, \tag{8.54}$$

The finite temperature behavior mirrors the finite frequency behavior of last subsection. We simply repeat the analysis leading to (8.20), starting with (8.54) rather than (8.3); somewhat predictably, at $\omega = 0$ but finite T we find

$$\chi^{(T)}(\vec{k}) = \chi_0 \frac{\sinh\left(\nu_k \log\left(\frac{T}{T_b}\right)\right)}{\sinh\left(\nu_k \log\left(\frac{T}{T_a}\right)\right)}, \tag{8.55}$$

where $T_{a,b}$ differ from $\omega_{a,b}$ by factors,

$$T_a = \frac{4\mu_*}{\pi} e^{\frac{\tilde{\alpha}}{\alpha}}, \qquad T_b = \frac{4\mu_*}{\pi} e^{\frac{\tilde{\beta}}{\beta}} . \tag{8.56}$$

Similarly to (8.26), the expression for $u < 0$ is obtained by analytically continuing (8.55) to obtain

$$\chi^{(T)}(\vec{k}) = \chi_0 \frac{\sin\left(\lambda_k \log\left(\frac{T}{T_b}\right)\right)}{\sin\left(\lambda_k \log\left(\frac{T}{T_a}\right)\right)} . \tag{8.57}$$

And again both (8.55) and (8.57) are analytic at $u = 0$ and reduce to the same function there

$$\chi^{(T)}(\vec{k}) = \chi_0 \frac{\log\frac{T}{T_b}}{\log\frac{T}{T_a}} + O(u,k^2) . \tag{8.58}$$

Similar to (8.22), the pole in (8.58) and (8.55) at $T = T_a$ should not concern us as this expression is supposed to be valid only for $T \ll \mu_* \sim T_a$. For nonzero ω, (8.55) generalizes to

$$\chi^{(T)}(\omega, k) = \chi_0 \frac{\sinh\left(\nu_k \left[\log\left(\frac{2\pi T}{\omega_b}\right) + \psi\left(\frac{1}{2} - i\frac{\omega}{2\pi T}\right)\right]\right)}{\sinh\left(\nu_k \left[\log\left(\frac{2\pi T}{\omega_a}\right) + \psi\left(\frac{1}{2} - i\frac{\omega}{2\pi T}\right)\right]\right)} \tag{8.59}$$

It is easy to check using the identities $\psi(\frac{1}{2}) = -\gamma_E - \log 4$ and $\psi(x \to \infty) \to \log x$ that this expression has the correct limiting behavior to interpolate between (8.55) and (8.20).

For $u > 0$, at a scale of

$$T \sim \Lambda_{\text{CO}} \sim \mu_* e^{-\frac{1}{\sqrt{u}}} \tag{8.60}$$

eq. (8.55) crosses over to an expression almost identical to (8.25) with ω replaced by T. For $u < 0$, at such small temperature scales equation (8.57) has poles at (for $k = 0$)

$$T_n = T_a \exp\left(-\frac{n\pi}{\sqrt{-u}}\right) = \frac{4\mu_*}{\pi} \exp\left(-\frac{n\pi}{\sqrt{-u}} + \frac{\tilde{\alpha}}{\alpha}\right), \qquad n \in \mathbb{Z}^+ . \tag{8.61}$$

Comparing to (8.28) and (8.44), we see that $T_n \sim \Lambda_n \sim 1/\zeta_n$. The first of these temperatures should be interpreted as the critical temperature

$$T_c = \frac{4\mu_*}{\pi} \exp\left(-\frac{\pi}{\sqrt{-u}} + \frac{\tilde{\alpha}}{\alpha}\right) \tag{8.62}$$

below which the scalar operator condenses. Including frequency dependence, one can check that $\chi^{(T)}(\omega, \vec{k})$ has a pole at

$$\omega_* = -\frac{2i}{\pi}(T - T_n) \tag{8.63}$$

For $T > T_n$ this pole is in the lower half-plane, and it moves through to the upper half-plane if T is decreased through T_n. Thus we see the interpretation of each of these T_n; as the temperature is decreased through each of them, one more pole moves through to the upper half-plane. There exist an infinite number of such temperatures with an accumulation point at $T = 0$; and indeed at strictly zero temperature there is an infinite number of poles in the upper half-plane, as seen earlier in (8.26). Of course in practice once the first pole moves through to the upper half-plane at $T_c = T_1$, the uncondensed phase is unstable and we should study the system in its condensed phase.

One can further study the critical behavior near the finite temperature critical point T_c. Here one finds mean field behavior and we will only give results. See

Appendix 8.B for details. For example the uniform static susceptibility has the form

$$\chi^{(T)} \approx \begin{cases} \frac{\chi_0}{2\nu_U \alpha\beta} \frac{T_c}{T-T_c} & T \to T_c^+ \\ \frac{\chi_0}{4\nu_U \alpha\beta} \frac{T_c}{T_c-T} & T \to T_c^- \end{cases} \tag{8.64}$$

The result that $\chi(T_c^-)$ has a prefactor twice as big as $\chi(T_c^+)$ is a general result of Landau theory.

Similarly, the correlation length near T_c is given by

$$\xi^{-2} = \frac{6\mu_*^2(-u)^{\frac{3}{2}}}{\pi T_c}(T - T_c) \ . \tag{8.65}$$

Note that the prefactor of $T - T_c$ diverges exponentially as $u \to 0$, and should be contrasted with the behavior (8.14) at the quantum critical point. Finally we note that at the critical point $T = T_c$, we find a diffusion pole in $\chi^{(T)}(\omega, \vec{k})$ given by

$$\omega_* = -i\frac{T_c}{3\mu_*^2(-u)^{\frac{3}{2}}}k^2 \tag{8.66}$$

which is of the standard form for this class of dynamic critical phenomena (due to the absence of conservation laws for the order parameter, this is Model A in the classification of [138]; see also [139] for further discussion in the holographic context). Note that the diffusion constant goes to zero exponentially as the quantum critical point is approached.

In Fig. 8-4 we summarize the finite temperature phase diagram.

8.5 Summary: the nature of a bifurcating critical point

In this chapter we studied the physics close to a "bifurcating" quantum critical point, i.e. the quantum critical point obtained by tuning the AdS_2 mass of the bulk scalar field through its Breitenlohner-Freedman bound. The results obtained were quite novel, and in this conclusion we attempt to interpret them.

Much of the physics can be understood from the expression for the dynamic susceptibility at zero temperature (8.20),

$$\chi(\omega, \vec{k}) = \chi_0 \frac{\sinh\left(\nu_k \log\left(\frac{-i\omega}{\omega_b}\right)\right)}{\sinh\left(\nu_k \log\left(\frac{-i\omega}{\omega_a}\right)\right)} + \cdots \tag{8.67}$$

where $\nu_k = \sqrt{u + \frac{k^2}{6\mu_*^2}}$ and $u = 0$ is the location of the quantum critical point. Note

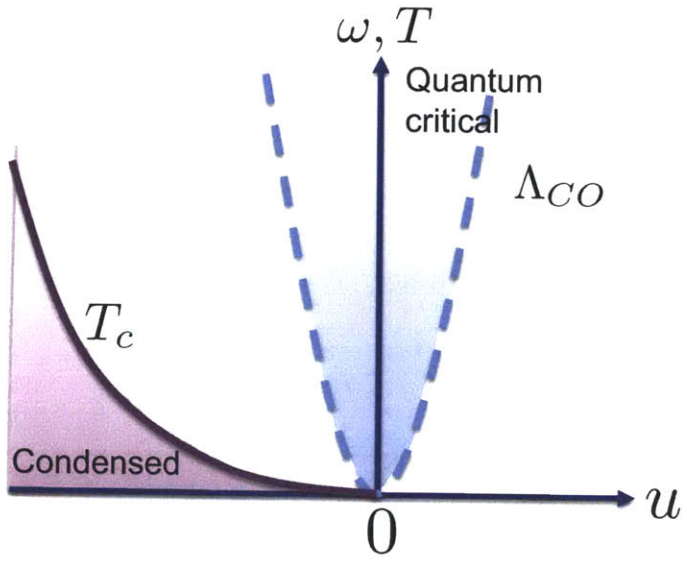

Figure 8-4: Finite temperature phase diagram with the quantum critical region for bifurcating criticality as a function of u. $\Lambda_{\rm CO}$ denotes a crossover scale, but note that it is unknown up to an overall *power*, as in (8.68). The quantum critical region is bowl-shaped, unlike the usual funnel-like shape.

that this expression actually defines a crossover scale as in (8.24)

$$\Lambda_{CO} \sim \mu_* \exp\left(-\frac{\#}{\nu_k}\right), \tag{8.68}$$

where the expression is actually not sensitive to the precise # appearing in the exponent. If we study frequencies ω such that $\omega \gg \Lambda_{CO}$, then it is safe to expand the arguments of the hyperbolic to obtain the universal and scale-free form (8.22) for the dynamic susceptibility,

$$\chi(\omega, \vec{k}) = \chi_0 \frac{\log\left(\frac{\omega}{\omega_b}\right) - i\frac{\pi}{2}}{\log\left(\frac{\omega}{\omega_a}\right) - i\frac{\pi}{2}} + O(u, k^2) \tag{8.69}$$

This expression should be viewed as the susceptibility defined by the quantum critical theory. It applies in a bowl-shaped quantum critical region in Figure 8-4. There is a finite temperature generalization of this formula found by taking $\nu_k \to 0$ in (8.59), which can now be applied all the way down to zero frequency provided that the

temperature $T \gg \Lambda_{CO}$,

$$\chi^{(T)}(\omega, \vec{k}) = \chi_0 \frac{\log\left(\frac{2\pi T}{\omega_b}\right) + \psi\left(\frac{1}{2} - i\frac{\omega}{2\pi T}\right)}{\log\left(\frac{2\pi T}{\omega_a}\right) + \psi\left(\frac{1}{2} - i\frac{\omega}{2\pi T}\right)} \,. \tag{8.70}$$

Note that we find interesting non-analytic behavior only in ω, and not in k; this behavior is called "local quantum criticality" in the condensed matter literature and is thought to lie behind a theoretical description of the phase transitions of various heavy fermion compounds (e.g. [85, 86] and references therein). In our description this arises from the fact that the AdS_2 that is at the heart of the non-analytic behavior has nontrivial scaling isometries only in time and not in the field theory spatial directions.

If we are outside the quantum-critical region, the susceptibility takes rather a different form, which is essentially the $\omega \to 0$ limit of (8.67),

$$\chi(k) = \chi_0 \left(\frac{1 + \nu_k \frac{\tilde{\beta}}{\beta}}{1 + \nu_k \frac{\tilde{\alpha}}{\alpha}}\right) \tag{8.71}$$

This should be viewed as the static susceptibility. The $u \to 0$ limit of this expression demonstrates rather different behavior, corresponding to approaching the critical point from outside the bowl in Figure 8-4.

Interestingly, the susceptibility does *not* diverge approaching the critical point. However, even if the susceptibility has no gapless poles in k it does contain branch cut singularities in the k plane that approach the origin as $u \to 0$. Upon Fourier transformation to coordinate space, these singularities lead to a correlation length that diverges at the critical point,

$$\xi = \frac{1}{\sqrt{6}\mu_* \sqrt{u}} \tag{8.72}$$

This appears to be a standard mean-field divergence, but the overall coordinate-space expression is suppressed by extra powers of x relative to the mean-field expression, as shown in (8.13). Similarly, precisely *at* the critical point, we find yet extra suppression, leading to a power law-falloff $G(x) \sim x^{-3}$.

Finally, if we set $k \to 0$ we see that the susceptibility develops a branch cut singularity at $u = 0$, as $\nu_{k=0} = \sqrt{u}$; it is trying to bifurcate into the complex plane as we cross $u = 0$. Indeed, for $u < 0$ from the bulk point of view we have violated the AdS_2 BF bound; from the IR CFT point of view, the two conformal fixed points corresponding to alternative and standard quantization have merged and annihilated. Conformality is lost [126], the scalar condenses, and a new scale should be generated,

$$\Lambda_{IR} = \mu_* \exp\left(-\frac{\pi}{\sqrt{-u}}\right) \tag{8.73}$$

This is the analog of the crossover scale on the uncondensed side, but on this side of the quantum critical point this scale determines precise observables (such as the

critical temperature and the scalar vev) and so we can determine the precise prefactor in the exponent. We note that the existence of this scale was already evident from the original expression (8.67); if we take $u < 0$ in that expression the hyperbolic sine is replaced by a normal sine and we see a geometric series of poles in the upper-half-plane at

$$\omega_n = i\omega_a \exp\left(-\frac{n\pi}{\sqrt{-u}}\right), \tag{8.74}$$

the $n = 1$ case of which is the scale described above. These are at exponentially small energies and so are not visible in the quantum critical expression (8.69). At the $O(1)$ temperatures assumed in (8.70) we are above T_c and so the poles are all in the lower-half plane.

The existence of these poles in the upper-half plane indicates that the $\phi = 0$ state is unstable and the true vacuum has a condensed scalar. A study of the full nonlinear response curve indicates a remarkable spiral structure, shown in Figure 8-2, that is a manifestation of the fact that even though continuous conformality has been lost a discrete subgroup of the scale transformations survives. We thus find an infinite tower of excited "Efimov" states with geometrically spaced expectation values

$$\langle \mathcal{O} \rangle_n \sim \mu^\Delta \left(\frac{\Lambda_{IR}}{\mu}\right)^{\frac{n}{2}}, \quad n = 2, 3, \cdots . \tag{8.75}$$

A thorough examination of the nonlinear response spiral, as performed in Section 8.3.2 above helps illustrate how the thermodynamics manages to develop the nontrivial vacuua described above while still not having a divergent susceptibility at the quantum critical point.

It is fascinating to note that nowhere on the uncondensed side do we see a coherent and gapless quasiparticle pole, which usually appears close to a quantum phase transition and indicates the presence of soft order parameter fluctuations. The fact that the susceptibility (8.71) does not diverge at the critical point is clearly another manifestation of the lack of this coherent quasiparticle pole. The bifurcating transition that we study appears not to be driven by such a pole. This does not mean that there are no gapless modes close to the critical point – rather there is a great deal of *incoherent* spectral density at low frequencies arising from the IR CFT associated with the AdS_2 region. It is the collective fluctuations of this incoherent spectral density that drives the transition – as we cross through to the unstable side it appears that these soft modes coalesce to form the sharp instabilities seen in (8.74).

There are by now several holographic models [127, 128] that realize such a quantum phase transition (called "holographic BKT") from the top down, using explicit constructions that essentially allow one to tune some control knob (e.g. a magnetic field) in a field theory to tune the mass of an effective order parameter field through a Breitenlohner-Freedman bound. It thus appears that this behavior genuinely exists and is accessible in various concrete models. While our discussion was entirely holographic, it actually seems likely that such behavior should be generic to any phase transition where the critical theory is not itself a CFT with one relevant direction (as is usually the case in the Landau-Ginzburg-Wilson paradigm of phase transitions),

but rather the merger of two different CFTs (as is the case in our construction [126]). It would be very interesting to understand the physics described in this section in purely field theoretical terms, and we leave this for later work.

8.A Analytic properties of $a_\pm$, $b_\pm$

Here we discuss the properties of $a_\pm(\omega,k)$, $b_\pm(\omega,k)$ appearing in (8.3), which as discussed in Chapter 4 are obtained by solving the scalar wave equation (4.13) perturbatively in ω in the UV region. Their k-dependence comes from two sources, from dependence on ν_k via the boundary condition (4.19) and from k^2 dependence in the equation (4.13) itself. Since the geometry is smooth throughout the UV region we expect the dependence on both ν_k and k^2 to be analytic. In fact we can think of $b_\pm$ and $a_\pm$ as *functions* of ν_k; i.e. there exists a function $b(\nu_k,k^2,\omega)$, *analytic in all its arguments*, such that $b_\pm = b(\pm\nu_k,k^2,\omega)$. This is clear from the boundary condition (4.19) (and its generalization for higher orders in ω) and from the fact that there is no other dependence on ν_k from the equation of motion itself.

Let us now look at the behavior of $a_\pm^{(0)}, b_\pm^{(0)}$ in the limit of $\nu_k \to 0$ in some detail. Note that this limit should be considered as a double limit $k^2 \to 0$ and $u \to 0$. First, we note that in the limit $\nu_k \to 0$, the basis of functions introduced in (4.19) can be expanded as

$$\eta_\pm^{(0)} = \eta^{(0)}(z) \pm \nu_k \tilde{\eta}^{(0)}(z) + O(\nu_k^2) \tag{8.76}$$

which leads to

$$b_\pm^{(0)} = \beta \pm \nu_k\tilde{\beta} + (c_1k^2 + d_1u) + \cdots, \qquad a_\pm^{(0)} = \alpha \pm \nu_k\tilde{\alpha} + (c_2k^2 + d_2u)\cdots. \tag{8.77}$$

In the above equations the linear order terms directly come from the linear order term in (8.76), while the quadratic order terms also receive contributions from equation of motion itself (not just the boundary conditions) and cannot be expressed in terms of ν_k^2 alone. The important point is that the quadratic order terms are independent of the signs before ν_k and thus are the same for $a_\pm$ and $b_\pm$ repsectively. Similarly approaching $\nu_k = 0$ from the imaginary $\nu_k = -i\lambda_k$ side, we have for small λ_k,

$$b_\pm^{(0)} = \beta \mp i\lambda_k\tilde{\beta} + \cdots, \qquad a_\pm^{(0)} = \alpha \mp i\lambda_k\tilde{\alpha} + \cdots. \tag{8.78}$$

Again the quadratic order terms should be the same for $a_\pm$ and $b_\pm$.

Note also that ν_k itself becomes *non-analytic* in k^2 at $u = 0$ (see (4.17)) and as a result through formula such as (8.77) $a_\pm, b_\pm$ will also develop non-analytic behavior in k^2 at $u = 0$. This fact is important for understanding the critical behavior around the critical point $u = 0$ discussed in the main text.

We conclude this section by noting that coefficients $a_\pm, b_\pm$ are not independent. For example evaluating the Wronskian of (4.13) (for $\omega = 0$)[9] for $\eta_\pm^{(0)}$ and demanding

[9]The Wronskian of equation (4.13) is given by

$$W[\phi_1,\phi_2] = \frac{f}{z^2}(\phi_1\partial_z\phi_2 - \phi_2\partial_z\phi_1) \tag{8.79}$$

that it be equal at infinity and at the horizon, we find the elegant relation:

$$a_+^{(0)}(k)b_-^{(0)}(k) - a_-^{(0)}(k)b_+^{(0)}(k) = \frac{\nu_k}{\nu_U} \ . \tag{8.80}$$

A similar analysis on $\eta, \tilde{\eta}$ results in

$$\alpha\tilde{\beta} - \beta\tilde{\alpha} = -\frac{1}{2\nu_U} \ . \tag{8.81}$$

Interestingly, this particular combination of coefficients appears many times throughout this paper.

We conclude this section by specifying the explicit values for these constants for a neutral scalar moving on the pure Reissner-Nordstrom background; in this model by requiring $\nu_{k=0} = 0$ we fix the value of the mass to be $m^2R^2 = -\frac{3}{2}$, and thus we can (numerically) compute the coefficients once and for all to be:

$$\alpha = 0.528 \qquad \tilde{\alpha} = 0.965 \tag{8.82}$$

$$\beta = 0.251 \qquad \tilde{\beta} = -0.640 \ . \tag{8.83}$$

One can check that to within numerical error these values satisfy (8.81) with $\nu_U = \frac{\sqrt{3}}{2}$.

In this Appendix we give the gravity analysis of the critical behavior near the bifurcating quantum critical point approaching from the condensed side, i.e. $u < 0$.

8.B Finite-temperature line near bifurcating critical point

The bifurcating quantum phase transition is the endpoint of a line of finite-temperature phase transitions. In this section we present some calculations near this line. As argued earlier this is a rather standard mean-field second-order transition, so we do not present much detail. One novel feature is that close to the quantum critical point then we are at exponentially small temperatures and so we have a great deal of analytic control over the calculations, allowing us to verify explicitly many of the features expected of such a transition.

8.B.1 Dynamic critical phenomena near finite-T transition

We first turn on a finite ω and k^2 and study the critical behavior close to the finite-temperature critical line. The leading ω behavior comes from the dependence of the IR Green's function in (8.54) on ω/T. At finite ω this IR Green's function is no longer a pure phase, and to lowest order we find

$$\mathcal{G}_k(\omega;T) = \left(\frac{\pi T}{\mu_*}\right)^{-2i\lambda_k} \frac{\Gamma(i\lambda_k)}{\Gamma(-i\lambda_k)} \frac{\Gamma\left(\frac{1}{2} - i\lambda_k\right)}{\Gamma\left(\frac{1}{2} + i\lambda_k\right)} \left(1 - \frac{\pi\omega}{2T}(\lambda_k + \mathcal{O}(\lambda_k^2))\right) \tag{8.84}$$

which is independent of z.

Recall that $u = g - g_c$ measures the distance from the critical point. The leading k^2 dependence comes from expanding λ_k in powers of k^2 close to the critical point:

$$\lambda_k = \sqrt{-u} - \frac{k^2}{6\mu_*^2\sqrt{-u}} + \mathcal{O}(k^4) \tag{8.85}$$

Note that a sufficiently large k will take us out of the imaginary ν phase and invalidate this expansion; while this could presumably be dealt with, it would complicate the analysis, and thus throughout we will simply assume that k^2 is parametrically small: $k^2 \ll (g_c - g)$. In this regime the UV contributions to the k^2 dependence can be ignored, as they will be higher order in $(g_c - g)$.

We now insert these expansions into (8.54). The denominator of the Green's function then takes the form

$$G_R(\omega, k; T)^{-1} \sim \sin\left(\log\left(\frac{T}{T_a}\right)\left(\lambda_0 + \frac{d\lambda}{dk^2}k^2\right)\right) - i\frac{\omega\lambda_0\pi}{2T}e^{-i\lambda_0\log\left(\frac{T}{T_a}\right)} \tag{8.86}$$

We now further expand the *temperature* in the vicinity of the n-th "Efimov temperature" T_n, defined in (8.61). We now find

$$(-1)^n G_R(\omega, k; T)^{-1} \sim \frac{\lambda_0(T - T_c^{(n)})}{T_c^{(n)}} + \frac{n\pi}{6\mu_*^2\lambda_0^2}k^2 - i\frac{\omega\pi\lambda_0}{2T_c^{(n)}} \tag{8.87}$$

Let us now study this expression, first setting $k \to 0$; we find then that the Green's function has a pole at

$$\omega_* = -\frac{2i}{\pi}(T - T_n) \tag{8.88}$$

For $T > T_n$ this pole is in the lower half-plane, and it moves through to the upper half-plane if T is decreased through T_n. Thus we see the interpretation of each of these Efimov temperatures; as the temperature is decreased through each Efimov temperature, one more pole moves through to the upper half-plane. There exist an infinite number of Efimov temperatures with an accumulation point at $T = 0$; and indeed at strictly zero temperature there is an infinite number of poles in the upper half-plane, as can be seen in (8.27).

Of course in practice once the first pole moves through to the upper half-plane, the uncondensed phase is unstable and we should study the system in its condensed phase; thus we see that the true critical temperature is precisely at the first Efimov temperature, $T_c = T_1 = T_a \exp\left(-\frac{\pi}{\sqrt{-u}}\right)$.

We can also set $\omega \to 0$ and study the static correlation length; we see that near each Efimov temperature (including the critical temperature) we have a standard finite correlation length ζ with a mean-field scaling in $(T - T_c)$:

$$\zeta^{-2} = \frac{6\mu_*^2(-u)^{\frac{3}{2}}}{T_n n\pi}(T - T_n) \tag{8.89}$$

This correlation length exhibits an intriguing scaling in $-u$.

Finally, we can keep both ω and k^2 nonzero and sit at the critical point $T = T_c^{(n)}$; we then find a diffusion mode

$$\omega_* = -i\frac{n}{3\mu_*^2(-u)^{\frac{3}{2}}}k^2 \tag{8.90}$$

which is of the standard form for this class of dynamic critical phenomena (due to the absence of conservation laws for the order parameter, this is Model A in the classification of [138]; see also [139] for further discussion in the holographic context).

8.B.2 Susceptibility across the critical point

We now compute the linear susceptibility near the critical point as we approach from the uncondensed side, i.e. $T > T_c$. We already have all of the ingredients; from (8.57) we have

$$\chi^{(T)} = \chi_0 \frac{\sin\left(\lambda_0 \log\left(\frac{T}{T_b}\right)\right)}{\sin\left(\lambda_0 \log\left(\frac{T}{T_a}\right)\right)} \tag{8.91}$$

Now expanding near $T = T_c = T_a \exp\left(-\frac{\pi}{\lambda_0}\right)$ we find

$$\chi^{(T)} \approx \chi_0 \frac{T_c \log\left(\frac{T_a}{T_b}\right)}{T - T_c} = \frac{\chi_0}{2\nu_U \alpha\beta}\frac{T_c}{T - T_c}, \tag{8.92}$$

where as usual we have used (8.81).

We will now perform the analogous calculation from the *condensed* side. This will require some understanding of the nonlinear solution close to the critical point. We will use analyticity properties of nonlinear classical field configurations on black hole backgrounds; these are precisely analogous to the analyticity arguments in the Landau theory of phase transitions. Similar arguments led us in [21] to conclude that for finite temperature phase transitions we find mean field critical exponents.

First we express A, B as functions of the horizon value of the scalar field, ϕ_h. We have

$$\frac{B}{\mu_*^{-\Delta}} = b_+(T)\phi_h + b_3(T)\phi_h^3 + \ldots \tag{8.93}$$

and the corresponding expression for A:

$$\frac{A}{\mu_*^{\Delta-3}} = a_+(T)\phi_h + a_3(T)\phi_h^3 + \ldots \tag{8.94}$$

For small values of the scalar linear response must apply, and thus the a_+ and b_+ appearing above are the same as those used throughout this paper in calculating linear response functions. Now from the calculation above we know that close to the critical temperature we have $a_+(T) \sim \tilde{a}(T - T_c)$; matching to (8.92) above we see

that

$$\frac{b_+(T_c)}{\tilde{a}} = \frac{T_c}{2\nu_U \alpha^2} \tag{8.95}$$

Now we see that for $T < T_c$ we have a nontrivial zero in A (and thus a normalizable bulk solution) at

$$\phi_h = \left(\frac{\tilde{a}(T - T_c)}{a_3}\right)^{\frac{1}{2}} \equiv \phi_{norm} \tag{8.96}$$

The definition of the nonlinear susceptibility χ_L is the derivative of the vacuum expectation value (i.e. B) with the source as we approach the normalizable solution on the condensed side, i.e.

$$\chi_L = \mu_*^{2\nu_U} \left.\frac{dB}{dA}\right|_{A\to 0} = \mu_*^{2\nu_U} \left.\frac{dB}{dA}\right|_{\phi_h = \phi_{norm}} . \tag{8.97}$$

Evaluating the derivatives this works out to be

$$\chi_L = \mu_*^{2\nu_U} \left.\frac{dB}{d\phi_h}\frac{d\phi_h}{dA}\right|_{\phi_h=\phi_{norm}} = \frac{\chi_0}{4\nu_U \alpha\beta}\frac{T_c}{T_c - T} \tag{8.98}$$

Compare this to the linear susceptibility χ calculated in (8.92); we see that the leading divergence in χ_L has a a prefactor that is half that of χ. This fact is a general result of Landau theory and follows from the symmetry and analyticity arguments that allowed us to write down (8.93) and (8.94).

8.C Fourier transforms

Here we perform various Fourier transforms that are discussed earlier in the chapter.

8.C.1 Generalities

In several sections in the main text we use some contour manipulations to extract the long-distance behavior of various Fourier transforms. Here we perform those integrals[10]. The basic idea in most of these is the following; we have various expressions in momentum space that depend analytically on the IR conformal dimension ν_k:

$$\nu_k = \sqrt{m^2 R_2^2 + \frac{k^2}{6\mu_*^2} + \frac{1}{4}} \equiv \frac{1}{\sqrt{6}\mu_*}\sqrt{k_0^2 + k^2}, \tag{8.99}$$

where for convenience we define $k_0^2 = 6\mu_*^2\left(\frac{1}{4} + m^2 R_2^2\right) = 6\mu_*^2 u$. We will often need to evaluate integrals of the form

$$I(x) \equiv \int dk\ F(\nu_k) e^{ikx} \tag{8.100}$$

[10]We would like to thank Daniel Park for exceedingly helpful assistance in this endeavour.

We will assume that the analytic structure of F is such that the only singularities in the complex k-plane are at the beginning of the branch cuts in ν, that is at $k = \pm ik_0$. If that is so, then we can take the two branch cuts to go upwards and downwards in the complex k-plane and then (for positive x) by deforming the contour upwards we can rewrite the above integrand as

$$I(x) = i \int_{k_0}^{\infty} d\kappa \left[F\left(-i\sqrt{\kappa^2 - k_0^2}\right) - F\left(+i\sqrt{\kappa^2 - k_0^2}\right) \right] e^{-\kappa x} \tag{8.101}$$

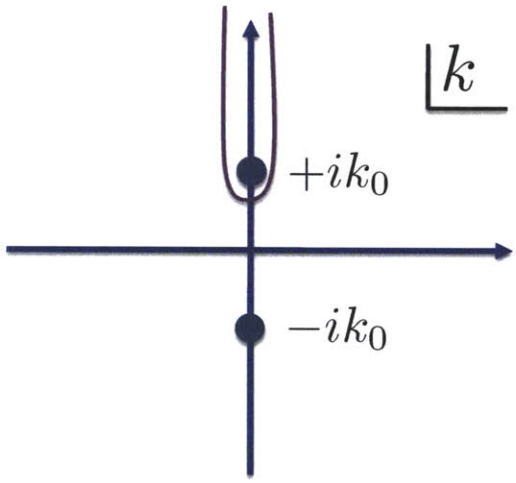

Figure 8-5: Contour manipulations used in derivation of (8.101).

Now in the limit of large x we expect the integral to be dominated by the lower limit of the integrand $\kappa \sim k_0$; thus we can expand the sub-exponential part of the integrand in powers of $(\kappa - k_0)$ and perform the integrals directly; thus it is clear that the leading x behavior will be of the form

$$I(x) \sim \frac{e^{-k_0 x}}{x^{\#}} \tag{8.102}$$

where the power appearing in # depends on the exact form of the integrand. The key point here is the the location of the branch cut sets a scale which determines the correlation length in the integral. We now perform the specific integrals in question.

8.C.2 Correlators near criticality

We first perform integrals near criticality, which correspond to tuning k_0 in (8.99) to be very small 0. The specific integral in question is

$$I(x) = \int dk_x dk_y \frac{1}{C + \sqrt{k_x^2 + k_y^2 + k_0^2}} e^{ik_x x} \text{ ., } \tag{8.103}$$

where we have put the spatial separation in the x direction. We assume that $k_0 \ll C$ (which is sensible near criticality) and attempt to extract an asymptotic formula at large x. Then the only relevant analytic structure is the branch cuts described above and the integral can be done by the techniques described above. We do the k_x integral first, where the integrand has a branch cut at $k_x = \pm i\sqrt{k_y^2 + k_0^2} \equiv i\tilde{k}_0$ instead of $\pm ik_0$. Performing the contour manipulations described above,

$$I(x) = \int dk_y \int_{\tilde{k}_0}^{\infty} id\kappa \left(\frac{1}{C + i\sqrt{\kappa^2 - \tilde{k}_0^2}} - \frac{1}{C - i\sqrt{\kappa^2 - \tilde{k}_0^2}} \right) e^{-\kappa x} . \tag{8.104}$$

Now since we only care about the large x behavior, we can expand the sub-exponential part of the integrand in a power series about $k \sim k_0$. We then find

$$I(x \to \infty) \sim \int dk_y \int_{k_0}^{\infty} d\kappa \frac{2\sqrt{2k_0}}{C^2} \sqrt{\kappa - \tilde{k}_0} \exp(-\kappa x) = \int dk_y \frac{\sqrt{2\pi \tilde{k}_0}}{C^2 x^{3/2}} e^{-\tilde{k}_0 x} . \tag{8.105}$$

It is now staightforward to do the k_y integral:

$$I(x) \sim \int_{-\infty}^{\infty} dk_y \frac{\sqrt{2\pi (k_y^2 + k_0^2)^{\frac{1}{2}}}}{C^2 x^{\frac{3}{2}}} e^{-\sqrt{k_y^2 + k_0^2} x} = 2 \int_{k_0}^{\infty} dv \frac{v}{\sqrt{v^2 - k_0^2}} \frac{\sqrt{2\pi v}}{C^2 x^{\frac{3}{2}}} e^{-vx} \tag{8.106}$$

where we have made the substitution $v = \sqrt{k_y^2 + k_0^2}$ and the overall 2 comes from the fact that both positive and negative k_y contribute. Again, as $x \to \infty$ the main contribution to the integral comes from the neighborhood of $v \sim k_0$, and we can expand the subexponential part of the integrand there. We find

$$I(x) \sim \frac{2k_0\sqrt{\pi}}{C^2 x^{\frac{3}{2}}} \int_{k_0}^{\infty} \frac{e^{-vx}}{\sqrt{v - k_0}} = \frac{2\pi k_0}{C^2 x^2} e^{-k_0 x} \tag{8.107}$$

An interesting feature of these integrals is that there is an overall extra suppression by factors of k_0 in the numerator. This does not happen if we are performing an integral with the usual kind of pole, e.g. $\frac{1}{k^2 + k_0^2}$; this appears to be due to the fact that the singularity at $k \sim \pm ik_0$ is of a weaker sort. It suggests however that the $k_0 \to 0$ limit of the above integrals is somewhat nontrivial and is not captured by the above expressions (since they simply vanish in that limit). We now directly compute the integral (8.103) at $k_0 = 0$; this requires different techniques.

8.C.3 Integrals at criticality: $k_0 = 0$.

We now perform an integral directly at criticality. We would like to evaluate

$$I_c(x) \equiv \int d^2k \frac{1}{C + |\vec{k}|} e^{ikx} . \tag{8.108}$$

This time we first perform the angular integral to find

$$I_c(x) = 2\pi \int_0^\infty \frac{k}{C+k} J_0(kx) = \pi \int_0^\infty \frac{k}{C+k} \left(H_0^{(1)}(kx) + H_0^{(2)}(kx) \right) \tag{8.109}$$

Here J_0 and H_0 are the Bessel and Hankel functions. Now the integral is along the real (positive) k-axis; however, since $H^{(1)}$ is well-behaved in the upper-half plane and $H^{(2)}$ is well-behaved in the lower, we can we can split the integral into two halves. We rotate one contour up and the other down, finding

$$I_c(x) = \pi \int_0^\infty id\kappa \left(\frac{i\kappa}{C+i\kappa} H_0^{(1)}(i\kappa x) + \frac{i\kappa}{C-i\kappa} H_0^{(2)}(-i\kappa x) \right) \tag{8.110}$$

which after some more manipulation gives

$$I_c(x) = 4 \int_0^\infty d\kappa \frac{\kappa^2}{\kappa^2 + C^2} K_0(\kappa x) \tag{8.111}$$

where we have used the definition of the modified Bessel function $H_0^{(1)}(i\kappa x) = -\frac{2i}{\pi} K_0(\kappa x)$ and the fact that it is real (and hence the Hankel function is imaginary) for real κx. Finally, if we expand the sub-Bessel part of the integrand in powers of κ we can get an expansion in powers of $1/x$; the leading term works out to be,

$$I_c(x \to \infty) \sim \frac{4}{C^2 x^3} \int_0^\infty dv\, v^2 K_0(u) = \frac{2\pi}{C^2 x^3} \,. \tag{8.112}$$

We have verified this behavior by numerical computation of the original integral and found perfect agreement. Note that the exponent of the power-law falloff in x is larger than that in the finite k_0 integral (8.107), as anticipated by the extra suppression of k_0 in the numerator.

Chapter 9

Conclusion

Far back, in the Introduction, we began our discussion by writing down the starting point for a conventional understanding of quantum field theory, the free field:

$$\mathcal{L} = \int d^4x \left[\frac{1}{2}(\nabla\phi)^2 + \frac{1}{2}m^2\phi^2 \right] . \tag{9.1}$$

Deformations of this theory define the structure of perturbative quantum field theory, the basis for our current microscopic understanding of physical reality. However, we quickly realized that this Lagrangian – or others like it – is not necessarily a suitable starting point for tackling all problems. There exist real-life systems in which strong interactions play an essential role, and in the Introduction we touched on two in particular. These case studies were the quark-gluon plasma and the strange metal phase of the high T_c cuprates.

We then turned away from these problems. Real-life systems are rather complicated. We do not have a gravity dual for $SU(3)$ QCD. The cuprates are even more complicated; there are doubtlessly many different aspects of condensed matter physics contributing to the full phase diagram, and we are very far from understanding what a true gravity dual for even the strange metal phase alone would look like. A direct assault on these problems is not a sensible task for a holographer.

We thus spent the next eight chapters studying a *different* set of strongly correlated problems – those which *do* admit a treatment using the techniques of gauge-gravity duality. This forced us into the study of theories that are conformal in the ultraviolet, and whose microscopic descriptions involve a great deal of supersymmetry. We chose to ignore these facts, studied systems at finite temperature and density, and focused on low-energy physics, where the spectacular symmetries of the conformal vacuum appear to play no role.

We studied diffusion on black hole horizons, and demonstrated that this was precisely equivalent to diffusion in a strongly coupled gauge theory plasma that was not dissimilar to the quark-gluon plasma. We studied a finite-density state via holography, and argued that within its phase diagram there existed a point that was not dissimilar to the strange metal phase of the cuprates, possessing a Fermi surface but no quasiparticles, and a resistivity that is linear in temperature. We found new types

of quantum phase transitions, driven by locally critical quantum fluctuations.

Along the way, we began to build an intuition for a new way to think about quantum field theory. Many familiar ideas – the renormalization group, symmetry breaking – took on fascinating new shape, manifesting themselves via elegant geometric pictures. The separation of energy scales became a physical separation in an extra holographic dimension. Charge diffusion happened when gauge excitations fell into black hole horizons. The buffeting of Fermi quasi-particles by a quantum critical sector became the physical stretching of its wavefunction down an AdS_2 throat. We framed our understanding of these field theories in a language that had nothing to do with the microscopic ingredients of Lagrangians like (9.1).

Of course, we did not solve either of the two systems mentioned in the Introduction. However, within our black holes and curved spacetimes we saw *caricatures* of their behavior, and we learned a new way to think about them. One would like to take our descriptions to a level more accurate than caricature; this will not be easy and in many ways it is not immediately clear how to do this. Nevertheless there exist many concrete directions for further research: these have been spelled out in the various individual chapters, and we do not repeat them here.

The study of physical applications of holography is in its infancy. Even at this stage, however, it seems undeniable that there is now a new base camp for the assault on strongly correlated systems. It looks nothing like (9.1); rather it is based on geometry and it looks like:

$$ds^2 = R^2 \frac{\eta_{\mu\nu} dx^\mu dx^\nu + dz^2}{z^2}. \tag{9.2}$$

From this new starting point we may finally have the opportunity to liberate our understanding of quantum field theory from the constraints of perturbation theory. It remains to be seen what we discover along the way.

Appendix A

Solvable spinor examples

In Chapter 2.2 a formalism was developed for holographically computing real-time response functions of fermionic operators. In this Appendix we illustrate this formalism by explicitly solving two concrete examples.

The first is spinors moving on a pure AdS_{d+1} bulk background. The computation we will perform will result in the two-point function of a fermionic operator in the vacuum of a CFT_d; this is exactly solvable because of the conformal symmetry associated with the vacuum.

The second example is spinors moving on a BTZ black hole [155, 156] in three bulk dimensions; this will allow us to calculate fermionic correlators in a thermal state in a CFT_2. This is also exactly solvable, which is perhaps more surprising. From a field theoretical point of view this is possible because the finite-temperature state in a CFT_2 is a conformal transformation of the vacuum (see e.g. Chapter 4 of [83]). This is dual to the fact that the BTZ black hole is locally precisely the same as the the AdS_3 vacuum, as it must be since in three dimensions the Riemann tensor is locally determined by the Ricci tensor; it is only the global structure that is different, as the BTZ black hole may be viewed as a quotient of global AdS_3 [156]. From a practical point of view it is thus not at all surprising that all wave equations on BTZ are just as solvable as those on AdS_3.

A.1 Pure AdS

The Euclidean vacuum two-point function for a spinor operator $\mathcal{O}$ in a CFT, which is dual a fermonic field ψ in a pure AdS, was obtained in closed form before in [76] (see also [77, 78]). The corresponding retarded function can then obtained from it by analytic continuation using (2.20). Here we calculate the retarded function directly using the prescription developed earlier as a check of our formalism.

For pure AdS, the metric is given by

$$ds^2 = r^2(-dt^2 + d\vec{x}^2) + \frac{dr^2}{r^2} \tag{A.1}$$

with associated nonzero spin connection components given by

$$\omega_{tr} = -r dt, \quad \omega_{ir} = r dx^i \ . \tag{A.2}$$

The Dirac equation in momentum space is then given by

$$r\Gamma^r \partial_r \psi + \frac{i}{r}\Gamma \cdot k\psi + \frac{d}{2}\Gamma^r \psi - m\psi = 0 \tag{A.3}$$

Using (2.41), equation (A.3) now becomes coupled equations for $\psi_\pm$

$$\psi_+ = -\frac{i\gamma \cdot k}{k^2} A(-m)\psi_-, \qquad \psi_- = \frac{i\gamma \cdot k}{k^2} A(m)\psi_+ \tag{A.4}$$

where we have used (2.43) or (2.44) for d even or odd and

$$A(m) = r\left(r\partial_r + \frac{d}{2} - m\right) \tag{A.5}$$

from which we obtain

$$k^2 \psi_+ = A(-m)A(m)\psi_+ \ . \tag{A.6}$$

Note that (A.6) is now a group of decoupled scalar equations, which implies that the $\mathcal{T}$ matrix defined in (2.62) will be proportional to the identity matrix. Equation (A.6) can be solved exactly using Bessel functions, and the solution satisfying the in-falling boundary condition at the horizon is

$$\psi_{R+} = \begin{cases} r^{-\frac{d+1}{2}} K_{m+\frac{1}{2}}\left(\frac{\sqrt{|\vec{k}|^2 - \omega^2}}{r}\right) a_+ & k^2 > 0 \\ r^{-\frac{d+1}{2}} H^{(1)}_{m+\frac{1}{2}}\left(\frac{\sqrt{\omega^2 - |\vec{k}|^2}}{r}\right) a_+ & \omega > |\vec{k}| \\ r^{-\frac{d+1}{2}} H^{(2)}_{m+\frac{1}{2}}\left(\frac{\sqrt{\omega^2 - |\vec{k}|^2}}{r}\right) a_+ & \omega < -|\vec{k}| \end{cases} \tag{A.7}$$

where a_+ is an arbitrary constant spinor. The story for the spacelike case $k^2 > 0$ is exactly the same as that of Euclidean correlator and the retarded correlator is real. For the timelike case $\omega > |\vec{k}|$, we find the corresponding A, B coefficients as defined in (2.60) as

$$A = -\frac{1}{\Gamma(\frac{1}{2} - m)}\left(\frac{k}{2}\right)^{-(m+\frac{1}{2})} a_+, \qquad B = \frac{e^{-(m+\frac{1}{2})\pi i}}{\Gamma(m + \frac{3}{2})}\left(\frac{k}{2}\right)^{(m+\frac{1}{2})} a_+, \quad k = \sqrt{\omega^2 - |\vec{k}|^2} \tag{A.8}$$

giving

$$\mathcal{T}_\beta{}^\alpha = \delta_\beta{}^\alpha \frac{\Gamma(-m - \frac{1}{2})}{\Gamma(m + \frac{1}{2})}\left(\frac{k}{2}\right)^{2m+1} e^{-(m+\frac{1}{2})\pi i} \tag{A.9}$$

Using (2.61), we then find that

$$G_R(k) = \frac{2e^{-(m+\frac{1}{2})\pi i}}{k^2}\frac{\Gamma(-m+\frac{1}{2})}{\Gamma(m+\frac{1}{2})}\left(\frac{k}{2}\right)^{2m+1}(\gamma\cdot k)\,\gamma^t, \qquad \omega > |\vec{k}| \tag{A.10}$$

For the other possible timelike case $\omega < -|\vec{k}|$ we simply change the phase factor $e^{-(m+\frac{1}{2})\pi i}$ to $e^{(m+\frac{1}{2})\pi i}$.

A.2 BTZ Black Hole

We now consider fermionic correlators in a BTZ black hole background [155, 156]. Previous work [80] found that the quasinormal modes of a BTZ black hole precisely coincide with the poles in the retarded propagator of the appropriate operator of the dual theory (whose form is essentially fixed by conformal invariance). Here we will closely follow [80, 81] to solve the wave equation but slightly extend these results by finding the full correlator from the gravity side.

A BTZ black hole with a mass M and angular momentum J describes a boundary 2d CFT in a sector with

$$L_0 = \frac{1}{2}(M+J), \qquad \bar{L}_0 = \frac{1}{2}(M-J)\ . \tag{A.11}$$

The system has a finite entropy and non-vanishing left and right temperatures. Here we are interested in probing this sector using fermionic operators with spin $s = \frac{1}{2}$. Such an operator $\mathcal{O}_\pm$ is characterized by conformal weights (h_L, h_R) with

$$h_L + h_R = \Delta, \qquad h_L - h_R = \pm\frac{1}{2} \tag{A.12}$$

where the $\pm$ sign denotes its chirality. As described in the previous section each $\mathcal{O}_+$ (or $\mathcal{O}_-$) is described by a Dirac spinor ψ in the bulk, with different chiralities corresponding to different boundary conditions and opposite bulk mass. We will now find the retarded correlators of $\mathcal{O}_\pm$ by solving the Dirac equation for ψ in the BTZ geometry.

The metric of a BTZ black hole can be written as

$$ds^2 = -\frac{(r^2-r_+^2)(r^2-r_-^2)}{r^2}dt^2 + \frac{r^2dr^2}{(r^2-r_+^2)(r^2-r_-^2)} + r^2\left(d\phi - \frac{r_+r_-}{r^2}dt\right)^2 \tag{A.13}$$

where ϕ is an angular coordinate of period 2π. The mass, angular momentum, and left and right moving temperature of the system are given by

$$M = \frac{r_+^2+r_-^2}{8G}, \qquad J = \frac{r_+r_-}{4G}, \qquad T_L = \frac{r_+-r_-}{2\pi} \qquad T_R = \frac{r_++r_-}{2\pi} \tag{A.14}$$

where G is the 3d Newton constant. To solve the Dirac equation in (A.16), it is

convenient to switch to a new coordinate system (ρ, T, X)

$$r^2 = r_+^2 \cosh^2\rho - r_-^2 \sinh^2\rho, \qquad T+X = (r_+ + r_-)(t+\phi), \qquad T-X = (r_+ - r_-)(t-\phi) \tag{A.15}$$

in which the metric is

$$ds^2 = -\sinh^2\rho dT^2 + \cosh^2\rho dX^2 + d\rho^2 \tag{A.16}$$

and the spin connections are given by

$$\omega_{T\rho} = -\cosh\rho dT \qquad \omega_{X\rho} = \sinh\rho dX \ . \tag{A.17}$$

We will work in Fourier space on each constant-ρ slice; a plane wave can be decomposed in either the (X, T) or (ϕ, t) coordinate system:

$$\psi = e^{-ik_T T + ik_X X}\psi(\rho, k_\mu) = e^{-i\omega t + ik\phi}\psi(\rho, k_\mu) \tag{A.18}$$

where using (A.15) and (A.14) we can see that the momenta in the original coordinate system (ω, k) are related to (k_T, k_X) by

$$k_T + k_X = \frac{\omega + k}{2\pi T_R}, \qquad k_T - k_X = \frac{\omega - k}{2\pi T_L} \ . \tag{A.19}$$

The Dirac equation can then be written as

$$\left[\Gamma^\rho\left(\partial_\rho + \frac{1}{2}\left(\frac{\cosh\rho}{\sinh\rho} + \frac{\sinh\rho}{\cosh\rho}\right)\right) + i\left(\frac{k_X\Gamma^X}{\cosh\rho} - \frac{k_T\Gamma^T}{\sinh\rho}\right) - m\right]\psi = 0 \tag{A.20}$$

We choose a gamma matrix representation where $\Gamma^\rho = \sigma^3, \Gamma^T = i\sigma^2, \Gamma^X = \sigma^1$ and write $\psi^T = (\psi_+, \psi_-)$. Now following [81] and letting

$$\psi_\pm \equiv \sqrt{\frac{\cosh\rho \pm \sinh\rho}{\cosh\rho\sinh\rho}}(\chi_1 \pm \chi_2), \qquad z = \tanh^2\rho \ , \tag{A.21}$$

then in terms of $\chi_{1,2}$ and z, the Dirac equation becomes

$$\begin{aligned} 2(1-z)\sqrt{z}\partial_z\chi_1 - i\left(\frac{k_T}{\sqrt{z}} + k_X\sqrt{z}\right)\chi_1 &= \left(m - \frac{1}{2} + i(k_T + k_X)\right)\chi_2 \\ 2(1-z)\sqrt{z}\partial_z\chi_2 + i\left(\frac{k_T}{\sqrt{z}} + k_X\sqrt{z}\right)\chi_2 &= \left(m - \frac{1}{2} - i(k_T + k_X)\right)\chi_1 \ . \end{aligned} \tag{A.22}$$

Note that the horizon is at $z = 0$ and the boundary at $z = 1$. It is now possible to eliminate one of the fields $\chi_{1,2}$ to obtain a second-order equation in the other field. The solutions to that equation are given in terms of hypergeometric functions. We are interested in evaluating the retarded correlator, and so we pick the solutions that

are infalling at the horizon. These take the form[1]

$$\chi_2(z) = z^{\alpha}(1-z)^{\beta}F(a,b;c;z)$$
$$\chi_1(z) = \left(\frac{a-c}{c}\right) z^{\frac{1}{2}+\alpha}(1-z)^{\beta}F(a,b+1;c+1;z) \tag{A.23}$$

where the parameters are

$$\alpha = -\frac{ik_T}{2} \qquad \beta = -\frac{1}{4}+\frac{m}{2} \tag{A.24}$$

and

$$a = \frac{1}{2}\left(m+\frac{1}{2}\right) - \frac{i}{2}(k_T - k_X), \quad b = \frac{1}{2}\left(m-\frac{1}{2}\right) - \frac{i}{2}(k_T + k_X), \quad c = \frac{1}{2} - ik_T\,. \tag{A.25}$$

From (A.21), we know that at the AdS boundary ψ has the following asymptotic behavior

$$\psi_+ \sim A(1-z)^{\frac{1}{2}-\frac{m}{2}} + B(1-z)^{1+\frac{m}{2}} \qquad \psi_- \sim C(1-z)^{1-\frac{m}{2}} + D(1-z)^{\frac{1}{2}+\frac{m}{2}}, \tag{A.26}$$

Our earlier analysis tells us that if $m > 0$ we can identify $A = \chi_0$ as the source and $D = \langle \mathcal{O}_- \rangle$ as the response, and so the retarded correlator in this frame is given by

$$\tilde{G}_R = i\frac{D}{A} \tag{A.27}$$

We now explicitly expand the solutions (A.23) near the boundary to extract the coefficients D, A. The relevant ratio works out to be

$$\tilde{G}_R(k_T,k_X) = -i\frac{\Gamma\left(\frac{1}{2}-m\right)}{\Gamma\left(\frac{1}{2}+m\right)}\frac{\Gamma\left(\frac{1}{4}(1-2i(k_T-k_X)+2m)\right)\Gamma\left(\frac{1}{4}(3-2i(k_T+k_X)+2m)\right)}{\Gamma\left(\frac{1}{4}(1-2i(k_T+k_X)-2m)\right)\Gamma\left(\frac{1}{4}(3-2i(k_T-k_X)-2m)\right)} \tag{A.28}$$

Using the relations (A.19) this can be rewritten in terms of momenta in the (t,ϕ) coordinate system as

$$\tilde{G}_R = -i\frac{\Gamma\left(\frac{1}{2}-m\right)}{\Gamma\left(\frac{1}{2}+m\right)}\frac{\Gamma\left(h_L - i\frac{\omega-k}{4\pi T_L}\right)\Gamma\left(h_R - i\frac{\omega+k}{4\pi T_R}\right)}{\Gamma\left(\tilde{h}_L - i\frac{\omega-k}{4\pi T_L}\right)\Gamma\left(\tilde{h}_R - i\frac{\omega+k}{4\pi T_R}\right)} \tag{A.29}$$

where we have introduced

$$h_L = \frac{m}{2}+\frac{1}{4}, \qquad h_R = \frac{m}{2}+\frac{3}{4} \tag{A.30}$$

[1]In order to display consistency of these solutions with the equations of motion (A.22), it can be helpful to use the hypergeometric identity $-aF(a+1,b+1,c+1,z) + \frac{c}{1-z}F(a,b,c,z) + \frac{c-a}{z-1}F(a,b+1,c+1,z) = 0$ [73].

and

$$\tilde{h}_L = -\frac{m}{2} + \frac{3}{4}, \qquad \tilde{h}_R = -\frac{m}{2} + \frac{1}{4}\,. \tag{A.31}$$

Note that (A.29) has a nice factorized form for left and right sectors. The correlator has a pole whenever either of the two gamma functions in the numerator has an argument that is a negative integer; thus we find the following two sequences of poles

$$\omega = -k - 4\pi i T_R\,(n + h_R) \qquad \omega = k - 4\pi i T_L\,(n + h_L) \qquad n \in \mathbb{Z}_+ \tag{A.32}$$

As demonstrated in [80], these two sequences of poles are precisely those appearing in the finite-temperature retarded correlator of an operator in a 2D CFT with conformal weights (h_L, h_R). Since $h_L - h_R = -\frac{1}{2}$, this is consistent with our expectation that ψ corresponds to $\mathcal{O}_-$.

If $m < 0$, we then find that ψ_- is the source and ψ_+ is the response. Thus we are looking the correlation function of $\mathcal{O}_+$. One can immediately find the correlator from the results above, as the roles of D and A are reversed; we find that this results in a different pole structure consistent with the correlator of an operator of conformal dimensions $(\tilde{h}_L, \tilde{h}_R)$, indeed corresponding to a boundary spinor of positive chirality.[2]

Finally we note one last point which is important if one wishes to determine the overall normalization of the correlator. Note that the above expression was computed in the (X, T) coordinate system; however we see from (A.15) that the relation between this and the (t, ϕ) coordinate system involves scaling the left-moving coordinate by $(r_+ - r_-)$ and the right-moving coordinate by $(r_+ + r_-)$, i.e. by the left and right temperatures respectively. Thus the correlator in the (t, ϕ) frame is[3]

$$G_R(\omega, k) = (2\pi T_L)^{2h_L - 1}(2\pi T_R)^{2h_R - 1}\tilde{G}_R(k_T, k_X)\,. \tag{A.33}$$

This rescaling is important for the extremal limit $T_L \to 0$. In this limit, using the Stirling formula in (A.29), we find that $\tilde{G}_R$ blows up

$$\tilde{G}_R \to -i\frac{\Gamma\left(\frac{1}{2} - m\right)}{\Gamma\left(\frac{1}{2} + m\right)}\frac{\Gamma\left(h_R - i\frac{\omega+k}{4\pi T_R}\right)}{\Gamma\left(\tilde{h}_R - i\frac{\omega+k}{4\pi T_R}\right)}\left(\frac{-i(\omega - k)}{4\pi T_L}\right)^{2h_L - 1}, \tag{A.34}$$

but G_R does have a finite limit

$$G_R(\omega, k) = -i(2\pi T_R)^{2h_R - 1}\left(\frac{-i(\omega - k)}{2}\right)^{2h_L - 1}\frac{\Gamma\left(\frac{1}{2} - m\right)}{\Gamma\left(\frac{1}{2} + m\right)}\frac{\Gamma\left(h_R - i\frac{\omega+k}{4\pi T_R}\right)}{\Gamma\left(\tilde{h}_R - i\frac{\omega+k}{4\pi T_R}\right)}\,. \tag{A.35}$$

[2]Note that in attempting to compare our assignment of conformal dimensions directly with [80], one should keep in mind two issues: m in this paper is $-m$ in [80], and our choice of gamma matrices means that a 3d spinor ψ_+ with positive eigenvalue of Γ^ρ has opposite 2d helicity here than it does in [80]; thus our assignment of h_L and h_R is switched relative to them.

[3]-1's in the exponents of the expression below are due to the fact that this is an expression in momentum space.

This expression can be verified by direct calculation using the bulk spacetime for the extremal BTZ black hole with $T_L = 0$. Note that (A.35) again has a nice factorized form with the left-moving sector given by the vacuum expression.

Appendix B

The Breitenlohner-Freedman Bound

In this Appendix we provide an elementary treatment of the celebrated Breitenlohner-Freedman bound [125], which tells us precisely when a bulk massive scalar field in AdS_{d+1} goes tachyonic. While the existence and derivation of this bound is a very well-known subject, we feel a careful and pedagogical discussion using only elementary techniques is still of some value.

We will work in units where $L_{AdS} = 1$ and the metric is given by

$$ds^2 = \frac{dz^2 - dt^2 + d\vec{x}^2}{z^2} = \frac{\eta_{AB} dx^A dx^B}{z^2} \tag{B.1}$$

where A, B run over all $d+1$ directions.

B.1 Wave equation in Schrodinger form

The bulk scalar action is

$$S = -\frac{1}{2}\int d^{d+1}x\sqrt{-g}\left((\nabla\phi)^2 + m^2\phi^2\right) = -\frac{1}{2}\int d^{d+1}x\, z^{1-d}\left(\eta^{AB}\partial_A\phi\partial_B\phi + \frac{m^2}{z^2}\right) \tag{B.2}$$

The equation of motion can be easily obtained from here to be

$$\phi'' + \frac{(1-d)}{z}\phi' - \left(k^2 + \frac{m^2}{z^2}\right)\phi = 0 \tag{B.3}$$

where I have assumed a field theory spacetime depedence e^{ikx}, so k^2 is the momentum $-\omega^2 + \vec{k}^2$. By writing $\phi = z^{\frac{d-1}{2}}\psi$ we find

$$-\psi'' + \left[\vec{k}^2 + \frac{1}{z^2}\left(m^2 - \frac{1-d^2}{4}\right)\right]\psi = \omega^2\psi \tag{B.4}$$

This is a perfectly normal looking Schrodinger equation, with potential $V(z)$ given by the quantity in square brackets and "energy" given by ω^2. Note that a negative-"energy" solution corresponds to imaginary ω, which means that the solution is growing exponentially in time; this is the instability we are looking for. For the remainder of our discussion we will set $\vec{k} = 0$.

Now this differential equation will always have solutions for all values of ω, both real and imaginary, but not all of them will be "normalizable". A normalizable solution to the AdS wave equation is one that has finite energy, in a sense that we will now make precise; in particular, normalizable in the bulk AdS wave equation sense will be closely related to normalizability in the usual QM sense (i.e. $\int dz|\psi(z)|^2 < \infty$).

B.2 Normalizable solutions to the AdS wave equation

We begin by first noting that if any spacetime has an isometry generated by a Killing vector ξ^μ, the current $j^\nu = T^{\mu\nu}\xi_\mu$ (where $T_{\mu\nu}$ is the stress tensor) is covariantly conserved: $\nabla_\nu j^\nu = 0$, as can be easily checked using the Killing equation and the conservation of $T_{\mu\nu}$. Thus given a region R of $d+1$ dimensional space

$$0 = \int_R d^{d+1}x\sqrt{-g}\nabla_\nu j^\nu = \int_{\partial R} d^d x\sqrt{h}n^\mu\xi^\nu T_{\mu\nu} \tag{B.5}$$

where ∂R is the boundary of R and h is the determinant of the induced metric on this boundary. Let us now specialize to AdS_{d+1} and let the Killing vector be $\xi = \partial_t$. Let us also take R to be a giant chunk of AdS, extending across all space $z \in [0, \infty)$ but bounded in the past and the future by two spacelike slices at t_i and t_f, i.e. $t \in [t_i, t_f]$. In that case ∂R has three components; the two spacelike slices at $t = t_i, t_f$, and the timelike slice at the AdS conformal boundary at $z = 0$ (I will assume that all fields decay away exponentially at $z \to \infty$; the boundary term at $z = 0$ will turn out to be important). This integral then becomes

$$\int_0^\infty dz\, z^{1-d}T_{tt}\Big|_{t=t_i}^{t=t_f} - \int_{t_i}^{t_f} dt\, z^{1-d}T_{tz}\Big|_{z=0} = 0 \tag{B.6}$$

The second term is the flux of energy-momentum out the AdS boundary; if this is zero then this equation implies that the first integral has the same value at t_f and at t_i and should be interpreted as the statement of energy conservation. Now let us explicitly work out what the relevant components of $T_{\mu\nu}$ are in our case. For a scalar field with action (B.2) the stress-energy tensor is

$$T_{\mu\nu} = \nabla_\mu\phi\nabla_\nu\phi - \frac{1}{2}g_{\mu\nu}\left[g^{\rho\sigma}\nabla_\rho\phi\nabla_\sigma\phi - m^2\phi^2\right] \tag{B.7}$$

I would now like to write this in terms of ψ. This is mostly very easy except for the term in $(\partial_z\phi)^2$, which we manipulate with an integration by parts as follows

$$\int_0^\infty dz z^{1-d}(\partial_z\phi)^2 = \phi z^{1-d}\partial_z\phi\Big|_{z=0}^{z=\infty} - \int_0^\infty dz\ \phi\partial_z(z^{1-d}\partial_z\phi) \tag{B.8}$$

$$= -\phi z^{1-d}\partial_z\phi\Big|_{z=0} - \int_0^\infty dz\ \psi\left[\partial_z^2\psi + \frac{1-d^2}{4z^2}\psi\right] \tag{B.9}$$

Similarly, we will manipulate the second term in (B.6) with a similar integration by parts (except on t)

$$-\int_{t_i}^{t_f} dt\ z^{1-d}T_{tz}\Big|_{z=0} = -\frac{1}{2}\left[\int_{t_i}^{t_f} dt\ z^{1-d}(\partial_t\phi\partial_z\phi - \phi\partial_t\partial_z\phi) + z^{1-d}\phi\partial_z\phi\Big|_{t=t_i}^{t=t_f}\right]_{z=0} \tag{B.10}$$

Putting the pieces together to assemble (B.6), we see that the boundary terms from each of the two parts cancel and we obtain the following equation

$$\int_0^\infty dz\frac{1}{2}\left[\partial_t\psi\partial_t\psi + \psi\left(-\partial_z^2 + V(z)\right)\psi\right]\Big|_{t=t_i}^{t=t_f} - \frac{1}{2}\left[\int_{t_i}^{t_f} dt\ z^{1-d}(\partial_t\phi\partial_z\phi - \phi\partial_t\partial_z\phi)\right]_{z=0} = 0 \tag{B.11}$$

where $V(z)$ is the potential from the Schrodinger equation (B.4)

$$V(z) = \frac{1}{z^2}\left(m^2 - \frac{1-d^2}{4}\right) \tag{B.12}$$

Now let us take a step back and think about what we require of a solution to the wave equation. It seems reasonable to require that the energy (defined by the first integral above) is finite, and also that it is *conserved.* We have seen that energy conservation requires that the second term vanish above vanish. Introducing a Fourier expansion in ω, $\phi(t) = \int d\omega\phi(\omega)e^{i\omega t}$, we see that this implies that

$$\int d\omega'\, d\omega \int_{t_i}^{t_f} dt e^{it(\omega+\omega')}\left[\omega\phi(\omega)\partial_z\phi(\omega') - \omega'\phi(\omega)\partial_z\phi(\omega')z^{1-d}\right]_{z=0} = 0 \tag{B.13}$$

Note that the fact that this must hold for all t_i, t_f essentially means it must hold for all ω, ω'. To put this into a form that will turn out to be more useful, we swap ω and ω' in the second term to obtain

$$\int d\omega'\, d\omega\ \omega z^{1-d}\left[\phi(\omega)\partial_z\phi(\omega') - \phi(\omega')\partial_z\phi(\omega)\right]_{z=0} = 0 \tag{B.14}$$

Finally, we write ϕ in terms of ψ and notice that the reality of $\phi(t)$ implies that $\phi(\omega) = \phi(-\omega)^*$ to write this equation as

$$\psi(\omega)^*\partial_z\psi(\omega') - \psi(\omega')\partial_z(\psi(\omega)^*) = 0 \quad \text{at } z = 0 \tag{B.15}$$

This equation embodies the statement that "nothing important is leaving through the AdS boundary," and will turn out have rather important consequences in the effective quantum mechanics problem that we will solve next.

Let us return now to the criterion of "finiteness of the energy". This simply requires that the first bracketed term in (B.11) is finite. Evaluating it at arbitrary t, we see that the energy is simply

$$E(t) = \frac{1}{2}\int d\omega' d\omega dz \left[-\omega\omega'\psi(\omega)\psi(\omega') + \psi(\omega)\left(-\partial_z^2 + V(z)\right)\psi(\omega')\right] e^{it(\omega+\omega')} \quad \text{(B.16)}$$

We have so far nowhere used the fact that we are evaluating this energy functional *on-shell*, that is, on a solution to the equations of motion (B.4). Using this fact, noticing that it is exactly the Schrodinger operator that appears in the second term above, and switching $\omega \to -\omega$, we end up with the following expression for the energy

$$E(t) = \frac{1}{2}\int d\omega' d\omega dz \left[+\omega\omega' + \omega'^2\right] \psi(\omega)^*\psi(\omega')e^{it(\omega'-\omega)} \quad \text{(B.17)}$$

This is promising. Now let us think very hard; the Schrodinger operator in (B.4) is probably Hermitian. Thus its eigenfunctions with different eigenvalues are orthogonal. These eigenfunctions are nothing but the $\psi(\omega)$, and so we should have $\int dz\psi(\omega)^*\psi(\omega') = \delta(\omega - \omega')$. Thus we find

$$E(t) = \int d\omega dz \omega^2 |\psi(\omega)|^2 \quad \text{(B.18)}$$

And so finiteness of the energy requires that the wavefunctions $\psi(\omega)$ have finite norm in the usual quantum mechanical sense.

However, it now appears that there is some discrepancy; we saw earlier that the energy would be conserved only if the boundary condition (B.15) was met, yet we also just found an explicit formula for the energy that is *time-independent*. Clearly the two conditions must be related. More precisely, we assumed that the Schrodinger operator appearing in (B.4) is Hermitian–is this necessarily true? Consider the operator acting on two eigenfunctions with real eigenvalues

$$\left[-\partial_z^2 + V(z)\right]\psi(\omega) = \omega^2\psi(\omega) \qquad \left[-\partial_z^2 + V(z)\right]\psi^*(\omega') = \omega'^2\psi^*(\omega') \quad \text{(B.19)}$$

Now multiply the first equation by $\psi^*(\omega')$, the second by $\psi(\omega)$, subtract the second from the first, and integrate them both over z. We obtain

$$-\int_0^\infty dz \left[\psi^*(\omega')\partial_z^2\psi(\omega) - \psi(\omega)\partial_z^2\psi^*(\omega')\right] = \left(\omega^2 - \omega'^2\right)\int_0^\infty dz\, \psi^*(\omega')\psi(\omega) \quad \text{(B.20)}$$

If $\omega \neq \omega'$, the eigenfunctions have different eigenvalues and the expression on the right-hand side is nonzero and proportional to the inner product of the eigenfunctions. If this operator is Hermitian, these eigenfunctions must be orthogonal, which means that the left-hand side of this expression better vanish. However, if we integrate by parts on this left-hand side, we see that it is not zero but in fact equal to a boundary

term

$$-\left[\psi(\omega')^*\partial_z\psi(\omega) - \psi(\omega)\partial_z(\psi(\omega')^*)\right]\Big|_{z=0} = \left(\omega^2 - \omega'^2\right)\int_0^\infty dz\, \psi^*(\omega')\psi(\omega) \qquad \text{(B.21)}$$

Thus the Schrodinger operator is not Hermitian unless this particular boundary term is zero. This boundary term is precisely the one that we found earlier in (B.15), and is proportional to the energy flux out the boundary of AdS. We summarize our findings below:

1. If the Schrodinger operator corresponding to the AdS wave equation is Hermitian on a particular set of eigenfunctions, then those eigenfunctions correspond to classical field configurations with a bulk AdS energy (i.e. the charge under the bulk time translational Killing vector) that is conserved. The condition for Hermiticity is precisely equivalent to the condition that no energy leak out the AdS boundary.

2. Furthermore, if a particular eigenfunction is normalizable in the normal QM sense (i.e. $\int dz|\psi(z)|^2 < \infty$), then it corresponds to a classical field configuration that has finite bulk AdS energy.

We now finally have a well-posed quantum mechanics problem; find normalizable negative-energy eigenstates of the Schrodinger operator (B.4) that satisfy the boundary condition (B.15).

B.3 An effective quantum mechanics problem

The Schrodinger problem we are solving is

$$\left(-\partial_z^2 + \frac{\alpha}{z^2}\right)\psi = -\beta^2\psi \qquad \text{(B.22)}$$

where $\alpha = \left(m^2 - \frac{1-d^2}{4}\right)$. We now want to examine the behavior of the solutions as a function of α; in particular, we are seeking negative-energy solutions, which with the convention used in (B.22) corresponds to real β. We should note that this particular potential has a venerable history; in our own treatment we will largely follow [157].

In any case, the solutions to (B.22) are writable in terms of Bessel functions:

$$\psi(z) = \sqrt{z}\left[C_1 J_\gamma(i\beta z) + C_2 Y_\gamma(i\beta z)\right] \qquad \text{(B.23)}$$

were $\gamma = \frac{1}{2}\sqrt{1+4\alpha}$. Already we see that something peculiar will happen at the particular value of $\alpha = -1/4$. To find the spectrum, we would like to impose various conditions on the wavefunction–first, let us examine the large z behavior. The asymptotic behavior of the Bessel functions with imaginary argument is

$$J_\gamma(i\beta z) \sim \sqrt{\frac{2}{i\beta z}}\cosh(\beta z) \qquad Y_\gamma(i\beta z) \sim -i\sqrt{\frac{2}{i\beta z}}\sinh(\beta z) \qquad \text{(B.24)}$$

where I have neglected some factors of $\pi/4$, etc. in the argument of the exponentials. It is clear that we need the linear combination appearing in ψ to decay exponentially at large z, which means that ψ takes the form

$$\psi(z) = C\sqrt{z}\left[J_\gamma(i\beta z) + iY_\gamma(i\beta z)\right] \tag{B.25}$$

Now we examine this at small z, where it becomes

$$\psi(z) = C\sqrt{z}\left[\frac{1}{\Gamma(\gamma+1)}\left(\frac{i\beta z}{2}\right)^\gamma - i\frac{\Gamma(\gamma)}{\pi}\left(\frac{2}{i\beta z}\right)^\gamma\right] \tag{B.26}$$

Now we finally need to worry about the true nature of $\gamma = \frac{1}{2}\sqrt{1+4\alpha}$. If $\alpha > -1/4$, then γ is real. Is this wave function then normalizable as we approach $z \to 0$? Actually, *yes*, it is; the relevant terms in $|\psi(z)|^2$ go like $z^{1+2\gamma}$, z, and $z^{1-2\gamma}$ respectively; these are actually all integrable at $z \to 0$ for sufficiently small γ, even if it is real. It appears that even if $\alpha > -\frac{1}{4}$ we can obtain *normalizable* negative energy bound states; furthermore we can get them for any value of β, i.e. a continuous spectrum of negative energy states.

To obtain a more realistic spectrum, we must recall our other boundary condition (B.15); evaluating this on two solutions (B.26) with different energies β_1, β_2 we obtainthe condition

$$\left(\frac{\beta_2}{\beta_1}\right)^\gamma + \left(\frac{\beta_1}{\beta_2}\right)^\gamma = 0 \tag{B.27}$$

This condition is never satisfied, regardless of the values of β_1, β_2 real. Thus we conclude that for real γ (i.e. $\alpha > -1/4$) we can never have a negative-energy bound state that satisfies the Hermiticity condition.

Finally, we move on to the case of interest, where $\alpha < -1/4$ and thus γ is imaginary; we write it as $\gamma = ig$, where g is a real number. Our large z analysis goes through untouched, and thus (B.25) is still the correct form for the wavefunction. On the other hand, in the small-z analysis, z is now raised to an imaginary power and so is oscillatory $z^{ig} \sim \exp[ig\log(z)]$. We find that at small z $\psi(z)$ is proportional to

$$\psi(z) \sim \sqrt{z}\cos\left[g\log\left(\frac{z\beta}{2}\right) + \delta\right] \tag{B.28}$$

δ is a g-dependent phase. This oscillates around 0 and so is probably normalizable at the boundary. Now we finally find that imposing the boundary condition (B.15) results in

$$g\left(\cos\left[g\log\left(\frac{z\beta_1}{2}\right) + \delta\right]\sin\left[g\log\left(\frac{z\beta_2}{2}\right) + \delta\right]\right) - 1 \leftrightarrow 2 = -g\sin[g(\log\beta_1 - \log\beta_2)] = 0 \tag{B.29}$$

This boundary condition can be solved, and the answer is that the (negative) energies

β_1, β_2 must be related by

$$\beta_1 = \exp\left(\frac{n\pi}{g}\right)\beta_2, \qquad n \in \mathbb{Z} \tag{B.30}$$

Thus we have a discrete spectrum. Note that $\beta = 0$ is an accumulation point of the spectrum. And indeed, given some way to fix one of the energies in the spectrum, we can fix the entire set. However, we will not pursue this any further, and simply write down the punchline:

If $\alpha < -1/4$, we have normalizable negative-energy states on which the Schrodinger operator is Hermitian.

Now recall that a "negative-energy" state is actually an instability of the classical AdS wave equation, and $\alpha = \left(m^2 - \frac{1-d^2}{4}\right)$. Thus the criterion for the existence of a finite-(and conserved)-energy instability is simply

$$m^2 L_{AdS}^2 < -\frac{d^2}{4}, \tag{B.31}$$

where we have restored the factors of L_{AdS}. This is the Breitenlohner-Freedman bound.

Bibliography

[1] S. Jeon and L. G. Yaffe, "From Quantum Field Theory to Hydrodynamics: Transport Coefficients and Effective Kinetic Theory," Phys. Rev. D **53**, 5799 (1996) [arXiv:hep-ph/9512263].

[2] D. J. Gross, F. Wilczek, "Asymptotically Free Gauge Theories," Phys. Rev. D **8**, 3633 (1973); H. D. Politzer, "Reliable Perturbative Results for Strong Interactions?," Phys. Rev. Lett. **30**, 1346 (1973).

[3] M. Luzum and P. Romatschke, "Conformal Relativistic Viscous Hydrodynamics: Applications to RHIC results at s(NN)**(1/2) = 200-GeV," Phys. Rev. C **78**, 034915 (2008) [Erratum-ibid. C **79**, 039903 (2009)] [arXiv:0804.4015 [nucl-th]].

[4] D. T. Son and A. O. Starinets, "Viscosity, black holes, and quantum field theory," Ann. Rev. Nucl. Part. Sci. **57**, 95 (2007) [arXiv:0704.0240 [hep-th]]

[5] K. S. Bedell (Ed.) Strongly Correlated Electronic Materials, Addison Wesley, New York (1989).

[6] P. Anderson and P. A. Lee in *High Temperature Superconductivity*, Proceedings of the 1989 Los Alamos Symposium, ed. K. S. Bedell, et. al., Addison-Wesley, Redwood City CA, 1990; P. A. Lee, N. Nagaosa and X.-G. Wen, Rev. Mod. Phys. 78, 17 (2006) and references therein; S. Marten *et al*, Phys. Rev. B41, (1990) 846.

[7] R. Shankar, "Renormalization group for interacting fermions in $d > 1$," Physica A **177**, 530 (1991).

[8] J. Polchinski, "Effective field theory and the Fermi surface," arXiv:hep-th/9210046.

[9] J. M. Maldacena, "The large N limit of superconformal field theories and supergravity," Adv. Theor. Math. Phys. **2**, 231 (1998) [Int. J. Theor. Phys. **38**, 1113 (1999)] [arXiv:hep-th/9711200].

[10] S. S. Gubser, I. R. Klebanov and A. M. Polyakov, "Gauge theory correlators from non-critical string theory," Phys. Lett. B **428**, 105 (1998) [arXiv:hep-th/9802109];

[11] E. Witten,"Anti-de Sitter space and holography," Adv. Theor. Math. Phys. **2**, 253 (1998) [arXiv:hep-th/9802150]

[12] S. Coleman, "Aspects of Symmetry," Cambridge University Press, New York 1985.

[13] K. S. Thorne, R. H. Price and D. A. Macdonald, "Black holes: the membrane paradigm," Yale University Press, New Haven 1986.

[14] N. Iqbal and H. Liu, "Universality of the hydrodynamic limit in AdS/CFT and the membrane paradigm," Phys. Rev. D **79**, 025023 (2009) [arXiv:0809.3808 [hep-th]].

[15] N. Iqbal and H. Liu, 'Real-time response in AdS/CFT with application to spinors," Fortsch. Phys. **57**, 367 (2009) [arXiv:0903.2596 [hep-th]].

[16] H. Liu, J. McGreevy, and D. Vegh, "Non-Fermi liquids from holography," arXiv:0903.2477 [hep-th]

[17] S.-S. Lee, "A Non-Fermi Liquid from a Charged Black Hole; A Critical Fermi Ball," Phys. Rev. D **79**, 086006 (2009) [arXiv: 0809.3402 [hep-th]]

[18] M. Cubrovic, J. Zaanen, and K. Schalm, "String Theory, Quantum Phase Transitions and the Emergent Fermi-Liquid," Science **325**, 439–444 (2009) [arXiv:0904.1993 [hep-th]].

[19] T. Faulkner, H. Liu, J. McGreevy and D. Vegh, "Emergent quantum criticality, Fermi surfaces, and AdS2," arXiv:0907.2694 [hep-th].

[20] T. Faulkner, N. Iqbal, H. Liu, J. McGreevy and D. Vegh, "Strange Metal Transport Realized by Gauge/Gravity Duality," Science **329**, 1043–1047 (2010) [arXiv:1003.1728 [hep-th]].

[21] N. Iqbal, H. Liu, M. Mezei and Q. Si, "Quantum phase transitions in holographic models of magnetism and superconductors," Phys. Rev. D **82**, 045002 (2010) [arXiv:1003.0010 [hep-th]].

[22] V. L. Berezinskii, Zh. Eksp. Teor. Fiz. **59**, 907 (1970) [Sov. Phys. JETP **32**, 493 (1971)].

J. M. Kosterlitz and D. J. Thouless, "Ordering, metastability and phase transitions in two-dimensional systems," J. Phys. **C6**, 1181 (1973).

[23] O. Aharony, S. S. Gubser, J. M. Maldacena, H. Ooguri and Y. Oz, "Large N field theories, string theory and gravity," Phys. Rept. **323**, 183 (2000) [arXiv:hep-th/9905111].

[24] E. D'Hoker and D. Z. Freedman, "Supersymmetric gauge theories and the AdS / CFT correspondence," arXiv:hep-th/0201253.

[25] J. Polchinski, "Introduction to Gauge/Gravity Duality," arXiv:1010.6134 [hep-th].

[26] S. A. Hartnoll, "Lectures on holographic methods for condensed matter physics," Class. Quant. Grav. **26**, 224002 (2009) [arXiv:0903.3246 [hep-th]].

[27] J. McGreevy, "Holographic duality with a view toward many-body physics," Adv. High Energy Phys. **2010**, 723105 (2010) [arXiv:0909.0518 [hep-th]].

[28] J. Casalderrey-Solana, H. Liu, D. Mateos, K. Rajagopal and U. A. Wiedemann, "Gauge/String Duality, Hot QCD and Heavy Ion Collisions," arXiv:1101.0618 [hep-th].

[29] D. Marolf, "States and boundary terms: Subtleties of Lorentzian AdS/CFT," JHEP **0505**, 042 (2005) [arXiv:hep-th/0412032].

[30] K. Skenderis and B. C. van Rees, "Real-time gauge/gravity duality: Prescription, Renormalization and Examples" [arXiv:0812.2909 [hep-th]].

[31] B. C. van Rees, "Real-time gauge/gravity duality and ingoing boundary conditions," [arXiv:0902.4010 [hep-th]].

[32] I. Papadimitriou and K. Skenderis, "AdS/CFT correspondence and Geometry," [arXiv:hep-th/0404176].

[33] I. Papadimitriou and K. Skenderis, "Correlation Functions in Holographic RG Flows," JHEP **0410** 075 (2004) [arXiv:hep-th/0407071].

[34] P. Kovtun, D. T. Son and A. O. Starinets, "Holography and Hydrodynamics: diffusion on stretched horizons," JHEP **10** 064 (2003) [arXiv:hep-th/0309213]

[35] O. Saremi, "Shear waves, sound waves on a shimmering horizon," [arXiv:hep-th/0703170].

[36] A. O. Starinets, "Quasinormal spectrum and the black hole membrane paradigm," Phys. Lett. **B670**, 442-445 (2009). [arXiv:0806.3797 [hep-th]].

[37] M. Fujita, "Non-equilibrium thermodynamics near the horizon and holography," [arXiv:0712.2289 [hep-th]]

[38] J. Kapusta and C. Gale, "Finite Temperature Field Theory: Principles and Applications," Cambridge University Press, New York 2006.

[39] J. Casalderrey-Solana and D. Teaney, "Heavy quark diffusion in strongly coupled N = 4 Yang Mills," Phys. Rev. D **74**, 085012 (2006) [arXiv:hep-ph/0605199]; J. Casalderrey-Solana and D. Teaney, "Transverse momentum broadening of a fast quark in a N = 4 Yang Mills plasma," JHEP **0704**, 039 (2007) [arXiv:hep-th/0701123]; S. S. Gubser, "Momentum fluctuations of heavy quarks in the gauge-string duality," Nucl. Phys. B **790**, 175 (2008) [arXiv:hep-th/0612143].

[40] M. Parikh and F. Wilczek, "An action for black hole membranes," Phys. Rev. D **58** 064011 (1998) [arXiv:gr-qc/9712077]

[41] R. H. Price and K. S. Thorne, "Membrane viewpoint on black holes: Properties and evolution of the stretched horizon," Phys. Rev. D **33** 915 (1986).

[42] D. T. Son, A. O. Starinets, "Minkowski space correlators in AdS / CFT correspondence: Recipe and applications," JHEP **0209**, 042 (2002). [arXiv:hep-th/0205051].

[43] C. P. Herzog and D. T. Son, "Schwinger-Keldysh propagators from AdS/CFT correspondence," JHEP **0303**, 046 (2003) [arXiv:hep-th/0212072].

[44] A. Adams, K. Balasubramanian, and J. McGreevy, "Hot Spacetimes for Cold Atoms" [arXiv:0807.1111 [hep-th]]; J. Maldacena, D. Martelli, and Y. Tachikawa, "Comments on string theory backgrounds with non-relativistic conformal symmetry," [arXiv:0807.1100 [hep-th]]; C. P. Herzog, M. Rangamani, and S. F.'Ross, "Heating up Galilean holography," [arXiv:0807.1099 [hep-th]].

[45] K. Landsteiner and J. Mas, "The shear viscosity of the non-commutative plasma," JHEP **0707**, 088 (2007) [arXiv:0706.0411 [hep-th]].

[46] A. Buchel and J. T. Liu, Phys. Rev. Lett. "Universality of the shear viscosity in supergravity" **93**, 090602 (2004) [arXiv:hep-th/0311175]

[47] D. T. Son and A. O. Starinets, "Hydrodynamics of R-charged black holes, JHEP **0603** 052 (2006) [arXiv:hep-th/0601157]

[48] K. Maeda, M. Natsuume, and T. Okamura, "Viscosity of gauge theory plasma with a chemical potential from AdS/CFT correspondence Phys. Rev. D **73**, 066013 (2006) [arXiv:hep-th/0602010]

[49] O. Saremi, "The Viscosity Bound Conjecture and Hydrodynamics of M2-Brane Theory at Finite Chemical Potential," JHEP **0610** 083 (2006) [arXiv:hep-th/0601159]

[50] P. Benincasa, A. Buchel and R. Naryshkin, "The shear viscosity of gauge theory plasma with chemical potentials," Phys. Lett. B **645** 309 (2007) [arXiv:hep-th/0610145]

[51] J. Mas, "Shear viscosity from R-charged AdS black holes," JHEP **0603** 016 (2006) [arXiv:hep-th/0601144]

[52] P. Kovtun, D. T. Son, A. O. Starinets, "Viscosity in strongly interacting quantum field theories from black hole physics," Phys. Rev. Lett. **94**, 111601 (2005). [arXiv:hep-th/0405231].

[53] A. Buchel, "On universality of stress-energy correlation functions in supergravity," Phys. Lett. B **609** 392 (2005) [arXiv:hep-th/0408095]

[54] S. R. Das, G. H. Gibbons and S. D. Mathur, "Universality of Low Energy Absorption Cross Sections for Black Holes" Phys. Rev. Lett. **78**, 417 (1997) [arXiv:hep-th/9609052]

[55] M. Brigante, H. Liu, R. C. Myers, S. Shenker and S. Yaida, "Viscosity Bound Violation in Higher Derivative Gravity," Phys. Rev. D **77**, 126006 (2008) [arXiv:0712.0805 [hep-th]];

[56] M. Brigante, H. Liu, R. C. Myers, S. Shenker and S. Yaida, "The Viscosity Bound and Causality Violation," Phys. Rev. Lett. **100**, 191601 (2008) [arXiv:0802.3318 [hep-th]].

[57] Y. Kats and P. Petrov, "Effect of curvature squared corrections in AdS on the viscosity of the dual gauge theory," JHEP **0901**, 044 (2009) [arXiv:0712.0743 [hep-th]].

[58] R. Brustein and A. J. M. Medved, "The ratio of shear viscosity to entropy density in generalized theories of gravity," Phys. Rev. D **79**, 021901 (2009) [arXiv:0808.3498 [hep-th]].

[59] A. Buchel, J. T. Liu, A. O. Starinets, "Coupling constant dependence of the shear viscosity in $\mathcal{N} = 4$ supersymmetric Yang-Mills theory," Nucl. Phys. B **707** 56 (2005) [arXiv:hep-th/0406264]

[60] S. C. Huot, P. Kovtun, G. D. Moore, A. Starinets, and L. Yaffe, "Photon and dilepton production in supersymmetric Yang-Mills plasma," JHEP **12** 015 (2006) [arXiv:hep-th/0607237]

[61] P. Kovtun and A. Ritz, "Universal conductivity and central charges," Phys. Rev. D **78**, 066009 (2008) [arXiv:0806.0110 [hep-th]].

[62] C. P. Herzog, P. Kovtun, S. Sachdev and D. T. Son, "Quantum Critical Transport, duality and M theory," Phys. Rev. D **75** 085020 [arXiv:hep-th/0701036]

[63] D. Z. Freedman, S. D. Mathur, A. Matusis and L. Rastelli, "Correlation functions in the CFT(d)/AdS($d+1$) correspondence," Nucl. Phys. B **546**, 96 (1999) [arXiv:hep-th/9804058].

[64] T. Damour and M. Lilley, "String Theory, Gravity and Experiment," arXiv:0802.4169 [hep-th]

[65] J. Polchinski, "Renormalization And Effective Lagrangians," Nucl. Phys. B **231**, 269 (1984).

[66] S. S. Gubser, S. S. Pufu, and F. D. Rocha, "Bulk viscosity of strongly coupled plasmas with holographic duals,", JHEP **08** 085 (2008) [arXiv:0806.0407 [hep-th]]

[67] P. Benincasa, A. Buchel and A. O. Starinets, "Sound waves in strongly coupled non-conformal gauge theory plasma", Nucl. Phys. B **733**, 160 (2006), [arXiv:hep-th/0507026]

[68] A. Buchel, "Bulk viscosity of gauge theory plasma at strong coupling," Phys. Lett. B **663**, 286 (2008), [arXiv:0708.3459 [hep-th]]

[69] A. Yarom, "Notes on the bulk viscosity of holographic gauge theory plasmas," JHEP **1004**, 024 (2010) [arXiv:0912.2100 [hep-th]].

[70] C. Eling and Y. Oz, "A Novel Formula for Bulk Viscosity from the Null Horizon Focusing Equation," arXiv:1103.1657 [hep-th].

[71] J. Polchinski, "String Theory: Volume I," Cambridge University Press, New York 2001.

[72] E. Witten, "Anti-de Sitter space, thermal phase transition, and confinement in gauge theories," Adv. Theor. Math. Phys. **2** 505 (1998) [arXiv:hep-th/9803131].

[73] M. Abramowitz and I. A. Stegun, "Handbook of Mathematical Functions," Dover, New York 1965.

[74] V. Balasubramanian, P. Krauss, "A stress tensor for Anti-de Sitter gravity", Commun. Math. Phys. **208**, 413 (1999) [arXiv:hep-th/9902121].

[75] J.D. Brown and J.W. York, "Quasilocal energy and conserved charges derived from the gravitational action," Phys. Rev. **D 47**, 1407 (1993) [arXiv:gr-qc/9209012]

[76] M. Henningson and K. Sfetsos, "Spinors and the AdS/CFT correspondence," Phys. Lett. B **431**, 63 (1998) [arXiv:hep-th/9803251].

[77] W. Mueck and K. S. Viswanathan, "Conformal field theory correlators from classical field theory on anti-de Sitter space. II: Vector and spinor fields," Phys. Rev. D **58**, 106006 (1998) [arXiv:hep-th/9805145].

[78] M. Henneaux, "Boundary terms in the AdS/CFT correspondence for spinor fields," [arXiv:hep-th/9902137].

[79] I. Klebanov and E. Witten, "AdS/CFT Correspondence and Symmetry Breaking," Nucl. Phys. B **556** 89 (1999) [arXiv:hep-th/9905104]

[80] D. Birmingham, I. Sachs, S. N. Solodukhin, "Conformal Field Theory Interpretation of Black Hole Quasi-normal Modes," Phys. Rev. Lett. **88**, 151301 (2002) [arXiv:hep-th/0112055]

[81] S. Das, A. Dasgupta, "Black hole emission rates and the AdS/CFT correspondence," JHEP **9910** 025 (1999) [arXiv:hep-th/9907116]

[82] J. A. Hertz, "Quantum critical phenomena," Phys. Rev. B **14**, 1165–1184 (1976).

[83] S. Sachdev, "Quantum Phase Transitions," Cambridge University Press, Cambridge 1999.

[84] Focus issue: Quantum phase transitions, Nature Phys. **4**, 167–204 (2008).

[85] P. Gegenwart, Q. Si, and F. Steglich, "Quantum criticality in heavy-fermion metals," Nat. Phys. **4**, 186–197 (2008).

[86] Q. Si, S. Rabello, K. Ingersent, and J. L. Smith, "Locally critical quantum phase transitions in strongly correlated metals," Nature **413**, 804–808 (2001).

[87] H. v. Löhneysen, A. Rosch, M. Vojta, and P. Wölfle, "Fermi-liquid instabilities at magnetic quantum phase transitions," Rev. Mod. Phys. **79**, 1015–1075 (2007).

[88] T. Senthil, A. Vishwanath, L. Balents, S. Sachdev, and M. P. A. Fisher, "Deconfined quantum critical points," Science **303**, 1490–1494 (2004).

[89] L. J. Romans, "Supersymmetric, cold and lukewarm black holes in cosmological Einstein-Maxwell theory," Nucl. Phys. B **383**, 395 (1992) [arXiv:hep-th/9203018].

[90] A. Chamblin, R. Emparan, C. V. Johnson and R. C. Myers, "Charged AdS black holes and catastrophic holography," Phys. Rev. D **60**, 064018 (1999) [arXiv:hep-th/9902170].

[91] T. Faulkner, N. Iqbal, H. Liu, J. McGreevy and D. Vegh, "Holographic non-Fermi liquid fixed points," arXiv:1101.0597 [hep-th].

[92] C. M. Varma, Z. Nussinov, W. van Saarloos, "Singular Fermi liquids," Phys. Rep. vol. **361**, 267-417 (2002) [arXiv:cond-mat/0103393].

[93] G. R. Stewart, "Non-Fermi-liquid behavior in d- and f-electron metals," Rev. Mod. Phys. **73**, 797 (2001).

[94] F. Denef, S. A. Hartnoll and S. Sachdev, "Black hole determinants and quasinormal modes," Class. Quant. Grav. **27**, 125001 (2010) [arXiv:0908.2657 [hep-th]].

[95] F. Denef, S. A. Hartnoll and S. Sachdev, "Quantum oscillations and black hole ringing," Phys. Rev. D **80**, 126016 (2009) [arXiv:0908.1788 [hep-th]].

[96] S. A. Hartnoll and D. M. Hofman, "Generalized Lifshitz-Kosevich scaling at quantum criticality from the holographic correspondence," Phys. Rev. B **81**, 155125 (2010) [arXiv:0912.0008 [cond-mat.str-el]].

[97] S. Sachdev, M. Mueller, "Quantum criticality and black holes," J. Phys: Condens. Matter **21** 164216 (2009) [arXiv:0810.2005 [cond-mat.str-el]].

[98] S. S. Gubser, "Phase transitions near black hole horizons," Class. Quant. Grav. **22**, 5121-5144 (2005), [arXiv:hep-th/0505189].

[99] S. S. Gubser, "Breaking an Abelian gauge symmetry near a black hole horizon," Phys. Rev. D **78**, 065034 (2008) [arXiv:0801.2977 [hep-th]];

[100] S. A. Hartnoll, C. P. Herzog and G. T. Horowitz, "Building a Holographic Superconductor," Phys. Rev. Lett. **101**, 031601 (2008) [arXiv:0803.3295 [hep-th]].

[101] S. A. Hartnoll, C. P. Herzog and G. T. Horowitz, "Holographic Superconductors," JHEP **0812**, 015 (2008) [arXiv:0810.1563 [hep-th]].

[102] C. P. Herzog, "Lectures on Holographic Superfluidity and Superconductivity," J. Phys. A **42**, 343001 (2009) [arXiv:0904.1975 [hep-th]].

[103] G. T. Horowitz, "Introduction to Holographic Superconductors," arXiv:1002.1722 [hep-th].

[104] S. J. Rey, "String Theory on Thin Semiconductors," Progress of Theoretical Physics Supplement No. 177 (2009) pp. 128-142; [arXiv:0911.5295 [hep-th]].

[105] T. Faulkner, G. T. Horowitz and M. M. Roberts, "Holographic quantum criticality from multi-trace deformations," arXiv:1008.1581 [hep-th].

[106] T. Faulkner, G. T. Horowitz, J. McGreevy, M. M. Roberts and D. Vegh, "Photoemission 'Experiments' on Holographic Superconductors," arXiv:0911.3402 [hep-th].

[107] T. Faulkner and J. Polchinski, "Semi-Holographic Fermi Liquids," arXiv:1001.5049 [hep-th].

[108] F. Denef and S. A. Hartnoll, "Landscape of superconducting membranes," arXiv:0901.1160 [hep-th].

[109] S. A. Hartnoll, J. Polchinski, E. Silverstein and D. Tong, "Towards strange metallic holography," arXiv:0912.1061 [hep-th].

[110] C. M. Varma, P. B. Littlewood, S. Schmitt-Rink, E. Abrahams, and A. E. Ruckenstein, "Phenomenology of the normal state of Cu-O high-temperature superconductors," Phys. Rev. Lett. **63**, 1996 – 1999 (1989).

[111] P. W. Anderson, ""Luttinger-liquid" behavior of the normal metallic state of the 2D Hubbard model," Phys. Rev. Lett. **64** 1839 (1990)

[112] M. F. Paulos, "Transport coefficients, membrane couplings and universality at extremality," JHEP **1002**, 067 (2010) [arXiv:0910.4602 [hep-th]].

[113] T. Holstein, R. E. Norton and P. Pincus, "de Haas-van Alphen Effect and the Specific Heat of an Electron Gas," Phys. Rev. B **8**, 2649 (1973).

[114] M. Y. Reizer, "Relativistic effects in the electron density of states, specific heat, and the electron spectrum of normal metals," Phys. Rev. B **40**, 11571 (1989).

[115] G. Baym, H. Monien, C. J. Pethick, and D. G. Ravenhall, "Transverse interactions and transport in relativistic quark-gluon and electromagnetic plasma," Phys. Rev. Lett. **64** (1990) 1867.

[116] S. A. Hartnoll, P. K. Kovtun, M. Mueller, S. Sachdev, "Theory of the Nernst effect near quantum phase transitions in condensed matter, and in dyonic black holes," Phys. Rev. B **76** 144502 (2007) [arXiv:0706.3215 [cond-mat]]

[117] J. Polchinski, "Low-energy dynamics of the spinon gauge system," Nucl. Phys. B **422**, 617 (1994) arXiv:cond-mat/9303037.

[118] C. Nayak and F. Wilczek, "Non-Fermi liquid fixed point in (2+1)-dimensions," Nucl. Phys. B **417**, 359 (1994) [arXiv:cond-mat/9312086]; "Renormalization group approach to low temperature properties of a non-Fermi liquid metal," Nucl. Phys. B **430**, 534 (1994) [arXiv:cond-mat/9408016].

[119] B. I. Halperin, P. A. Lee and N. Read, "Theory of the half filled Landau level," Phys. Rev. B **47**, 7312 (1993).

[120] S. A. Hartnoll and A. Tavanfar, "Electron stars for holographic metallic criticality," arXiv:1008.2828 [hep-th].

[121] S. A. Hartnoll, D. M. Hofman and A. Tavanfar, "Holographically smeared Fermi surface: Quantum oscillations and Luttinger count in electron stars," arXiv:1011.2502 [hep-th].

[122] S. A. Hartnoll and P. Petrov, "Electron star birth: A continuous phase transition at nonzero density," arXiv:1011.6469 [hep-th].

[123] V. G. M. Puletti, S. Nowling, L. Thorlacius and T. Zingg, "Holographic metals at finite temperature," JHEP **1101**, 117 (2011) [arXiv:1011.6261 [hep-th]].

[124] M. Cubrovic, J. Zaanen and K. Schalm, "Constructing the AdS dual of a Fermi liquid: AdS Black holes with Dirac hair," arXiv:1012.5681 [hep-th].

[125] P. Breitenlohner and D. Z. Freedman, "Stability In Gauged Extended Supergravity," Annals Phys. **144**, 249 (1982).

[126] D. B. Kaplan, J. W. Lee, D. T. Son and M. A. Stephanov, "Conformality Lost," Phys. Rev. D **80**, 125005 (2009) [arXiv:0905.4752 [hep-th]].

[127] K. Jensen, A. Karch, D. T. Son and E. G. Thompson, "Holographic Berezinskii-Kosterlitz-Thouless Transitions," arXiv:1002.3159 [hep-th].

[128] K. Jensen, "More Holographic Berezinskii-Kosterlitz-Thouless Transitions," Phys. Rev. D **82**, 046005 (2010) [arXiv:1006.3066 [hep-th]].

[129] S. S. Gubser and A. Nellore, "Ground states of holographic superconductors," Phys. Rev. D **80**, 105007 (2009) [arXiv:0908.1972 [hep-th]].

[130] G. T. Horowitz and M. M. Roberts, "Zero Temperature Limit of Holographic Superconductors," JHEP **0911**, 015 (2009) [arXiv:0908.3677 [hep-th]].

[131] J. P. Gauntlett, J. Sonner and T. Wiseman, "Holographic superconductivity in M-Theory," Phys. Rev. Lett. **109**, 151601 (2009) [arXiv:0907.3796 [hep-th]].

[132] J. P. Gauntlett, J. Sonner and T. Wiseman, "Quantum Criticality and Holographic Superconductors in M-theory," JHEP **02**, 060 (2010) [arXiv:0912.0512 [hep-th]].

[133] S. S. Gubser, S. S. Pufu and F. D. Rocha, "Quantum critical superconductors in string theory and M-theory," Phys. Lett. B **683**, 201-204 (2010) [arXiv:0908.0011[hep-th]

[134] S. S. Gubser, C. P. Herzog, S. S. Pufu and T. Tesleanu, "Superconductors from Superstrings," Phys. Rev. Lett. **103** 141601 (2009) [arXiv:0907.3510 [hep-th]]

[135] S. S. Gubser and F. D. Rocha, "The gravity dual to a quantum critical point with spontaneous symmetry breaking," Phys. Rev. Lett. **102** 061601 (2009) [arXiv:0807.1737 [hep-th]]

[136] T. Hertog and K. Maeda, "Black holes with scalar hair and asymptotics in N = 8 supergravity," JHEP **0407**, 051 (2004) [arXiv:hep-th/0404261]

[137] T. Hertog and K. Maeda, "Stability and thermodynamics of AdS black holes with scalar hair," Phys. Rev. D **71**, 024001 (2005), [arXiv:hep-th/0409314].

[138] P. C. Hohenberg and B. I. Halperin, "Theory Of Dynamic Critical Phenomena," Rev. Mod. Phys. **49**, 435 (1977).

[139] K. Maeda, M. Natsuume and T. Okamura, "Universality class of holographic superconductors," Phys. Rev. D **79**, 126004 (2009) [arXiv:0904.1914 [hep-th]].

[140] S. S. Gubser and S. S. Pufu, "The gravity dual of a p-wave superconductor," JHEP **0811**, 033 (2008) [arXiv:0805.2960 [hep-th]].

[141] A. Auerbach, *Interacting Electrons and Quantum Magnetism*, Springer-Verlag, New York (1994).

[142] F. D. M. Haldane, "Nonlinear Field Theory of Large-Spin Heisenberg Antiferromagnets: Semiclassically Quantized Solitons of the One-Dimensional Easy-Axis Nel State," Phys. Rev. Lett. **50**, 1153 (1983).

[143] S. Chakravarty, B. I. Halperin, and D. R. Nelson, "Two-dimensional quantum Heisenberg antiferromagnet at low temperature," Phys. Rev. B **39**, 2344 (1989).

[144] N. Read and S. Sachdev, "Continuum Quantum Ferromagnets at Finite Temperature and the Quantum Hall Effect," Phys. Rev. Lett. **75**, 3509–3512 (1995).

[145] S. Coleman, "There are no Goldstone bosons in two dimensions," Commun. Math. Phys. **31**, 259 (1973).

N. D. Mermin and H. Wagner, "Absence of ferromagnetism or antiferromagnetism in one- or two- dimensional isotropic heisenberg models," Phys. Rev. Lett. **17**, 1133 (1966).

P. C. Hohenberg, "Existence of long-range order in one and two dimensions," Phys. Rev. **158**, 383 (1967).

[146] D. Anninos, S. A. Hartnoll and N. Iqbal, "Holography and the Coleman-Mermin-Wagner theorem," Phys. Rev. D **82**, 066008 (2010) [arXiv:1005.1973 [hep-th]].

[147] T. Faulkner, H. Liu and M. Rangamani, "Integrating out geometry: Holographic Wilsonian RG and the membrane paradigm," arXiv:1010.4036 [hep-th].

[148] S. S. Lee, "Low energy effective theory of Fermi surface coupled with U(1) gauge field in 2+1 dimensions," arXiv:0905.4532 [cond-mat.str-el].

[149] P. A. Lee and N. Nagaosa, "Gauge theory of the normal state of high-Tc superconductors," Phys. Rev. B **46**, 5621 (1992).

[150] K. Goldstein, S. Kachru, S. Prakash and S. P. Trivedi, "Holography of Charged Dilaton Black Holes," arXiv:0911.3586 [hep-th].

[151] M. Edalati, J. I. Jottar and R. G. Leigh, "Transport Coefficients at Zero Temperature from Extremal Black Holes," arXiv:0910.0645 [hep-th].

[152] G. Mahan, *Many-Particle Physics*, Second Edition, Plenum Press.

[153] S. Caron-Huot and O. Saremi, "Hydrodynamic Long-Time Tails from Anti De Sitter Space," JHEP **1011**, 013 (2010) [arXiv:0909.4525 [hep-th]].

[154] V. Efimov, "Energy levels arising from resonant two-body forces in a three-body system," Phys. Lett. **B33**, 563 (1970).

[155] M. Banados, C. Teitelboim, J. Zanelli, "Black hole in three-dimensional spacetime," Phys. Rev. Lett. **69** 1849 (1992) [arXiv:hep-th/9204099]

[156] M. Banados, M. Henneaux, C. Teitelboim, J. Zanelli, "Geometry of the 2+1 black hole," Phys. Rev. D **48** 1506 (1993) [arXiv:gr-qc/9302012]

[157] K. M. Case, "Singular Potentials," Phys. Rev. **80**, 797 (1950)